

# Semisynthesis of light switchable human STAT6 variants and their characterization

---

## Dissertation

zur Erlangung des akademischen Grades  
eines Doktors der Naturwissenschaften  
(Dr. rer. nat.)

des Fachbereichs Chemie der TU Dortmund

Angefertigt am Max-Planck-Institut für molekulare Physiologie  
in Dortmund (Germany)

Sunanda Lahiri

aus Mumbai (Indien)

*Mom, Dad*

*&*

*Sis*

# Erklärung/ Declaration

Die vorliegende Arbeit wurde am Max-Planck-Institut für molekulare Physiologie, Dortmund, Germany in der Abteilung Physikalische Biochemie von Prof. Dr. Roger S. Goody, unter Anleitung von Prof. Dr. Christian Becker und Prof. Dr. Martin Engelhard durchgeführt. Der experimentelle Teil wurde vom September 2004 bis November 2008 angefertigt. Hermit versichere ich an Eides statt, dass ich die vorliegende Arbeit selbständig und nur mit den angegebenen Hilfsmitteln angefertigt habe.

The present work was accomplished in the Max-Planck Institute for Molecular Physiology, Dortmund, Germany in the department of Prof. Dr. Roger S. Goody under the supervision of Prof. Dr. Christian Becker and Prof. Dr. Martin Engelhard. I hereby declare that I performed the work presented independently and did not use any other but the indicated aids.

1. Berichterstatter : Prof. Dr. M. Engelhard
2. Berichterstatter : Prof. Dr. Peter Eilbracht

Dortmund, November 2008

Sunanda Lahiri



# Wisdom begins with wonder

Socrates (469 BC – 399 BC)

# Contents

## Introduction

<b>1.1. Overview</b>	<b>1</b>
1.1.1 STATs	1
1.1.2 Structure of STATs	3
1.1.3 Activation mechanism of STATs	6
1.1.4 STAT6	10
<b>1.2. Chemical protein synthesis</b>	<b>11</b>
1.2.1. Native chemical ligation	12
1.2.2. Expressed protein ligation	16
1.2.3. Caged compounds	19

## Aim

<b>2.1. Aim of the project</b>	<b>22</b>
--------------------------------	-----------

## Materials and methods

<b>3.1. Materials and instruments</b>	<b>24</b>
3.1.1 Materials	24
3.1.2 Instruments and suppliers	25
<b>3.2. Chemical Methods</b>	<b>26</b>
3.2.1 Synthesis of caged phosphorylated tyrosine building block	26
3.2.2 1-(2-nitrophenyl) ethanol (NPE- OH) <b>(2)</b>	26
3.2.3 O-1-(2-nitrophenyl) ethyl-O'- $\beta$ -cyanoethyl-N,N-diisopropyl phosphoramidite <b>(3)</b>	27
3.2.4 N- $\alpha$ -Fmoc-L-tyrosine tert- butyl Ester <b>(5)</b>	28
3.2.5 N- $\alpha$ -Fmoc-phospho (1-nitrophenylethyl-2-cyanoethyl)-L-tyrosine tert-butyl ester. <b>(7)</b>	29
3.2.6 N- $\alpha$ -Fmoc-phospho (1-nitrophenylethyl-2-cyanoethyl)-L-tyrosine <b>(8)</b>	30
3.2.7 Synthesis of Cy5-NHS and coupling to the $\epsilon$ -amino group of Lysine	31

3.2.8	Synthesis of cysteine capture beads	32
3.2.9	Peptide synthesis	32
3.2.10	Cleavage of peptides attached to Wang resin	33
3.2.11	Peptide purification	33
<b>3.3.</b>	<b>Biochemical methods</b>	<b>34</b>
3.3.1	Buffers and Media	34
3.3.2	Expression of recombinant STAT6 (aa 1 - 634) $\alpha$ -COSR in <i>E. coli</i>	35
3.3.3	Purification of STAT6MxeCBD	35
3.3.4	Determination of Protein Concentration	36
<b>3.4.</b>	<b>Analytical methods</b>	<b>36</b>
3.4.1	Electro Spray Ionisation (ESI) - Mass spectrometry	36
3.4.2	Matrix-assisted laser desorption ionization (MALDI)	36
3.4.3	Nuclear Magnetic Resonance Spectroscopy	37
3.4.4	Thin-Layer Chromatography (TLC)	37
3.4.5	Sodium dodecyl sulfate polyacrylamide gel electrophoresis	38
3.4.6	Silver staining	39
3.4.7	Non-denaturing gels	40
3.4.8	Western blots	41
<b>3.5.</b>	<b>Native chemical ligation</b>	<b>41</b>
3.5.1	Purification of semisynthetic STAT6	42
3.5.2	Separation of peptide from ligation product	42
<b>3.6.</b>	<b>Bioactivity methods</b>	<b>43</b>
3.6.1	Electrophoretic mobility shift assay	43
3.6.2	Cell culture	44
3.6.3	Microinjection	45
3.6.4	Photo activation	46
3.6.5	Fluorescence measurement	46

## Results

<b>4.1</b>	<b>Peptide synthesis</b>	<b>47</b>
4.1.1.	Synthesis of Peptide 1	51
4.1.2.	Synthesis of Peptide 2	54
4.1.3.	Synthesis of Peptide 3	55
4.1.4.	Synthesis of Peptide 4	57
4.1.5.	Synthesis of Peptide 5	58
4.1.6.	Synthesis of Peptide 6	59
4.1.7.	Synthesis of Peptide 7	60
<b>4.2</b>	<b>Expressed protein ligation</b>	<b>62</b>
4.2.1	Expression and purification of STAT6MxeCBD protein	62
4.2.2	Preparation of STAT6-1	67
4.2.3	Preparation of STAT6-2	72
4.2.4	Preparation of STAT6-3	73
4.2.5	Preparation of STAT6-4	75
4.2.6	Preparation of STAT6-5	76
4.2.7	Preparation of STAT6-6	77
<b>4.3</b>	<b>Bioactivity of semisynthetic STAT6</b>	<b>80</b>
4.3.1	Decaging of caged phospho tyrosine in STAT6 variants	80
4.3.2	Binding of STAT6 variants to ds DNA	83
4.3.3	Monitoring the STAT6 and ds GAS-DNA by FRET	95
4.3.4	<i>In vivo</i> analysis of STAT6 variants	95

## Discussion

<b>5.1</b>	<b>Biological background of STAT6</b>	<b>106</b>
<b>5.2</b>	<b>Caged phosphorylated tyrosine building block</b>	<b>109</b>
<b>5.3</b>	<b>Generation of semisynthetic STAT6 variants</b>	<b>112</b>
<b>5.4</b>	<b>Choice of fluorophore</b>	<b>115</b>
<b>5.5</b>	<b>Bioactivity of STAT6 proteins</b>	<b>116</b>

## **Summary and Outlook**

**6.1 Summary 123**

**6.2 Outlook 125**

**Acknowledgement 126**

**Reference list 127**

**Appendix 144**



## Abbreviations

---

aa	Amino acids
APS	Ammonium persulphate
BOC	tert-butyloxycarbonyl
CBD	Chitin binding domain
CDI	Carbonyl diimidazole
COSR	C-terminal thioester
C-terminus	Carboxy terminus
DCM	Dichloromethane
dd H <sub>2</sub> O	Distilled water
DDM	n-dodecyl $\beta$ -D-maltoside
DIEA	diisopropyl ethylamine
DMEM	Dulbeccos's modified Eagle's medium
DMF	Dimethylformamide
DMSO	Dimethylsulfoxide
DNA	Dioxy ribonucleic acid
<i>E.coli</i>	<i>Escherichia coli</i>
EDTA	Ethylene diamine tetraacetate
em	Emission
ex	Excitation
EPL	Expressed protein ligation
ESI-MS	Electrospray ionization massspectrometry
FCS	Fetal calf serum
Fmoc	Fluorenylmethoxycarbonyl
FPLC	Fast protein liquid chromatography
FRET	Fluorescence resonance energy transfer
HBTU	2-(1H-benzotriazole-1yl)-1,1,3,3-tetramethyluronium hexafluorophosphate
His-tag	Histidine tag
HOBT	N-hydroxybenzotriazole
HPLC	High performance liquid chromatography

## Abbreviations

---

IPTG	Isopropyl- $\beta$ -D-thiogalactopyranoside
JAK	Janus kinase
kDa	Kilo dalton
MALDI	Matrix assisted laser desorption ionization
MesNa	Sodium $\beta$ -mercaptoethane sulphonate
MW	Molecular weight
NCL	Native chemical ligation
NTA	Nitrilo tri acetic acid
NPE	1-(2-nitrophenyl) ethanol
N-terminus	Amino terminus
OD	Optical density
PBS	Phosphate buffer saline
rpm	Revolution per minute
RT	Room temperature
SDS-PAGE	Sodium dodecyl sulfate polyacrylamide gel electrophoresis
SPPS	Solid phase peptide synthesis
STAT6	Signal transducer and activator of transcription 6
Tamra	Tetra-methyl 6-carboxy rhodamine
TBE	Tris Borate buffer
TCEP	Tris-(2-carboxyethyl) phosphine
TEMED	N, N, N, N-tetramethylethylenediamine
TFA	Trifluoroacetic acid
TLC	Thin layer chromatography
Tris	2-amino-2-(hydroxymethyl)-1,3-propanediol hydrochloride
UV	Ultraviolet
$\epsilon$	Extinction coefficient
$\lambda$	Wavelength

# Abbreviations

---

## Amino acids

Alanine	A	Ala	Leucine	L	Leu
Arginine	R	Arg	Lysine	K	Lys
Asparagine	N	Asn	Methionine	M	Met
Aspartate	D	Asp	Phenylalanine	F	Phe
Cysteine	C	Cys	Proline	P	Pro
Glutamine	Q	Gln	Serine	S	Ser
Glutamate	E	Glu	Threonine	T	Thr
Glycine	G	Gly	Tryptophan	W	Thp
Histidine	H	His	Tyrosine	Y	Tyr
Isoleucine	I	Ile	Valine	V	Val

# Chapter 1

---

Introduction

## 1.1. Overview

### 1.1.1 STATs

Communication is one of the fundamental premises of life and occurs by sensing signals from within or outside of cells and subsequent processing of these signals. Such events are observed in both prokaryotes and eukaryotes. Multi-cellular organisms have to coordinate a large number of physiological functions such as cell proliferation, differentiation, response to external stimuli, which are orchestrated by complex mechanisms known as a signal transduction cascades. There are several proteins, peptides and small molecules that carry out cell-cell communications, for as cytokines. Cytokines comprise a large number of peptides secreted by a variety of cells and regulating events such as cell growth, development, neuronal, hemapoietic and embryonic development of an organism, inflammatory processes and immune response thus, they are of considerable medical importance.

Many of these molecules and their cognate receptors were functionally and genetically characterized during the 1980s<sup>1</sup>. Cytokines are ligands for membrane bound receptors which then transmit intracellular signals via second messengers to alter gene expression levels. The known cytokines include interleukins (ILs)<sup>2</sup>, type 1 interferons (eg. IFN- $\alpha$ , IFN- $\beta$ , IFN- $\omega$ )<sup>3</sup> and type 2 interferons e.g. IFN- $\gamma$ , TGF- $\beta$  family, chemotactic factors and growth factors which have sub families<sup>4</sup>. The cytokine receptors are transmembrane proteins with extracellular ligand binding motifs. The active form of cytokine receptors is composed of homo-dimers, hetero-dimers, trimers or higher oligomers. The vast majority of the receptors are hetero oligomers where one subunit is shared among different ligands. This structural similarity allows cytokines receptors to recognize and respond to more than one ligand, which is the basis for high cross-reactivity and redundancy.

Over the past decade, research has clarified how cytokines transmit signals via pathways using the cytoplasmic Protein Tyrosine Kinases (PTKs), Janus Kinases (JAK)

## Introduction

and the Signal Transducer and Activator of Transcription (STAT) proteins. The study of cytokines led to the identification of Signal transducer and activators of transcription (STAT) in 1990s initially known as ligand induced transcription factors<sup>5,6</sup>. STAT and JAK proteins are central components in the signal transduction events in hematopoietic and epithelial cells.

The human STATs genes (STAT1, STAT2, STAT3, STAT4, STAT5A, STAT5B and STAT6) have been identified in three chromosomal clusters on chromosomes 2, 12 and 17<sup>7,8</sup>. Table (figure 1.1) shows various cytokines responsible for STAT activation.

<b>STATs</b>	<b>Total no. of amino acids</b>	<b>Cytokines (Ligands)</b>	<b>Phosphorylation site</b>
<b>STAT1</b>	750	IFNs, IL-6, EGF	701
<b>STAT2</b>	851	IFNs	689
<b>STAT3</b>	770	IL-6, IL-10, LIF, OM, C-T1, G-TFS, Leptin, EGF	705
<b>STAT4</b>	748	IL-12, IFN	722
<b>STAT5A</b>	734	PRL, GH, EPO	694
<b>STAT5B</b>	734	PRL, GH, EPO	694
<b>STAT6</b>	848	IL-4, IL-13	641

**Figure 1.1: Table of STATs and their respective ligands and phosphorylation site.**

EGF: epidermal growth factor; LIF: leukemia inhibitory factor; CNTF: ciliary neurotrophic factor; OM: oncostatin M; CT-1: cardiotrophin-1; G-CSF: granulocyte colony-stimulating factor; GM-CSF: granulocyte-macrophage colony stimulating factor; Epo: erythropoietin, PRL: prolactin

STATs play a regulatory role in the development and differentiation of T-cells, during inflammations, apoptosis and oncogenesis<sup>9-13</sup>. Due to their involvement in different diseases STATs have gained momentum as potential pharmaceutical targets. STAT1 and STAT2 were discovered as parts of the IFN signaling pathways. The generation of STAT1 knockout mice confirmed that IFN- $\alpha$  and IFN- $\gamma$  induced expression of a wide

## Introduction

---

range of proteins such as Major Histocompatibility Complex (MHC) class II protein, interferon regulatory factor-1 (IRF-1), guanylate-binding protein 1 (GBP-1), the MHC class II transactivating protein (CIITA), and the complement protein C3. They were absent or diminished in STAT1 knockout mice. These mice were defective in IFN dependent immune responses to both viral and microbial agents. Biochemical studies demonstrated that these mice failed to induce transcription of STAT1 target genes in response to IFN- $\alpha$  and IFN- $\gamma$ <sup>14</sup>.

STAT2<sup>15,16</sup> has 78% homology to STAT1 and differs only in its carboxy terminal region. STAT2 is activated by type 1 IFNs and plays a role in promoting antiviral immune responses. STAT3<sup>17-19</sup> is activated by IL-6 and is found in active murine and human tumor cells. STAT4<sup>20,21</sup> is activated by IL-12 and IFN cytokines and plays a critical role in the development of Th1 cells which is associated with rheumatoid arthritis disease. STAT5A and STAT5B share 96% similarity. They are activated by prolactin, growth hormone (GH) and erythropoietin (EPO) and can be found in all tissues. STAT5 is also found in cancer cells, similar to STAT3<sup>22,23</sup>.

STAT6<sup>24,25</sup> is activated by interleukin (IL) -4 and -13 cytokines. IL-4<sup>26,27</sup> plays a crucial role in stimulating T-cells using STAT6 as the signaling protein, which promotes Th2 cell differentiation and induces the expression of basal cell lymphoma-extra large (Bcl2L1/Bcl-xl)<sup>28-30</sup> proteins. The Bcl-xl gene which contains a STAT6 binding motif regulates the apoptotic and autophagic cell death pathway. STAT6 is found to be activated in Th2 cell, although STAT6 is present in Th1 and Th2 cell types. STAT6 deficient mice showed profound defects in their ability to develop Th2 cells. STAT6 activation has been connected to breast cancer and chronic diseases such as asthma<sup>31-</sup>  
33.

### 1.1.2 Structure of STATs

STATs are large proteins (85 -115 kDa) existing in the cytoplasm in their monomeric inactive state and as active dimers in the nucleus. As parts of signal transduction

## Introduction

---

cascades, they are multi domain proteins, which enable them to carry out a variety of functions. STAT1 and STAT3 structural features were first reported by Chen *et. al*<sup>34</sup>. and Becker *et al* in 1998<sup>35</sup>. Sequence comparison of these STATs has led to the identification of several well-conserved domains; the protein consists of an SH2 domain which is highly conserved. Carboxyl terminal to this domain is the tyrosine that becomes activated by phosphorylation in response to ligands (cytokine, epidermal growth factors, peptides) (figure 1.1) and subsequently mediates dimerization providing protein-protein interaction sites in SH2 domain that is required to form homo-dimers or hetero-dimers between two phosphorylated STAT monomers<sup>36</sup> (figure 1.2, A). Another conserved domain, separated by ~80 amino acids from the amino terminus, is the DNA binding domain helping also for protein-protein interactions during dimerization. The coiled-coiled domain does not participate during the dimerization of STATs. The crucial process of dimerization and STATs back and forth migration from cytoplasm to the nucleus during signal transduction is still poorly understood.

The structure of an activated STAT1 (aa 132 - 713, MW = 67.3 kDa), crystallized with an 18-mer duplex DNA containing a binding site for one STAT-1 dimer was determined at 2.9 Å resolution was first shown by Chen *et. al.* in 1998 (figure 1.2, A). The structure consists of four tandem domains such as coiled-coil domain as the first domain (aa 136 - 317) consists of four long helices ( $\alpha$ 1 - 4), the DNA-binding domain follows next (aa 318-488) and contains an immunoglobulin-type fold. The next domain links the DNA-binding domain to the SH2 domain, called as linker domain (aa 488 - 576). The SH2 domain (aa 577 - 683) is at the C-terminal end of the core structural unit. The C-terminal tail segment (aa 700 - 708) is phosphorylated on Tyr<sup>701</sup> and is connected to the SH2 domain by a flexible linker of 17 residues. The coiled-coiled domain of STATs ranges between residues 130 and 315 consists of a four-stranded helical coiled-coiled domain. This domain associates with a number of potentially important IFN regulatory factors (IRF)-9<sup>37</sup>.



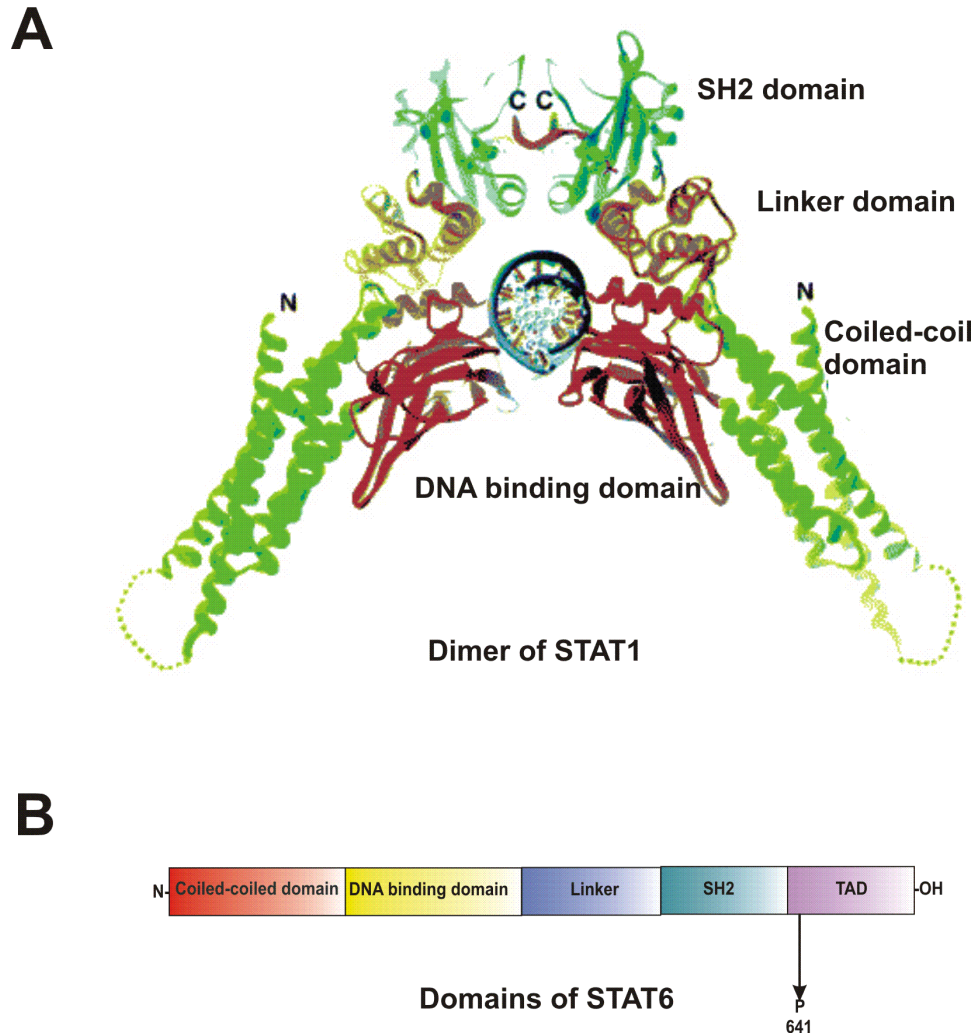


**Figure 1.2: Structure of STAT1**

**A:** Crystal structure of STAT1 phosphorylated dimer solved by Chen *et. al.* in 1998 indicating the different domains. **B:** Domain organization of STAT6.

The two coiled-coil domains project outward from the C-shaped core in opposite directions and is not involved in the interactions with the DNA or with the other monomer in the dimer. It has four  $\alpha$ -helices, two long ones ( $\alpha$  1 and  $\alpha$  2, 50 residues each) and two shorter ones ( $\alpha$  3 and  $\alpha$  4, 32 and 23 residues, respectively). The coiled-coil domain is followed by a DNA-binding domain from amino acids 320 to 475. It is structurally very similar to the immunoglobulin-like DNA-binding domain. Moreover, a DNA-binding fold between residues 320 and 490 contains several  $\beta$ -sheets that are folded similarly to those found in the DNA-binding domains of the transcription factors NF- $\kappa$ B<sup>32</sup> or p53<sup>38</sup>. The  $\beta$  strands in the domain mainly run parallel to the major axis of

## Introduction

---

the domain, and this axis is oriented perpendicular to the direction of the DNA axis. This binding domain determines the DNA-binding specificity for each STAT protein<sup>19</sup>.

The linker domain links the DNA binding domain with the SRC- homology-2 (SH2) domain. The SH2 domain consists of amino acid residues 600 to 700. It is required for the recruitment of unphosphorylated STATs to the phosphorylated residue of the receptor tail which occurs through the interaction of the SH2 domain on the STAT with the phosphorylated tyrosine present on the docking site of the receptor. Further due to reciprocal SH2-phosphotyrosine interaction between two monomeric STATs, dimers are formed<sup>39</sup>. The differences in the STAT SH2 domain bring about the selectivity of the STAT protein-binding to the different cytokine receptors. The last domain is the transactivation domain (TAD) which is the largest part (aa ~350-750) of the STAT and is involved in transcription of gene in the nucleus in addition to translocation of STAT to the cytoplasm from the nucleus after transcription is completed.

### 1.1.3 Activation mechanism of STATs

The STAT proteins receive signals from receptor domains located in the cytoplasm and transmit these signals to the nucleus. This occurs by passing of STATs through the nuclear membrane to functionally link extracellular signals with the promoters of cytokine-responsive genes. In the cytoplasm, STATs exist in an unphosphorylated monomeric state and translocate to the nucleus in their active homo or heterodimeric phosphorylated form. STAT proteins become activated by means of a variety of soluble factors, such as cytokines, growth factors, and hormones. STATs are phosphorylated on Tyr at their C-terminal domain which is catalyzed by JAK<sup>40,41</sup>.

JAKs are important intracellular protein tyrosine kinases (PTKs). In mammals, the JAK family has four members, JAK1, JAK2, JAK3 and Tyrosine kinase 2 (Tyk2). They are very large proteins of 120 - 140 kDa containing ~1,100 amino acids. JAKs contain several characteristic domains named JAK homo domain-1 (JH1) immediately adjacent

## Introduction

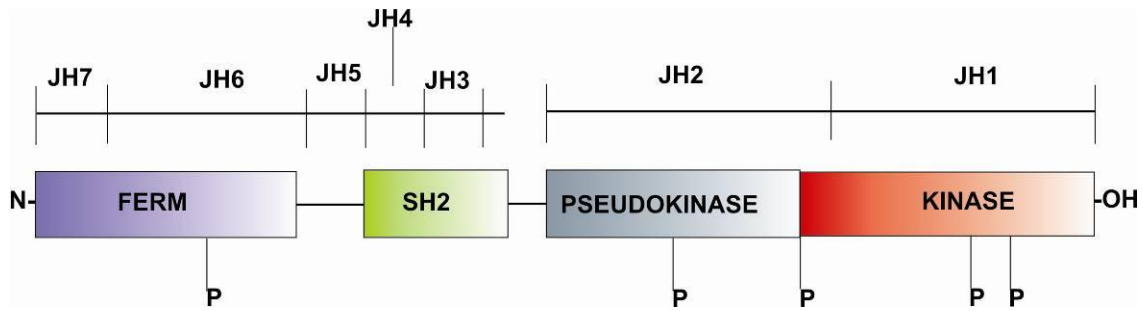


**Figure 1.3: Domains of Janus Kinase (JAK)**

to a kinase-like domain (JH2), and five additional JAK homology domains (JH3-JH7). The N-terminal domain contains a FERM (four point one, ezerin, radixin, moesin) domain (JH7-6) which is useful for catalytic activity by binding with the common  $\gamma$  chain ( $\gamma_c$ ) a shared subunit of transmembrane proteins like cytokine receptors for interleukin (IL) 2, 4, 7, 9, and 15<sup>42-44</sup> (figure 1.3).

The canonical signaling cascade of JAK-STAT pathway is initiated when a ligand interacts with two independent cytokine receptor chains, thereby promoting receptor dimerization<sup>45-47</sup>. This leads to the activation of JAK and cross activation of the neighboring kinases, which is believed to be associated with the cytoplasmic tails of the cytokine receptors. Activation of JAK may take place in the homo dimeric or hetero oligomeric cytokine receptor complexes. Once active, JAK phosphorylates certain tyrosine residues on the receptor, which generates docking sites for STAT monomers. Monomeric STAT present in the cytoplasm binds to these docking sites on the receptor tail through the C-terminal tail of STAT which has a phosphotyrosine binding domain known as the SH2 domain<sup>48</sup>. Having bound to the phosphotyrosine on the receptor, the STATs themselves become phosphorylated on Tyr residues, which enable them to form homo or hetero dimers<sup>49</sup>. The STAT proteins are activated by tyrosine phosphorylation and this modification serves as a molecular switch to allow binding to its recognized GAS-DNA. The active STAT dimers translocate rapidly to the nucleus, where they activate or repress the expression of target genes by binding with the promoter region of cytokines and thereby transcribing the responsive genes<sup>50</sup>. Since STAT6 is the main topic in this thesis the activation scheme shown below is explained by using STAT6 as

## Introduction

a model<sup>51</sup> (figure 1.4). STAT6, similar to other STATs, receive and carry transducer signal from their respective cytokines and upon activation by JAKs forms dimer and migrates to the nucleus where they bind to the promoter region of interleukin's and transcribe genes responsive to their signals. This field is of great interest in pharmaceutical companies for which STATs receive great significance.

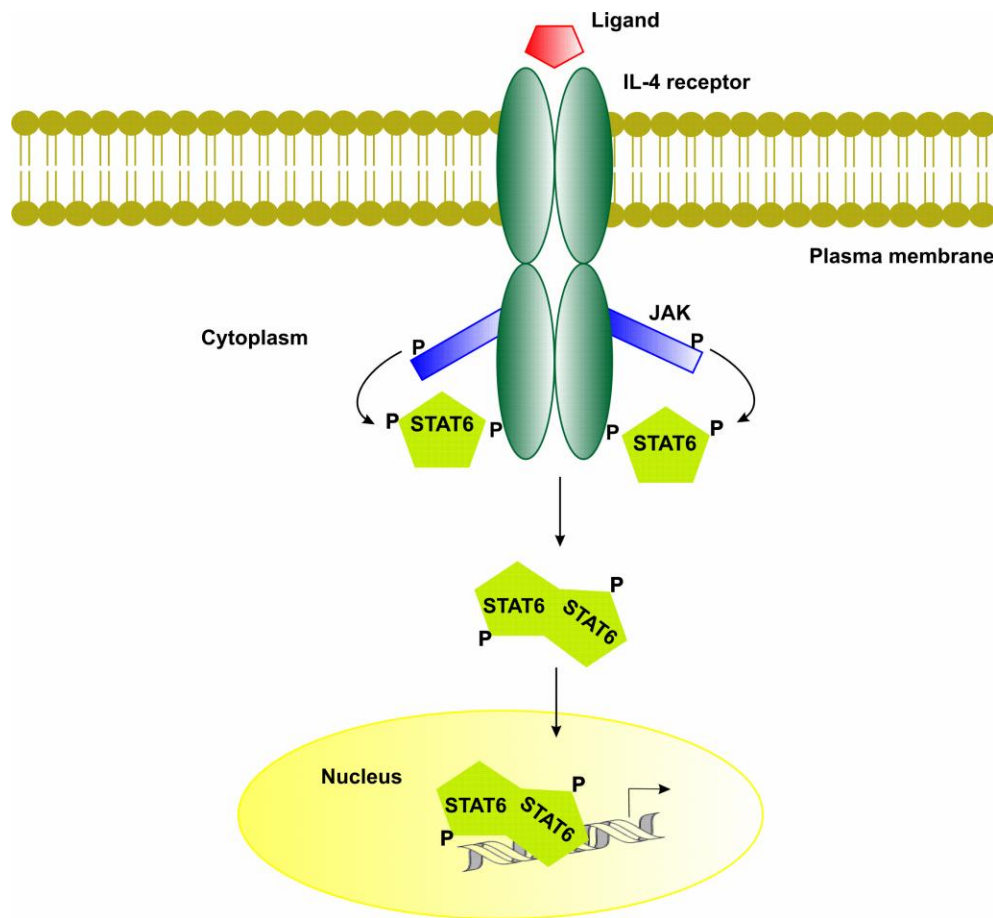


**Figure 1.4:** Scheme describing JAK-STAT6 pathway.

Cytokine ligands such as IL-4 specific for STAT6 bind to its receptor IL-4R activating JAK, which phosphorylates monomeric STAT6 from the cytosol. Upon phosphorylation, STAT6 dimerizes and migrates to nucleus and binds to its specific GAS-DNA to induce transcription of specific genes.

Therefore, nuclear localization is very crucial for STATs. However, STATs are structurally and functionally similar but their localization is distinctly regulated. Nuclear localization signals (NLSs)<sup>52</sup> and nuclear export signals (NESs) are recognized by

## Introduction

---

amino acid sequences on STATs. These signals for import and export of STATs from nucleus to cytoplasm work on post-translation modifications on STATs or their interactions with other proteins, and can alter the conformation of the protein thereby varying its localization. Dephosphorylation of STATs can occur by many phosphatases such as SH2 domain-containing tyrosine phosphatase 1 (SHP1), SHP2, protein tyrosine phosphatase 1B (PTP1B) and others. STATs interact with the specific cofactors to mediate the specificity of their promoters<sup>53</sup>. DNA binding ability of STATs is responsible for gene expression. This mechanism is not fully understood for STATs. It is only known that STATs bind the Gamma-activated sequence (GAS) motif whose consensus sequence is TTC (N)<sub>2-4</sub> GAA with N denoting any nucleotide.<sup>54-58</sup>

The inhibition of STAT dimerization in a cellular context is regulated by cytokine-inducible SH2-containing protein (CIS), suppressor of cytokine signaling (SOCS)<sup>59-61</sup>, JAK binding protein (JAB), STAT-induced STAT inhibitor (SSI), protein inhibitor of activated STAT (PIAS)<sup>62</sup>, by phosphatases, or by protein degradation via the ubiquitin-proteasome pathway. Direct targeting of STAT domains is of great interest in molecular therapies that can directly inhibit the dimerization of STAT and modulate the interaction of STAT with other proteins. From a pharmaceutical point of view, STATs are very attractive targets since the lack of responsiveness and resistance to existing drugs, delivery problems and manufacturing costs make the search for new anti-inflammatory agents necessary. As STATs possess transcriptional activity only after dimerization, hence blocking of this event can prevent the STAT mediated transcription of STAT target genes. Peptidomics have been used to achieve inhibition of STAT3 activity in tumor cells by using S3I-201 as an inhibitor<sup>63,64</sup>.

### 1.1.4 STAT6

Work in this thesis has been performed solely on STAT6 which has similar domains as STAT1 (figure 1.2, B). However, no 3-D structure of STAT6 is available until now. The only information obtainable was from NMR studies which have been carried out to show its interaction with NF-Kappa  $\beta$ <sup>65-67</sup>. Tyr<sup>641</sup> is the crucial phosphorylation site in STAT6,

## Introduction

present in the C-terminal region of the TAD. STAT6<sup>68-70</sup> mediates a multitude of action produced from the signal of interleukins (IL-4 and -13) which are relevant to pathogenesis of allergic disease, airway hyper responsiveness (AHR), eosinophilic inflammation<sup>71,72</sup>, mucus production of late phase allergic responses of mast cells<sup>73</sup>,<sup>74,75</sup> (figure 1.5).

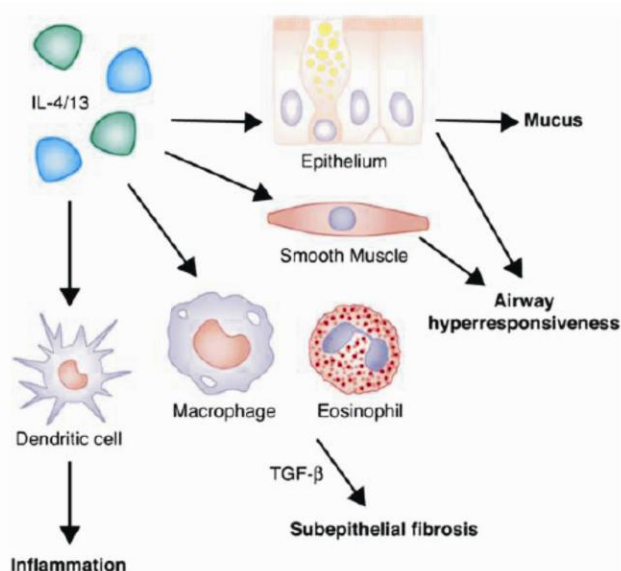


**Figure 1.5: Interleukin (IL-4) and Interleukin (IL-13) responsive diseases<sup>76</sup>.**

IL-4/13 affects various cells such as dendritic cells causing inflammation, eosinophil and macrophages through TGF- $\beta$  causing sub epithelial fibrosis, smooth muscle epithelial cells causing airway hyper responsiveness.

STAT6 is also found in cancerous cells<sup>77-79</sup> and hence is a good target for molecular cancer therapy. Phosphorylated STAT6 has been found in patient samples isolated from prostate cancer tissues, Hodgkin lymphomas<sup>80,81</sup>. The mechanism that leads to increase in STAT6 activation in tumors is still not very clear hence more knowledge has to be gained at its molecular level.

There are four naturally occurring isoforms of STAT6 (STAT6a, STAT6b, STAT6c and STAT6d) which compete with the STAT6 signaling. The phosphorylation and dephosphorylation<sup>82,83</sup> of STAT6 at Tyr<sup>641</sup> has been studied in many cell based experiments. IL-4 binding to its IL-4R $\alpha$  receptor and IL-13 binding to its IL-13R $\alpha$ 1 and

## Introduction

---

IL-13R $\alpha$ 2 causes many phosphorylation events in the cell by which JAK1 and JAK3 (both JAK linked with IL-4R $\alpha$ ) are phosphorylated as explained above (section 1.1.3) leading STAT6 to phosphorylate and dimerize. This is a key event as STAT6 upon dimerization carries the signal from cytokines (IL-4 and -13) to the nucleus and transcribes the specific genes which are responsible for fatal diseases such as cancer and inflammatory diseases such as asthma (figure 1.4). There are still unanswered questions about the STAT6 nuclear import and export and the significance of their post-translational modifications on C-terminus. Hence, in this thesis a light switchable system that allows to turn STAT6 dimerization (as an activation process) was constructed by combining chemical and biochemical strategies.

### 1.2. Chemical protein synthesis

To study bioactive proteins means to control, at the molecular level, the mechanisms and principles governing their structural and functional properties. In order to investigate bioactive proteins it is necessary to obtain large amount of material to work with, hence various methods to obtain native proteins such as natural sources, heterologous expression and chemical methods were introduced. Obtaining proteins in native state directly from the organism or organs is the most desirable option but the disadvantage of this system is that obtaining an organism of choice and organ with high expression level is rather expensive, difficult and there is no scope of performing any desired modifications to study the proteins. Next choice is heterologous expression where protein can be synthesized in high yield for which a host organism such as bacterial cells, yeast cells or higher eukaryotic cells (mammalian cells and insect cells) has to be selected. Expression of engineered proteins in such cells is well understood but it is extremely difficult with standard expression techniques to generate proteins with desired site-specific modifications or post translational modifications (PTMs)<sup>84</sup> such as to incorporate unnatural amino acids, small fluorescent molecules, pegylations and glycosylations into the protein chain to understand the structure and function of the protein.

## Introduction

---

Chemical synthesis has opened new areas to synthesize proteins in large quantities with high purity. Organic synthesis has helped in generating natural amino acids which can be combined together as per the desired sequence of a peptide from C-terminus to N-terminus by a method known as solid phase peptide synthesis (SPPS)<sup>85-90</sup>. Automated SPPS first introduced by Merrifield increased the speed and efficiency of the peptide synthesis. The SPPS method was a major breakthrough in peptide science, which enabled us to obtain proteins or peptides in higher yield facilitating the understanding of protein-protein interactions and cellular networking on a deeper level by using chemical modification. Peptides are normally synthesized from C- to N-terminus which is opposite to the natural protein synthesis. To synthesize short peptides via SPPS requires  $\alpha$ -protecting amino group which is either base sensitive 9-fluorenylmethoxycarbonyl (Fmoc) or acid sensitive tert-butoxycarbonyl (Boc). On cleavage of Fmoc and Boc groups next protected amino acid with an activated carboxyl group can be coupled to the unprotected resin bound amine. Boc methodology requires HF for final cleavage and release of peptides, which is extremely toxic and not well situated for phospho and glycopeptides whereas Fmoc methodology is an attractive tool to generate these chemically sensitive peptides. Short peptides can be joined together to generate large proteins ~50 kDa by methods such as native chemical ligation (NCL) introduced by *Dawson et. al.*<sup>91</sup> and chemoselective ligation strategies.

### 1.2.1. Native chemical ligation

Native chemical ligation (NCL)<sup>92-96</sup> chemistry involves a chemoselective reaction between a peptide carrying C-terminal thioester ( $\alpha$ -COSR) and a second peptide or protein with N-terminal Cysteine residue. An initial transthioesterification reaction followed by a spontaneous intramolecular S $\rightarrow$ N acyl transfer generates the desired full length peptide with a native peptide bond, which upon successful folding gives the native protein or protein domains (figure 1.6).

The ligation can be carried out in aqueous conditions in the absence or presence of chaotropes such as 6M Guanidine HCl between two unprotected peptide fragments<sup>97,98</sup>.



## Introduction

To prevent the thiol of the N-terminal Cysteine from oxidation, and thus forming an unreactive disulfide linked dimer, it is necessary to add thiols or other reducing reagents like tris-(2-carboxyethyl) phosphine (TCEP) to the reaction mixture. Furthermore, the addition of excess thiol not only keeps the thiol-functions reduced but also increases the reactivity by forming new more reactive thioester through transthioesterification.

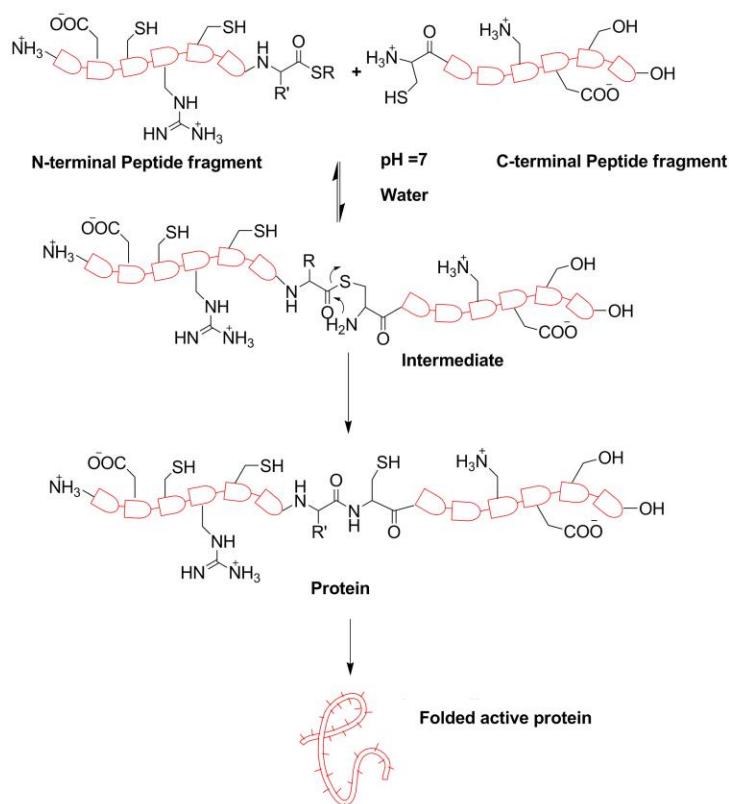


**Figure 1.6: Scheme of Native Chemical ligation.**

The N-terminal peptide segment having C-terminal  $\alpha$ -thioester reacts with its C-terminal portion having an N-terminal Cysteine residue in a native chemical ligation reaction.

The most common strategy of native chemical ligation is described in figure 1.6. Using this chemoselective coupling reaction a fully unprotected synthetic peptide based on the predicted gene sequence ~99 amino acid long peptide of human immune deficiency virus 1 (HIV-1) protease enzyme was generated in Kent Lab<sup>99</sup>, in aqueous solution at pH 7. Many important peptides such as H-Ras<sup>100,101</sup>, erythropoiesis<sup>102</sup>, TASP<sup>103</sup>, glycopeptides synthesis<sup>104</sup> and total chemical synthesis of crambin shown by Bang *et.*

## Introduction

*al.*<sup>105</sup>. Although, NCL is carried out in solution, it has been reported that the same can also be carried out on solid support as well as inside a living cell using cyclic peptides demonstrated by Camarero *et. al.*<sup>106</sup> To obtain thioester by NCL<sup>87</sup> is the key step for synthesizing the desired protein (figure 1.7). Back bone amide linker BAL<sup>107</sup>, safety catcher linker.

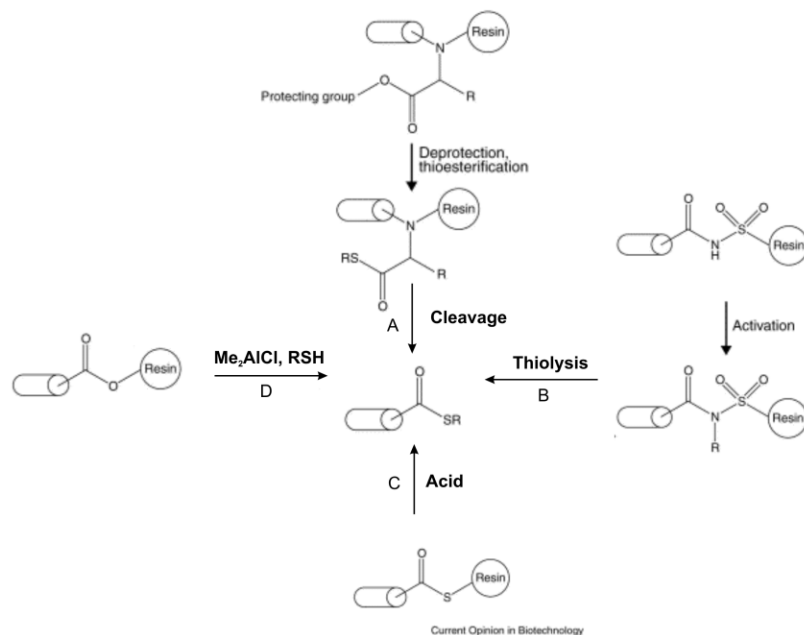


**Figure 1.7: Methods to obtain thioester at C-terminal end of peptide or protein<sup>108</sup>.**

**A.** Protective group cleavage, backbone amide linker<sup>109</sup>. **B.** Thiolysis on peptide, "safety catch" linker<sup>110</sup>.  
**C.** Acidolysis, Lewis acid activated cleavage<sup>111</sup>. **D.** auxiliary methods, mercaptoalkyl linkers<sup>112</sup>

A limitation of NCL method is that at every ligation site an N-terminal Cysteine residue have to be generated hence the use of non-Cysteine residue has been developed based on auxiliary approach<sup>113</sup> in which thiol-containing auxiliaries are used (figure 1.7, D). A second limitation found was that only proteins containing ~150 amino acid residues could be generated since there are enormous challenges remaining to produce larger proteins. The difficulty faced in synthesizing larger peptides was often too many ligations steps and hence purification problems such as the secondary structure formation during synthesis resulting in many by products which are often difficult to separate. Membrane spanning peptides have always been found to be the most challenging peptides to synthesize due to their poor solubility in aqueous solvents.

## Introduction

Recently, the use of lipid bilayer systems and detergents for NCL has been shown to give good NCL efficiencies for membrane peptides and proteins<sup>114,115</sup>.

Various chemoselective ligation strategies are available to understand the spatial and temporal function of protein. These strategies include thioester-forming ligation<sup>116</sup> (figure 1.8, A), thioether-forming ligation<sup>117</sup> (figure 1.8, B), oxime-forming ligation<sup>118,119</sup>, (figure 1.8, C), thiazolidine-forming ligation<sup>120</sup> (figure 1.8, D), copper (I)-catalyzed [3+2] cycloadditions of an azide and an alkyne to form a triazole structure, termed as “click-” chemistry<sup>121</sup> (figure 1.8, E) and Staudinger ligations (figure 1.8 F).

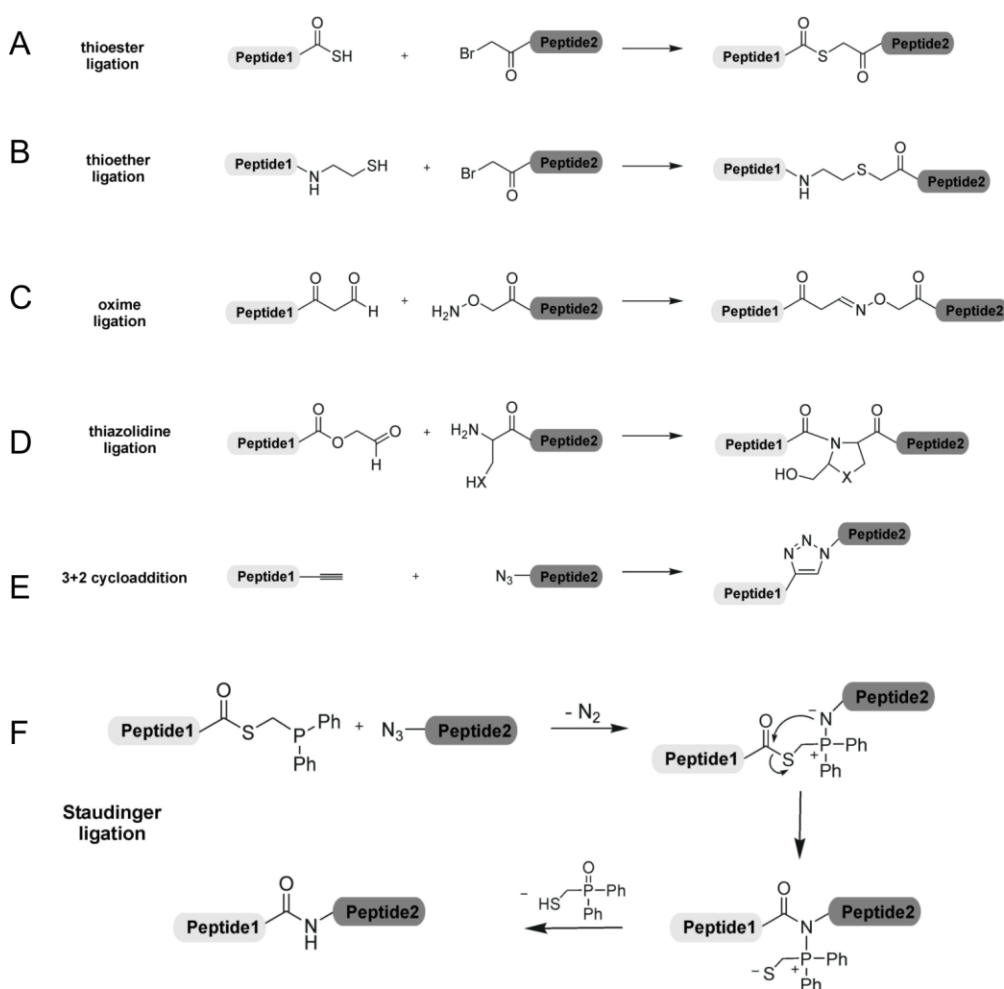


Figure 1.8: Different chemoselective ligation strategies (A-F) are useful for generating small proteins and protein domains<sup>122</sup>

### 1.2.2. Expressed protein ligation

Expressed protein ligation (EPL)<sup>123-130</sup> is a highly useful extension of native chemical ligation (NCL). Combining the two approaches of recombinant expression of protein and SPPS it is possible to make a modification on a specific domain of even very large protein. The main advantage of EPL over total chemical synthesis of protein is that it does not limit the size of the protein. EPL requires an  $\alpha$ -COSR at the C-terminal of the recombinant protein and N-terminal Cysteine at the synthetic peptide building blocks. DNA mutagenesis techniques are used to generate the recombinant protein with an intein fusion which is expressed in bacterial. *Mycobacterium xenopi* DNA gyrase A (*Mxe GyrA*)<sup>131,132</sup> or *Saccharomyces cerevisiae* vacuolar ATPase (*Sce VMA1*) are some of the common inteins which are self-splicing protein fragments. Protein splicing involves the removal of the intein from a precursor protein and the ligation of the two flanking sequences to produce a mature protein.

The fusion protein can be bound to the affinity resin (chitin beads) where the developing  $\alpha$ -COSR can be trapped with small molecule thiols, thus eluting the recombinant protein with a C-terminal  $\alpha$ -COSR leaving the intein protein on the affinity resin (figure 1.9). Various molecules are used as thiols for protein splicing reactions e.g.  $\beta$ -mercaptoethane sulphonic acid (MesNa) and thiophenol. A C-terminal  $\alpha$ -COSR, which is generated on the recombinant protein, undergoes initial reversible transthioesterification reaction followed by spontaneous irreversible S $\rightarrow$ N acyl shift with the N-terminal  $\alpha$ -Cysteine of the synthetically modified peptide to obtain the desired semisynthetically modified full-length protein (figure 1.9).

## Introduction

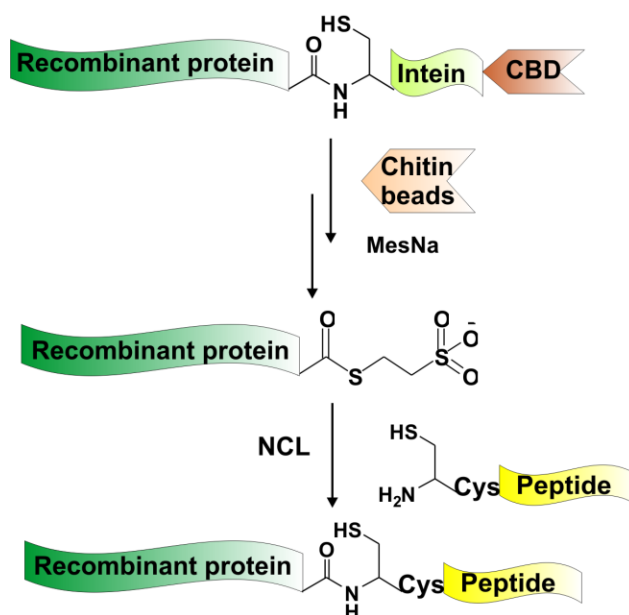


**Figure 1.9: Scheme of Expressed protein ligation.**

Expressed protein ligation deals with the expression of recombinant protein with an intein fusion protein which undergoes a transthioesterification reaction to generate  $\alpha$ -thioester at its C-terminal followed by native chemical ligation to bind with the desired peptides having free  $\alpha$ -Cys.

EPL has been used to investigate several important proteins: Muir *et al.* synthesized a semisynthetic C-terminal Src kinase (Csk) protein (50 kDa) that catalyzes the phosphorylation of a highly conserved tyrosine within the C-terminal tail of Src family. This modification results in an intramolecular interaction between the Src homology 2 (SH2) domain and the C-terminal phosphotyrosine within Src, this association leads to a significant conformational change and catalytic repression *in vivo*. Hence, Csk which lacks the C-terminal activating tyrosine-containing loop, as well as an N-terminal myristoylation site. An extension of CsK was carried out by semisynthetic strategy to observe the conformation and catalytic behavior. Phosphorylated semisynthetic terminus of Csk showed evidence of an intramolecular phosphotyrosine-Src homology 2 interactions and an unexpected increase in catalytic phospho transfer efficiency towards a physiologically relevant substrate compared with the terminus which lacked phosphorylation as a control. Human interleukin (IL) -8, a neutrophil-activating and chemotactic cytokine, known to play an important role in the pathogenesis of a large number of neutrophil-driven inflammatory diseases was first time generated by

## Introduction

---

semisynthesis and was found to be active. Several important proteins such as Smad-2<sup>133,134</sup>, Rab7GTPases<sup>135,136</sup> and protein phosphatase<sup>137</sup> have been modified using EPL.

EPL has also been reported for ligation of two recombinant proteins and the positions that should be modified. Depending on the size of the protein of interest, number of ligation sites can be increased. Several groups have also shown that inteins can be cut into two pieces, which individually have no activity but upon combination give rise to an active intein. The splicing process of these inteins is known as protein-trans splicing. Thus, EPL has been successfully used to investigate protein-protein interactions, isotopic labeling<sup>138</sup>, protein cyclization<sup>139,140</sup>, incorporation of unnatural amino acids and cytotoxic proteins<sup>141</sup> and many more. Many bioactive proteins such as protein phosphatase<sup>142</sup>, ion channels<sup>143,144</sup>, labeled dihydrofolate reductase<sup>145</sup> have been synthesized. Caged compounds<sup>146</sup> have also been used to control EPL reactions.

### 1.2.3. Caged compounds

Caged compounds<sup>147-149</sup> have been introduced in cell biology, molecular physiology, and pharmacology since Kaplan *et. al.* developed caged ATP in 1978<sup>150,151</sup>. Caging a molecule of interest renders it biologically inert by chemical modification with a photo removable group. Caging the biological molecule facilitates in studying the inert (or caged) state of the molecule which upon uncaging their active state. Caged ATP, GTP, neurotransmitters, second messengers, inhibitory peptides, enzymes and fluorescent dyes have been widely studied using this approach.

The caging groups are generally small molecules such as 2-nitrobenzyl which can be covalently attached to polar groups in a biologically relevant substances rendering them inactive. These photolabile protecting groups are rapidly cleaved upon exposure to UV light (depending on light intensity), hence it is a very useful tool to study fast reactions and processes (figure 1.9, A). Studies with caged compounds have revealed spatial and temporal information inaccessible by other methods. The absolute speed for uncaging depends on the application but is generally faster than cellular processes. Applying

## Introduction

---

caged compounds to investigate signal transduction cascades in a biological system, such as, by constructing switchable STAT6 by caging their phosphorylation site to see their monomeric behavior and upon decaging of the caged group their dimeric behavior can open new areas to understand protein-protein interactions of STAT6.

Light sources used for uncaging can be flash lamps (xenon or mercury lamps) or lasers. Quantification of the uncaging reaction *in situ* is often very challenging and requires fluorophore conjugation. To explore the cell adhesion events, cell adhesive (RDG) peptides that promote integrin<sup>152</sup> mediated cell adhesion were prepared by Svea Petersen *et. al.*, 2008<sup>153</sup> which showed no integrin binding activity in their caged form, however, on illumination with UV light decaged RGD effectively mediated cell adhesion to surfaces with spatiotemporal precision. Caged phosphopeptides<sup>154-158</sup> are recently being studied to investigate the key phosphorylation in cellular process. Photochemical gated Ca<sup>2+</sup> channels<sup>159,160</sup> have been generated recently.

Caged compounds attached to the peptides or proteins<sup>161</sup> can be brought into to the cell by various methods like microinjection, patch pipette, passive diffusion, cell penetrating peptides (CPPs)<sup>162</sup> and detergent membrane permeabilization. Microinjection<sup>163,164</sup> is one of the fastest method to load the peptides or proteins into the cells there by giving a wide platform to study the inactive form of the biological molecule. The only disadvantage is the expensive equipment that is required and laborious practice to master the technique and relatively small number of cells that can be microinjected.

## Introduction

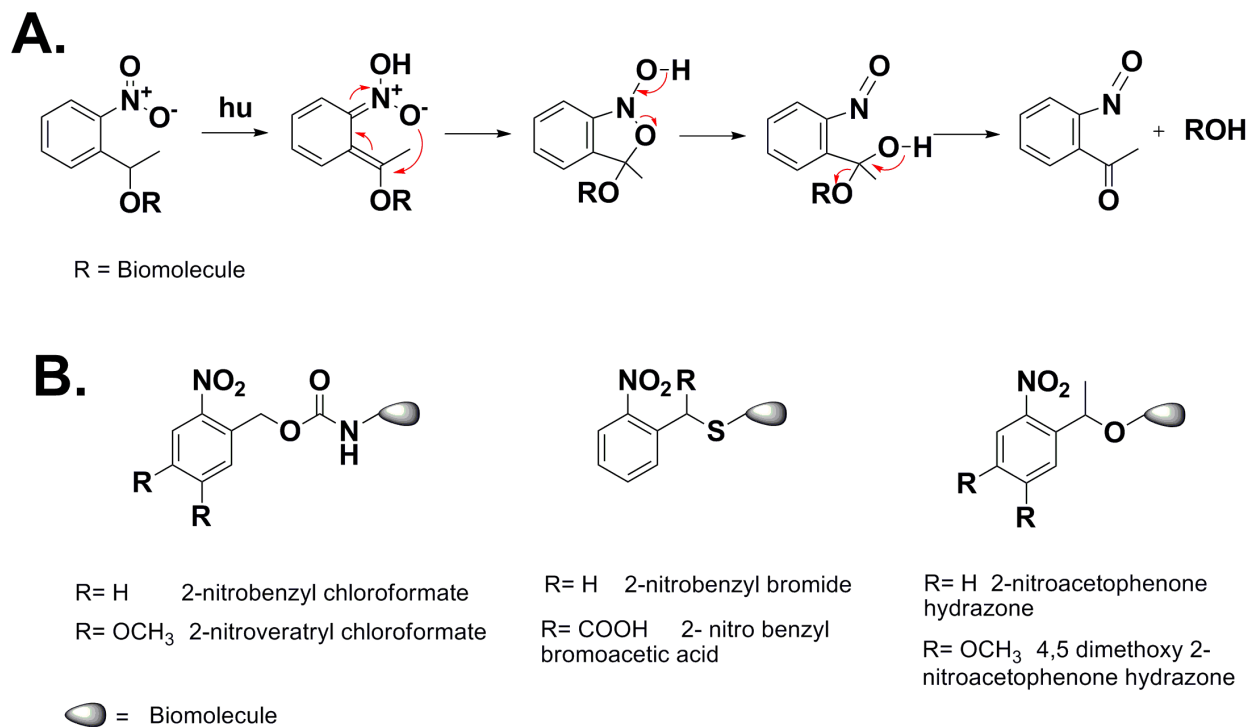


**Figure 1.10: Mechanism of light induced removal of caged group<sup>165</sup>.**

**A:** Scheme of photolysis of caged compounds. **B:** Examples of functional groups that can be caged.

Caged molecules can be attached to peptides and proteins by three different techniques, by using chemical synthesis<sup>166</sup> or SPPS<sup>167</sup>, nonsense codon suppression techniques<sup>168,169</sup>. Chemical modification can be carried out by different methods depending on the side chains. Amino groups in peptide or proteins can be modified with chloroformate or chlorocarbamate and the urethane bond can be cleaved off by UV irradiation (figure 1.10 A and B). Thiol groups in peptides and proteins can be modified by 2-nitrobenzyl bromide. Pan *et. al.*, 1997<sup>170</sup> used this method to prepare a caged derivative of C-kemptide which is a substrate of cyclic AMP-dependent protein kinase. Carboxyl groups in peptides or proteins can be modified with diazo-derivatives. SPPS enables to make caged peptides in a straightforward method in larger scales by using Fmoc- and Boc- amino acids derivatives. NCL methods have been used extensively to incorporate Fmoc-amino acid derivatives of Tyrosine<sup>158</sup>, Threonine and Serine<sup>171</sup> containing photolabile group which can be easily prepared and incorporated in the peptide sequence. Muir *et. al.*, demonstrated the activity of Smad-2<sup>172,173</sup> (~50 kDa) in



## Introduction

live cells by using semisynthetic protein chemistry to generate caged Smad-2 a cellular signaling protein. Smad-2 is phosphorylated on two C-terminal serine residues by TGF $\beta$  receptor. This event is the key step in Smad-2 activation, and results in accumulation of Smad-2 in the nucleus where it acts as a transcription factor to modify expression of hundreds of target genes.

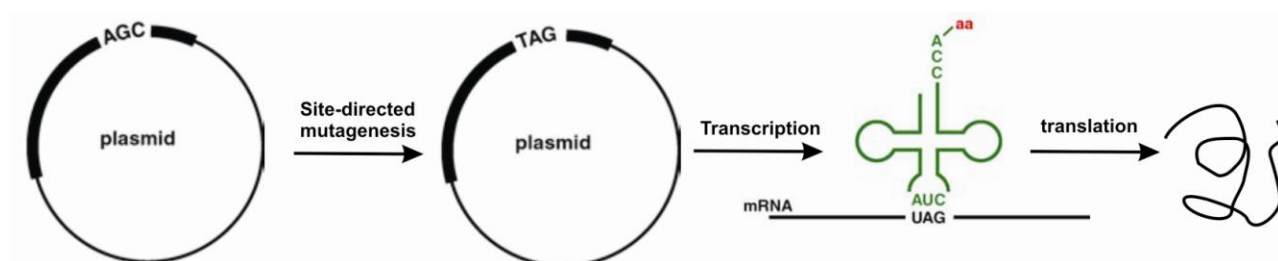


**Figure 1.11:** Nonsense codon suppression methodology to insert unnatural amino acid into proteins.<sup>174</sup>

Nonsense codon suppression technique<sup>175</sup> is the most critical method to generate caging on peptides or proteins. This method involves incorporating a non sense mutation into the sequence encoding the amino acid of interest (figure 1.11). Caged protein is synthesized by an *in vitro* or *in vivo* translation system. Caged lysozyme (T4L) containing an aspartyl  $\beta$ -nitrobenzyl ester in the active site was generated by Schulz group using this method. T4L is a stable, well-characterized enzyme whose lysis of *E. coli* provides a convenient and sensitive assay for catalytic activity. To accomplish this, an amber mutant (D20-TAG) of T4L was constructed and suppressor tRNA linked to nitrobenzyl aspartic acid was synthesized. Using an *in vitro* translation system, caged protein was synthesized, that was catalytically active upon exposure to UV irradiation (figure 1.11). Caged neurotransmitters and caged second messengers have been utilized to study fast and local biological processes such as synaptic neurotransmission.

# Chapter 2

---

Aim

## 2.1. Aim of the project

The aim of this thesis was to generate a light switchable system which turns STAT6 dimerization (activation process) and visualize it's *in vivo* localization. It was previously identified that misregulations in JAK-STAT pathway can increase STAT6 activation leading to diverse kinds of diseases such as cancer and asthma . Therefore, any method to deactivate STAT6 can open new understanding of their behavior at a molecular level to enhance knowledge on formulating future therapeutic applications.

### Semisynthesis strategy for C-terminally truncated STAT6

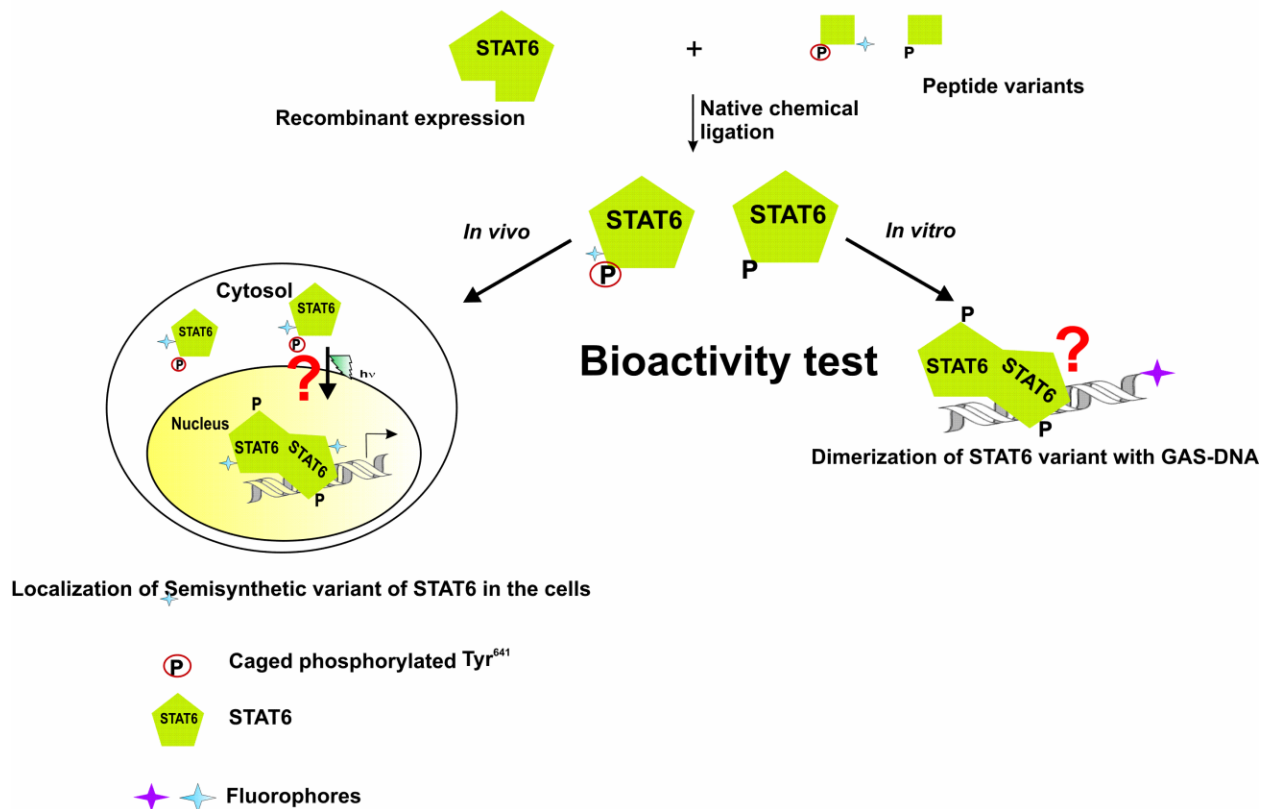


**Figure 2.1: Aim of the project**

Semisynthetic truncated STAT6 generated by using expressed protein ligation (EPL) can help in understanding the posttranslational modifications at its C-terminus and bioactivity should be demonstrated by microinjection, EMSA and FRET experiments.

## Aim

---

It was hypothesized that a semisynthetic caged phosphorylated STAT6 can only form dimer upon irradiation with UV light in view of the fact that STAT6 is biologically active only upon phosphorylation. Such semisynthetic truncated caged phosphorylated STAT6 should move to the nucleus and not bind to GAS-DNA whereas the semisynthetic phosphorylated variants should mimic the known physiological behavior. The idea was to employ chemical synthesis for carrying out phosphorylation of STAT6, which is performed by JAK in a physiological environment.

To investigate the bioactivity of semisynthetic truncated STAT6 protein variants, novel techniques of expressed protein ligation (EPL), solid phase synthesis (SPPS), organic synthesis, tissue culture have been used. Organic synthesis can be applied to synthesize the caged phosphorylated tyrosine, which can subsequently be incorporated into a C-terminal of STAT6 peptide obtained by SPPS. The large N-terminal fragment can be obtained by expressing the protein with an intein fusion protein in bacterial cells. To visualize semisynthetic STAT6 variants in cell based experiments, fluorophore such as Cy5 can be incorporated at the C-terminal fragment of the protein instead of large natural fluorophores such as GFP or CFP. Thus, EPL can be used to explore the spatio-temporal aspect of pharmaceutically important large proteins such as STAT6 by controlling its site-specific post-translational modifications and bioactivity. The challenging part would be to build such a large protein, which requires several steps of chemical, and biochemical synthesis and further to judge, the bioactivity of such a post translationally modified protein.

Bioactivity of semisynthetic truncated STAT6 variant can therefore be investigated by using sophisticated cell based (*in vivo*) methods such as microinjection followed by photolysis experiments to mimic the physiological activity of STAT6. Similarly *in vitro* studies on semisynthetic STAT6 were designed based on western blotting, electrophoretic mobility shift assay (EMSA) and fluorescent resonance energy transfer (FRET) principles.

# Chapter 3

---

Materials and methods

## 3.1. Materials and instruments

### 3.1.1 Materials

#### Chemicals:

Sigma (Steinheim), Aldrich (Heidenheim), Fluka (Neu-Ulm), Baker (Groß-Gerau), Bio-Rad (Munich), Merck (Darmstadt), Roth (Karlsruhe), Applied Bioscience (Berlin) and Serva (Heidelberg).

#### Biological materials:

Ni-NTA superflow

Oligonucleotides

Plasmid

6 x Orange G

Low molecular weight marker

High molecular weight marker

Dialysis kit

Dialysis tube

Silver staining kit

Centricons

Mattrek dishes

Microinjection needles

Nitrocellulose paper

Quartz cuvette (5 µl, 12 µl, 1 cm)

#### Suppliers

Qiagen, Hilden, DE

Eurofins MWG, Ebersberg, DE

New England Biolabs, Frankfurt, DE

Fermentas, St. Leon Rot, DE

Amersham Pharmacia Biotech,  
Freiburg, DE

Invitrogen, Karlsruhe, DE

Pierce

Spectrum (Gardena, CA, USA)

Pierce

Amicon-Milipore, Schwalbach, DE

Matrek Corporations, USA

Eppendorf AG, Hamburg, DE

Schleicher & Schull (Dassel, DE)

Hellma Optik GmbH, Jena, DE

## Materials and Methods

---

### 3.1.2 Instruments and suppliers

#### Instruments

HPLC

ÄKta prime system with REC112

Recorder (FPLC)

Spex Fluoromax-3 spectrofluorometer

UV/Visible-spectroscopy

HPLC-ESI-MS

MALDI

FLA-5000 (fluorescence image reader) Fujifilm, Japan

NMR

$^1\text{H}$  (400 MHz),  $^{13}\text{C}$  (100.6 MHz)

$^1\text{H}$  (500 MHz),  $^{13}\text{C}$  (125.8 MHz)

PH-meter 761

Sephadex columns

Rotors SS-34

Cell harvesting, Avanti J-20 XP

Centrifuge, JLA 8.1 000 rotor

Centrifuge 5415C/D benchtop

Cell lysis in Microfluidizer

Ultra sonic cell disruptor (SONIFER)

Gel electrohoris system

#### Suppliers

Systems Gold and Waters, Beckman  
coulter Palo Alto, CA, USA

Äkta, Munich, DE

Jobin Yvon Horiba Group (NJ, USA)

Beckman Coulter (Palo Alto, USA)

LCQ, Finnigan, Bremen, DE

Voyager-DE Pro Biosystems,  
Weiterstadt, DE

Bruker DRX 400

Bruker DRX 500

Calimatic knick ,Berlin, DE

Amersham Pharmacia Biotech, Freiburg

Sorvall, Bad Homburg

Beckman coulter Palo Alto, CA, USA

Beckman coulter Palo Alto, CA, USA

Eppendorf, Hamburg, DE

M-110, Microfluidics Corporation,  
Newton, MA, USA

Branson (Danbury, CT, USA)

Biorad (Munich, DE)

## 3.2. Chemical Methods

### 3.2.1 Synthesis of caged phosphorylated tyrosine building block

Solution phase synthesis over 5 steps yielded a caged phosphorylated tyrosine building block. All procedures are based on from Rothman *et. al.* 2003<sup>176</sup>

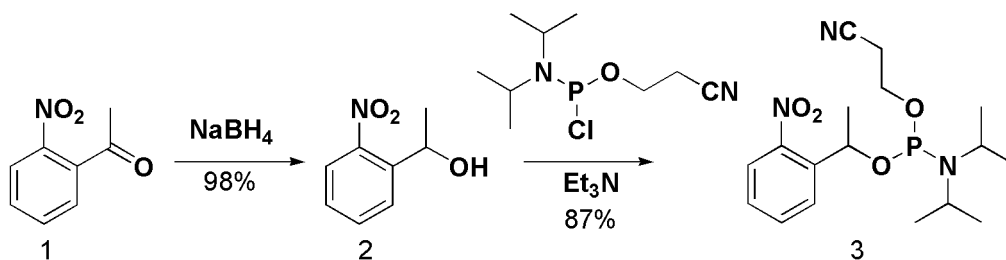


Figure 3.1. Synthesis of (3)

### 3.2.2 1-(2-nitrophenyl) ethanol (*NPE-OH*) (2)

2-nitroacetophenone (**1**) was added to (1.0 g, 6.05 mmol) in 14.4 ml of methanol/dioxane (3:2) (v/v) in a dry round bottom flask Sodium borohydride (687 mg, 18.17 mmol) was added slowly and stirred at 0°C for 20 min. The mixture was allowed to stir for 2.5 h at room temperature (progress monitored by TLC in chloroform). The reaction was quenched by addition of 50 ml of water and stirring at room temperature for 30 minutes. The mixture was extracted with chloroform (3 x 30 ml), the organic phase was dried over sodium sulfate and concentrated under reduced pressure. The alcohol was dried in vacuum over night to give yellow oil, 990.9 mg (97.9%).

<sup>1</sup> H NMR (500 MHz, CDCl<sub>3</sub>) δ (ppm): 7.7 (d, J<sub>HH</sub>= 8 Hz, 1H); 7.64 (d, J<sub>HH</sub>= 8 Hz, 1 H); 7.48 (t, J<sub>HH</sub>= 8 Hz, 1 H); 7.26 (t, J<sub>HH</sub>= 7 Hz, 1 H); 5.23 (q, J<sub>HH</sub>=7 Hz, 13 Hz, 1 H); 3.95 (s, 1 H); 1.35 (d, J<sub>HH</sub>=7 Hz, 3 H).

<sup>13</sup> C NMR (500 MHz, CDCl<sub>3</sub>) δ (ppm): 141.21; 133.80; 128.26; 127.74; 127.74; 124.43; 65.7, 24.5



## Materials and Methods

---

### 3.2.3 O-1-(2-nitrophenyl)ethyl-O'- $\beta$ -cyanoethyl-N,N-diisopropylphosphoramidite (**3**)

2-cyanoethyl diisopropyl chlorophosphoramidite (471  $\mu$ L, 2.11 mmol) in 1.7 ml of dry DCM was added to solution of (**2**) (294 mg, 1.76 mmol) in freshly distilled triethylamine (589  $\mu$ L, 4.23 mmol) and 8.8 ml of dry DCM at room temperature in the dark. The reaction was monitored by the disappearance of (**2**) by TLC in methanol/ chloroform/ water 65:25:4 (v/v). The reaction mixture was washed twice with 10% NaHCO<sub>3</sub> solution (30 ml). The organic layer was then dried over Na<sub>2</sub>SO<sub>4</sub> and concentrated under reduced pressure. The product was dried in vacuum overnight to give dark yellow oil, (392 mg), 98% yield.

<sup>1</sup>H NMR (500 MHz, CDCl<sub>3</sub>)  $\delta$  (ppm): 7.8 (m, 1 H); 7.5 (m, 1 H); 7.3 (m, 2 H); 5.4 (m, 1 H); 3.7 (m, 2 H); 3.5 (m, 2 H); 2.5 (m, 2 H); 1.5 (m, J<sub>HH</sub>= 5 Hz, 7 Hz, 3 H); 1.2 (m, 12 H).

<sup>31</sup>P NMR (400 MHz, CDCl<sub>3</sub>)  $\delta$  (ppm): 148.2 (d, J<sub>HH</sub>=61); 15.0

## Materials and Methods

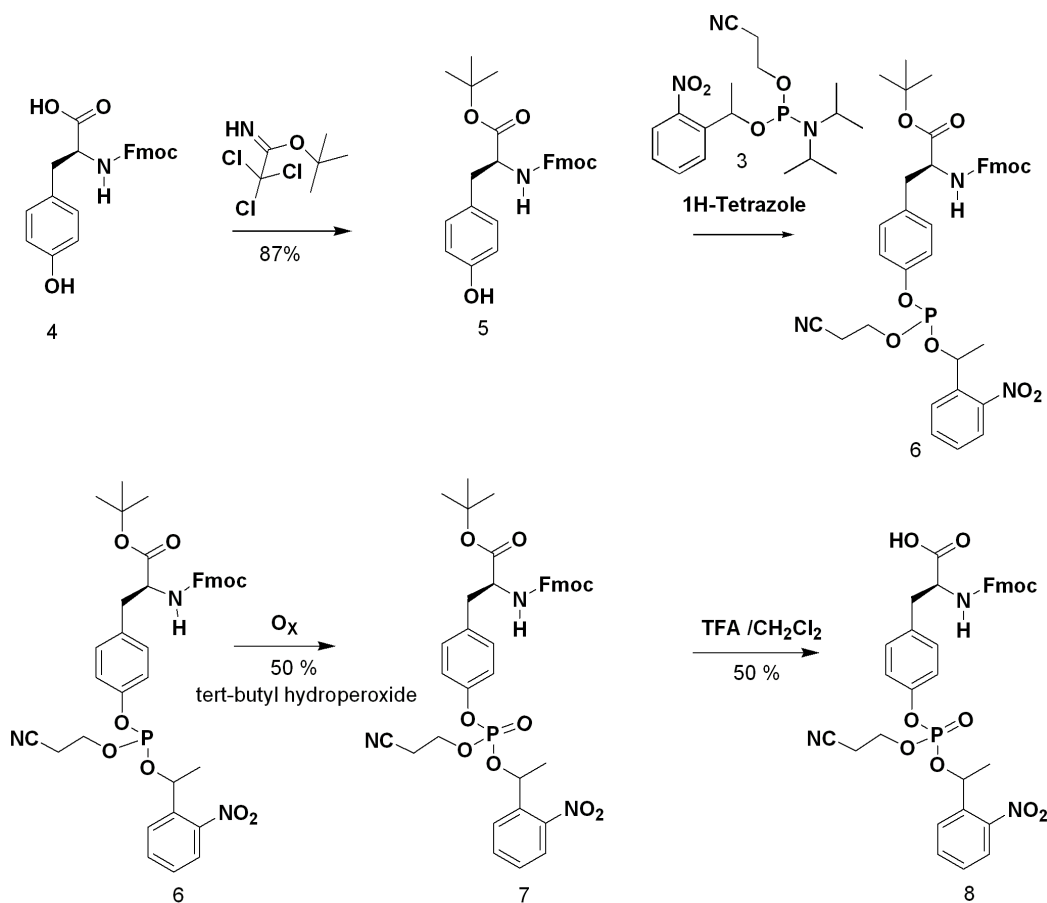


Figure 3.2. Synthesis of caged phosphorylated tyrosine (8)

### 3.2.4 N- $\alpha$ -Fmoc-L-tyrosine *tert*-butyl Ester (5)

N- $\alpha$ -Fmoc-L-tyrosine (**4**) (440 mg, 1.10 mmol) was added in a dry 25 ml round-bottom flask in DCM/THF (4 ml, 4:1) (v/v) and cooled to 0°C under argon, and *tert*-butyl trichloroacetimidate (720 mg, 3.28 mmol) was added to the resulting solution. The reaction mixture was allowed to stir overnight at room temperature. DCM (100 ml) was added, and the solution was washed with 2.5%  $NaHCO_3$  (2 x 50 ml). The organic layer was dried with  $Na_2SO_4$  and concentrated. The residue was purified by flash column chromatography (1:1 EtOAc/hexanes) to give the desired product as a sticky solid (342 mg) in 68% yield.

## Materials and Methods

---

**<sup>1</sup>H NMR (400 MHz, CDCl<sub>3</sub>) δ (ppm):** 7.7-7.6 (d,  $J_{\text{HH}} = 7$  Hz, 2 H); 7.5-7.4 (m, 2 H); 7.3 (m, 2 H); 7.2-7.3 (m, 2 H); 6.9-7.0 (d,  $J_{\text{HH}} = 8$  Hz, 2 H); 6.67- 6.65 (d,  $J_{\text{HH}} = 8$  Hz, 2 H); 4.4-4.2 (m, 3 H); 4.13 (m, 1 H); 2.9 (m, 2 H); 1.5 (s, 1 NH); 1.3 (d, 9 H).

**<sup>13</sup>C NMR(500 MHz, CDCl<sub>3</sub>) δ (ppm):** 171.0; 155.8; 155.0; 144; 141.0; 141.5; 130,8; 128.1; 127.9; 127.3; 125.3; 120.1; 115.5; 82.6; 67.1; 55.5; 47.4; 37.8; 28.2

**ESI-MS:**  $[\text{M} + \text{Na}]^+_{\text{obs}}$  : 482.13 ,  $[\text{M} + \text{H}]^+_{\text{cal}}$ : 459.13

### 3.2.5 N- $\alpha$ -Fmoc-phospho (1-nitrophenylethyl-2-cyanoethyl)- L-tyrosine *tert*-butyl ester. (7)

(**5**) (440 mg, 0.96 mmol) was dissolved in dry THF (4 ml) in a round bottom flask provided with 4 Å molecular sieves (400 mg). In a separate flask (**3**) was dissolved (600 mg, 1.63 mmol) in 1H-tetrazole in 98% acetonitrile (115 mg, 1.63 mmol) and dry THF (4 ml). After 5 min activation the mixture was added to the Fmoc- L-tyrosine *tert*-butyl ester solution, and the resulting mixture was allowed to stir in the dark for overnight under argon. The reaction mixture was filtered over Celite and concentrated under reduced pressure, and the residue was redissolved in DCM (25 ml) and washed with 1% NaHCO<sub>3</sub> (2 x 25 ml). The combined organic layers were dried over Na<sub>2</sub>SO<sub>4</sub> and concentrated under reduced pressure. The oily residue was redissolved in dry DCM (25 ml), and *tert*-butyl hydroperoxide was added drop wise to the solution (300  $\mu$ L of 5 - 6 M solution in decane). The reaction was stirred for 1 h at room temperature and then washed with 2% NaHCO<sub>3</sub> (2 x 50 ml). The organic layer was dried with Na<sub>2</sub>SO<sub>4</sub> and concentrated under reduced pressure. The resulting residue was purified by flash column chromatography (1:1 hexanes/ EtOAc) (v/v) to give the product (442 mg) in 63% yield.

**<sup>1</sup>H NMR (400 MHz, CDCl<sub>3</sub>) δ (ppm):** 7.9-7.4 (m, 7 H); 7.33 (t, 2 H); 7.26 (t, 2 H); 7.24 (t, 2 H); 7.22 (t, 2 H); 7.0 (d, 1 H); 6.94-6.96 (d, 1 H); 6.97-6.99 (d,  $J_{\text{HH}} = 5$

## Materials and Methods

---

Hz, 8 Hz, 1 H); 6.2 (m, 1 H); 4.1-4.0 (m, 6 H); 2.9 (m, 2 H); 2.55-2.50 (m, 2 H); 1.66-1.68 (m, 3 H); 1.35 (s, 9 H).

**<sup>13</sup>C NMR (400 MHz, CDCl<sub>3</sub>) δ (ppm):** 170.5; 155.7; 149.2; 147.0; 144.0; 143.9; 141.5; 137.0; 134.1; 133.0; 131.10; 129.2, 129.1; 127.9; 127.8; 127.2, 125.3; 124.7, 120.1; 120.0; 119.9; 116.2; 82.8; 74.0; 67.0; 62.7; 55.2; 47.4; 37.7; 28.2; 24.4; 19.7.

**<sup>31</sup>P NMR (400 MHz, CDCl<sub>3</sub>) δ (ppm):** 7.93 ;7.85; -7.077; -7.140; -7.140.

**ESI-MS:** [M+ Na]<sup>+</sup><sub>obs</sub> : 764.13 [M+H]<sup>+</sup><sub>cal</sub>: 741.13

### 3.2.6 N-α-Fmoc-phospho (1-nitrophenylethyl-2-cyanoethyl)-L-tyrosine (8)

(7) (440 mg, 590 μmol) was dissolved in dry DCM (8 ml) in a 25 ml round-bottom flask, and the solution was cooled to 0°C. TFA (8 ml) was slowly added to the solution, and the reaction mixture was allowed to stir in the dark for 1 h at room temperature under argon. The solvents were removed under reduced pressure, and the residue was redissolved in chloroform and concentrated again to eliminate any residual TFA. The residue was purified by flash column chromatography (1% AcOH/5% MeOH/DCM) (v/v) to give the product (8) (329 mg) in 50% yield.

**<sup>1</sup>H NMR (500MHz, CDCl<sub>3</sub>) δ (ppm):** 8.4 (br, s, 1 H); 7.8 (d, J<sub>HH</sub>= 8 Hz, 1 H); 7.6 (m, 3 H); 7.5-7.4 (m, 3 H); 7.3-7.2 (m, 3 H); 7.17-7.19 (m, 2 H); 6.9 (m, 4 H); 6.1 (m, 1 H); 5.4 (m, 1 H); 4.52 (s, 1 H) ; 4.34 (s, 1 H); 4.25 (s, 2 H); 4.0 (s, 2 H); 3.0 (m, 2 H); 2.50 (m, 2 H); 1.64 (dd, J<sub>HH</sub>= 2 Hz, 6 Hz, 3 H).

**<sup>13</sup>C NMR (400 MHz, CDCl<sub>3</sub>) δ (ppm):** 177.8, 156.0, 149.1, 146.9, 143.9, 141.5, 136.8, 134.2, 134.1, 131.1, 129.2, 127.9, 125.2, 124.7, 120.2, 120.15, 120.1, 116.2, 74.3, 67.2, 63.0, 54.9, 47.3, 37.2, 24.3, 20.9.

**<sup>31</sup>P NMR (400 MHz, CDCl<sub>3</sub>) δ (ppm):** -7.74.

**ESI-MS:** [M+Na]<sup>+</sup><sub>obs</sub>: 708.13, [M+H]<sup>+</sup><sub>cal</sub>: 685.13

### 3.2.7 Synthesis of Cy5-NHS and coupling to the $\epsilon$ - amino group of Lysine

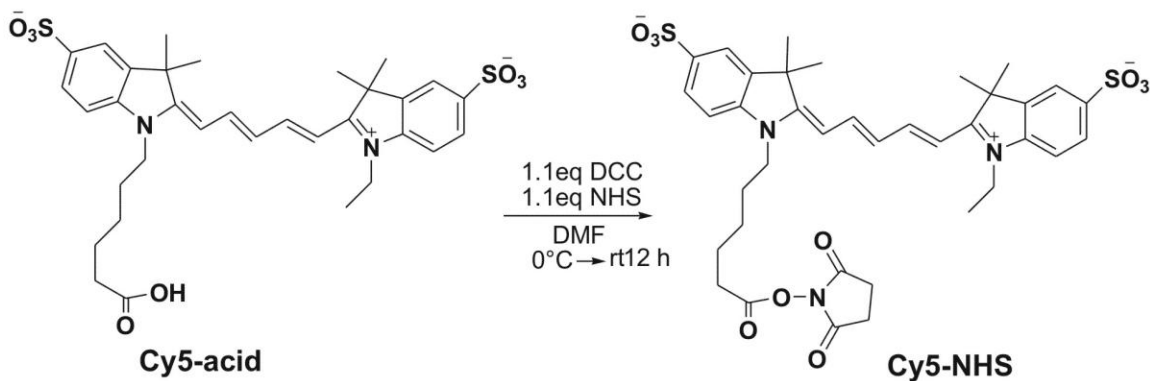


**Figure 3.3. Synthesis of Cy5-NHS**

Cy5<sup>177,178</sup> was used for fluorescent labeling of STAT6 as a highly useful fluorophore for *in vivo* imaging. Cy5-acid was first activated over night before it was coupled to the required peptides of STAT6. Boc protected N-terminal Cys was used instead of Fmoc since Cy5 can label any free amino group on the peptide. 50 mg of Cy5-COOH, 18 mg DCC (1.1 eq), NHS 10 mg (1.1 eq) in DMF (1 ml) was stirred ~12 h at 0°C to room temperature in the dark. DMF was removed on rotational evaporator. Dried Cy5-NHS was analyzed by MALDI by first dissolving it in CH<sub>3</sub>CN/H<sub>2</sub>O (1:1) (v/v) buffer. Linking of activated Cy5 to the required peptide was performed by removing a base labile ivDde group which protects  $\epsilon$ -amino group of Lys on the peptide. ivDde group cannot be removed by mild base such as 20% piperidine which was used during Fmoc group cleavage. It was removed with 3% hydrazine monohydrate in DMF (3 x 10 min). Coupling time was three overnight.

MALDI:  $[\text{M}+\text{Na}]^+_{\text{obs}}: 752.0$

## Materials and Methods

---

### 3.2.8 Synthesis of Cysteine capture beads

According to the procedure from Matteo *et. al.* 2001<sup>179</sup> capture beads were synthesized for which PEGA beads (2 g, 0.8 mM) were washed with DMF and a mix of succinic anhydride (0.800 g, 8.0 mM), with HBTU (1.08 g, 8.0 mM) and DIEA (1.390 ml, 8 mM), was added and left at RT overnight. Bead were washed with DMF, CDI (5.84 g, 32 mM in DMF) was added and reaction mixture was left for 30 min. Beads were washed again, amino acetaldehyde diethylacetal (24 mM, 3.192 g) with HOBT (2.16 g, 16 mM) were added and reaction mixture was left for 3 h at RT. Beads were finally washed with DMF and stored in CH<sub>3</sub>CN/H<sub>2</sub>O (1:1) at RT. Capture beads were tested by incubation with fluorescently labeled peptide containing an N-terminal Cys.

### 3.2.9 Peptide synthesis

Six variants of STAT6 peptides were synthesized using Fmoc based SPPS<sup>180,181</sup>. Peptide **1** (aa 635-668) with a caged phosphorylated Tyr<sup>641</sup> and Cy5 labeled, peptide **2** (aa 635-668) with only a caged caged phosphorylated Tyr<sup>641</sup>, peptide **3** (aa 635-668) with a phosphorylated Tyr<sup>641</sup> and Cy5 labeled, peptide **4** (aa 635-666) with only a phosphorylated Tyr<sup>641</sup>, peptide **5** (aa 635-666) with a non-phosphorylated Tyr<sup>641</sup> and peptide **6** (aa 635-668) with a non-phosphorylated Tyr<sup>641</sup> and Cy5 labeled peptides were synthesized on solid phase using Fmoc strategy. All the above mentioned carry a C-terminal His<sub>6</sub>-tag<sup>182</sup> at the C-terminal region. The reactive side chain of the following amino acids was protected as follows His(Trt), Lys(ivDde), Glu(OtBu), Thr(tBu), Gln(trt), Asp(OtBu), Arg(Pbf), Thr(tBu), Lys(Boc), Thr(tBu), Tyr(PO(NMe<sub>2</sub>)<sub>2</sub>), Cys(Trt).

The synthesis was carried out in a reaction vessel attached to the vacuum. Wang resin preloaded with Fmoc-His-(Trt)-Wang (0.2 mmol) was swelled for 2 h in DMF. Resin was washed for 1 min with DMF. The base labile Fmoc group was

## Materials and Methods

---

removed by 20% piperidine in DMF (3 x 12 min). Each Fmoc protected amino acids (1 mmol) were activated by using HBTU<sup>183</sup> (4.5 eq from 0.5 M stock solution in DMF) followed by addition of DIEA (10 eq, 2 mmol) for 3 min and immediately added on to the resin. Coupling time for each amino acid was for 30 min. Resin was washed again with DMF (1 x 1 min) before starting the next coupling cycle. Couplings were checked by Kaiser's test<sup>184</sup>. Attachment of the unnatural amino acid **(8)** caged phosphorylated Tyr was performed similarly except the coupling time was prolonged for 2 h. Cy5 was coupled to the peptide as mentioned in 3.2.7. Finally, resin-bound peptide was washed with DMF, DCM and MeOH followed by drying over night in vacuum.

### 3.2.10 Cleavage of peptides attached to Wang resin

Peptides were cleaved from Wang resin by dissolving in a mixture of 95% TFA + 2.5% H<sub>2</sub>O and 2.5% TIS for 3 h. Peptides were finally precipitated with diethyl ether and cooled on ice. Precipitated peptides were dissolved in (1:1) CH<sub>3</sub>CN/H<sub>2</sub>O (v/v) and separated from the resin by vacuum filtration. Peptide solutions were frozen in liquid nitrogen followed by lyophilization.

### 3.2.11 Peptide purification

Purification of peptides for analytical purposes was performed over analytical C4 (125 x 4mm, Beckman coulter) columns with 1 ml/min flowrate and bulk purification was performed over preparative C4 (250 x 22 mm) columns with 7 to 10 ml/min flowrate. For bulk purification each peptide (70 - 200 mg) was dissolved in 6 M Guanidine-HCl, 100 mM NaPi, at pH 5 and a linear gradient from 5% buffer A (H<sub>2</sub>O + 0.1% TFA) to 70% buffer B (CH<sub>3</sub>CN + 0.08% TFA) eluted the peptide at 30% - 40% of buffer B. Absorbance was monitored at 214 nm and 280 nm or 585 nm (for Cy5 detection). Fractions were analyzed by ESI-

## Materials and Methods

---

MS and MALDI-TOF followed by lyophilization of the desired fractions and stored at -20°C.

### 3.3. Biochemical methods

#### 3.3.1 Buffers and Media

2 TY - Medium:	16 g Trypton 10 g yeast 5 g NaCl pH 7.2 - 7.4
STAT6 buffer:	1 M NaCl 50 mM NaH <sub>2</sub> PO <sub>4</sub> 1 mM TCEP 1 mM EDTA pH 8.0 +/- DDM
Lysis buffer:	1 M NaCl 50 mM NaH <sub>2</sub> PO <sub>4</sub> , 1 mM TCEP, pH 8.0,
Washing buffer:	200 mM NaCl 50 mM NaH <sub>2</sub> PO <sub>4</sub>
Imidazole buffer:	10 - 250 mM Solution in STAT6 buffer
Ampicillin:	1 g in 10 ml dd H <sub>2</sub> O
IPTG:	2.38 g in 10 ml dd H <sub>2</sub> O
Purification:	Ni - NTA super flow Chitin beads Centricon (10 - 50 kDa) Dialysis kit (10 - 50 kDa) Nap5



## Materials and Methods

---

Biobeads

Gel filtration columns (S - 75 and S - 200 analytical)

### 3.3.2 Expression of recombinant STAT6MxeCBD in *E. coli*

A single colony of plasmid (pTXB1) containing STAT6 (aa 1 - 634) and His<sub>7</sub>-tag as insert was inoculated in 2 ml of 2 TY - medium containing ampicillin (100 µg/ml) and shaken at 37°C for nearly 8 h at 150 rpm. 250 ml preculture containing ampicillin (100 mg/ml, 0.250 ml) were prepared and shaken at 37°C for overnight at 150 rpm. Cells with OD<sub>578</sub> = 0.05 from this overnight culture were grown in 1.5 l volume of 2 TY - medium in six 5 l flasks containing 100 µg/ml ampicillin, shaken at 37°C, 150 rpm. 1 mM of IPTG (238 mg/ml) was added for induction at 18°C when OD<sub>578</sub> = 0.6 - 0.8 was obtained. Cells were harvested after 4 h, the pellet washed with washing buffer, centrifuged at 5000 rpm at 4°C for 15 min. The supernatant was discarded and pellets were stored at -80°C.

### 3.3.3 Purification of STAT6MxeCBD

Cells were thawed and suspended in lysis buffer and protease inhibitor 3 tablets/ 100 ml and suspended cells were lysed by microfluidizer at 850 KPa pressure. Immediately the lysed cells were centrifuged at 18,000 rpm in SS - 34 rotor for 30 min, 4°C. The supernatant was immediately loaded on 5 ml of Ni - NTA super flow beads pre - equilibrated with 10 mM - 20 mM imidazole in STAT6 buffer with varying concentrations of DDM (see results). Washing of Ni-NTA beads was carried out with STAT6 buffer containing 5 mM - 20 mM imidazole followed by elution of the protein by using 250 mM imidazole solution in STAT6 buffer + DDM (0.05% - 0.1%) or glycerol (25% - 50%). The protein was dialyzed against non - imidazole containing STAT6 buffers through membranes or by ultrafiltration having 5 - 10 kDa cutoff size. Imidazole free protein was loaded on chitin beads

## Materials and Methods

---

to undergo cleavage reaction using MesNa. Finally by eluting the protein from chitin beads, STAT6 MesNa  $\alpha$ -COSR was flash freezeed and stored at -80°C.

### 3.3.4 Determination of Protein Concentration

Concentration of fluorescently labelled protein was determined by measuring absorption at 649 nm for Cy5 using glass cuvette, 1 cm width. Concentration of non Cy5 labeled protein was estimated by comparison with protein bands on SDS - PAGE and Bradford test using absorption at 280 nm.

## 3.4. Analytical methods

### 3.4.1 Electro Spray Ionisation (ESI) - Mass spectrometry

All peptides and synthesized amino acids were identified and analyzed by this method using LCQ machine. Samples were dissolved in volatile solvents such as MeOH, EtOH or 1:1 Acetonitrile/ dd H<sub>2</sub>O.

### 3.4.2 Matrix-assisted laser desorption ionization (MALDI)

Alternatively the molecular weight of amino acids, peptides, activated Cy5-NHS were determined by matrix-assisted laser desorption ionization (MALDI). A concentrated amino acid were dissolved in ethanol and peptide was dissolved with a mixture of water/ Acetonitrile solution (1:1) + 0.1% TFA and matrix (for peptides > 10 kDa: saturated sinapinic acid and peptides < 10 kDa: saturated  $\alpha$ -cyano-4-hydroxy cinnamic acid) were used to measure MALDI. Data were acquired on a Voyager DE- Pro (Applied Biosystems).

### 3.4.3 Nuclear Magnetic Resonance Spectroscopy

$^1\text{H}$  and  $^{13}\text{C}$  NMR spectras for the synthesis of the building block of caged phosphorylated tyrosine were recorded on one of the following instruments Varian Mercury 400, Bruker DRX 400/ 500. Tetramethylsilane (TMS) was used as the internal reference. The chemical shifts are provided in  $\delta$  (ppm) and the coupling constants in Hz. The abbreviations for multiplicities used are: s, singlet; d, doublet; dd, double doublet; t, triplet; q, quadruplet; m, multiplet; br, broad; ar, aromatic.

### 3.4.4 Thin-Layer Chromatography (TLC)

Thin-layer chromatography (TLC) plates were obtained from Merck (Silica gel 60, F254). The TLCs were visualized by UV light ( $\lambda = 254 \text{ nm}$ ,  $366 \text{ nm}$ ) or by staining with one of the following stains:

Stain A: 0.3 g Ninhydrin, 3 ml acetic acid, 97 ml ethanol.

Stain B: 1.6 g  $\text{KMnO}_4$ , 10 g  $\text{K}_2\text{CO}_3$ , 2.5 ml 5% NaOH, 200 ml  $\text{H}_2\text{O}$ .

## Materials and Methods

### 3.4.5 Sodium dodecyl sulfate polyacrylamide gel electrophoresis (SDS-PAGE)

To check the molecular weight and purity of protein samples SDS-PAGE was used, following the procedure first described by Schägger and von Jagow<sup>185</sup>.

	4% stacking gel for 1 gel	10% Separating gel
<b>Gel buffer</b>	0.600 ml	1.250 ml
<b>Dd H<sub>2</sub>O</b>	1.450 ml	1.730 ml
<b>Acrylamide 49.5%</b>	0.180 ml	0.775 ml
<b>TEMED</b>	0.002 ml	0.002 ml
<b>APS 10%</b>	0.012 ml	0.019 ml

**Figure 3.4. Reagents for 10% Schägger /Jagow gels**

Gel buffer	3.0 M TrisHCl, 0.3% SDS, pH 8.45
Acrylamide	48% acrylamide, 1.5% bisacrylamide
Cathode buffer	0.1 M Tris HCl, 0.1% SDS, 0.1% Tricine, pH 8.25
Anode buffer	0.2 M Tris pH 8.9
2 x SDS	6% SDS, 35% glycerol, 120 mM Tris HCl, 0.41 M Monothioglycerol, 0.05% bromophenol blue, pH 8.0).
Staining solution	0.1% Coomassie Brilliant blue R 250, 40% ethanol, 10% acetic acid
Distaining solution	10% acetic acid, 5% ethanol
Glass-Slides	0.75 mm (Bio-rad)

Gels were run in BioRad electrophoresis chamber by using constant voltage settings from 95 mV - 120 mV.

## Materials and Methods

---

Low molecular weight protein marker (LMW):	Phosphorylase (97.0 kDa), Albumin (66.0 kDa), Ovalbumin (45 kDa), Carboanhydrase (30.0 kDa), Trypsin inhibitor (20.1 kDa), $\alpha$ -Lactalbumin (14.4 kDa) were the mixture of Low molecular protein marker
High molecular weight protein marker (HMW):	Myosin (250 kDa), Phosphorylase (148 kDa), BSA (98 kDa), Glutamic Dehydrogenase (64 kDa), Alcohol Dehydrogenase (50 kDa), Carbonic Anhydrase (50 kDa), Carbonic anhydrase (36 kDa), Myoglobin Red (22 kDa), Lysozyme (16 kDa), Aprotin (6 kDa), Insulin, B chain (4 kDa) were mixture of HMW.

### 3.4.6 Silver staining

Solution 1 (Fixer):	40% MeOH, 10% Acetic acid
Solution 2:	15 ml EtOH, NaOAc.3H <sub>2</sub> O (2 mM), Na <sub>2</sub> S <sub>2</sub> O <sub>3</sub> (31 $\mu$ M),
Washing:	(3 x 5 min, dd H <sub>2</sub> O)
Solution 3:	0.05 g AgNO <sub>3</sub> , 30 $\mu$ l Formaldehyde
Washing:	(3 x 20 s, dd H <sub>2</sub> O)
Solution 4:	0.5 mM Na <sub>2</sub> CO <sub>3</sub> .1 H <sub>2</sub> O, 15 ml EtOH
Solution 5:	Stopping Solution 0.04 M EDTA, pH 8.0, 0.745 g EDTA

After the completion of the run, the gel was stored in solution 1 for 30 min. On discarding the fixer, solution 2 was added for 10 min which was followed by washing the gel with water. The gel was further soaked in solution 3 for 10 min followed by washing with water and finally solution 4 was added. Gel was shaken till the bands were visible. The reaction was stopped by addition of solution 5.

## Materials and Methods

### 3.4.7 Non-denaturing gels

	5% Acryl amide for 2 gels	12% Acryl amide for 2 gels
<b>10x TBE</b>	1.000 ml	1.000 ml
<b>dd H<sub>2</sub>O</b>	7.292 ml	4.958 ml
<b>Acrylamide 30%</b>	1.666 ml	4.000 ml
<b>TEMED</b>	0.012 ml	0.012 ml
<b>APS 10%</b>	0.030 ml	0.030 ml

**Figure 3.5. Reagents for making non-denaturing gels**

10 x TBE: 107,8 g Tris-HCL, 55 g Boric acid, 7.44 g Di Na-EDTA in 1 l of dd H<sub>2</sub>O, pH 8.0

Loading buffer: 30 mM Tris-HCl, pH 7.5, 40% sucrose, 0.2% bromophenol blue  
Orange G (Fermenta)

Silver staining for non-denaturing gels was carried out by using silver staining kit from Pierce as the proteins bands were not visible after using silver staining method described in 3.4.4. The gel was run by using 100 mV in ice. Coomassie staining was performed by the same method used for SDS-PAGE.

## Materials and Methods

---

### 3.4.8 Western blots

Cathode buffer	300 mM Caproic acid, 30 mM Tris, pH 8.6 - 8.7
Anode buffer	300 mM Tris, 100 mM Tricine, pH 8.7 - 8.8
Anti body	Phosphotyrosine-HRP (Zymed)

Non-stained SDS-PAGE was sandwiched in the following order from top to bottom: two sheets of nitrocellulose paper soaked in cathode buffer: SDS-PAGE: Whatmann filter paper: two sheets of nitrocellulose paper soaked in anode buffer. This stack was placed in Fast blot apparatus (Biometra). Transfer of the proteins was achieved by passing 5 mA/cm<sup>2</sup> current for 20 min. After the transfer of the protein on the nitrocellulose membrane, the same was blocked for 2 h in 10% PBS + 5% non-fat dry milk powder. Next, phosphotyrosine-HRP antibody in the ratio of 1:10000 with the buffer (10% PBS+ 5% non-fat dry milk powder + 0.1% Tween) was rinsed with the membrane for 1 h followed by washing with 10% PBS + 0.1% Tween (3 x 15 min). Membrane was incubated with the enhanced chemiluminescence kit (ECL) according to the manufacture's protocol (Amersham, UK).

### 3.5. Native chemical ligation

Recombinant STAT6 MesNa  $\alpha$ -COSR and peptides **1-6** were ligated via native chemical ligation obtain six variants of semisynthetic STAT6 (**1-6**). Proteins were mixed with excess of peptide with addition of ~250  $\mu$ M MesNa. The reaction mixture was mixed on rotating wheel at RT for three days. Each day ligation reaction was monitored by SDS-PAGE. Ligation products containing fluorophore were additionally indentified by fluorescence scanner.

## Materials and Methods

---

### 3.5.1 Purification of semisynthetic STAT6

Protein was loaded on 1 ml of Ni-NTA super flow beads, pre equilibrated with 10 - 20 mM imidazole in STAT6 buffer+ 0.1% - 0.05% DDM or glycerol (25% - 50%). Washing was performed with STAT6 buffer with 5 mM - 20 mM imidazole. Elution of protein was carried out by 250 mM imidazole in STAT6 buffer + (0.1% to 0.05%) DDM or glycerol (25% - 50%) at pH 8.0. Further dialysis against imidazole free buffer gave semisynthetic STAT6 variants.

### 3.5.2 Separation of peptide from semisynthetic STAT6

Since ligated STAT6 variants and peptides **1-6** carry C-terminal His<sub>6</sub>-tag, excess peptide was removed by capture beads, and subsequent gel filtration or ultrafiltration over centricon membrane with Molecular weight cutoffs (5 - 30 kDa). 500 µl of freshly synthesized capture beads were added with protein/ peptide mixture and rotated at 4°C for 14 h. Gel filtration was carried out via NAP<sup>TM</sup>5, Sephadex -75 and -200 analytical columns. Molecules larger than the largest pores in the Sephadex matrix are excluded and elute first. STAT6 buffers were used to loading and elution by keeping the flow rate 1 ml/min. Ligated protein was concentrated by ultrafiltration using 5 - 50 kDa molecular weight cutoffs.



### 3.6. Biological activity

#### 3.6.1 Electrophoretic mobility shift assay (EMSA)

Oligonucleotides	Sequence
Recognized DNA	Tamra 5'-TC GAC TTC CCAA GAA CA GAG -3' 3'-AG CTG AAG GGTT CTT GT CTC -5'
Mismatch DNA	Tamra 5'-TC GAC TTC CCCA GAA CA GAG -3' 3'-AG CTG AAGGGT CTT GT CTC -5'
Random DNA	Tamra 5'- GTC TG GGT AGCG ACG GC TCT -3' 3'- CAG AC CCA TCGC TGC CG AGA -5'

**Figure 3.6. Sequences to make DNA variants**

Binding buffer: 10 mM Tris-HCL, 50 mM NaCl, 10 mM EDTA  
in dd H<sub>2</sub>O, pH 7.2 - 7.4

The electrophoretic mobility shift assays also known as the gel retardation assay or gel shift assay is a widely used method that allows studying the interactions of proteins with DNA or RNA respectively. Binding specificity and kinetics of a given system can be studied. The assay is based on the observation that complexes of protein and DNA or RNA migrate through a non-denaturing polyacrylamide gel slowly than double stranded.

The oligonucleotides comprising the consensus recognition sequence of STAT6 binding region in the protein were obtained from Eurofins MWG (Ebersberg) with Tamra as fluorophore was incorporated at 5' Terminal region of one of the oligonucleotide sequence. 20 μM of binding DNA, 10 μM of mismatched DNA and 20 μM random DNA were hybridized by dissolving respective oligonucleotide sequences (fig 3.6) in the binding buffer and heating them at 95°C for 5 min, followed by rapid cooling in 1 h to rt and stored at 4°C overnight. Hybridization of

## Materials and Methods

---

DNA was checked by running them over a 12% polyacrylamide gel at 0°C and 60 mV constant voltages.

DNA-binding experiments were carried out with 5 µM of STAT6 and 20 µM of DNA variant, mixed at room temperature from 5 min to 1 h. Binding was checked by a 5% polyacrylamide gel (section 3.4.5) using 100 mV voltage at 0°C. Stock solutions of oligonucleotides and DNA were flash frozen and stored at -80°C. Gels were first analyzed by Fujitsu scanner to detect the Tamra fluorescent followed by Coomassie or silver staining.

### 3.6.2 Cell Culture

Mammalian cells:	A 431, COS-7, MDCK
Media:	Dulbeccos's modified Eagle's medium (DMEM) 450 ml + (50 ml) of 10% fetal calf serum + 5 ml P/S antibiotic penicillin. (GIBCO, Invitrogen) Trypsin
PBS buffer:	137 mM NaCl, 2.7 mM KCl, 4.3 mM Na <sub>2</sub> HPO <sub>4</sub> , 1.4 mM KH <sub>2</sub> PO <sub>4</sub> , pH 7.5
Materials	Mattrek dishes, Needles
Confocal Microscope	Leica TCS SP5 X, Leica TCS SP1

To recultivate cryopreserved stocks of A431, COS-7 and MDCK cells were supplemented with 10% DMSO, the cells were thawed at 37°C in a water bath or by hand and  $1.5 \times 10^5$  cells were added under sterile workbench to 10 cm dishes and incubated with 10 ml DMEM for two hours at 37°C, 7.5% CO<sub>2</sub> and relative humidity of 95%. After cell adhesion, the medium was aspirated to remove DMSO and fresh medium (DMEM + 10% FCS) containing antibiotic (P/S: Penicillin, 100 U/ml; Streptomycin, 100 µg/ml) was added and incubated under similar condition. Each plate was maintained up to a cell density of 80% confluence at 37°C and 7.5% CO<sub>2</sub> with 95% humidity. Shortly before complete

## Materials and Methods

---

confluence, as monitored under a light microscope, the cells were passaged to new subcultures. The medium was aspirated; cells were washed with sterile PBS and treated with Trypsine-EDTA for 5 - 10 minutes at 37°C, 7.5% (CO<sub>2</sub>) and relative humidity of 95%. Once the cells were detached, fresh medium was added to resuspend the cells. Cell density was counted by using a Neubauer cell counter were, the average number of cells in four wells out of a total of sixteen were multiplied by  $1 \times 10^4$  to calculate the cell density (cells/ml).  $1 \times 10^5$  cells were thereafter transferred to new containers or mattrrek dishes.

### 3.6.3 Microinjection:

Cytoplasm of the cells was microinjected with peptide **1** and STAT6-1 by using an Eppendorf microinject Man NI 2/Femtojet system. Hoechst 33445 and propidium iodide were used as nuclear marker. Rab $\Delta$ YFP was used as cytoplasm marker. Excitation of Cy5 was performed using helium laser, Argon laser for exciting YFP and propidium iodide and UV 405 diode was used for excitation of Hoechst 33445.

Samples for microinjection should be free of particulates and aggregates to avoid clogging the microcapillary tip. Samples were therefore centrifuged in cold room at 15,000 g for 10 - 20 min. The needles were loaded with the supernatant of the centrifuged sample (0.5 to 1.0  $\mu$ l). The needles used for microinjection are borosilicate glass capillaries drawn to a fine tip 0.2 - 0.5  $\mu$ M in diameter using microprocessor-controlled capillary puller or excellent commercial microcapillaries were purchased from Eppendorf (Fermotips) and are designed to operate with the Eppendorf capillary holder. The base pressure of the system was adjusted via the visual adjustment. Cells were microinjected in the chamber at 5% CO<sub>2</sub> and 37°C. During imaging, cells were incubated in imaging solution from PAN Biotech and placed under an inverted Leica SP5 microscope equipped with an AOTF/AOBS (Acousto-Optical Tunable Filter/Beam Splitter), HCL-X-PL-APO lambda Blau 63.0x N.A 1.40 OIL IMM objective.

## Materials and Methods

---

### 3.6.4 Photo activation

Decaging of caged phosphor Tyr was achieved with a Xenon lamp adjusted at 365 nm *in vitro*. To deprotect the same group within the cell a UV diode laser ( $\lambda = 405$ ) was used.

### 3.6.5 Fluorescence measurement

(Fluorescence resonance energy transfer) FRET was performed by acceptor photo bleaching with a Fluoromax 3 spectrophotometer. Cy5 labeled STAT6-3 in presence of binding buffer was added to a quartz micro cuvette of 12  $\mu$ l volume capacity and emission maxima of Cy5 at 660 nm was observed. Similarly emission maximum at 580 nm for Tamra ds DNA was observed in the presence of binding buffer. Binding assay was performed by addition of small aliquots of Tamra ds GAS-DNA to STAT6-3 in binding buffer. Negative control was performed by STAT6-3 and Tamra ds random DNA. The change in the fluorescence was corrected for dilution for each reading. A plot of fluorescence intensities of Cy5 against the concentration of DNA (nM) determined the binding reaction.

# Chapter 4

---

Results

### 4.1 Peptide synthesis

Previous studies of STAT6 protein were all based on cellular experiments<sup>186,187</sup>. The structure of STAT6 and its biological pathway is still under investigation. Earlier studies on STAT were carried out by enzymatically phosphorylating the essential tyrosine following the canonical JAK-STAT pathway that occurs in the natural environment within the cell by indispensable interleukin (IL)/ interferon (IFNs) stimulations by using various biological catalyst like kinases that were activated by IL/ IFN stimulation (section 1.13)<sup>188</sup>. To investigate the behavior of monomeric and dimeric form of STAT6 *in vivo* and *in vitro*, a combination of biochemical methods such as expressed protein ligation (EPL) and chemical methods (figure 4.1) were used to obtain different variants of native STAT6.

The generation of full-length, site specifically modified STAT6 C-terminal portion was impossible by total chemical synthesis with the presently existing methods due to the large size of the protein (95 kDa), hence; truncated isoform of STAT6/MxeCBD was expressed in *E coil* cells until amino acid residue 634. STAT6 MesNa  $\alpha$ -COSR was generated with MxeCBD protein (figure 4.1). The remaining C-terminal part containing aa 635 - 668 was generated by Fmoc based SPPS (figure 4.2) having one glycine to cysteine mutation at position 635 which is required for native chemical ligation. The C-terminal fragment also included a His<sub>6</sub>-tag and a Lys for incorporating the fluorophore Cy5 and Gly as a spacer. EPL enabled to incorporate C-terminal site specifically modified peptides **(1-6)** to the N-terminal fragment of STAT6 MesNa  $\alpha$ -COSR to generate six variants of semisynthetic truncated STAT6 **-(1-6)** very efficiently in good yield. Seven different analogues of STAT6 (aa 635 - 660) peptides were synthesized (figure 4.2) as described in section 3.2.9 by SPPS.

## Results

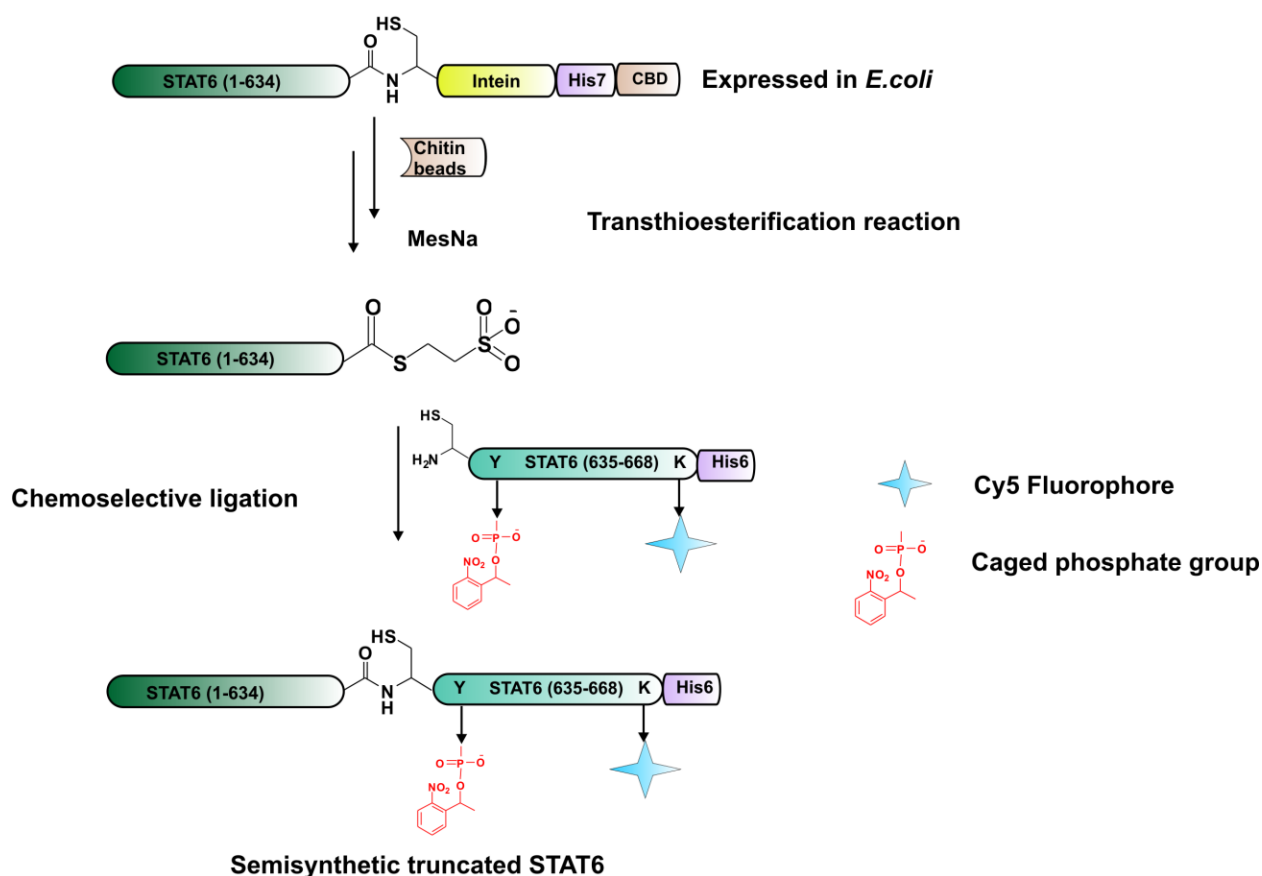


**Figure 4.1: Scheme of EPL to produce site specifically modified STAT6.**

Scheme representing recombinant STAT6MxeCBD expressed in *E. coli* cells, which undergoes transthioesterification reaction in presence of MesNa to generate STAT6 MesNa  $\alpha$ -COSR. STAT6 MesNa  $\alpha$ -COSR is thus capable to ligate the remaining C-terminal part obtained from SPPS with required modification.

To generate light switchable semisynthetic STAT6, peptide with caged phosphorylated Tyr<sup>641</sup> was synthesized by using solution phase synthesis following the procedure from Rothman, D *et. al.* 2003<sup>176</sup>. Over five steps, *N*- $\alpha$ -Fmoc-phospho-(1-nitrophenylethyl-2-cyanoethyl)-L-tyrosine (**5**) was synthesized with an yield of 50% (figure 3.1 and 3.2). O-1-(2-nitrophenyl)-ethyl-O'- $\beta$ -cyanoethyl-N,N-diisopropyl phosphoramidite (**2**) as the photolabile caged analogue of phosphate bonded with tyrosine was synthesized over two steps. The key P-O bond construction was carried out using a reactive trivalent phosphoramidite species, and phosphite was then oxidized to the corresponding phosphate by using *tert*-Butylhydroperoxide. The  $\beta$ -Cyanoethyl protecting group was

## Results

---

retained until the next Fmoc-amino acid was coupled. Commercially available tyrosine building block *N*- $\alpha$ -Fmoc-L-tyrosine was converted to *N*- $\alpha$ -Fmoc-L-tyrosine-*tert*-butyl ester (**4**) using *tert*-2, 2, 2-butyltrichloroacetimidate. Final coupling of *N*- $\alpha$ -Fmoc-phospho-(1-nitrophenylethyl-2-cyanoethyl)-L-tyrosine (**5**) was performed manually to the STAT6 peptide, which was synthesized until Val<sup>642</sup> or by using a peptide synthesizer (figure 4.2). All synthesis steps are explained in detail in the section 3.2.1. NPE group can be released by illumination with far UV light of 365 nm that does not severely damage cells during *in vivo* analysis. The byproducts generated during photolysis of the caged group are non-toxic to cells. NPE was also stable during basic Fmoc group removal in SPPS synthesis and strong acidic treatment during cleavage.

To synthesize peptides by SPPS, an insoluble solid support such as the resin (Fmoc-His-(Trt)-Wang) was selected to incorporate amino acids natural and modified depending on the native STAT6 sequence. Furthermore, because of the repetitive nature of peptide synthesis (deprotection, washing, coupling, washing, deprotection), the use of an insoluble support in a single reaction vessel allows for automatization of the processes in contrast to the solution phase chemistry where product has to be isolated, purified each time with the retardation in the yield of the final product. Byproducts during SPPS are removed by simple vacuum filtration. Another advantage of using SPPS was to incorporate small fluorophores such as Cy5 to study the progression of ligations as well as to investigate the activity of STAT6 *in vivo* and *in vitro* which was linked to Lys<sup>661</sup> by cleaving the ivDde protecting group. His<sub>6</sub>-tag was incorporated in all the peptides for the purpose of purification via Ni-NTA superflow beads.



## Results

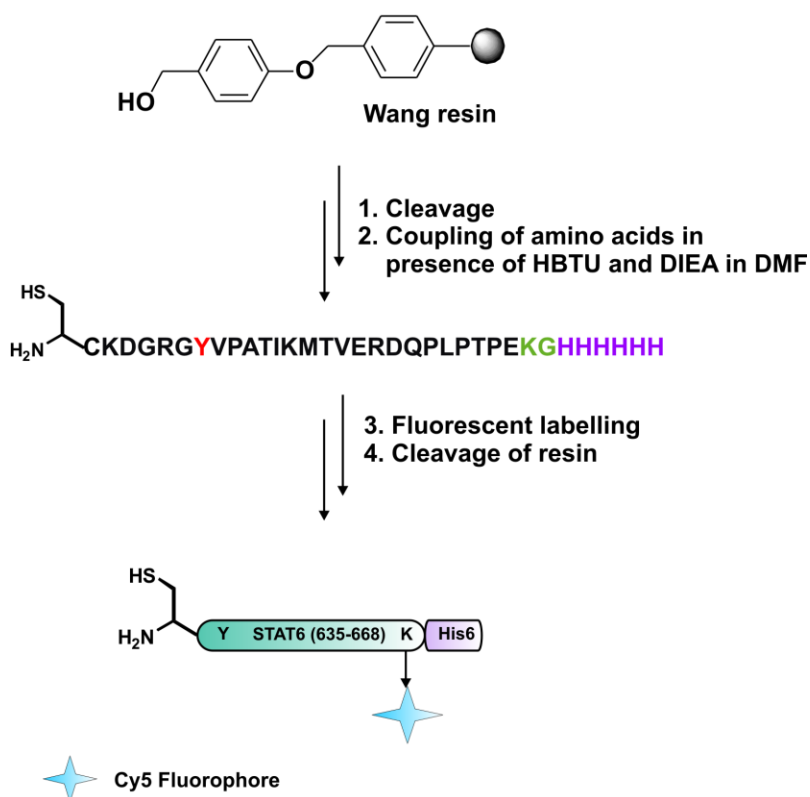


**Figure 4.2: Scheme for Fmoc based SPPS**

Modifications on STAT6 peptides were carried out at Tyr<sup>641</sup> and with or without Cy5 at Lys<sup>661</sup>. STAT6 peptide with caged phosphorylated tyrosine was synthesized with Cy5 (figure 4.3, peptide 1) and without Cy5 (figure 4.3, peptide 2). To synthesize the non-caged phosphorylated STAT6 variant, Fmoc-Tyr-[PO(OBz)OH]-OH was used and two variants were generated, one with Cy5 (figure 4.3, peptide 3) and another without Cy5 (figure 4.3, peptide 4). Commercially available Fmoc-Tyr-OH was used to synthesize the wild type STAT6 along without (figure 4.3, peptide 5) and with Cy5 (figure 4.3, peptide 6). Peptide 7 was synthesized with N-terminal Fmoc on Cys to test the removal of NPE group (figure 4.3).

## Results

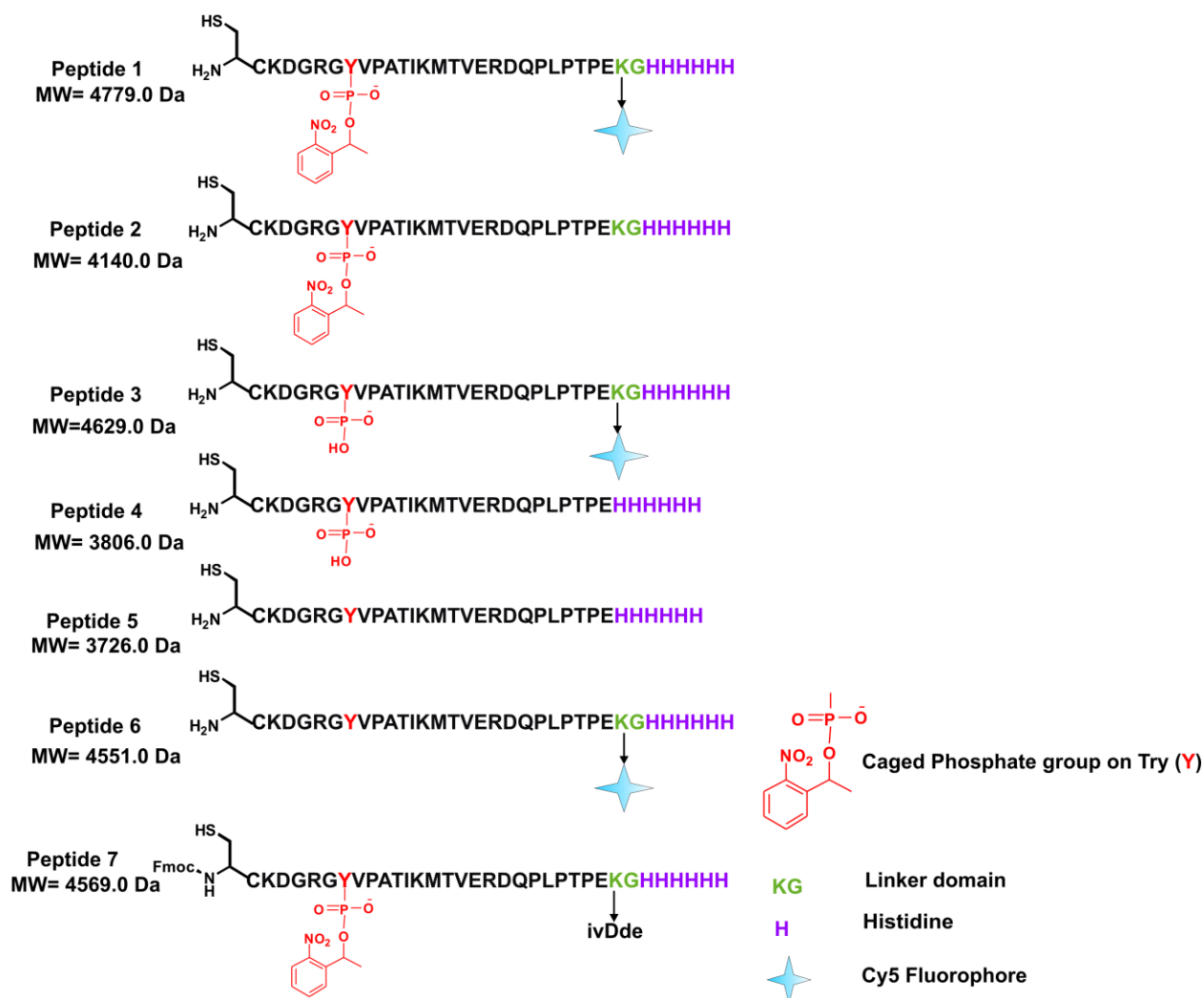


Figure 4.3: Different variants of STAT6 peptides synthesized by Fmoc based SPPS. Modifications of Tyr<sup>641</sup> and Lys<sup>661</sup> are as indicated.

### 4.1.1. Synthesis of Peptide 1

635 H-CKDGRGY<sup>X1</sup>VPATIKMTVERDQPLPTPEK<sup>X2</sup>GHHHHHH-OH 668  
MW = 4779.0 Da [X<sub>1</sub>= NPE-PO<sub>3</sub>, X<sub>2</sub>= Cy5]

Peptide 1 contains the caged phosphorylated Tyr<sup>641</sup> which will enable STAT6 to behave as native truncated monomeric form after NCL with STAT6 MesNa  $\alpha$ -COSR as described in section 4.2.2. Peptide 1 will also be used for *in vivo* experiments in the later sections. Modification on this peptide was achieved by incorporating synthesized *N*- $\alpha$ -

## Results

Fmoc-phospho (1-Nitrophenylethyl-2-cyanoethyl)-L-tyrosine (8), by labeling Cy5 on Lys<sup>661</sup> of the linker domain and His<sub>6</sub>-tag at the C-terminus thus having all combinations of modifications (figure 4.3, peptide 1).

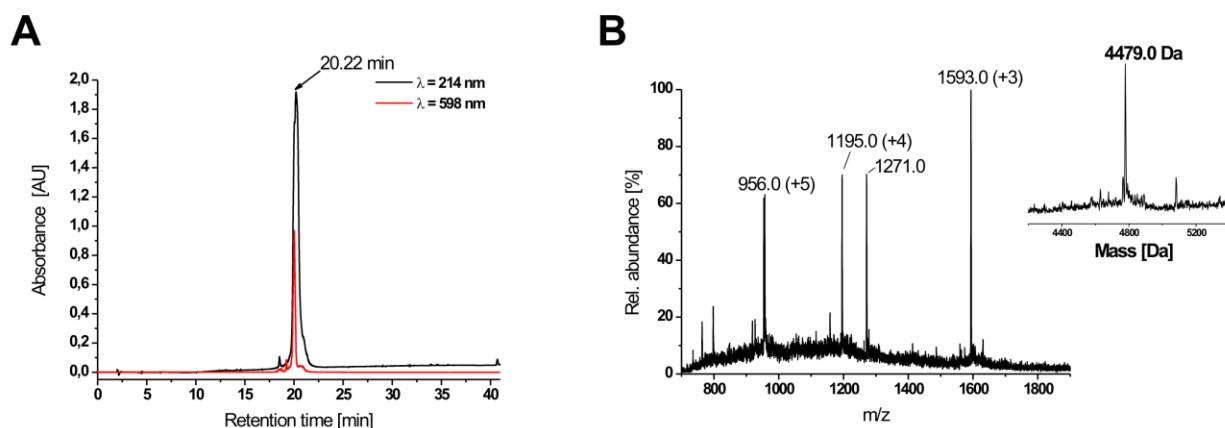


**Figure 4.4: Analysis of peptide 1**

**A:** Single peak of purified peptide **1** was eluted at a retention time of 20.22 min from analytical C4-RP-HPLC by using a gradient of buffer B from 5% (v/v) to 65% (v/v) in buffer A over 30 min with a flow rate of 1 ml/min. Cy5 signal was detected at  $\lambda = 596$  nm. **B:** ESI-MS of purified peptide **1**. MS signals at 956.0 Da, 1195.0 Da, and 1593.0 Da correspond to the desired ( $M_{\text{cal}} = 4779.0$  Da) pure peptide.

His<sub>6</sub>-tag was used to facilitate the purification after NCL with STAT6 MesNa  $\alpha$ -COSR. As shown in figure 4.2, the peptide was synthesized until Val<sup>642</sup> manually or by using peptide synthesizer on solid phase using Fmoc-His-(Trt)-Wang (0.2 mmol) resin (w/w) following the general strategy of Fmoc synthesis.<sup>189</sup> The remaining amino acid couplings to complete the sequence were carried out manually. Coupling of *N*- $\alpha$ -Fmoc-phospho (1-nitrophenylethyl-2-cyanoethyl)-L-tyrosine was carried out for 1 - 2 h. Activation of each amino acid and cleavage of Fmoc group at each step was carried out by standard procedures as described in section 3.2.10. Unsure couplings of the amino acids were monitored by Kaiser's test.

After completion of the entire sequence of the peptide, the resin was washed with DMF, DCM, MeOH and lyophilized overnight in the dark. Later 0.1 mmol (w/w) of the same resin was allowed to swell in DMF for 1 h to deprotect the side chain ivDde group from

## Results

---

Lys<sup>661</sup> to couple the fluorophore Cy5. Deprotection of ivDde group was carried out, by using 5 ml of 3% Hydrazine solution in DMF (3 x 12 min). Cy5-NHS ester was finally coupled in equimolar amounts in DMF for 72 h as described in section 3.2.7 in the dark. The coupling of Cy5 could not be analyzed by a negative Kaiser's test since Cy5 will block the free amino terminal of Lys<sup>661</sup> and due to the high solubility of unreacted Cy5 sticking to the resin which dissolves in any organic solvents. Alternatively, a test cleavage was carried out and MS analysis indicated the successful coupling of Cy5. Test cleavage of the resin was carried out in a solution of 95% TFA, 2.5% TIPS and 2.5% water for 3 h (section 3.2.10). The resulting peptide was precipitated with cold ether. The peptide was dissolved in water/ acetonitrile (1:1) (v/v) solution and separated from the resin by centrifugation or vacuum filtration followed by overnight lyophilization.

Lyophilized crude peptide was dissolved in 6 M Guanidium-HCL, 300 mM NaH<sub>2</sub>PO<sub>4</sub>, pH 7.5 for RP-HPLC purification on a preparative C4-RP-HPLC column with a linear gradient of 40% (v/v) to 60% (v/v) buffer B in buffer A over 80 min. Fractions from purification were analyzed by ESI-MS, lyophilized and stored at -20°C in the dark. From 200 mg of crude peptide, 10 mg (5% yields) of pure peptide were finally obtained. The preparative HPLC-purified peptide was rechromatographed on an analytical C4 RP-HPLC column. The purity of the peptide was detected by a single peak with a retention time of 20.22 min (figure 4.4, A) at absorption 595 nm in the chromatogram indicating the successful coupling of the fluorophore Cy5.

The ESI-MS shows different charge states of peptide **1**, with five (956.0 Da), four (1195.0 Da), and three (1593.0 Da) positive charges corresponding to a deconvoluted mass of 4779 Da ( $M_{cal} = 4779.0$  Da). The peak at 1271 m/z is caused by an artifact from HPLC purification since no mass corresponding to ( $M_{cal} = 3813.0$  Da), was found (figure 4.4, B). Since the same peptide was used for generating of peptide **2** where peak at 1271 m/z was not observed, it can be concluded that it was an artifact from HPLC.

## Results

### 4.1.2. Synthesis of Peptide 2

**635 H-CKDGRGY<sup>X</sup>VPATIKMTVERDQPLPTPEKGGHHHHH-OH 668**  
**MW = 4140.0 Da [X= NPE-PO3]**

Peptide **2** has a caged phosphorylated Tyr in position 641 similar to peptide **1** only no fluorophore was incorporated here. Peptide **2** when ligated with STAT6  $\alpha$ -COSR will generate native monomeric truncated STAT6 without fluorescent label as described in section 4.2.3. This variant was used to detect the decaging of the STAT6 in vitro as described in section 4.3.1. Peptide **2** is peptide **1**, which was synthesized without incorporating Cy5, hence the side chain protecting group ivDde from Lys<sup>661</sup> was removed. After completion of the sequence, the peptide was cleaved from the resin

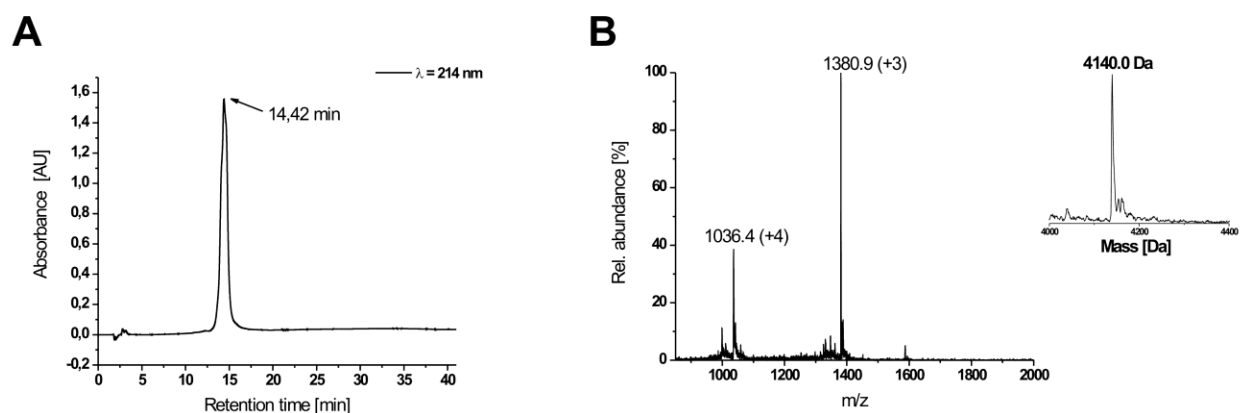


**Figure 4.5: Analysis of peptide 2.**

**A:** Single peak corresponding to purified peptide **2** was eluted at a retention time of 14.42 min from analytical C4-RP-HPLC by using buffer B from 5% (v/v) to 65% (v/v) in buffer A over 40 min with a flow rate of 1 ml/min. **B:** ESI-MS of purified peptide **2**. MS signals at 1036.4 Da, and 1380.9 Da, corresponds to the desired mass  $M_{\text{cal}} = 4140.0 \text{ Da}$  of pure peptide.

following the general technique of Fmoc cleavage (section 3.2.10) and 200 mg of crude peptide were obtained. The purification of the crude peptide was performed by using preparative C4-RP-HPLC column with a linear gradient of 40% (v/v) to 60% (v/v) buffer B in buffer A over 80 min. Fractions were analyzed by ESI-MS and required fraction was lyophilized and stored at  $-20^{\circ}\text{C}$  in the dark. 10 mg (20% yields) of pure peptide were

## Results

---

obtained from 50 mg of crude peptide after purification. The preparative HPLC-purified peptide was rechromatographed on C4-analytical RP-HPLC column. A single peak with a retention time of 14.42 min (figure 4.5, A) confirmed the purity of the peptide. ESI-MS data showed differently charged signals corresponding to peptide **2** with four (1036.4 Da) and three (1380.9 Da) positive charges of the deconvoluted mass of the pure peptide ( $M_{cal}= 4140.0$  Da) (figure 4.5, B).

### 4.1.3. Synthesis of Peptide 3

**635 H-CKDGRGY<sup>X1</sup>VPATIKMTVERDQPLPTPEK<sup>X2</sup>GHHHHHH-OH 668**  
**MW = 4629.0 Da [X<sub>1</sub>= PO<sub>4</sub>, X<sub>2</sub>= Cy5]**

Peptide **3** has two modifications on its usual sequence. It has no caged phosphorylated Tyr<sup>641</sup> as compared with peptide **1** and **2**. Peptide **3** was generated to mimic the native bioactive STAT6 which is found in dimeric form in the cytoplasm and enters nucleus to transcribe gene. Hence after its ligation with the STAT6 MesNa  $\alpha$ -COSR, *in vitro* experiments were carried out to prove the dimeric behaviour of STAT6 with the DNA as described in section 4.2.4. Peptide **3** was also used for western dot blot experiments as control as described in section 4.3.1.

In order to synthesize peptide **3**, commercially available Fmoc-Tyr[PO(OBz)OH]-OH (Novabiochem) was coupled at position 641 of the peptide. Similar to the above mentioned synthesis for peptide **1**, Fmoc-His-(Trt)-Wang resin in 0.2 mmol (w/w) was used to prepare peptide **3** keeping the peptide **1** sequence constant. Peptide **3** was labeled with Cy5 fluorophore following the procedure as described for labeling peptide **1**.

## Results

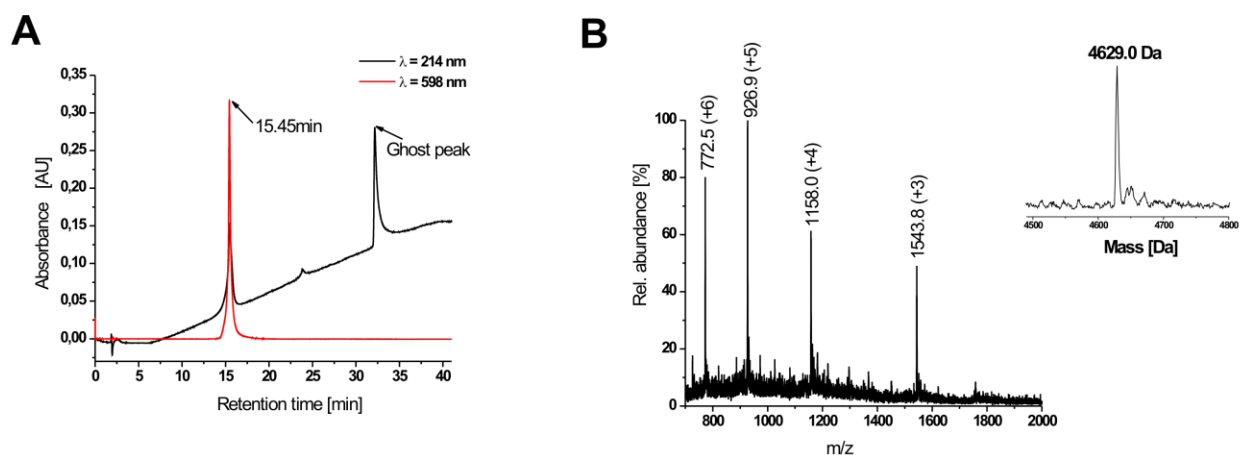


**Figure 4.6: Analysis of peptide 3**

**A:** Single peak of purified peptide **3** was eluted at a retention time of 15.45 min from analytical C4-RP-HPLC by using buffer B from 5% (v/v) to 65% (v/v) in buffer A over 40 min with a flow rate of 1 ml/min. Cy5 signal was detected at  $\lambda = 596$  nm. **B:** ESI-MS of purified peptide **3**. MS signals at 772.5 Da, 926.9 Da, 1158.0 Da and 1543.8 Da correspond to the desired mass of pure peptide ( $M_{\text{cal}} = 4629.0$  Da).

After completion of the sequence, peptide **3** was successfully cleaved from the resin following the general technique of Fmoc cleavage (section 3.2.10). 150 mg of the crude peptide was obtained after cleavage. Purification of the crude peptide was performed by using preparative C4-RP-HPLC column with a linear gradient of 10% (v/v) to 50% (v/v) buffer B in buffer A over 60 min. Fractions were analyzed by ESI-MS, pooled accordingly and stored at  $-20^{\circ}\text{C}$  in the dark. From 30 mg of crude peptide, 10 mg (33%) of pure peptide was obtained finally. A single peak from the analytical C4-RP-HPLC column confirmed the purity of the peptide with a retention time of 15.45 min. (figure 4.6, A) and absorption at 545 nm indicated the presence of Cy5 labeled peptide **3**. ESI-MS signals detected different charged states of peptide **3** with six (772.5 Da), five (926.9 Da), four (1158.0 Da) and three (1543.8 Da) positive charges corresponding to the desired deconvoluted mass of the pure peptide **3** ( $M_{\text{cal}} = 4629.0$  Da) (figure 4.6, B). Appearance of ghost peak at 32 min came from the C4 column, which was unavoidable. The peak was not a matter of concern since a pure peptide was obtained after final purification over preparative RP-HPLC.

## Results

### 4.1.4. Synthesis of Peptide 4

635 H-CKDGRGY<sup>X</sup>VPATIKMTVERDQPLPTPEHHHHH-OH 666

MW = 3806.0 Da [X= PO4]

The sequence of peptide **4** contains non-caged phosphorylated Tyr in position 641 synthesized by using commercially available Fmoc-Tyr[PO(OBz)OH]-OH (Novabiochem), Cy5 as fluorophore was not attached to the peptide, hence linker domain was not incorporated in the sequence (figure 4.7). Ligation of peptide **4** with STAT6 MesNa  $\alpha$ -COSR will generate STAT6 as a dimer as described in section 4.2.5. This was used for many DNA binding assay experiments as described in section 4.3.2.

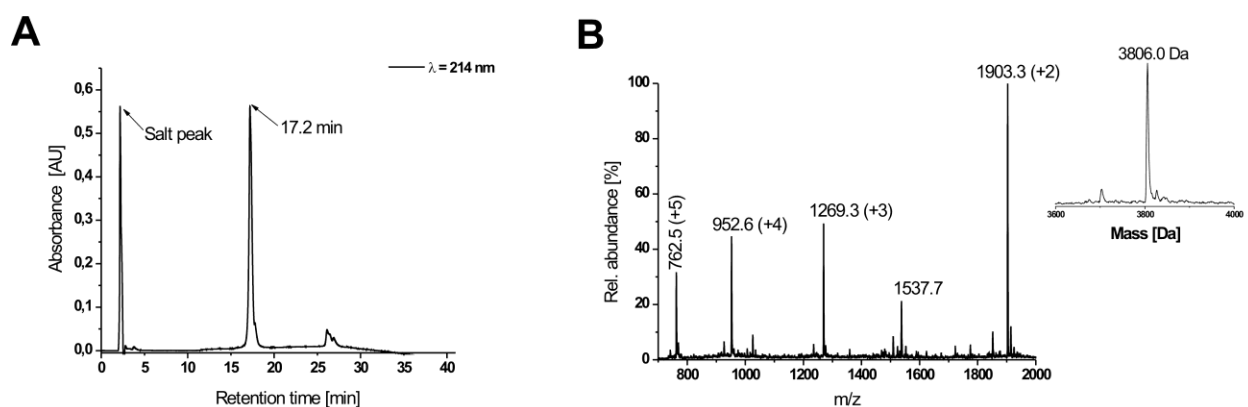


**Figure 4.7: Analysis of peptide 4**

**A:** Single peak of purified peptide **4** was eluted at a retention time of 17.2 min from analytical C4-RP-HPLC by using buffer B from 5% (v/v) to 65% (v/v) in buffer A over 40 min with a flow rate of 1 ml/min. **B:** ESI-MS of purified peptide **4**. MS signals at 762.5 Da, 952.6 Da, 1269.3 Da and 1903.3 Da corresponds to the desired mass of pure peptide ( $M_{\text{cal}} = 3806.0$  Da).

To generate peptide **4**, 0.2 mmol (w/w) of Fmoc-His-(Trt)-Wang resin was used to synthesize the sequence manually. Similar to the above mentioned peptides **1-3** synthesis and cleavage of this peptide was performed following the general technique of Fmoc synthesis. 300 mg of crude peptide was obtained after cleavage of the resin.



## Results

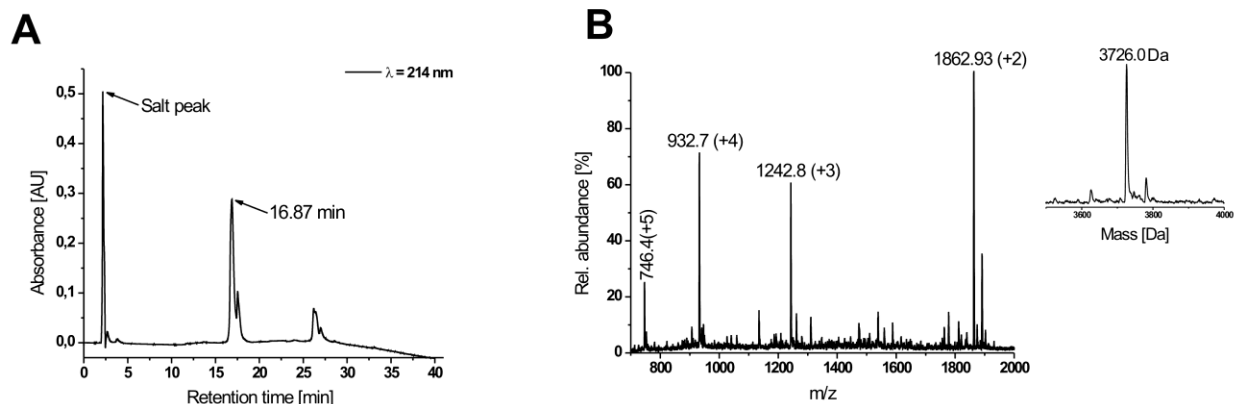
The purification of the crude peptide was performed by using preparative C4- RP-HPLC column with a linear gradient of 15% (v/v) to 55% (v/v) buffer B in buffer A over 60 min. Fractions were analyzed by ESI-MS and required fractions were lyophilized and stored at -20°C. From 30 mg of crude peptide, 10 mg (33%) of pure peptide was obtained finally. The preparative HPLC-purified peptide was rechromatographed on analytical C4-RP-HPLC column. The purity of the peptide was detected by a single peak with a retention time of 17.2 min (figure 4.7, A) at absorption 214 nm. ESI-MS signals detected different charged states of peptide **4** with five (762.5 Da), four (952.6 Da), three (1269.3 Da) and two (1903.3 Da) positive charges corresponding to the desired mass of pure peptide the ( $M_{cal}= 3806.0$  Da) shown in (figure 4.7, B). No corresponding mass of three (1537) charge state was observed.

### 4.1.5. Synthesis of Peptide 5

**635 H-CKDGRGYVPATIKMTVERDQPLPTPEHHHHHH-OH 666**

**MW = 3726.0 Da**

Peptide **5** was generated to obtain a truncated, wild type STAT6 after NCL with STAT6 MesNa  $\alpha$ -COSR as described in section 4.3.6. Peptide **5** when ligated to STAT6 MesNa  $\alpha$ -COSR will lead to the formation of monomeric STAT6 without Cy5 fluorophore. Peptide **5** consists of the same sequence as peptide **1-4** except Tyr<sup>641</sup> was not phosphorylated, labeling with Cy5 fluorophore was not included, hence linker domain was not incorporated.



## Results

---

### Figure 4.8: Analysis of peptide 5

**A:** Single peak of purified peptide **5** was eluted at a retention time of 16.87 min from analytical C4-RP-HPLC by using buffer B from 5% (v/v) to 65% (v/v) in buffer A over 40 min with a flow rate of 1ml/ min. **B:** ESI-MS of purified peptide **5**. MS signals at 746.4.Da, 932.7 Da, 1242.8 Da and 1862.9 Da corresponds to the desired mass of pure peptide ( $M_{cal}= 3726.0$  Da).

To synthesize peptide **5**, 0.1 mmol (w/w) resin pre-loaded peptide with the sequence of peptide **4** until Val<sup>642</sup> was used and the complete sequence was synthesized manually. Synthesis and cleavage of this peptide was performed following the general technique of Fmoc synthesis. 150 mg of the crude peptide was obtained after cleavage.

The purification of the crude peptide was performed as described above with a linear gradient of 10% (v/v) to 60% (v/v) buffer B in buffer A over 45 min. Fractions were analyzed by ESI-MS and fractions containing the right peptide **5** were lyophilized and stored at -20°C in darkness. From 30 mg of crude peptide, 10 mg (33%) of pure peptide was finally obtained. The purity of peptide **5** was analyzed in RP-HPLC by the detection of a single peak with a retention time of 16.87 min (figure 4.8, A) at 214 nm. ESI-MS signals detected four different charged states of peptide **5** with five (746.4.Da), four (932.7 Da), three (1242.8 Da) and two (1862.9 Da) positive charges which corresponds to a deconvoluted mass of the desired pure peptide ( $M_{cal}= 3726.0$  Da) (figure 4.8, B).

### 4.1.6. Synthesis of Peptide 6

**635 H-CKDGRGYVPATIKMTVERDQPLPTPEK<sup>X</sup>GHHHHHH-OH 668**

**MW = 4551 Da [X= Cy5]**

Peptide **6** was generated to obtain wild type Cy5 labeled STAT6 variant as described in section 4.2.7. Peptide **6** when ligated to STAT6 MesNa  $\alpha$ -COSR will lead to the formation of monomeric STAT6 with Cy5 fluorophore. Fmoc-His-(Trt)-Wang (0.2 mmol) resin (w/w) was used for synthesis of the complete sequence. Synthesis and cleavage of this peptide was performed following the general technique of Fmoc synthesis. ~150 mg of the crude peptide was obtained after cleavage from the resin. 30 mg of the peptide was dissolved in STAT6 buffer A.

## Results

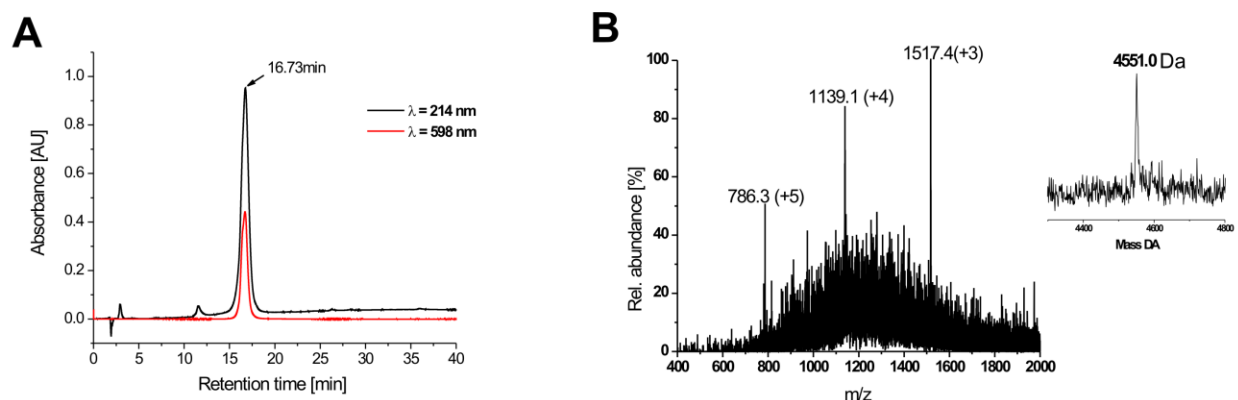


**Figure 4.9: Analysis of peptide 6**

**A:** Single peak of purified peptide **6** was eluted at a retention time of 17.2 min from analytical C4-RP-HPLC by using buffer B from 5% (v/v) to 65% (v/v) in buffer A over 40 min with a flow rate of 1 ml/min. **B:** ESI-MS of purified peptide **6**. MS signals at 786.3 Da, 1139.1 Da and 1517.4 Da which corresponds to ( $M_{\text{cal}} = 4551.0 \text{ Da}$ ) the pure peptide.

The purification of the crude peptide was performed as above, with a linear gradient of 15% (v/v) to 80% (v/v) buffer B in buffer A over 45 min. Fractions were analyzed by ESI-MS and required fractions were lyophilized and stored at  $-20^{\circ}\text{C}$  in the dark. From 30 mg of crude peptide, 10 mg (33%) of pure peptide was finally obtained. As above peptides a single peak with a retention time of 16.73 min at absorption 214 nm (figure 4.6, A) detected the purity of the peptide. ESI-MS signals detected different charged states of peptide **6** with five (786.3 Da), four (1139.1 Da) and three (1517.4 Da) positive charges corresponding to the pure desired mass of the peptide ( $M_{\text{cal}} = 4551.0 \text{ Da}$ ) shown in figure 4.9, B.

### 4.1.7. Synthesis of Peptide 7

635 H-<sup>X1</sup>CKDGRGY<sup>X2</sup>VPAIKMTVERDQPLPTPEK<sup>X3</sup>GHHHHHH-OH 668  
MW = 4567.0 Da [X1= Fmoc] [X2= NPE-PO3] [X3= ivDde]

## Results

Peptide **7** was generated with Fmoc protected Cys at position 635 region of the peptide chain. It was generated to investigate the removal of NPE group. The peptide was synthesized with similar sequence as peptide **1** and **2** without deprotecting ivDde group from Lys<sup>661</sup>. Peptide was not purified in HPLC since the ESI-MS showed 98% pure peptide after cleavage from the resin. Presence of impurity would not deter the decaging experiment nor the peptide would be used for any ligations with STAT6 MesNa  $\alpha$ -COSR. As above synthesis and purification procedures for peptides, peptide **7** after completion of the sequence was cleaved from the resin and ESI-MS signals detected different charged states with six (762.40 Da), five (914.53 Da), four (1142.03 Da) and three (1523.33 Da) positive charges corresponding to the desired mass of the peptide ( $M_{cal}= 4567.0$  Da) shown in figure 4.10.

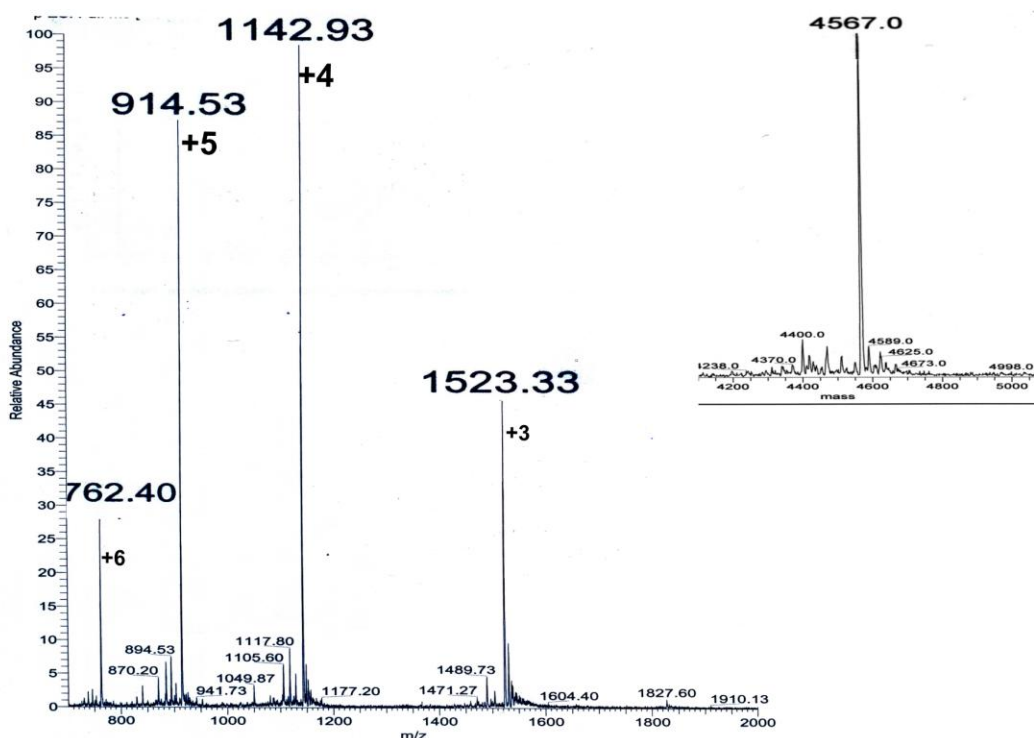


**Figure 4.10: ESI-MS of peptide 7**

ESI-MS signals 762.4 Da, 914.53 Da, 1142.03 Da and 1523.33 Da which corresponds to ( $M_{cal}= 4567.0$  Da) peptide **7**

## Results

### 4.2 Expressed protein ligation

#### 4.2.1 Expression and purification of STAT6MxeCBD protein

To study the activity of STAT6, which is ~118 kDa in size, a truncated isoform of STAT6 was designed so that specific modifications could be made at the C-terminal portion by chemical tools as described in the section 4.1. The truncated STAT6 was designed to have  $\alpha$ -COSR which can later undergo native chemical ligation with the modified peptides. STAT6 gene is cloned into an expression vector pTXB1 (New England Biolabs) as an N-terminal fusion to the intein from *Mycobacterium xenopi* (Mxe GyrA) followed by a His<sub>7</sub>-tag at its C-terminus finally leading to chitin binding domain (CBD) (figure 4.11). Expression of STAT6MxeCBD was carried out in *E.coli* cells and performed at 37°C until O.D<sub>598</sub>= 0.6 - 0.9 in 2 TY medium and ampicillin (100 µg/ml) as antibiotic. Highly expressed STAT6MxeCBD (protein band above 67 kDa, figure 4.12 A) was seen after 4 h of induction with IPTG at 14 - 18°C. Temperature was lowered to obtain high yield of soluble native STAT6MxeCBD since there are no folding methods available for this multi-domain proteins. Minor amount of protein was observed before induction (figure 4.12, A). Large amount of protein was observed in the inclusion bodies of *E.coli*, compared with the cytosolic fraction Purification from the cytosolic fraction of *E.coli* was detrimental since STAT6 MesNa  $\alpha$ -COSR was required in the native form and no standard method was developed to refold the protein after purification in denaturing conditions.

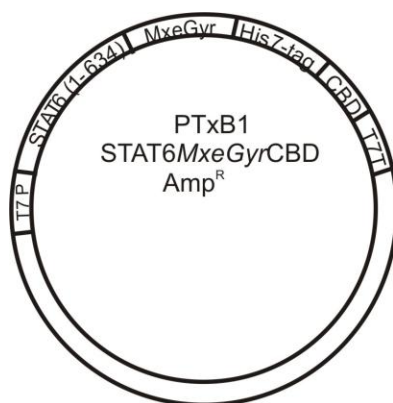


Figure 4.11: pTXB1 vector with STAT6MxeGyrCBD and His<sub>7</sub>-tag insert.

## Results

---

Expression was monitored at each 1 h after addition of IPTG at 14°C-18°C to obtain soluble STAT MesNa  $\alpha$ -COSR. Purification was performed using the crude *E.coli* cell extracts from the cytoplasm. First step in purification was carried out by Ni-NTA super flow beads as affinity chromatography as described in section 3.3.3 with the help of internal His<sub>7</sub>-tag. Purifying STAT6MxeCBD was found to be the most difficult part due to its instability while handling.

Two methods were performed to bind STAT6MxeCBD with pre-equilibrated Ni-NTA beads. First method was immediate loading of supernatant solution obtained after lysis of STAT6 pellets was performed in a flask in presence of 5 mM - 20 mM imidazole solution in STAT6 buffer + 0.1% DDM. The suspension of Ni-NTA beads and protein solution was rotated on table top rotating wheel at 4°C for 1 h to 2 h. Overnight binding with Ni-NTA beads with protein was found to be unstable leading to precipitation during further purification steps. Second method was performed by using gravity flow for loading impure protein solution over the column containing Ni-NTA beads. This was very time consuming and since protein was unstable direct mixing of protein with Ni-NTA beads was preferred, which saved purification time providing soluble protein.

Washing of Ni-NTA beads was very challenging because upon using STAT6 buffer containing 5 - 60 mM imidazole STAT6MxeCBD eluted with 30 mM imidazole solution onwards until 250 mM imidazole solution. Hence, larger volumes of washing with STAT6 buffer were used for removing impurities such as non-His-tag proteins and cell components. Finally, STAT6MxeCBD was eluted from Ni-NTA beads with 250 mM imidazole solution in STAT6 buffer + 0.1% DDM. Elution from the Ni-NTA matrix containing STAT6MxeCBD was dialyzed against 100 volumes of STAT6 buffer free of imidazole corresponding to the total volume of the Ni-NTA elution. Minor impurities were ignored in this step, as protein would be further purified over chitin beads through the chitin binding domain to obtain STAT6 MesNa  $\alpha$ -COSR and later again after native chemical ligation with the various analogues of the modified peptides to obtain semisynthetic STAT6 (aa 1 - 668 ) proteins.

## Results

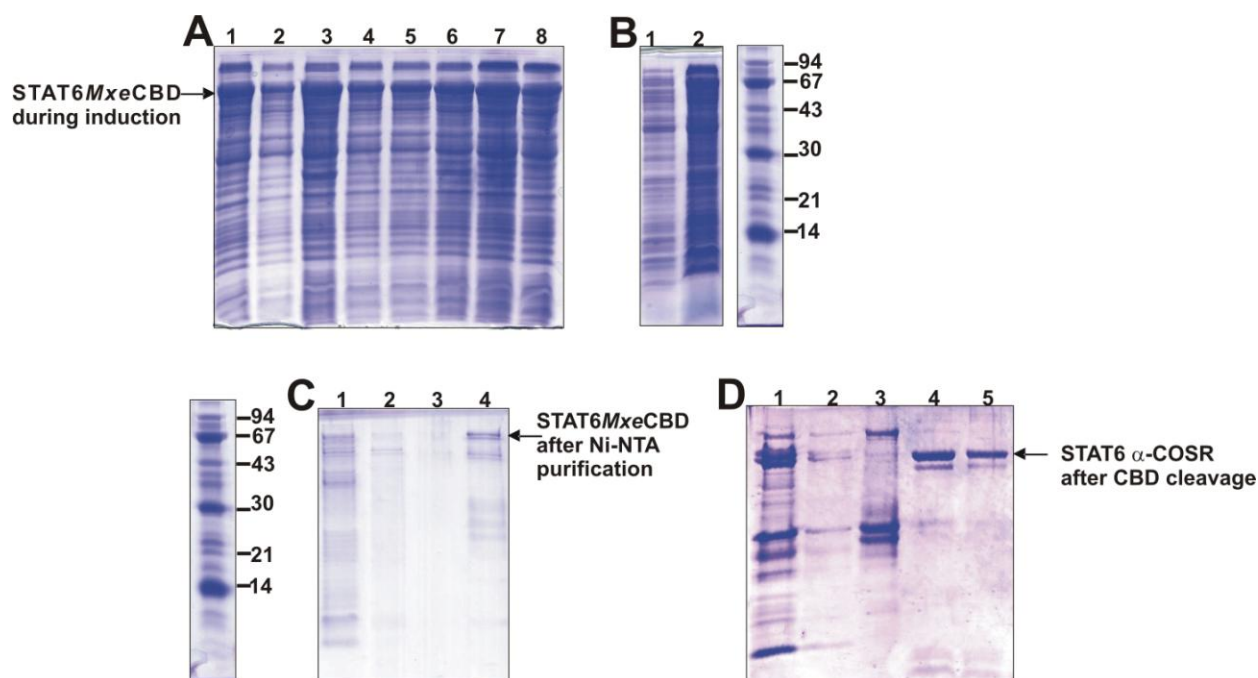


**Figure 4.12: Expression and purification of STAT6/MxeCBD protein**

**A:** SDS-PAGE showing expression of STAT6/MxeCBD protein in *E. coli* cells induced at O.D = 0.9. *E. coli* cell extracts after addition of 1 mM IPTG were analyzed at every 1 h (lanes 1, 10  $\mu$ l and lane 2, 5  $\mu$ l), 2 h (lanes 3, 10  $\mu$ l and lane 4, 5  $\mu$ l), 3 h (lanes 5, 5  $\mu$ l and lane 6, 10  $\mu$ l) and maximum yield was observed after 4 h of inductions (lanes 7, 10  $\mu$ l and lane 8, 5  $\mu$ l). **B:** SDS-PAGE analysis of the expression of STAT6/MxeCBD fusion protein. Crude cell extract from *E. coli* cells before induction (lane 1), after induction (above 67 kDa shown by an arrow) with IPTG at 18°C for 4 h (lane 2), inlay showing low molecular weight marker. **C:** STAT6/MxeCBD purifications with Ni-NTA. Washings with 10 mM - 20 mM imidazole in STAT6 buffer (lanes 1 - 3), final elution of the protein by 250 mM imidazole (lane 4) shown by an arrow. **D:** SDS-PAGE of intein splicing from STAT6/MxeCBD by loading it on chitin beads. Washing elution from chitin beads (lanes 1 - 2), chitin beads showing STAT6 and MxeCBD intein before cleaving with MesNA. (lane 3), pure STAT6 MesNa  $\alpha$ -COSR after cleavage from chitin beads (lanes 4 - 5) shown by an arrow.

Moderately pure STAT6/MxeCBD after Ni-NTA purification was loaded onto chitin beads, which was pre-equilibrated with STAT6 buffer + 0.1% DDM for 3 - 12 h at 4°C. The best results were obtained after 3 h of loading onto chitin beads. Strong binding of the protein with the chitin beads was observed when few amount of suspension of beads with protein were washed with STAT6 buffer, mixed with 2 x SDS, heated for 5 min at 95°C and later analyzed over SDS-PAGE (figure 4.12, D). After loading

## Results

---

suspension of chitin beads and protein, beads were washed with STAT6 buffer three times the bead volume. MesNA (~250 mM) was used to cleave the intein from STAT6. The amount of MesNA was varied to observe the yield of STAT6 MesNa  $\alpha$ -COSR. Higher concentration of MesNA lead to precipitation of the protein. The transthoesterification reaction was monitored before and after cleavage of the protein from the chitin beads by SDS-PAGE by heating the chitin beads as described above. The shift in the pure STAT6 MesNa  $\alpha$ -COSR band (figure 4.12, D, lane 4 and 5) compared to the non-cleaved STAT6MxeCBD on the SDS-PAGE (figure 4.12, D, lane 3) shows the successful transthoesterification reaction.

Concentration of protein at every step of purification was determined by using Bradford assay or by comparing the protein band against the standard LMW-bands from SDS-PAGE. Calculated yield of STAT6 MesNa  $\alpha$ -COSR after Bradford's test corresponds to 1 mg/ml from 9 l of culture corresponding to the concentration of 1 g/l calculated from Expasy, Prot pram.

It was necessary to purify STAT6 MesNa  $\alpha$ -COSR without detergent as it interfered with the interpretation of many bioactivity experiments as described in the section 4.3.2. Only once STAT6 MesNa  $\alpha$ -COSR was purified in absence of detergent and many bioactivity (DNA binding) experiments could be carried out without any problems. However, it was observed that purification of STAT6 MesNa  $\alpha$ -COSR was very challenging since in the absence of detergent protein was very unstable as precipitation being the major difficulty. Precipitation occurred at various stages, e.g. as during dialysis to remove imidazole from the protein solution. Hence, to avoid precipitation from dialysis, STAT6MxeCBD was loaded directly onto the chitin beads but later protein precipitated while concentrating the cleaved protein as thioester.

Precipitation was also seen while protein solution was stored on ice. Protein stabilizers such as DDM and Glycerol were tested during various stages of purification starting from the lysis of the bacterial cells, during Ni-NTA purification and finally during cleavage of the protein from the intein through chitin beads.



## Results

---

Best condition was found to be when stabilizers were used during lyses of bacterial cells and throughout the purification steps. Concentration of detergent (DDM) was reduced from 0.1% - 0.05% that avoided the precipitation in larger scale however; any amount of detergent was not compatible with EMSA experiments as described in 4.3.2. Hence, it was necessary to obtain native STAT6 MesNa  $\alpha$ -COSR in detergent free buffer to generate semisynthetic STAT6 protein. Several techniques to remove detergent as well as to purify STAT6 in detergent free buffer by using different other stabilizers were performed. First step was to use EMSA compatible stabilizers such as using Arg - glutamate (1:1) but it was not found to be the best method since peptide **1** was inseparable which was ligated to obtain semisynthetic truncated STAT6 (aa 1 - 668). Stabilizer such as Glycerol (25% - 50%) in STAT6 buffer was found to be the best stabilizer. The yield of purification was enhanced since in presence of DDM the yield of the protein was only 1 mg in total volume of 1 ml and in presence of 50% glycerol the total volume was 4 ml containing same concentration of protein 1 mg/ml. In addition, the DNA binding assay experiments could be carried out efficiently (section 4.3.2).

Next challenging part was to generate largest semisynthetic truncated STAT6 variants by mixing STAT6 MesNa  $\alpha$ -COSR and peptide variants, which followed the general method of chemoselective ligations. It was challenging to generate these semisynthetic variants since it involved many chemical and biochemical steps along with purification in each step. STAT6 stability during ligations and bioactivity test after ligations would be the essential elements to investigate. Below are the detailed description of the six variants of semisynthetic truncated STAT6-(**1-6**) obtained from six different peptides **1-6** are described.

## Results

### 4.2.2 Preparation of STAT6-1

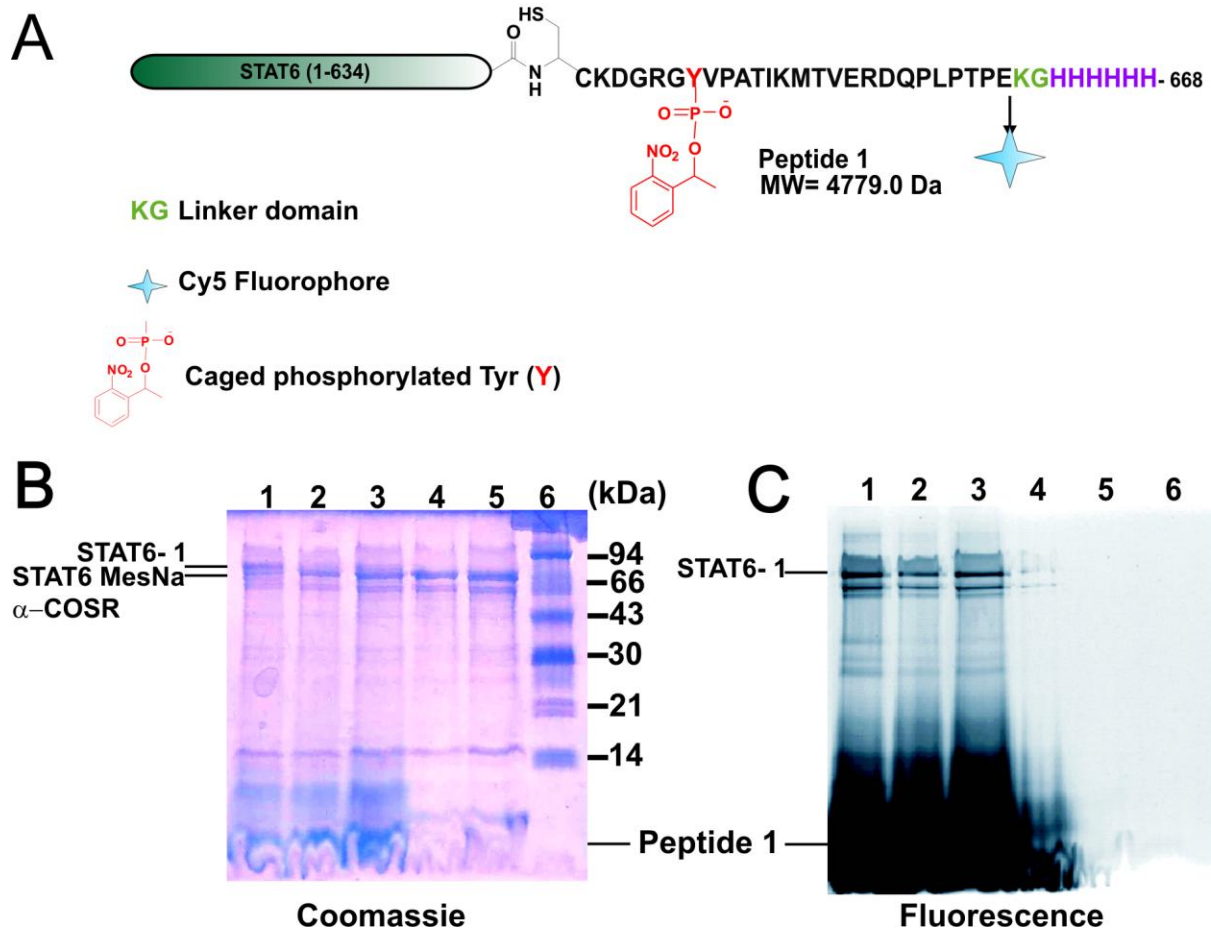


**Figure 4.13: NCL of STAT6-1**

**A:** Schematic representation of semisynthetic truncated STAT6-1. **B:** Ligation of STAT6 MesNa  $\alpha$ -COSR protein with peptide 1 was monitored by SDS-PAGE (lanes 1 - 3), STAT6 MesNa  $\alpha$ -COSR protein without peptide 1 (lanes 4, 5) and LMW (lane 6). **C:** Fluorescence scans of the corresponding gel at ex: 635 nm and em: 670 nm.

The first variant of STAT6-1 was obtained by ligating recombinant STAT6 MesNa  $\alpha$ -COSR (72 kDa) with peptide 1 (4.7 kDa) as shown in figure 4.13. STAT6-1 was assumed to behave as a monomer and was used for the decaging experiments (*in vivo*), which is described in section 4.3.1 and 4.3.3. To obtain this variant, STAT6 MesNa  $\alpha$ -COSR in 1 mg/ml concentration was mixed with excess of peptide 1 in the

## Results

---

presence of MesNa (200  $\mu$ M), STAT6 buffer + 0.1% DDM. Ligation mixture was rotated at room temperature in the dark. Each day the ligation was monitored by SDS-PAGE (shown by an arrow in figure 4.13, A) which was first scanned by fluorescence scanner at ex: 635 nm, em: 675 nm (figure 4.13, B) and subsequently stained with Coomassie.

Detection of the ligation product was facilitated by the presence of the fluorophore since fluorescent bands at the molecular weights corresponding to STAT6-1 could be seen (figure 4.13, B and lanes 1 - 3) when compared with the lanes showing no fluorescent band which was loaded with non-labeled STAT6 MesNa  $\alpha$ -COSR (figure 4.13, B, lanes 4 - 5). Ligation reaction was performed until the STAT6 MesNa  $\alpha$ -COSR band had completely disappeared along with the reduction of the band peptide **1** from the bottom of the SDS-PAGE. Coomassie stain of the SDS-PAGE showed ~95% formation of the ligated STAT6-1 after 72 h of overall reaction time. The difference in the protein band shift on the SDS-PAGE between ligated product and the STAT6 MesNa  $\alpha$ -COSR along with the fluorescent band proved the successful formation of STAT6-1. Scanning of the gel could only provide evidence of successful ligation reaction. STAT6-1 is in the monomeric form due to the caged group on phosphorylated Tyr<sup>641</sup>.

STAT6-1 was purified via Ni-NTA matrix by taking advantage of the His<sub>6</sub>-tag attached at the C-terminal region of the ligated protein to remove excess of STAT6 MesNa  $\alpha$ -COSR. Ni-NTA purification was carried out similarly to the procedure described for STAT6 MesNa  $\alpha$ -COSR purification. All the steps were analyzed by 10% SDS-PAGE. Gels were first scanned by fluorescence scanner and later stained with Coomassie. STAT6 MesNa  $\alpha$ -COSR was separated from the STAT6-1 but unreacted peptide **1**, which has a His<sub>6</sub>-tag at its C-terminus, could not be separated by this method. Final yield of STAT6-1 was 35%. Since STAT6-1 was constructed for *in vivo* experiments to obtain, pure protein was essential. Hence, to remove excess of peptide **1** different purification methods via NAP<sup>TM</sup>-5 column, Sephadex column, capture beads and ultracentrifugation was performed which are described below.

## Results

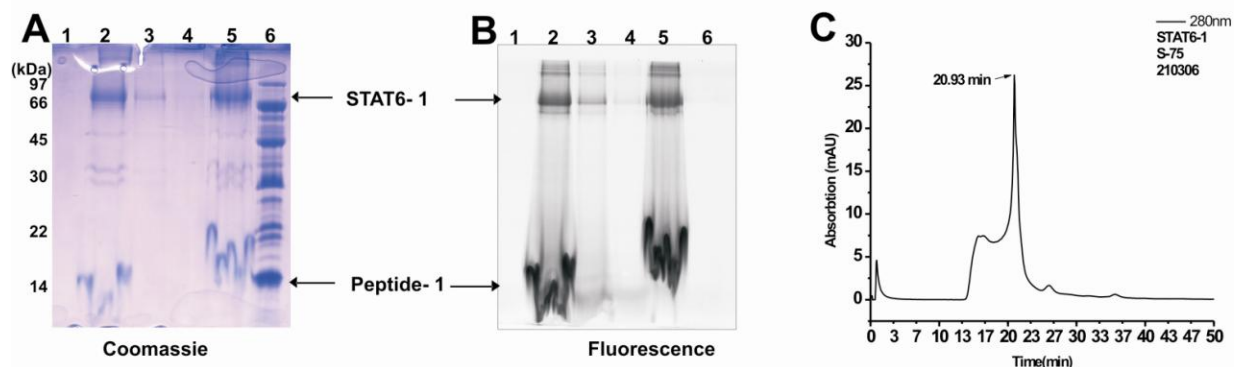


**Figure 4.14: Purification of STAT6-1 by NAP<sup>TM</sup>-5 and S-75**

**A:** Purification of STAT6-1 by NAP<sup>TM</sup>-5 column was monitored on SDS-PAGE. First elution from NAP<sup>TM</sup>-5 column (lane 1). Washings by STAT6 buffer in absence of detergent first washing shows the presence of both STAT6-1 and peptide 1 (lane 2), second and third washing from the column shows presence of minor amount of STAT6-1 (lanes 3 and 4). Final elution from the column containing both STAT6-1 and peptide 1 (lane 5), LMW (lane 6) **B:** Fluorescence of the corresponding gel. **C:** Gel filtration of STAT6-1 on S-75 analytical column and STAT6-1 was eluted together with peptide 1 at 20.93 min.

NAP<sup>TM</sup>-5 columns containing Sephadex with 5 kDa cutoff size were generally used for purification of oligonucleotides, DNA fragments, desalting and buffer exchange was equilibrated with STAT6 buffer + 0.1% DDM and loaded with the ligation product by gravity flow. The column was first washed with the loading buffer. Prior to loading of STAT6-1 over the column the protein was rotated on table top rotating wheel at 4°C with bio-beads which has a capacity to adsorb detergent. STAT6-1 (50 µl) was loaded to the column in a maximum volume of 0.5 ml volume with the STAT6 buffer in absence of detergent (as described in the company protocol). The eluted volume was concentrated by ultra filtration with 5 - 30 kDa molecular weight cutoff and analyzed over SDS-PAGE. Gels were first scanned by fluorescent scanner to observe Cy5 labeled protein bands followed by Coomassie staining. Filtrate showed the presence of both peptide 1 with STAT6-1 protein (figure 4.14, A and B, lanes 2 and 5 shown by an arrow) showing no separation of peptide 1 from the STAT6-1.

Further separation of STAT6-1 from excess of peptide 1 was attempted by gel filtration through Sephadex S-75 gel filtration column (figure 4.14, C). The gel filtration column

## Results

---

was equilibrated with STAT6 buffer + 0.1% DDM. It was observed that STAT6-1 (75 kDa) eluted together with the peptide **1** (Figure 4.14, C) and no separate peak for peptide **1** was observed. These experiments were repeated with detergent-free buffer. The eluted volume was concentrated by ultra filtration with 5 - 30 kDa molecular weight cutoff and the concentrated samples were analyzed on SDS-PAGE. Protein bands were detected first by fluorescence detector and later stained by silver staining. STAT6-1 (75 kDa) eluted together with the peptide **1** (4.7 kDa despite of the larger difference in size). This behavior can be explained by the formation of detergent micelle in the sample solution that changed the elution peak during the course of purification. Since peptide could not be separated by gel filtration it was not considered a probable method for purification and was not further used for optimization of the purification method.

The semi purified STAT6-1 protein was further purified via capture beads that specifically capture peptide with N-terminal free Cys. Capture beads were prepared freshly and washed with STAT6 buffer + 0.1% DDM before loading them with STAT6-1. Free peptide **1**, which has an N-terminal L-Cysteine, should form a thiozolidine with the aldehyde group on the capture beads (section 3.2.8). Ligated protein was incubated with capture beads for 4 - 12 h at 4°C. The protein was filtered and beads were washed 10 times the column volume. Capture beads turned blue in color due to the Cy5 labeled peptide indicating the success of the capture reaction. The eluted fraction was analyzed via SDS-PAGE and monitored first by fluorescence later gel and subsequent silver staining. SDS-PAGE showed the peptide band at the bottom of the gel showing that the capture beads were not able to remove all of the peptide **1** from the ligation.

## Results

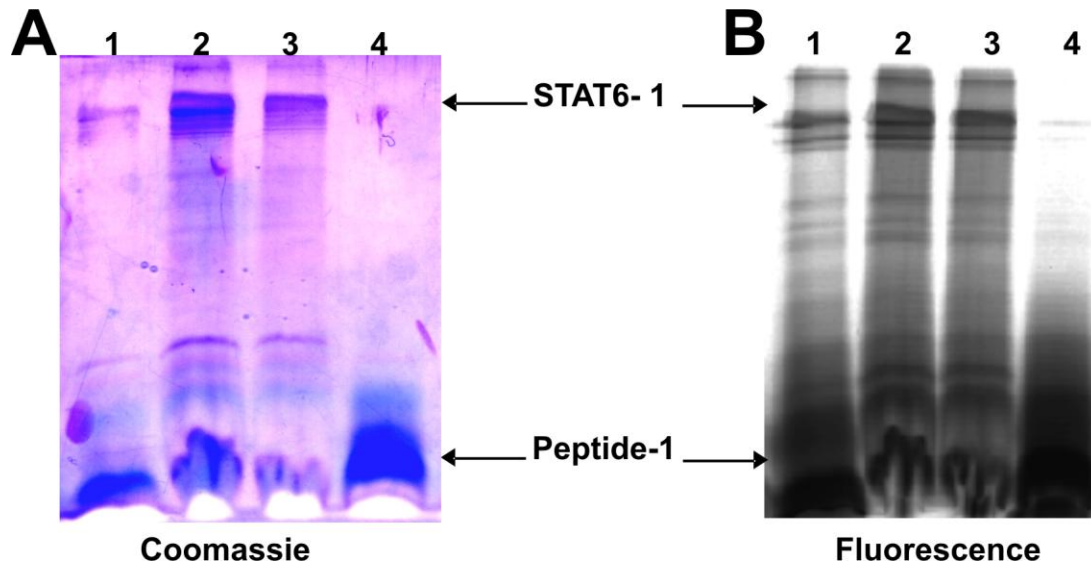


**Figure 4.15: Ultrafiltration of STAT6-1**

**A:** Coomassie stains of STAT6-1 before purification over Ni-NTA (lane 1). Ultrafiltration removed large amounts of peptide (lanes 2 - 3) as compared from lane 1. Peptide 1 as an elution from ultrafiltration (lane 4). **B:** Cy5 fluorescence scans of the corresponding gel.

The STAT6-1 was further purified by using ultrafiltration with a 50 kDa molecular weight cutoff where 80% of the peptide was removed by washing several times with detergent-free STAT6 buffer. The eluted fractions were checked by SDS-PAGE, which were fluorescently scanned and later stained by Coomassie. As shown in figure 4.15, A and B, lanes 2 - 3 minor amount of the peptide was always seen along with the protein which was assumed not to interfere with the *in vivo* and *in vitro* analysis of the protein. Fluorescence scan of the corresponding gel clearly shows the presence of peptide 1 due to the presence of Cy5 in peptide 1 before ultrafiltration (figure 4.15, A and B, lane 1) and absence of the same after ultrafiltration (figure 4.15, A and B, lane 2 and 3). Figure 4.15, B, lanes 1 containing STAT6-1 before ultrafiltration when compared with figure 4.15, B, lane 4 containing the elution from ultrafiltration showed approximately same Cy5 intensity due to the presence of excess peptide 1. Figure 4.15, B, lanes 2 and 3 shows the reduction in the intensity of Cy5 (shown by an arrow). Due to the ultrafiltration concentration of STAT6-1 had increased when compared to (figure 4.15) lane 1 against lane 2 and 3. The wavy shape of the band containing peptide 1 on the SDS-PAGE (figure 4.14 and 4.15) was seen due to the presence of high concentration

## Results

of DDM that accumulated during the ultracentrifugation step of STAT6-1. This indicates the presence of DDM in the STAT6 buffer.

### 4.2.3 Preparation of STAT6-2

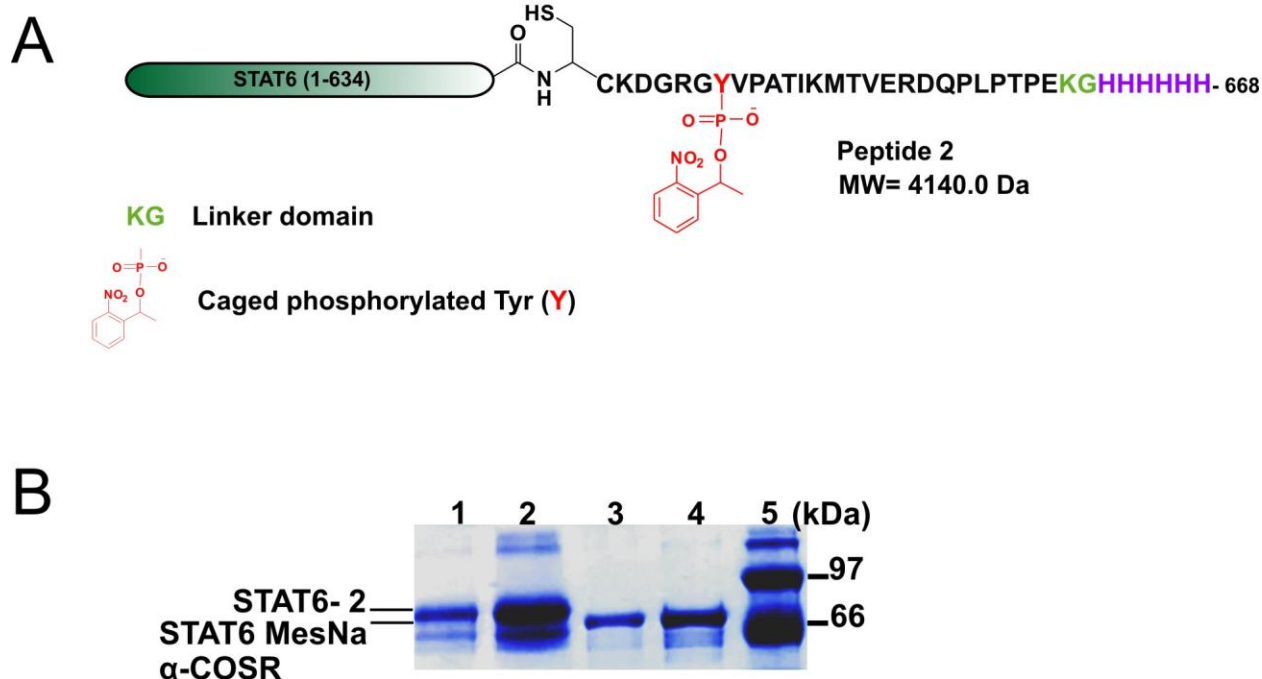


Figure 4.16: NCL of STAT6-2

**A.** Schematic representation of semisynthetic truncated STAT6-2. **B.** Ligation between STAT6 MesNa  $\alpha$ -COSR protein with peptide 2 monitored by SDS-PAGE to generate STAT6-2 (lanes 1, 2) shown by an arrow. STAT6 MesNa  $\alpha$ -COSR without peptide 2 (lanes 3, 4) and LMW (lane 5).

To study the decaging of the caged phosphorylated Tyr<sup>641</sup> *in vitro* STAT6-2 was generated, which was assumed to behave in monomeric form. This variant was used for DNA-binding assays and investigating the decaging of photolabile group using EMSA and western blot methods respectively. STAT6 MesNa  $\alpha$ -COSR was ligated with peptide 2 to form STAT6-2. It was synthesized following the similar protocol as described for STAT6-1 (section 4.2.2). An arrow in figure 4.16 indicates the ligation product, lanes 1 - 2. The difference in the protein band shift between the ligation product and the STAT6 MesNa  $\alpha$ -COSR on SDS-PAGE confirmed the successful formation of

## Results

---

the ligation product. The ligation was carried out for 72 h, and gave yield of ~95% from SDS-PAGE analysis. Final yield of STAT6-2 after purification was ~33%. Peptide **2** was also inseparable from STAT6-2 like peptide **1** from STAT6-1. Ligation was carried out in the presence of two different stabilizers like DDM 0.1% and glycerol 50%. It was necessary to find to different stabilizers since DDM interfered in interpretation of results in bioactivity test. More details for changing the buffer from DDM to glycerol are as described in section 4.3.2.

STAT6-2 in presence of 50% glycerol was not purified by Ni-NTA matrix. Since this variant was used to investigate the decaging of photolabile group by western blot methods which requires SDS-PAGE. It was hypothesized that presence of excess of peptide **2** would not interfere in determining the decaging reactions since decaged STAT6-2 having 75 kDa will not migrate faster than peptide **2** (4140.0 Da) over SDS-PAGE. Second advantage of not separating peptide **2** from STAT6-2 was that large amount of ligated product would be available for the investigation.

### 4.2.4 Preparation of STAT6-3

STAT6-3 was assumed to be in the dimeric form due to its free phosphate group on Tyr<sup>641</sup> and can mimic the native STAT6 found in physiological system. The benefit of the presence of Cy5 in STAT6-3 was utilized for FRET experiments to study the kinetics of dimerization as a control for the cell assays. STAT6-3 was generated by ligation between STAT6 MesNa  $\alpha$ -COSR and peptide **3** following similar conditions as described for ligation **1** in dark due to the presence of Cy5.



## Results

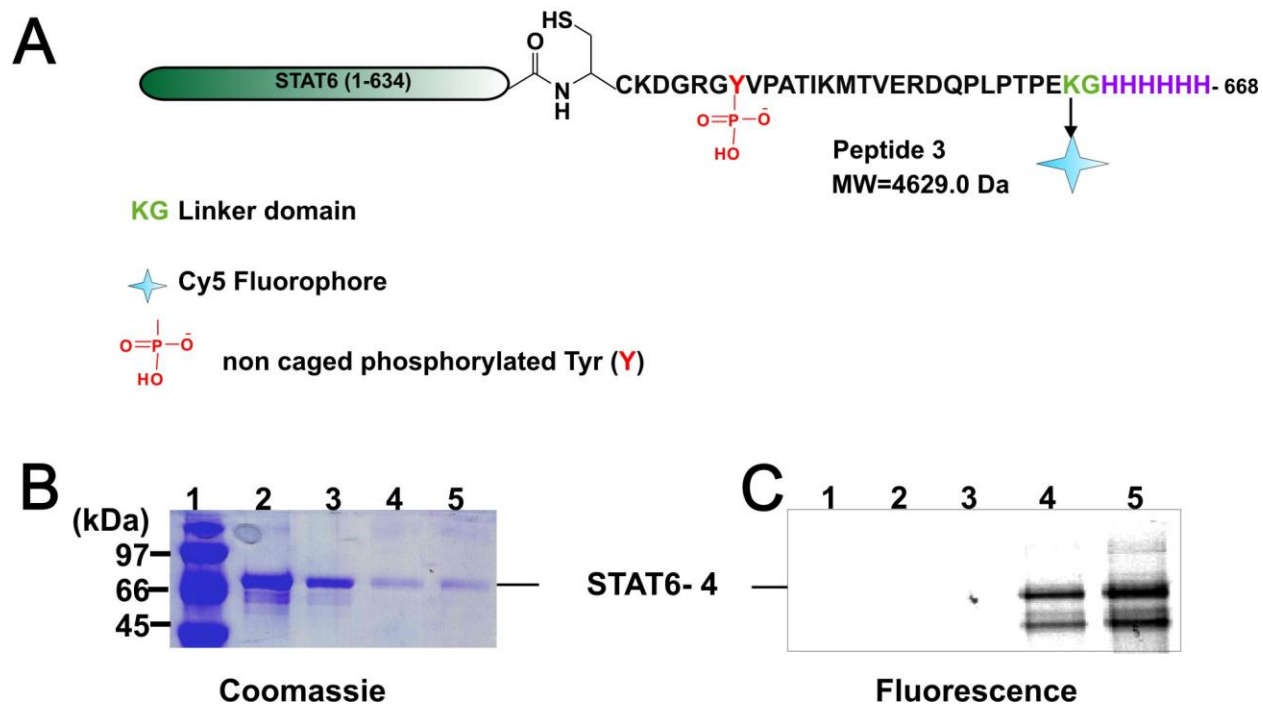


**Figure 4.17: NCL of STAT6-3**

**A:** Schematic representation of semisynthetic truncated STAT6-3. **B:** Ligation of STAT6 MesNa  $\alpha$ -COSR (lanes 2 and 3) without the presence of the peptide, STAT6 MesNa  $\alpha$ -COSR protein (lanes 4 and 5) and peptide 3 and LMW (lane 1). **C:** Fluorescence scanning of the corresponding gel at ex: 635 nm, em: 670 nm shows the ligation between STAT6 MesNa  $\alpha$ -COSR protein with peptide-3 (lanes 4 and 5) shown by an arrow, whereas shows lanes (2 - 3) no fluorescence band.

The ligation product is shown in figure 4.17 by an arrow. The formation of the ligation was analyzed by the presence of fluorescence band from Cy5 (figure 4.17, B and lanes 4 - 5) and absence of Cy5 bands (figure 4.17, B and lanes 2 - 3) which were loaded with STAT6 MesNa  $\alpha$ -COSR. The presences of minor fluorescence band below the ligation product were always seen which could be due to the COSR artifacts. The shift in the protein band between STAT6-3 and STAT6 MesNa  $\alpha$ -COSR on Coomassie staining over 10% SDS-PAGE was not observed very clearly since ligation product was not concentrated to avoid precipitation of protein during concentration step. In addition, a very small difference in the molecular weight of the peptide 3 and STAT6-3 made it difficult to analyze the difference in the band shift by Coomassie staining. The ligation yield was ~30% from SDS-PAGE analysis since loss in yield occurred during the Ni-

## Results

NTA purification. The ligation product was purified over Ni-NTA matrix and final yield was ~36%.

### 4.2.5 Preparation of STAT6-4

To study the dimeric behavior of STAT6 protein STAT6-4 was synthesized without the presence of Cy5. This variant like STAT6-3 was assumed to be also in dimeric form due to the phosphate group on Tyr<sup>641</sup> mimicking the native STAT6. It behaved as a very good positive control in western blot experiments against the decaging of NPE group for STAT6-1. STAT6-4 was also used for DNA-binding assays. Hence, this was one of the essential semisynthetic truncated STAT6 variant that was generated.

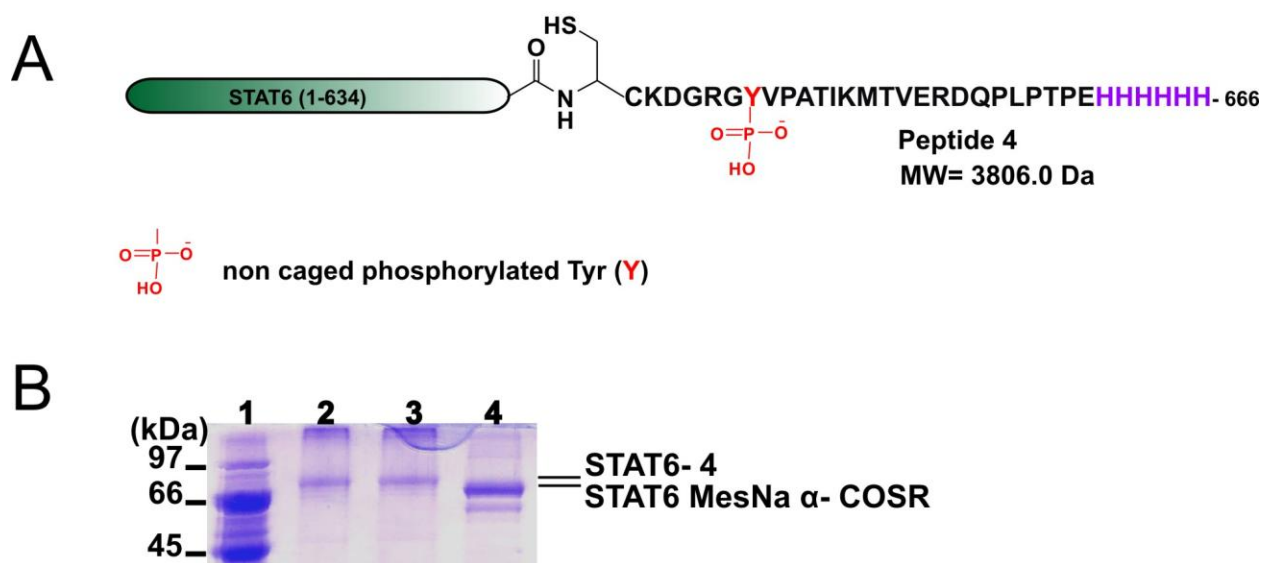


**Figure 4.18: NCL of STAT6-4**

**A.** Schematic representation of semisynthetic truncated STAT6-4. **B.** Ligation of STAT6 MesNa  $\alpha$ -COSR protein with peptide 4 was monitored by SDS-PAGE (lanes 2, 3) shown by an arrow, STAT6 MesNa  $\alpha$ -COSR protein without the presence of the peptide (lane 4) and LMW (lane 1).

STAT6 MesNa  $\alpha$ -COSR was ligated with peptide 4 to form STAT6-4 following the similar method used for STAT6-1. Due to the absence of any fluorophore, the formation of ligation product was analyzed by the shift in the band between STAT6-4 and STAT6 MesNa  $\alpha$ -COSR via SDS-PAGE (figure 4.18, B). Only 48 h were needed to generate

## Results

STAT6-4. Final yield of STAT6-4 after Ni-NTA purification was ~20%. Here again peptide **2** was unable to separate but it was not of much concern since this was not designed to be used for any *in vivo* experiments as it lacks fluorophore. STAT6-4 was used for DNA binding assays where it was necessary to remove DDM because it interfered with interpretation of data from DNA-binding assays. Ligation was carried out in presence of two different stabilizers (DDM 0.1% or glycerol 50%) due to the problems as described in section 4.3.2 with protein stability. Ligation product in presence of 50% glycerol was not purified via Ni-NTA matrix as explained in section 4.2.3. Consequently, good amount of STAT6-4 was generated after ligation, which can be used for further experiments such as for western blots and DNA-binding assays as described in sections 4.3.1 and 4.3.2 respectively.

### 4.2.6 Preparation of STAT6-5

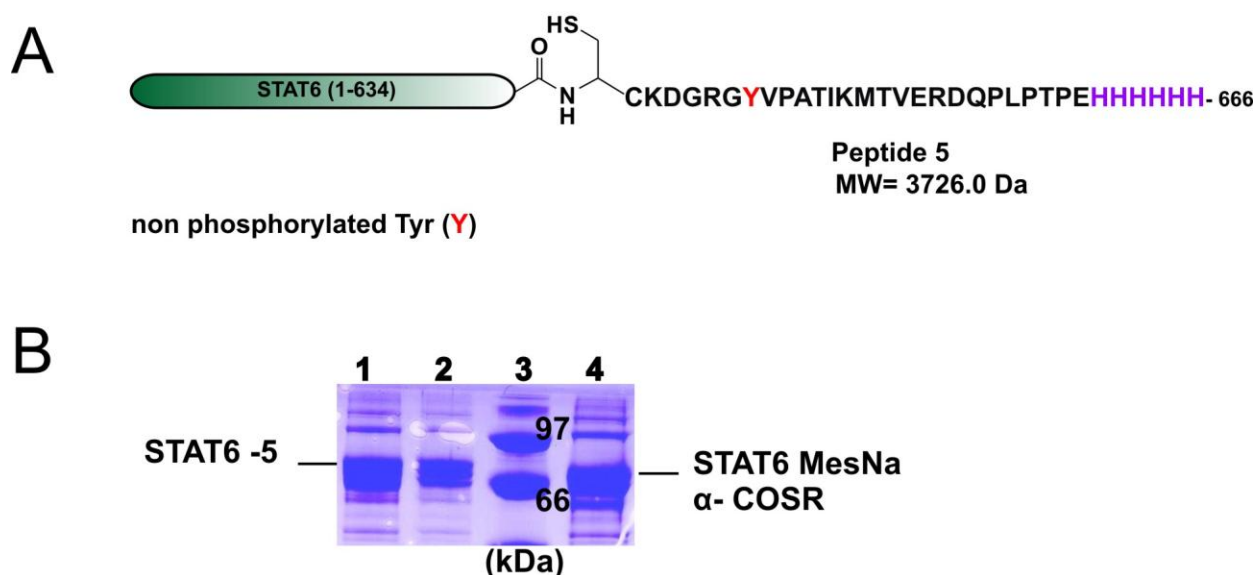


**Figure 4.19: NCL of STAT6-5**

**A:** Schematic representation of semisynthetic truncated STAT6-5. **B:** Ligation of STAT6 MesNa  $\alpha$ -COSR protein with peptide **5** was monitored by SDS-PAGE (lanes 1 and 2) shown by an arrow. STAT6 MesNa  $\alpha$ -COSR without peptide **5** (lane 4) and LMW (lane 3).

## Results

The wild type variant of STAT6 (STAT6-5) contains a non-phosphorylated Tyr in position 641, which was generated by mixing STAT6 MesNa  $\alpha$ -COSR and peptide 5 using the similar conditions as for previous ligations. STAT6-5 was assumed to behave as monomer due to the non-phosphorylated Tyr<sup>641</sup>. The presence of new band above 66 kDa from the formation of STAT6-5 figure 4.19, B, lanes 1 and 2 shows the successful NCL reaction after STAT6-5 was purified with Ni-NTA superflow beads to remove unreacted STAT6 MesNa  $\alpha$ -COSR. After purification, the ligation yield of STAT-5 was ~ 25% observed from SDS-PAGE analysis. Ligation was carried out in two different stabilizers such as DDM 0.1% and 50% glycerol as described in section 4.2.3. Ligation product in presence of 50% glycerol was not purified by Ni-NTA matrix, which is explained in detail in section 4.2.3.

### 4.2.7 Preparation of STAT6-6

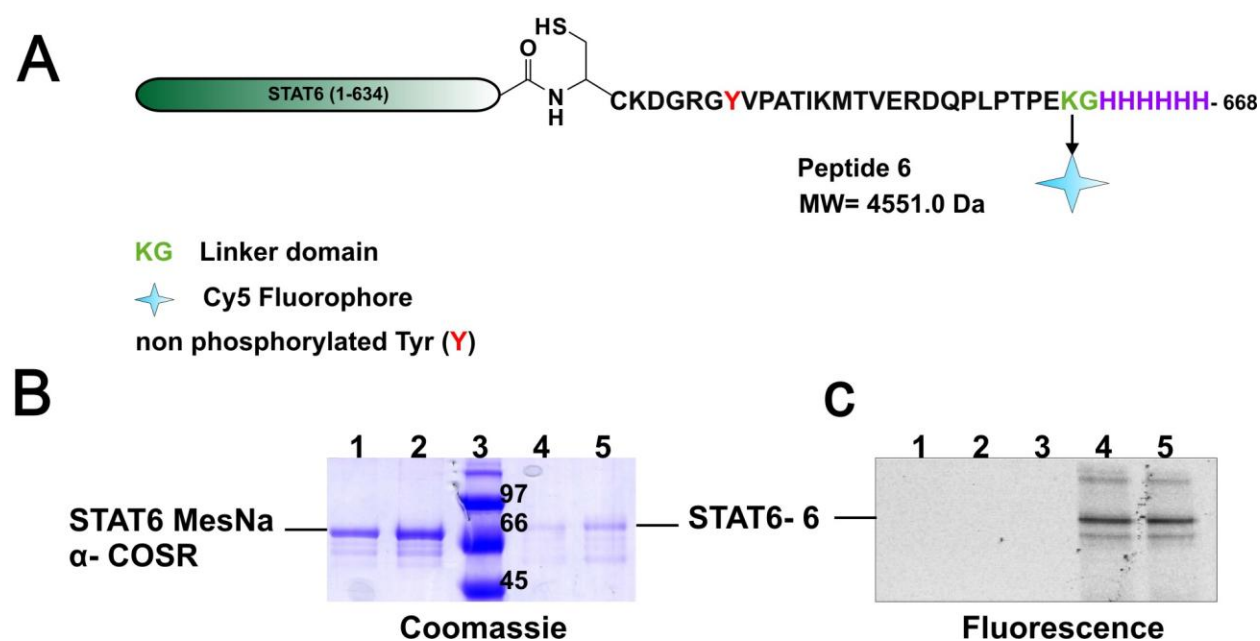


**Figure 4.20: NCL of STAT6-6**

**A:** Schematic representation of semisynthetic truncated STAT6-6. **B:** STAT6 MesNa  $\alpha$ -COSR protein without the presence of the peptide 6 (lanes 1, 2), LMW (lane 3) and ligation of STAT6 MesNa  $\alpha$ -COSR protein with peptide 6 (lanes 4, 5) shown by an arrow was monitored by SDS-PAGE. **C:** Fluorescence scanning of the corresponding gel at ex: 635 nm em: 670 nm shows the ligation between STAT6 MesNa

## Results

---

$\alpha$ -COSR protein with peptide **6** (lanes 4, 5) shown by an arrow whereas lanes (2, 3) shows no fluorescence band.

STAT6-**6** was a fluorescent derivative of STAT6-**5**. STAT6 MesNa  $\alpha$ -COSR was ligated with peptide **6** following the similar scale and conditions as described for ligation of STAT6-**1**. The ligation product is shown in figure 4.20, B, lanes 4 and 5 by an arrow. The ligation product was observed by the presence of Cy5 fluorescence and the difference in the protein band shift of the ligation product and the STAT6 MesNa  $\alpha$ -COSR shows the successful NCL reaction. Yield reduces during the purification during Ni-NTA chromatography and final yield was ~25%. Ligation was carried out in two different stabilizers such as DDM 0.1% and glycerol 50% as described in above sections. Ligation product in presence of glycerol 50% was not purified by Ni-NTA matrix, which is explained in detail in section 4.3.1

## Results

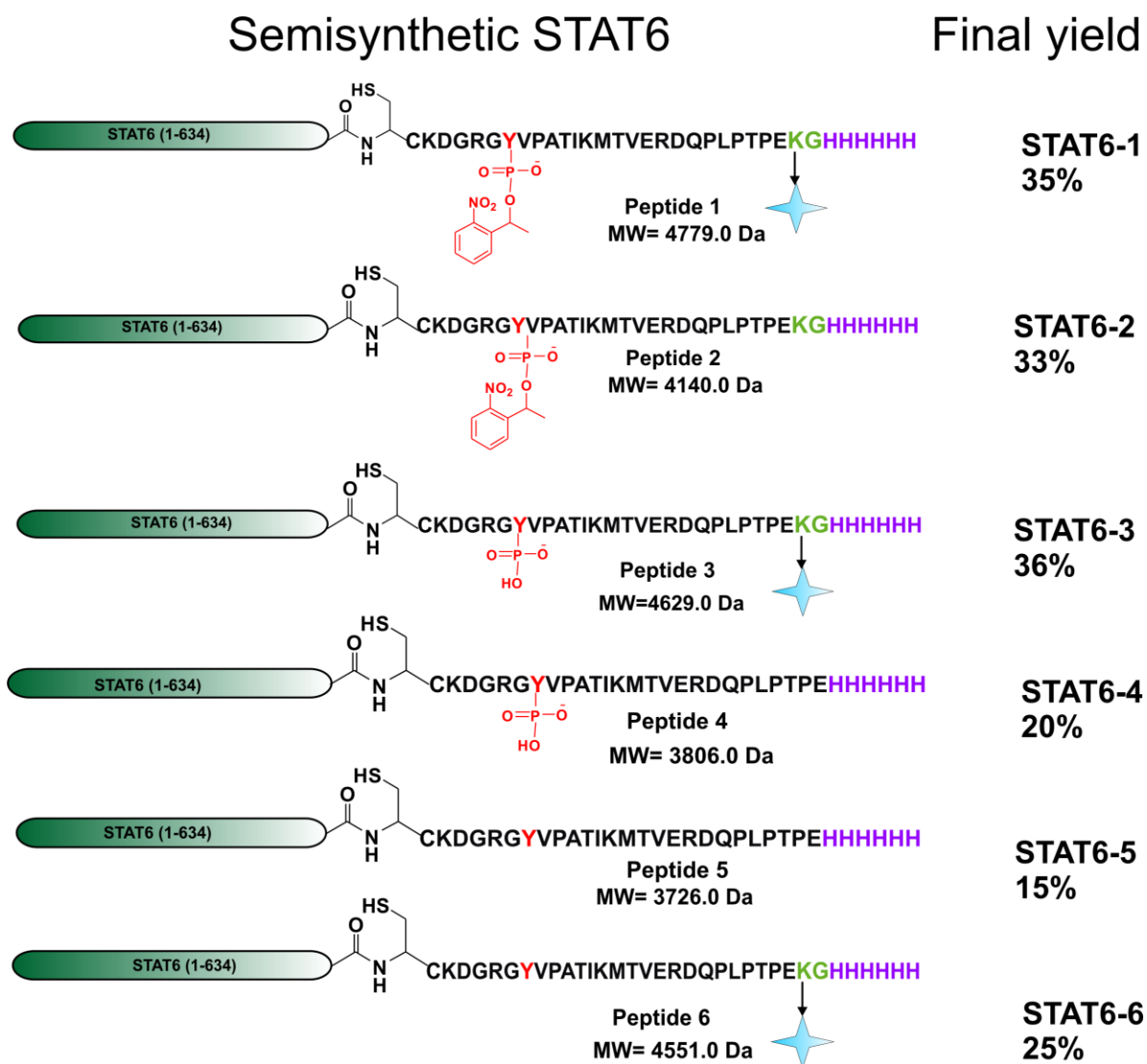


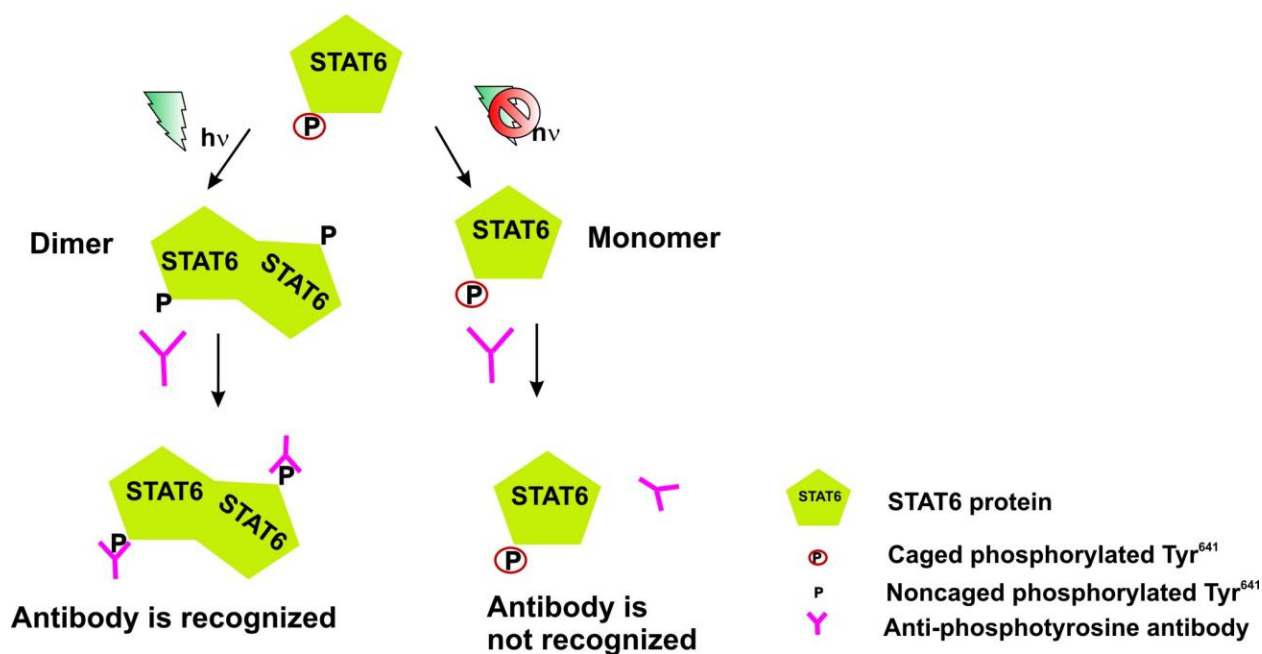
Figure 4.21: Different semisynthetic STAT6 -(1-6) with their final yields after purification.

Figure 4.21 shows the final yields of semisynthetic truncated STAT6-(1-6) after ligation of STAT6 MesNa  $\alpha$ -COSR with variants of peptides (1-6) as described in above sections. Next, step was to show the bioactivity of these semisynthetic variants for which first, the decaging of caged group was performed followed by DNA-binding assays and microinjections. These are described in detail in proceeding sections.

## 4.3 Bioactivity of semisynthetic STAT6

### 4.3.1 Decaging of caged phosphorylate tyrosine

Decaging of STAT6-2 will transform this variant into an activated STAT6-2 with free phosphate group on Tyr<sup>641</sup> that will enable it to form an active dimer. The challenging questions such as how the semisynthetic STAT6 will behave during and after exposure to UV light, whether STAT6-2 can perform its physiological activity by behaving like its native form and finally how to determine the photochemical reaction were to be answered. As shown in figure 4.22, decaged STAT6 should bind to a specific phospho tyrosine-HRP antibody which can be easily monitored by western blotting.



**Figure 4.22:** A phospho tyrosine specific antibody is used to test removal of the caging group on STAT6 variants.

Removal of the caged group by UV light converts the bio-inactive STAT6-1 into its activated dimeric form with a phosphorylated tyrosine. The decaged phospho tyrosine can be efficiently detected by western blotting using a specific anti-phospho tyrosine antibody. Caged phosphorylated STAT6 which has not been exposed to UV light should not bind to the antibody.

## Results

---

The concentration of anti-phospho tyrosine-HRP antibody to bind free phosphate group and its efficiency was determined using peptides **2** and STAT6-4 consisting of phosphorylated tyrosine as positive control and peptide **3** and **5** consisting of caged phosphorylated tyrosine and non phosphorylated Tyr was used as negative control for dot blot experiments. As shown in the scheme in figure 4.22, the decaged STAT6 should bind to a phospho tyrosine specific antibody which can be monitored by western blotting. Peptides **2**, **3**, peptide **5** and STAT6-4 were loaded directly onto a nitrocellulose membrane. 1  $\mu$ l from stock solution of peptide **3** (2.65  $\mu$ M, 12.2  $\mu$ g) was diluted in a series to make final concentration of 2.6 nM (figure 4.23, dot 1), 5.3 nM (figure 4.23, dot 2), 26 nM (figure 4.23, dot 3) and 88 nM (figure 4.23, dot 4) to load 1  $\mu$ l from each stock on nitrocellulose membrane. Figure 4.23, dot 5 contains 1  $\mu$ l from 245  $\mu$ g of peptide **3** stock solution. STAT6-4 (4.4  $\mu$ M, 132  $\mu$ g) at different concentrations ranging from 0.33  $\mu$ g to 3.3  $\mu$ g was directly loaded on nitrocellulose membrane. Peptide **5** from 89  $\mu$ M to 27 nM and Peptide **2** (0.95  $\mu$ g) dot 9 and 10 was used as negative control.

Spots were dried for a few sec and later analyzed by the western blotting with anti-phospho tyrosine-HRP antibody as described in section 3.4.8. The efficient binding of the antibody to peptide **3** (figure 4.23, A) and STAT6-4 (figure 4.23, B) confirmed the presence of phosphorylated Tyr<sup>641</sup>. The negative control for the experiment was carried out with peptide **5** which has no phosphorylated Tyr which did not show any signal after incubation with antibody. Another negative control for the experiment was peptide **2** which has caged phosphorylated Tyr, dot 9 shows a faint binding of phosphorylated Tyr<sup>641</sup> to the antibody as compared with the positive controls and dot 10 donot show any spots confirming the presence of caged phosphorylated Tyr<sup>641</sup>. The appearance of very faint signal from antibody can occur due to the minor exposure of the caged group in the visible light during loading of the sample (Figure 4.23, dot 9) which is very difficult to avoid.



## Results

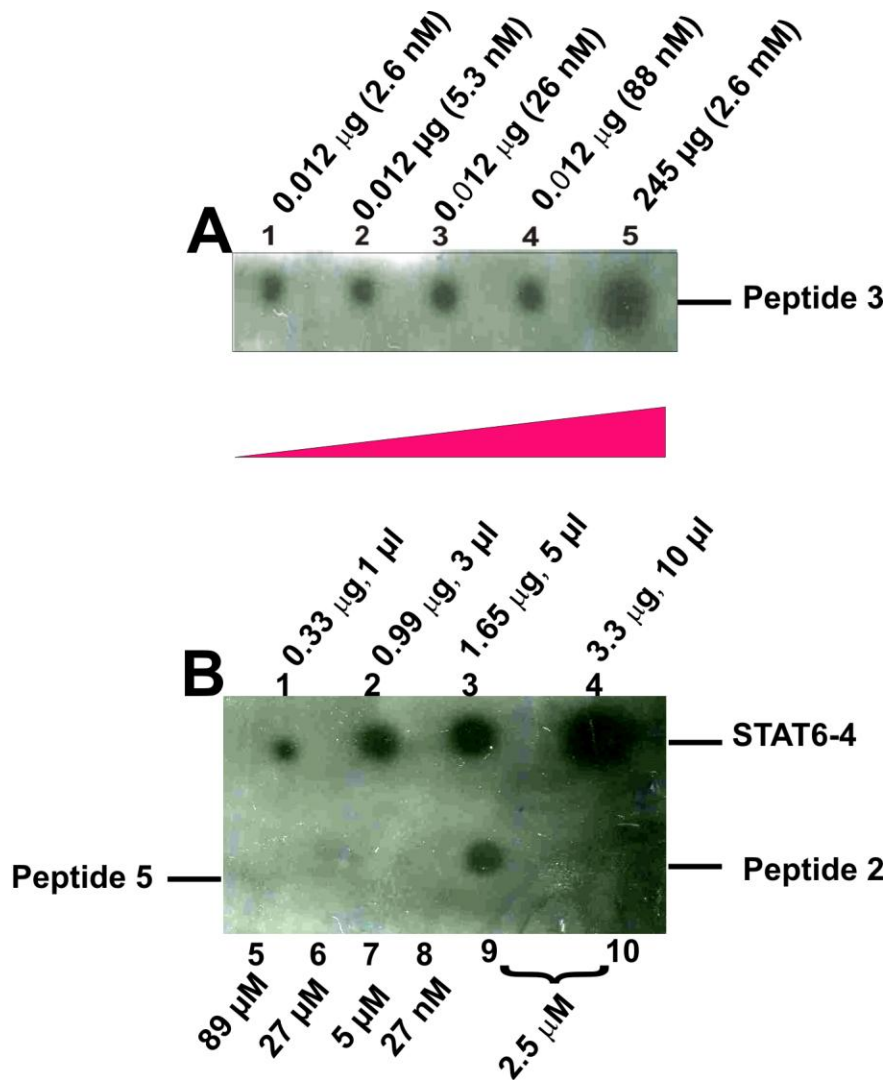


**Figure 4.23: Western dot blot analysis of peptides 2, 3 and STAT6-4**

**A:** Positive control for western blot was performed by using 1 µl of Peptide 3 at different concentration. 2.65 nM (dot 1), 5.3 nM (dot 2), 26.5 nM (dot 3), 88 nM (dot 4), 2.6 mM (dot 5). **B:** 1 µl of STAT6-4 at different concentrations. 0.33 µg (dot 1), 0.99 µg (dot 2), 1.65 µg (dot 3), 3.3 µg (dot 4) and negative control for the same was performed by using 1 µl Peptide 5 89 nM (dot 5), 27 nM (dot 6), 0.05 nM, 0.27 nM and Peptide 2 0.95 µg, 5 µl (dots 9 and 10).

The data suggests that the antibody is very specific for phosphorylated tyrosine of STAT6-3. Figure 4.23, red bar showed the change in the dot intensity from lower to

## Results

---

higher which was due to the increase in the concentration of the peptide **3** and STAT6-4 loaded onto the nitrocellulose membrane.

After obtaining evidence from the dot blot experiment described above for peptides **2**, **3** and STAT6-4 protein it is proved that antibody specific to free phospho tyrosine group can successfully bind to free phosphate group on Tyr<sup>641</sup>. Thus, antibody must detect the formation of free phosphate group on Tyr<sup>641</sup> present in STAT6-2 after its illumination with UV light. The decaging experiment was performed in a plastic cuvette with 5  $\mu$ M of STAT6-2 protein exposed to 800 W UV light for 10 min to ensure complete removal of caged group. SDS-PAGE followed by western blotting resolved the protein. The developed X-ray film shown by an arrow in figure 4.24 indicates a very high intensity band for dimeric and monomeric form of the decaged STAT6-2. Dimers of STAT6 were seen due to the tight binding between themselves which was not separated in the presence of detergents such as SDS. STAT6-2 which was not exposed to UV light had almost no binding to antibody indicating the absence of free phosphorylated Tyr<sup>641</sup>. STAT6-3 was used as a positive control for antibody binding as it has a free phosphate group on Tyr<sup>641</sup>. HMW protein marker which has fluorescent phosphorylase (Invitrogen) binds to the antibody and shows a band after western blotting (figure 4.24, lane 4). Lanes 1 and 3 in figure 4.24 shows STAT6-2 before and after exposure to UV light respectively. A significant increase in antibody binding in lane 3 shows that caged group in STAT6-2 is efficiently uncaged after 10 min of exposure to UV light showing the presence of free phosphate group in Tyr<sup>641</sup>. The very minor signal in figure 4.24 (lane 1) was similar to the signal in figure 4.23 (dot 9) which was due to the accidental removal of the caged group through visual light during the loading of the sample which cannot be avoided.

## Results

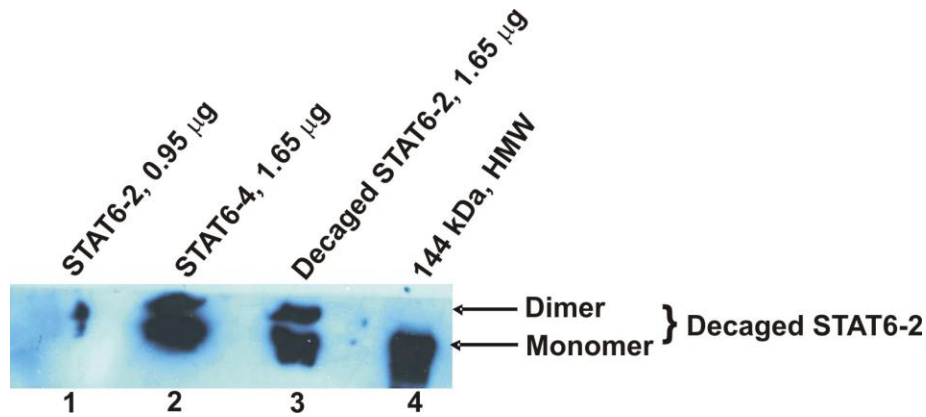


**Figure 4.24. Decaging of STAT6-2**

Western blot analysis on SDS-PAGE after removing caged group from STAT6-2 by flashing UV light of 800 W for 10 min: 0.95 µg of caged phosphorylated STAT6-2 (lane 1), 1.65 µg of phosphorylated STAT6-4 (lane 2), 0.95 µg decaged phosphorylated STAT6-2 (lane 3) and pre-stained HMW 5 µl (lane 4)

Similar western blot experiments were carried out and protein was resolved via 5% non-denaturing gel since it was important to find out the stability of semisynthetic STAT6-2 after exposure to UV light. Decaging experiments were carried out as described above by UV light. The obtained results showed a highly intense band on the X-ray film showing that STAT6-2 is in the native state (figure 4.25, lane 1) as it could migrate within 60 min through non-denaturing gel without any presence of aggregation. Several attempts with the decaging experiments showed the same intense band of STAT6-2 on non-denaturing gel. This can be explained due to the large pore size of the polyacrylamide gel which enables dimeric STAT6-2 (144 kDa) (1.9 µg) to spread over the gel without further migration when compared to STAT6-4 (0.42 µg) non caged phosphorylated Tyr<sup>641</sup> (figure 4.25, lanes 2 and 3) which did not show highly intensity band. The presence of STAT6-4 in native gels was proved by DNA-binding assays, explained in sections 4.3.2 which showed that it can only in the presence of dimeric form can bind to its specific DNA conjugated with Tamra fluorophore.

## Results

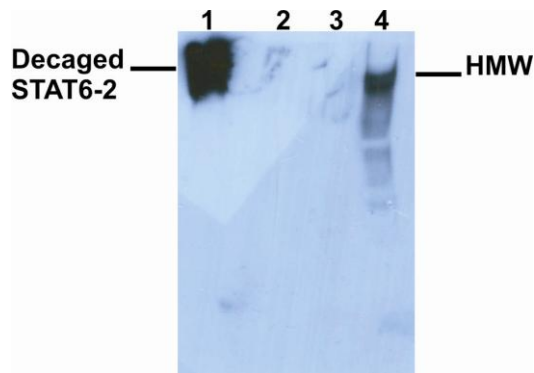


**Figure 4.25: Decaged STAT6-2 in native gel.**

STAT6-2 was decaged and ran over 5% non-denaturing gel followed by western blotting. The high intense decaged STAT6-2 (lane 1) showed that STAT6-2 on exposure to UV light did not precipitate. STAT6-4 (lane 2-3) and HMW (lane 4)

To further examine the release of caged group, *in vitro* analysis was performed. Peptide **7** when exposed to UV 365 nm from a Xe lamp present in a stop flow machine released NPE group in 20 min. Every 10 min sample was collected from the reaction mixture and was monitored via ESI-MS. Peptide **7** having caged phosphorylated Tyr<sup>641</sup> with a deconvoluted mass of  $M_{(obs)} = 4569.0$  Da and  $M_{(obs)} = 4419.0$  Da of the decaged phosphate group after 20 min shows the beginning of photolysis reaction on release of NPE group which converts into a peptide having a free phosphate group (figure 4.26, A). Figure 4.26, B shows the final conversion of the caged phosphate group into free phosphate with 100% yield since no trace of peptide with  $M_{(obs)} = 4569.0$  Da was observed. No external scavenger was added.

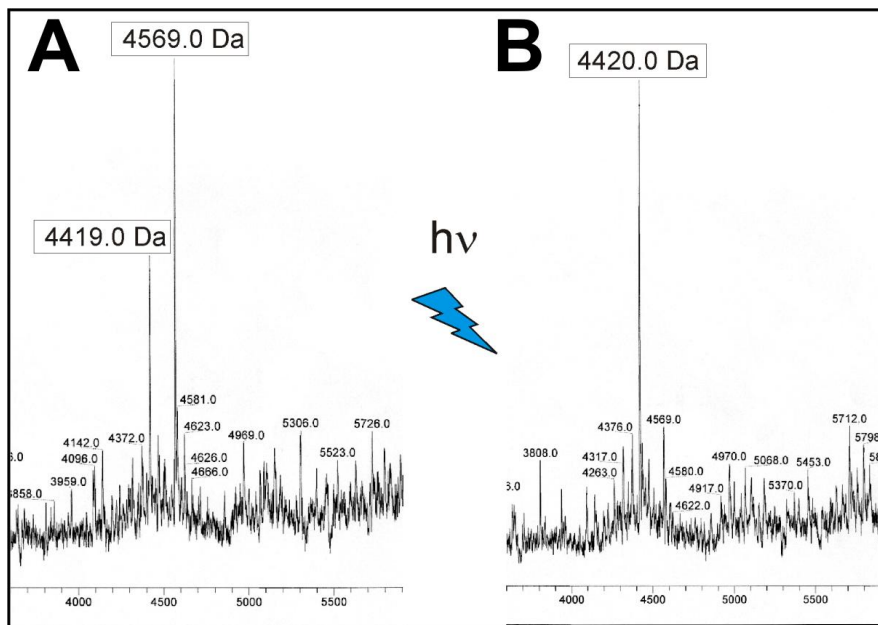


**Figure 4.26: Decaging of peptide 7**

**A:** Decaging of peptide **7** showing the release of NPE group. **B:** Peptide **7** with free phosphate group on tyrosine showing complete photolysis of NPE group.

## Results

### 4.3.2 Binding of STAT6 variants to ds DNA

Western blotting experiments demonstrate the successful decaging of semisynthetic STAT6-2. Further experiments were designed to provide evidence that semisynthetic STAT6 was functionally active to form dimer. From previous results from Georg B Ewert *et al*, 2001<sup>190</sup>, it is known that STATs bind to a consensus sequence known as Gamma activated sequence (GAS), N<sub>2-4</sub> motif 5'-TTCN<sub>2-4</sub>GAA-3' through its DNA binding domain. Other STAT family members do not bind to the sequence recognized by STAT6. To find more proof on semisynthetic STAT6 variants if they depict the specific binding of DNA of native STAT6, EMSA was demonstrated.

*In vivo* binding of STAT6 monomers occurs when they are released from the cytokine receptor tail after JAK/TyK phosphorylates the STAT6 proteins and forms dimers which are translocated to the nucleus where they bind to GAS-DNA to transcribe IL-4/IL-13 responsive genes. This phenomena of STAT6 binding to GAS-DNA can be demonstrated in the following experiments by applying the technique of electrophoretic mobility shift assay (EMSA). This technique was used to demonstrate the biological functionality of semisynthetic truncated STAT6-4 (72 kDa), which is a phosphorylated variant, assumed to form dimer and interact with ds GAS-DNA in its dimeric active form and STAT6-1 which has caged phosphorylated Try<sup>641</sup> was assumed as a monomer which should not bind to ds GAS-DNA (figure 4.27).

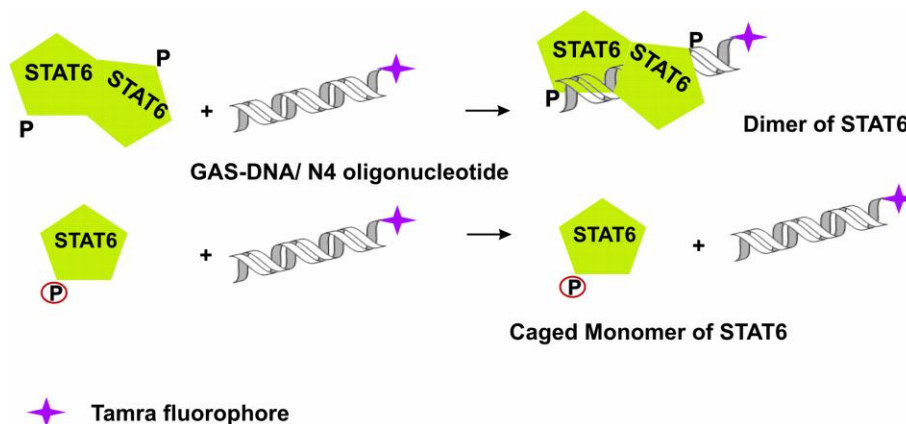


Figure 4.27: STAT6 binds to GAS-DNA

## Results

---

To obtain ds GAS-DNA, two complimentary oligonucleotides of 20 base pairs with (Tamra 5'-TCGACTTCCCAAGAACAGAG-3' and 3'-AGCTGAAGGGTTCTTGTCTC-5') in the (1:1) ratio of 20  $\mu$ M concentration was used. The presence of Tamra on one oligonucleotide allows easy monitoring of STAT6 binding to GAS-DNA with STAT6-4 dimer. The oligonucleotides were heated for 5 min at 95°C and cooled to 37°C in 1 h and immediately stored at 4°C over night. The binding buffer was 10 mM Tris HCl, 1 mM EDTA, 50 mM NaCl in ddH<sub>2</sub>O at pH 7.4 (section 2.6.1). The hybridization of DNA was followed in 12% non-denaturing acrylamide with 60 mV at 0°C and Orange G was used as the loading buffer for single and double stranded oligonucleotides. The gel was later scanned by a fluorescence scanner at Tamra ex: 510 nm, em: 575 nm (figure 4.28, C). The shift in the fluorescence band of Tamra shows the efficient hybridization of the oligonucleotides to form double stranded Tamra labeled GAS-DNA. Fluorescence scan data gives a very accurate detail to monitor the Gel-shift experiments (figure 4.28, C).

Initial tests were carried out with STAT6-4 (5  $\mu$ M), ds GAS-DNA (20  $\mu$ M) in 10  $\mu$ l of binding buffer which was incubated at RT with GAS-DNA at different time intervals protecting it from light to avoid bleaching of Tamra fluorophore. Mixture of STAT6-4 and GAS-DNA after incubation was divided equally (v/v) into two parts in 1.5 ml tube and later loading buffer was added and all samples were run at 100 mV, 0 degrees, via 5% native gel . It was observed that binding between STAT6-4 and GAS-DNA which was not indicated in the first experiment presumably due to micelles generated by DDM as STAT6-4 was stabilized in STAT6 buffer + 0.1% DDM. Recombinant STAT6 was hence purified in detergent free buffer as described in section 4.2. Similar binding reaction was performed in detergent free buffer. Results are shown in figure 4.28, A and B.

## Results

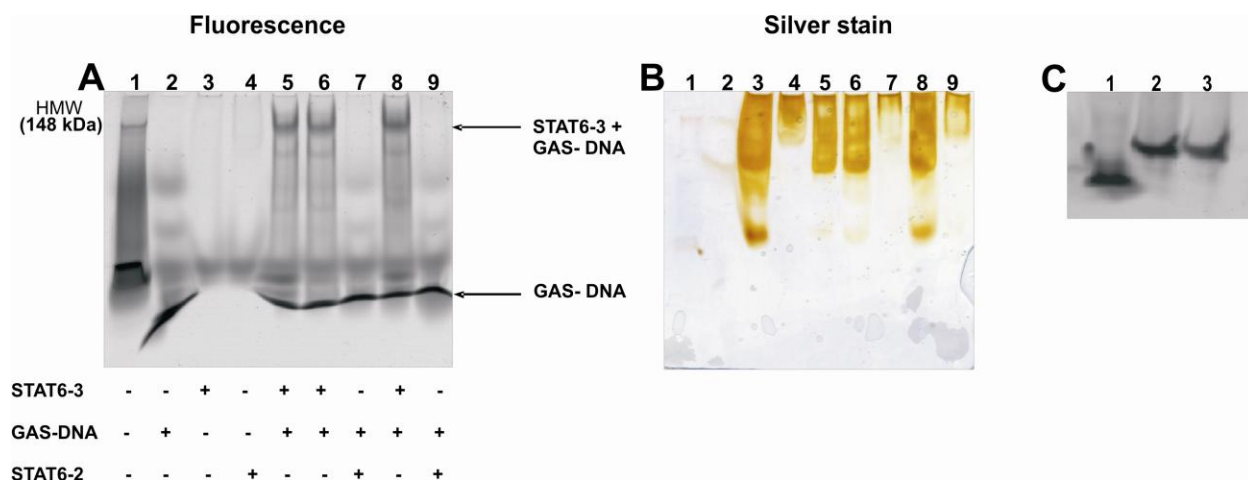


**Figure 4.28: Tamra ds GAS-DNA binding of semisynthetic STAT6-4**

**A:** EMSA analysis was carried out via 5% native gel, 100 mV at 0°C, which was monitored first by fluorescence scanning at ex: 510 nm and em: 575 nm. Binding complex of truncated semisynthetic variant STAT6-4 with Tamra ds GAS-DNA was performed for 5 min, 1 h and 3 h at RT (lanes 8, 6, & 5 respectively) shown by an arrow. The negative control was observed by mixing STAT6-2 with Tamra ds GAS-DNA for 5 min and 1 h (lanes 7 & 9 respectively). STAT6-4 (lane 3), STAT6-2 (lane 4), Tamra ds GAS-DNA (lane 2) shown by an arrow and pre-stained HMW protein marker (lane 1). **B:** Silver stain of the corresponding gel showed presence of the proteins in the absence of ds DNA (lanes 3, 4, 7 & 9). **C:** Hybridization of GAS-DNA was observed by running the DNA and the oligonucleotides over 12% polyacrylamide gels at 0°C, 60 mV. Fluorescence scanning of the corresponding gel at ex: 510 nm, em: 575 nm showed Tamra labeled oligonucleotides (lane 1) and hybridized DNA (lanes 2, 3)

The binding was indicated by a change in electrophoretic mobility of Tamra ds GAS-DNA (figure 4.28, A, lanes 5, 6 and 8) indicating the formation of a complex between semisynthetic STAT6-4 dimer and DNA. The Tamra fluorescence was observed on the top part of the 5% non-denaturing polyacrylamide gel with an excess of DNA at the bottom of the gel. When compared, the new Tamra band of ds GAS-DNA complexed with dimer of STAT6-4 (144 kDa) protein was in good agreement with the expected molecular weight of such a complex compared against the prestained HMW protein marker (Invitrogen) phosphorylase (148 kDa). This observation provides proof that semisynthetic STAT6-4 protein forms a functional dimer that binds to its known GAS recognition sequence *in vitro*. The negative controls were used to show that GAS-DNA only binds to the dimer of STAT6. STAT6-4 in the absence of Tamra ds GAS-DNA showed no Tamra fluorescence (figure 4.28, A, lane 3) also can be compared with silver

## Results

---

stained gel (figure 4.28, B, lane 3) showing the presence of STAT6-4. Similarly STAT6-2 in presence of Tamra ds GAS-DNA showed no binding due to the presence of caged phospho Tyr<sup>641</sup> group on the protein indicating STAT6-2 existing in its monomeric state (fig 4.28, A, lanes 7 and 9). The corresponding silver stain of the same native gel shows the presence of STAT6-2 protein in absence of Tamra ds GAS-DNA (figure 4.28, B, lane 4).

To ensure that only the consensus sequence GAS-DNA binds to the dimer of STAT6-4 further experiments were carried out. All the samples were prepared as described in section 3.6.1. For positive controls STAT6-4 (5  $\mu$ M and 3  $\mu$ M) in varying amounts was used for binding with Tamra ds GAS-DNA (20  $\mu$ M). To answer the question if the consensus ds GAS-DNA binds STAT6 specifically, Tamra ss GAS-DNA 5'-TCGACTTCCCAAGAACAGAG-3' was mixed in the ratio with the protein described before section 3.6.1. One set of samples were incubated for 5 min and the other for 1 h in dark in total volume of 10  $\mu$ l and later divided into two parts (v/v) followed by mixing with 40% sucrose loading buffer. The samples were run over standard 5% non-denaturing polyacrylamide gel, followed by scanning the gel in fluorescence scanner with Tamra ex: 510 nm, em: 575 nm.

Binding of semisynthetic STAT6-4 with Tamra ds GAS-DNA (figure 4.29, A and lanes 7 - 10) was reproducible as was confirmed by the appearance of Tamra fluorescence band which was in the range of a band in the prestained HMW protein marker (148 kDa) showing the dimeric form of STAT6-4 (144 kDa). The presence of high intensity bands containing STAT6-4 (5  $\mu$ M) (figure 4.29, lanes 9 and 10) and low intensity bands for STAT6-4 (3  $\mu$ M) (figure 4.29, lanes 7 and 8) with constant concentration of DNA (20  $\mu$ M) in the reaction mixture shows that varying concentrations of STAT6-4 did not affect the binding. The presence of the Tamra fluorescence band from ss GAS-DNA when mixed with STAT6-4 (shown by an arrow, figure 4.29, A, lanes 5 and 6) was found to be lower when compared to the complex of STAT6-4 and Tamra ds GAS-DNA shown in the figure 4.29, A and lanes 7 - 10. This gives an indication that STAT6-4 shows the absolute presence of dimeric form by only binding Tamra ds GAS-DNA and not Tamra



## Results

ss GAS-DNA. Thus, functional quantification of the binding of semisynthetic STAT6-4 to GAS-DNA was performed successfully by EMSA technique.

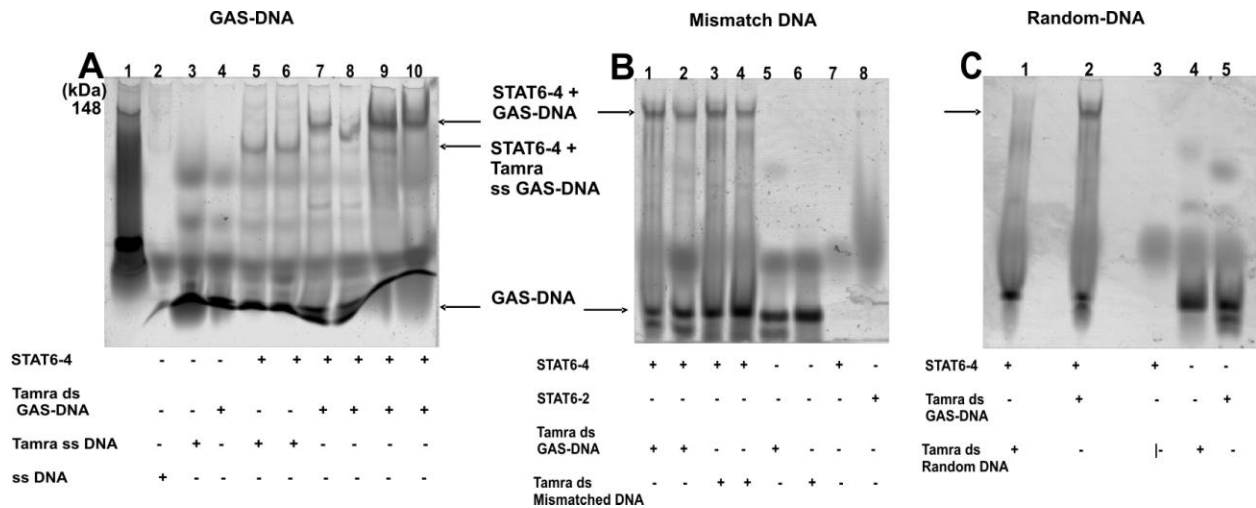


**Figure 4.29: Binding studies of STAT6 with different forms of DNA**

**A:** EMSA technique was used to study the non-specific binding of STAT6-4. The 5% native gels scanned at ex: 510 nm and em: 575 nm shows the non-specific complex of Tamra ss GAS- DNA with STAT6-4 figure (lanes 5 and 6) as shown by an arrow. Binding complex between STAT6-4 with Tamra ds GAS-DNA (lanes 7-10), Tamra ds GAS-DNA indicated by an arrow (lane 4), Tamra ss GAS-DNA (lane 3), ss GAS-DNA (lane 2) and prestained HMW (lane 1). **B:** Fluorescence scanning at ex: 510 nm, em: 575 nm. shows binding of STAT6-4 with Tamra ds GAS-DNA (lanes 1 and 2) indicated by an arrow, STAT6-4 complexed with Tamra ds mismatch DNA (lanes 3 and 4), Tamra ds GAS-DNA (lane 5) indicated by an arrow, Mismatch DNA (lane 6), STAT6-4 (lane 7) and STAT6-2 (lane 8). **C:** Fluorescence scans at ex: 510 nm, em: 575 nm shows non-binding of STAT6-4 with Tamra ds random DNA (lane 1) shown by an arrow, and binding of STAT6-4 with Tamra ds GAS-DNA (lane 2), STAT6-4 (lane 3), Tamra ds random DNA (lane 4) and Tamra ds GAS-DNA (lane 5).

To further, confirm the specificity of STAT6-4 for ds GAS-DNA, mismatch and random DNA sequences were generated from two complimentary oligonucleotides of 20 bases each equipped with a Tamra fluorophore for efficient monitoring during EMSA. The sequences for mismatch DNA were Tamra 5'-TCGACTTCCCGAGAACAGAG-3' and its complimentary sequence 3'-AGCTGAAGGGTCTTGTCTC-5' containing an A to C mutation at N<sub>3</sub> region. The sequence for random DNA were Tamra 5'-GTCTGGGTAGCGACGGCTCT-3' and its complimentary sequence 3'-

## Results

---

CAGACCCATCGCTGCCGAGA-5' without resemblance to the consensus sequence of GAS-DNA was used. The DNA was hybridized following the procedure used for ds GAS-DNA. The hybridization was monitored by 12% non-denaturing polyacrylamide gels followed by fluorescence scanning as mentioned above. Mobility shift of ds DNA compared to ss DNA showed successful hybridization.

To test the specific binding reactions two set of experiments were performed. In two 100  $\mu$ l tubes STAT6-4 (5  $\mu$ M) + mismatch DNA (20  $\mu$ M) and STAT6-4 (5  $\mu$ l) + random DNA (20  $\mu$ M) in 10  $\mu$ l volume were incubated for 5 min to 1 h at RT each in dark. The samples were run via 5% non-denaturing polyacrylamide gel with 100 mV on ice. The gels were scanned as described above. It was observed that one mutation from A to C, does not prevent binding of STAT6 (figure 4.29, B, lanes 3 and 4) when compared with the binding complex of STAT6-4 and ds GAS-DNA (figure 4.29, B, lanes 1 and 2) indicated by an arrow showing no major difference in Tamra absorption. No binding of random Tamra ds DNA and STAT6-4 was observed (figure 4.29, C, lane 1) whereas binding with Tamra ds GAS-DNA was always reproducible (figure 4.29, C, lane 2). The binding of STAT6-4 with single mutation from A to C at N<sub>3</sub> region provides evidence that both N<sub>3</sub> and N<sub>4</sub> nucleotide sequences bind to STAT6 proteins. These experiments proved that STAT6-4 was a functional dimer that binds to specific ds GAS-DNA with N<sub>3</sub> or N<sub>4</sub> palindromic sequences.

Concentration dependent studies with varying amounts of Tamra ds GAS-DNA (20 to 150  $\mu$ M) mixed with STAT6-4 (5  $\mu$ M) for binding reaction in a volume of 10  $\mu$ l was performed as above and divided into equal ratio (to investigate the effect of DNA-binding. One set of binding reactions containing STAT6-4 (5  $\mu$ M) with varying concentration of Tamra ds GAS-DNA (20  $\mu$ M-150  $\mu$ M in gel) for 5 min and another set of reactions with similar concentrations of STAT6-4 and ds GAS-DNA for 1 h in dark was carried out. Later the gel was analyzed as described above. Figure 4.30, lanes 1 - 10 indicates no increase or decrease in band intensities in the binding complex as observed by the fluorescence scan of the gel. Pink bar shows the increase in concentration of Tamra ds GAS-DNA.

## Results

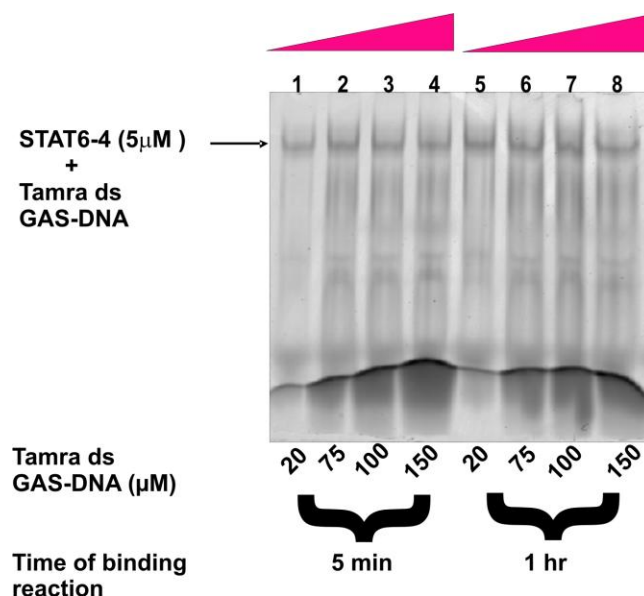


**Figure 4.30:** Different concentrations of Tamra ds GAS-DNA ranging from 20 - 150 μM incubated with 5 μM STAT6-4.

Semisynthetic STAT6-2 is prevented from dimerization by having a caged phosphorylated Tyr<sup>641</sup> and therefore does not bind to Tamra ds GAS-DNA as seen before in EMSA experiments (figure 4.28, A and B, lanes 4 and 9). The difficult and interesting experiment was to prove semisynthetic STAT6-2 as bioactive by becoming a functional dimer which would bind with ds GAS-DNA upon removal of caged group from phosphorylated Tyr<sup>641</sup> with UV light. To achieve the deprotection of caged group from phosphotyrosine, STAT6-2 (5 μM) in a 10 μl quartz cuvette was flashed with UV light for 5 min and 10 min. UV exposed STAT6-2 was later incubated with Tamra ds GAS-DNA following the above described procedure for binding reactions. The samples were run via 5% non-denaturing polyacrylamide gel followed by scanning for Tamra fluorescence and subsequent silver stain.

## Results

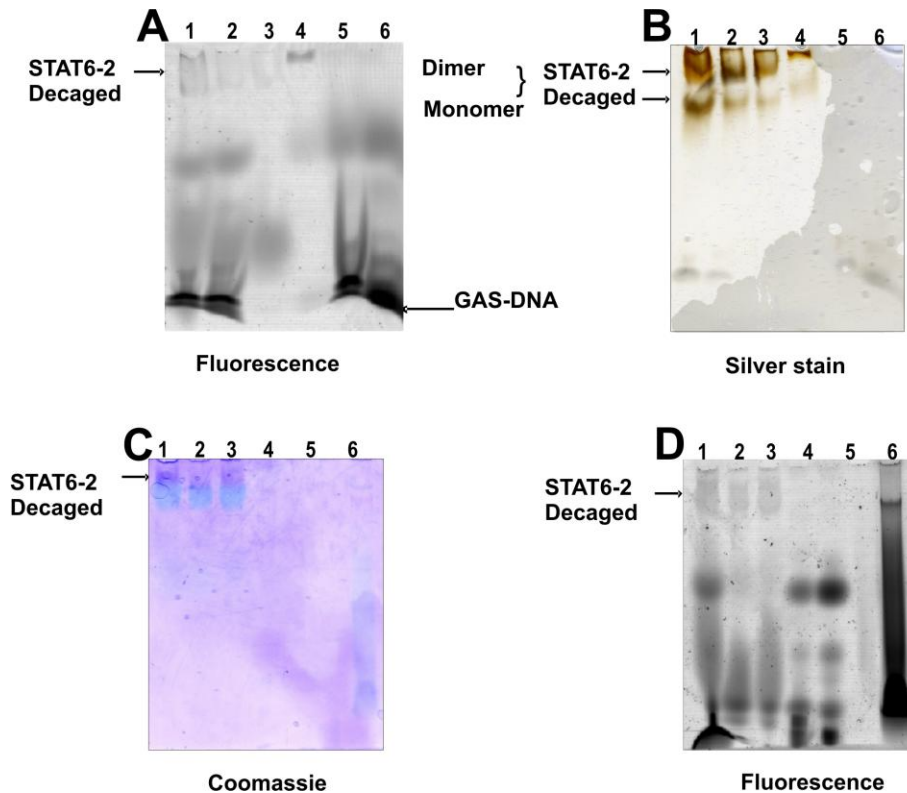


**Figure 4.31: DNA-binding assay of decaged STAT6-2 and Tamra ds GAS-DNA.**

**A:** The complex formation of decaged STAT6-2 and Tamra ds GAS-DNA was monitored by EMSA. The 5% gel was scanned at ex: 510 nm, em: 575 nm. Decaged STAT6-2 complexed with Tamra ds GAS-DNA 10 min and 5 min of exposure under UV light (lanes 1 and 2 respectively) shown by an arrow, decaged STAT6-2 in absence of Tamra ds GAS-DNA (lane 3) and non decaged STAT6-2 (lane 4), Tamra ds GAS-DNA (lane 5) and Tamra ss GAS-DNA (lane 6). **B:** Silver stain of the corresponding gel showing the new dimer of decaged STAT6-2 complexed with Tamra ds GAS-DNA and excess of monomer STAT6-2 shown by an arrow (lanes 1 and 2 respectively), STAT6-2 exposed to UV light for 5 min without the incubation with GAS-DNA (lane 3), non decaged STAT6-2 (lane 4). **C:** Coomassie stains of decaged STAT6-2 complexed with Tamra ds GAS-DNA (lane 1), decaged STAT6-2 in absence of Tamra ds GAS-DNA (lanes 2) and non-decaged STAT6-2 (lane 3). Tamra ds GAS-DNA (lane 4), Tamra ss GAS-DNA (lane 5) and prestained HMW (lane 6). **D:** Corresponding Fluorescence scans of **(C)**.

The fluorescence scan showed (figure 4.31, A shown by arrows) a faint band that corresponds to Tamra ds GAS-DNA bound to decaged STAT6-2 dimer. When compared with the corresponding silver stained gel (figure 4.31, B, lanes 1 and 2), two separate bands were seen as indicated by arrows. The first band was assumed to be the dimeric form of STAT6-2 and the lower band represents the monomeric form. The

## Results

---

unidentified fluorescence band was unexpectedly observed for decaged STAT6-2 in absence of Tamra ds GAS-DNA (figure.4.31, A, lane 3) and caged STAT6-2 (figure.4.31, A, lane 3). This observation was very exigent (figure 4.31, A and B, lanes 3 and 4) to determine the unidentified fluorescent bands obtained after fluorescent scans.

To find the reason for unidentified fluorescent bands seen in figure 4.31, A and B, lanes 3 and 4 yet again, similar decaged reaction on STAT6-2 was performed followed by DNA binding assay and the reactions were monitored via native gels, which were first scanned to find Tamra fluorescence band followed by Coomassie staining. Figure 4.31, C, lane 1 indicated that decaged STAT6-2 complexed with Tamra ds GAS-DNA has reduced mobility shift in native gel when compared with STAT6-2 without Tamra ds GAS-DNA (figure 4.31, C, lane 3) and non-decaged STAT6-2 (figure 4.31, C, lane 4) showing the successful formation of dimeric STAT6-2 after illumination with UV light. Coomassie band also showed unidentified fluorescent bands (figure 4.31, D, lanes 1 - 3). Tamra fluorescence scan showed fluorescence band of higher intensity for figure 4.31, lane 1 that contained decaged STAT6-2 complexed with Tamra ds GAS-DNA when compared with other lanes that did not contain Tamra ds GAS-DNA. The band for dimeric STAT6-2 (144 kDa) complexed with Tamra when compared with the prestained HMW fluorescent band position at 148 kDa showed the existence of decaged STAT6-2 in dimeric form. The same result can be compared with the binding reaction observed for STAT6-4 complexed with Tamra ds GAS-DNA (figure 4.28, A)

Finally, the evidence of decaging of STAT6-2 was observed from reduced mobility shift of decaged dimeric STAT6-2 complexed with GAS-DNA, indicated in Coomassie stain and faint Tamra fluorescence band for presence of retarded mobility shift of complexed Tamra GAS-DNA in fluorescence scans. Thus, the DNA binding assay indicates that semisynthetic STAT6-2 can be decaged and is functional as shown by its ability to bind with its recognized GAS-DNA. Decaging of STAT6-2 and observing its binding with Tamra ds GAS-DNA remained a challenge due to the presence of unidentified fluorescent bands and faint Tamra fluorescence band. The proof for decaged STAT6-2 experiment was briefly explained through western blot analysis in section 4.3.1.

## Results

Nevertheless, the challenging part was to interpret the presence of unidentified bands in those lanes (figure 4.31, C and D) that did not contain Tamra DNA and their corresponding Coomassie stained gels.

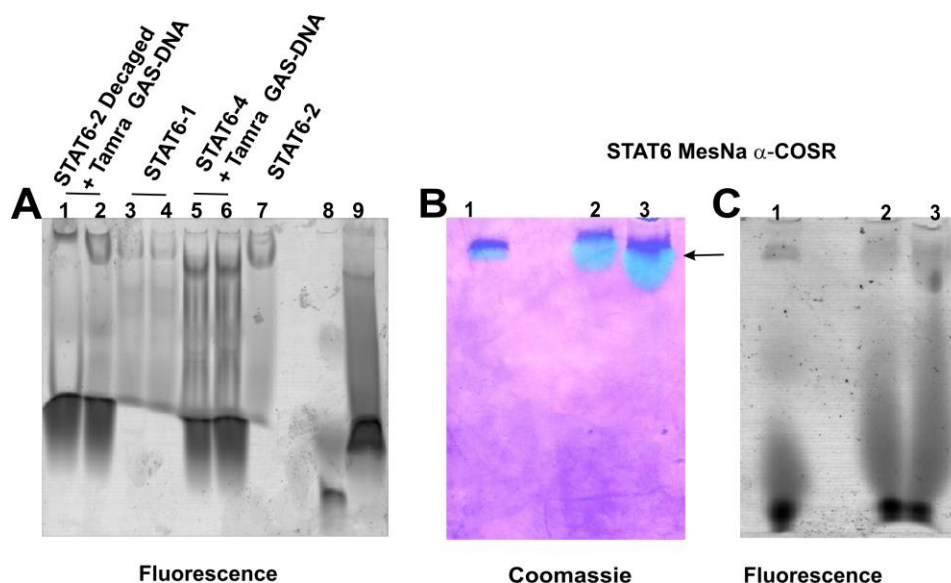


**Figure 4.32: Analysis of DNA binding assays with STAT6 variants and STAT6 MESNA  $\alpha$ -COSR on native gel.**

**A:** Fluorescence scan at ex: 510 nm, em: 575 nm of 5% native gel showing a complex of decaged STAT6-2 and Tamra ds GAS-DNA incubated for 1 h and 5 min at RT (lanes 1-2 respectively). Caged STAT6-1 mixed with Tamra ds GAS-DNA incubated for 1 h and 5 min at RT (lanes 3-4 respectively). STAT6-4 complexed with Tamra ds GAS-DNA for positive control following similar conditions for binding and incubated for 1 h and 5 min (lanes 5 and 6 respectively), STAT6-2 (lane 7), Tamra ds GAS-DNA (lane 8), prestained HMW (lane 9). **B:** STAT6 MesNa  $\alpha$ -COSR at different concentration run via 5% non-denaturing gel and stained with Coomassie (lanes 1 and 3) were fluorescent blue band from 0-1% DDM band indicated by an arrow. **C:** STAT6 MesNa  $\alpha$ -COSR at different concentration was run via 5% non-denaturing gel and scanned at Tamra fluorescence (lanes 1-3), faint band from 0-1% DDM indicated by an arrow.

To analyze in detail the unidentified fluorescence band (figure.4.32, A, lanes 3 and 4) in the samples which did not contain Tamra ds GAS-DNA; the following steps were carried out such as STAT6-2 (5  $\mu$ M) was mixed with Tamra ds GAS-DNA and was run via 5% native gel and scanned for Tamra fluorescence. The fluorescent band with high

## Results

---

intensities was observed (figure 4.32, A, lanes 1 and 2). A similar fluorescent band was also observed for STAT6-2 (5  $\mu$ M) which was loaded in absence of Tamra ds GAS-DNA (figure 4.32, A, lane 7) when compared with the figure 4.31, A, lane 3 and 4. STAT6-1 having Cy5 as the fluorophore was loaded without Tamra ds GAS-DNA (figure 4.32, A, lanes 3 and 4). STAT6-2 in absence of Tamra ds GAS-DNA produced the similar fluorescent band (figure 4.32, A, lane 7).

STAT6 MesNa  $\alpha$ -COSR purified with STAT6 buffer + 0.1% DDM was tested to see if it has the same effect on the native gel, as the same STAT6 MesNa  $\alpha$ -COSR was used to carry out the ligation with the peptides. The Coomassie stain of the STAT6 MesNa  $\alpha$ -COSR (figure 4.32, B, lanes 1 - 3) indicates an unidentified band, which disappeared within 5 min after destaining the gel giving an indication that the band occurred was from detergent (0.1% DDM) present in the STAT6 buffer. It also showed that STAT6 MesNa  $\alpha$ -COSR appeared near the sockets of the gel. This could be due to the large size of the protein as well as the protein in combination with the DDM micelle that hinders in the fast migration through the native gel. The fluorescent scan (figure 4.32, C, lanes 1 - 3) at Tamra absorption showed a band in spite of the absence of any Tamra ss/ds GAS-DNA.

Hence, it was observed that STAT6 MesNa  $\alpha$ -COSR and caged semisynthetic STAT6-1 and -2 variants showed a fluorescent band in the absence of Tamra ds GAS-DNA. Based on the information observed in figure 4.33, B, lanes 1 - 3 it was assured that STAT6 buffer containing 0.1% DDM used during ligations might be responsible for the fluorescent band that appeared in the native gels during the fluorescence scanning even in the absence of Tamra fluorophore in the reaction mixture. It was very essential to observe STAT6 MesNa  $\alpha$ -COSR and semisynthetic variants of STAT6 without the presence of the unidentified fluorescent band on scanning at Tamra fluorescence on the native gel.

Since STAT6 MesNa  $\alpha$ -COSR migration on the native gel was found near the sockets, first attempt to improve its migration was carried out. Due to the presence of big

## Results

---

polyacrylamide pores in 5% native gel it was assumed that DDM would migrate faster than STAT6 MesNa  $\alpha$ -COSR thereby separation of DDM from the protein could be achieved. Different conditions such as, changing the buffer from TBE to TRIS Borate, variation in pH from 8.0 to 9.0 and running the native gel overnight at 4°C were used. Gels were scanned at Tamra fluorescence. By changing the pH of the running TBE buffer from 8.0 to 9.0, STAT6 MesNa  $\alpha$ -COSR slowly migrated from the sockets to the middle of the gel but along with DDM which eventually showed unidentified fluorescent band in absence of Tamra ss/ds GAS-DNA. After these observations, it was clear that an unidentified band seen on figure 4.32, B, lanes 1 – 3 was caused by detergent in STAT6 buffer. Hence, it was essential to remove DDM from the STAT6 buffer to carry out the future expressed protein ligations.

It was very challenging question to remove DDM due to DDM's low CMC value. Hence, DDM was responsible for the formation of unidentified bands in EMSA data's as well as problems faced during peptide **1** separation from the ligation products (section 4.2.2). It was also observed that when STAT6 MesNa  $\alpha$ -COSR was ligated with peptide-**4** to make STAT6-**4**, the binding reactions could not be repeated. Hence, the expression of STAT6 MesNa  $\alpha$ -COSR as described in section 4.2.1 was carried out without detergent where several challenges were faced due to the instability of the STAT6 MesNa  $\alpha$ -COSR causing high loss in the yield of the protein due to aggregation during their preparation. As described in the earlier section 4.2.1, 50% glycerol was found to be the best suitable stabilizer. STAT6 MesNa  $\alpha$ -COSR in 50% glycerol when run over 5% non-denaturing gels, the fluorescence scan did not show any fluorescence band. Ligations were repeated after the above observation using STAT6 MesNa  $\alpha$ -COSR in 50% glycerol to synthesize STAT6-**2** and STAT6-**4**. As expected, no fluorescence band was observed when STAT6-**2** (5  $\mu$ M) in STAT6 buffer + 50% glycerol in presence of binding buffer was loaded onto the native gel. The binding reactions were also reproducible for STAT6-**4** in presence of 50% of glycerol.



## Results

---

### 4.3.3 Monitoring the STAT6 and GAS-DNA by FRET

Fluorescence resonance energy transfer (FRET) interaction is based on two species labeled with different fluorophores. This technique has emerged as a powerful tool to study interactions of ions, ligands, and molecular interactions *in vivo* or *in vitro*. To observe FRET, a fluorescence donor has to interact with an acceptor molecule which is separated by 2 - 10 nm from the donor. The interaction results in the transfer of the donor excitation energy to the acceptor manifested as, among others, quenching of donor fluorescence and enhancement, of acceptor fluorescence. In case of STAT6 and GAS-DNA, Cy5 conjugated to STAT6 was the acceptor and Tamra conjugated GAS-DNA was the donor. The methodology of highly sensitive FRET was applied to find more verification for DNA binding of semisynthetic STAT6 dimers, together with the analysis of the data obtained from EMSA (section 4.3.2). Semisynthetic truncated STAT6-3 (a phosphorylated and Cy5 labeled variant) was selected and FRET was measured at different concentrations of 5'-Tamra ds GAS-DNA and a Tamra labeled random ds DNA respectively.

The total volume of the FRET reaction mixture was 12  $\mu$ l and the experiment was performed in three sided quartz micro cuvette. All readings were taken in a Spex Fluoromax 3 spectrofluorometer instrument at 20°C. The binding assay was investigated by addition of 1.2  $\mu$ l of Tamra ds GAS-DNA each time to make a final concentration of 0.01  $\mu$ M and 2.0  $\mu$ l of STAT6-3 to make 0.1  $\mu$ M of final concentration in 12  $\mu$ l of binding buffer. The negative control was demonstrated by adding 1.2  $\mu$ l of Tamra ds random DNA to make a final concentration of 0.01  $\mu$ M each time in a reaction volume of 12  $\mu$ l containing binding buffer and 0.1  $\mu$ M of STAT6-3. The dilution factor was deducted for every reading taken. Fluorescence intensities of Tamra and Cy5 are recorded as a function of the concentration of DNA (nM).

FRET was observed as emission of Cy5 (660 nm) as an acceptor linked to STAT6-3 an excitation of Tamra ds DNA (548 nm) as donor. A ~1.5 fold increase in Cy5 emission (660 nm) for binding assays of STAT6-3 with Tamra ds GAS-DNA was observed when

## Results

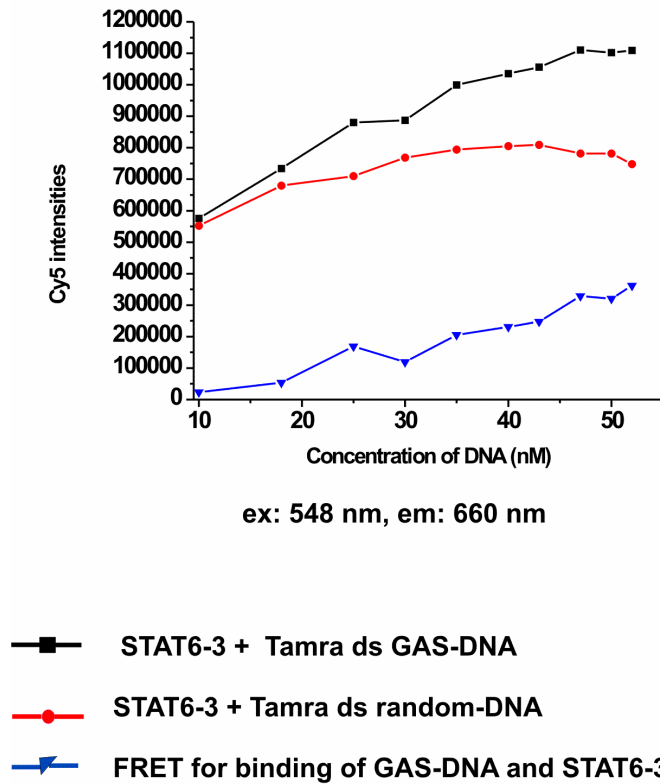


**Figure 4.33:** Fluorescence intensities of STAT6-3 with varying concentration of Tamra ds DNA  
A: FRET observation at Cy5 em: 660 nm excited at Tamra 548 nm.

compared with the background Cy5 emission obtained from non-binding assays (negative control) with Tamra ds random DNA (figure 4.33). The difference in the fluorescence intensities of Cy5 shows the actual FRET (figure 4.33) providing further evidence for the presence of dimeric semisynthetic STAT6-3 binding to ds GAS-DNA. The biophysical characterization of semisynthetic STAT6-3 was in agreement with the results obtained from EMSA (section 4.3.2) which proved that GAS-DNA binds only in the presence of dimeric STAT6 even in the presence of the Cy5 fluorophore attached to the linker domain and His<sub>6</sub>-tag at the C-terminus of the protein. No aggregation of protein was observed. Nevertheless, the challenging part was to work with very low concentration of STAT6, due to which DNA was added each time and dilution factor was subtracted. Further disadvantage was the overheating of the instrument which can lead to precipitation of sample during measurement. Hence short working time was preferred.

## Results

### 4.3.4 In vivo analysis of STAT6 variants

STAT6 as described in chapter 1 migrates to the nucleus only in its active dimeric form. To examine the localization of semisynthetic truncated STAT6, which is assumed to follow the same pathway from the cytoplasm to nucleus, the microinjection approach was selected which allows transferring the target protein into any mammalian cell. As shown in figure 4.34, STAT6-1, on being microinjected into the cytoplasm of mammalian cells, should localize into the cytoplasm due to the presence of caged phospho tyrosine that prevents it from forming a dimer and translocation to the nucleus. After illuminating the cells with UV light, the caged group is removed and STAT6-1 is expected to migrate to the nucleus showing the dimeric active state of STAT6-1.

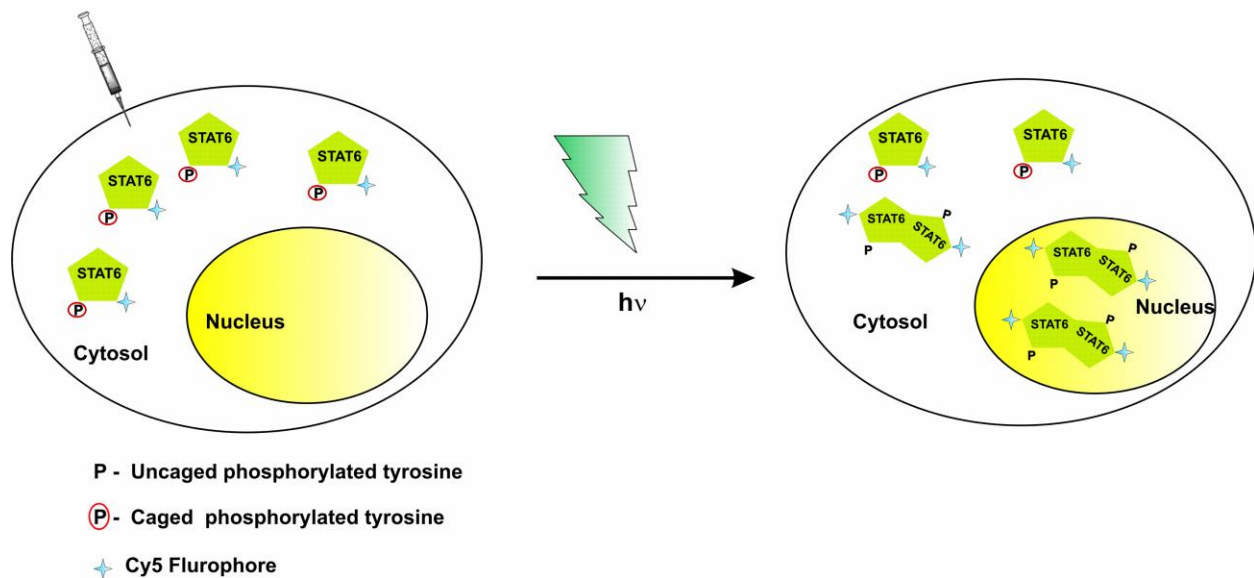


**Figure 4.34: Scheme for microinjection of STAT6-1**

Cartoon represents microinjected mammalian cell with STAT6-1, which is localized only in the cytosol. On illuminating the cell with UV light, the caged group on some of the phosphorylated tyrosine of STAT6-1 is removed and it migrates to the nucleus. This process can be observed by fluorescence microscopy.

To establish and standardize microinjection of STAT6-1 in the cytoplasm of cell and further illuminating the cell with UV light, various mammalian cell lines such as human epithelial carcinoma cell line (A431) species human, African green, kidney (COS-7) fibroblast species monkey and Madin Darby Canine Kidney (MDCK) epithelial cells

## Results

were used. Cells were cultured as described in section 3.6.2. Microinjection was carried out in a glass cage having an atmosphere of 5 % CO<sub>2</sub> and 37 °C.

STAT6-1 with the caged phosphorylated tyrosine (~1 pl from 5 μM in PBS) was microinjected into the cytoplasm of several A431 cells. This showed that STAT6-1 possessing caged phosphorylated tyrosine was present in the cytoplasm only (figure 4.35, A) which confirms the existence of STAT6-1 in the monomeric state and its larger size avoided the migration of the protein into the nucleus.

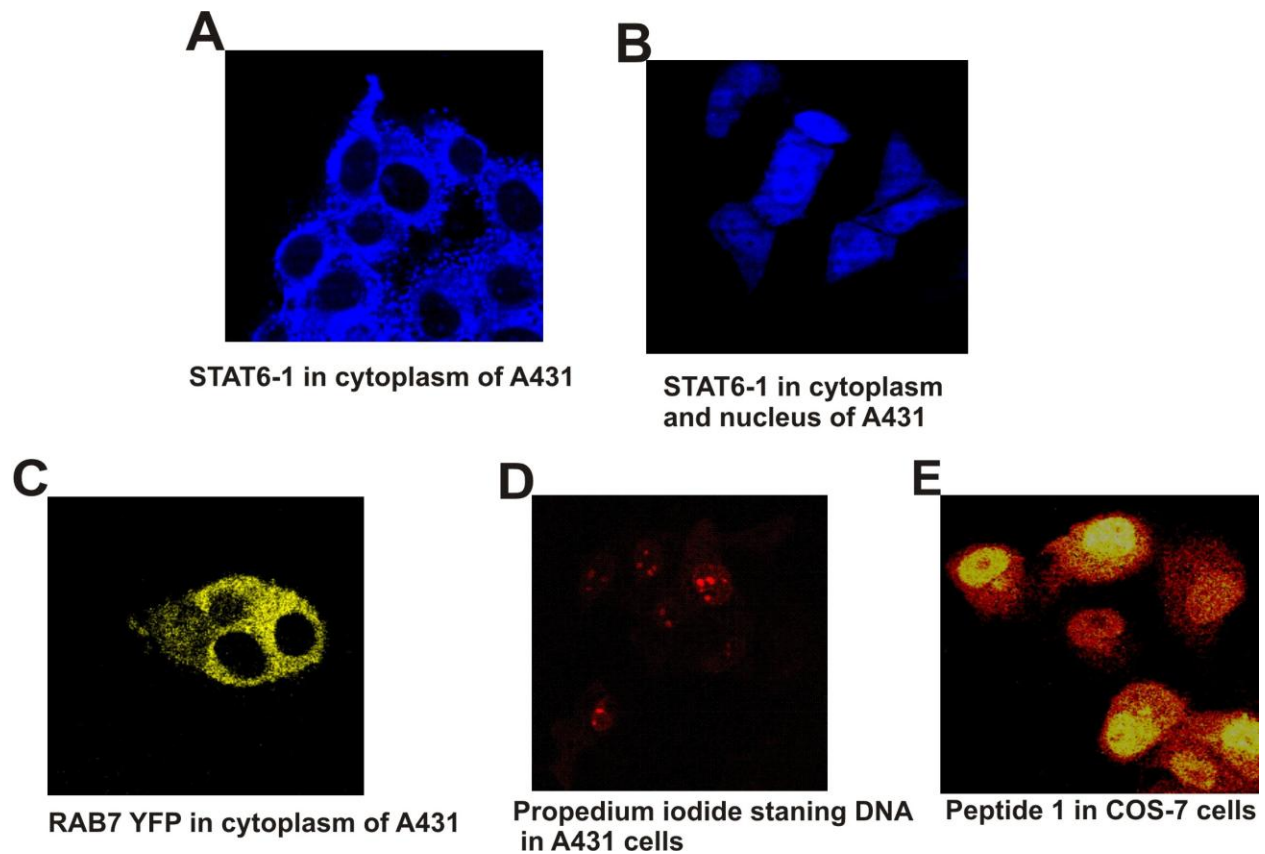


**Figure 4.35: Microinjection**

**A:** STAT6-1 is microinjected in A431 cells and Cy5 absorption shows the localization in the cytoplasm. **B:** STAT6-1 is microinjected in A431 cells and Cy5 absorption shows the localization in the cytoplasm and nucleus **C:** Localization of microinjected RAB $\Delta$ 7-YFP in cytoplasm at YFP absorption ex 500 nm and em 535 nm **D:** Microinjected A431 cells with Propidium iodide. **E:** Peptide 1 microinjected in COS cell line and Cy5 absorption at ex. 635 nm and em 670 nm from Confocal microscope, Leica SP5 shows the localization in the cytoplasm and nucleus.

## Results

---

Several problems were encountered during the microinjection. Only 10-20% of our experiments generated the similar results as above showed that STAT6-1 was found in fact in the nucleus and the cytoplasm this suggested that STAT6 was being uncaged in spite of the absence of UV light (figure 4.35, B). The sudden change in the behavior of STAT6-1 in the cell is difficult to explain. It was assumed that the presence of peptide 1 in the buffer of STAT6-1 that was not separated after several purification trials (section 4.2.2) could lead to the observation of fluorescence in the nucleus along with the minor decaging of STAT6-1 which can occur due to the absorption of UV light from the white light during handling of the sample. Enlargement of the confocal aperture from the microscope which focused high intensity light on the sample during microinjection can also decaged the caged group on STAT6-1.

As a control experiment, the first attempt was made by RAB $\Delta$ 7-YFP (30 kDa) that was microinjected into the cytoplasm of A431 cells (figure 4.35, C). The fluorescence image at YFP ex: 500 nm and em: 535 nm showed that RAB $\Delta$ 7-YFP did not migrate into the nucleus immediately due to its larger size and was localized only in the cytoplasm that later migrates to the nucleus in 5 - 10 min of incubation. Thus, larger protein does not migrate in the nucleus immediately like smaller peptides. Propidium iodide was microinjected in the cytoplasm of A431 that immediately traveled to the nucleus and stained DNA (figure 4.35, D).

Next, solublizing peptide 1 conjugated to Cy5 (4.7 kDa) in PBS buffer and microinjecting it into the cytoplasm of COS-7 cells (section 3.6.3). Concentration was not determined since minor amount of peptide 1 was taken at the tip of the spatula and dissolved in 50  $\mu$ l of PBS buffer. Fluorescence image from confocal microscope showed localization of peptide 1 throughout the cell due to its smaller size that can easily diffuse through the plasma membrane of the nucleus (figure 4.35, E).

The most challenging part was observed when the micro capillary containing STAT6-1 was brought close to the cell wall; cells underwent disintegration even before the cells

## Results

were microinjected with the sample. Changing the cell line from A431 to COS7 showed similar effects. Changing the concentration of STAT6-1 did not damage the cells but due to low fluorescence from Cy5, it was very difficult to interpret the results.

Finally, MDCK cell line proved to be better suited for microinjection of STAT6-1. It was microinjected into one cell out of three cells that are in close proximity of each other and no damage to the cells after microinjection was observed. Fluorescence image of the Cy5 channel shows that STAT6-1 is localized in the cytoplasm of MDCK cell before illuminating with UV light (figure 4.36, A, Cy5 channel 1). Finally upon exposure to UV light using 405 nm diode laser, STAT6-1 migrated to the nucleus (figure 4.36, A, Cy5 channel, 2-3) forming an activated dimer with an increase in Cy5 fluorescence intensity. The nucleus is marked by Hoechst 33445 excited by 405 diode laser. Due to high intensity of laser, Hoechst appears to be saturated (figure 4.36, B, 2 - 3)

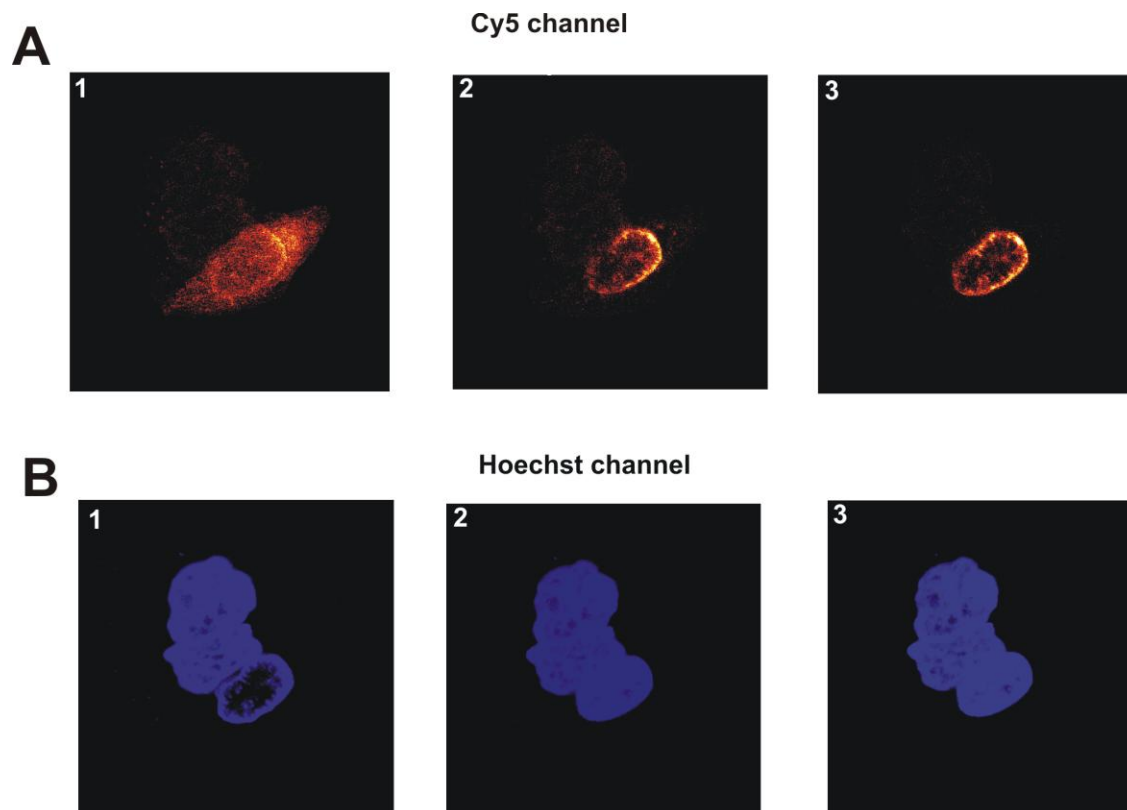
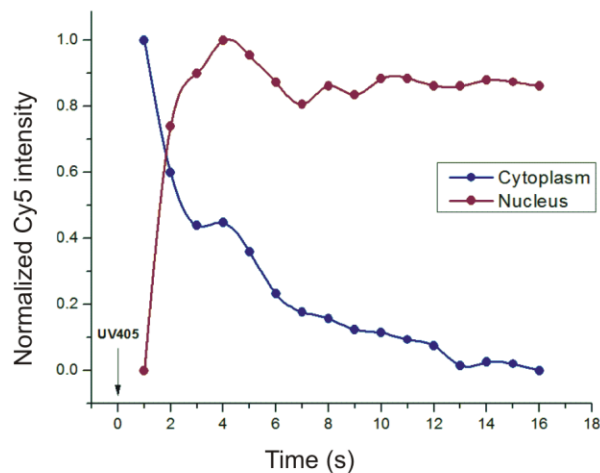


Figure 4.36: Transition of monomeric STAT6-1 to dimer.

## Results

**A:** Cy5 channel represents the microinjected STAT6-1 in the cytoplasm in the absence of UV (A 1), On flashing UV light of 405 nm from Leica SP5 confocal microscope equipped with a Diode laser , fast uncaging of caged group dimerizes the STAT6-1 with increase in the Cy5 intensity and migration of the same to the nucleus (A 2-4). **B:** Hoechst 33445 channel showing three nucleus stained with Hoechst 33445 nuclear marker.

A normalized Cy5 intensity (figure 4.37) was plotted by demarking an area in cytoplasm and nucleus which shows the exponential increase in Cy5 intensity in the nucleus due to the immediate formation of STAT6-1 dimer and rapid migration to the nucleus on removing the cage group after illuminating cells with UV light and exponential decrease in Cy5 intensity in the cytoplasm. The cells were illuminated with the UV laser for another 15 min to observe the migration of STAT6-1 in the cytoplasm which did not show any change in the localization of the protein which can be observed by no linear or exponential decrease of Cy5 intensity in the nucleus nor increase of the same in the cytoplasm.



**Figure 4.37: Translocation of STAT6-1 shown by a plot of Cy5 fluorescent intensity against time.**

Translocation of STAT6-1 from cytoplasm to nucleus is shown by an exponential increase of Cy5 intensity in the nucleus due to decaging of the caged group and formation of activated, dimeric STAT6-1 with an exponential decrease in Cy5 intensity in the cytoplasm (blue).

## Results

---

This showed that semisynthetic truncated STAT6-1 exists as a monomer in the cytoplasm and after uncaging the phosphorylated tyrosine forms a dimer, becomes biologically active and migrates to the nucleus immediately showing a functional protein. Thus actual JAK-STAT pathway was mimicked by semisynthetic protein in physiological conditions without the presence of cytokines and JAK to induce activation and phosphorylation. Deletion of C-TAD in the semisynthetic truncated STAT6-1 did not change its bioactivity. However, the truncated STAT6-1 cannot carry out gene transcription in the nucleus due to the missing TAD portion at its C-terminus hence gene expression studies were not carried out. Thus, signal transduction pathway of STAT6 protein by using EPL technique is a step forward in understanding many more vital functions of STAT6.



# Chapter 5

---

Discussion

### 5.1 Biological background of STAT6

Expressed protein ligation (EPL) is an intein-based approach, which has paved the way for investigating the structure and function of proteins through site-specific modifications by introducing unnatural amino acids, small fluorophores, isotope labels, spin resonance probe and cross-linkers (section 1.2.2). This approach provides an advantage over traditional methods to prepare proteins in *E. coli*, yeast, mammalian cell lines. In order to analyze the effects of C-terminal tyrosine phosphorylation events semi-synthetic truncated STAT6 **-(1-6)** variant was synthesized using EPL technique.

Progress in understanding of the JAK-STAT signaling pathway is of high interest as this pathway consists of a variety of interesting pharmaceutical targets due to the tight regulation transcriptional activation<sup>191</sup>. STATs mediate signals from extracellular cytokines to the nucleus of a cell upon activation by JAK. As described in section 1.1 cytokines are responsible for immune responses, gene regulation, proliferation and differentiations in immune cells. Abnormalities in cytokines and JAKs have been shown to be the cause of many inflammatory diseases and cancers. Hence both cytokines and JAKs have long been used for therapeutic usage and studies.

Research on inflammatory diseases which are related to JAK-STAT pathway have been found focusing more on JAK3 for drug development because of its selective expression in T-cells and its activation by IL-2 cytokines<sup>192</sup>. Extensive work over the last few years has provided evidence that JAK kinases play important roles in the generation of responses for interferons, which are cytokines that exhibit important anti-tumor activities. There is also accumulating evidence that constitutive activation of different JAKs and STATs mediates neoplastic transformation and promotes abnormal cell proliferation in various malignancies. It has been found that JAK mutations also lead to active or hyperactive JAK proteins which play a crucial role in hematopoietic malignancies<sup>193</sup>. When expressed in cells and bound to membrane cytokine receptors, mutant JAK proteins are no longer inactive and constantly activate STAT proteins. This activity promotes oncogenic transformation and uncontrolled blood cell production.

## Discussion

---

STAT signaling has been widely observed in a wide array of human cancers (breast, leukemia, lymphomas, prostate, and head, and neck). STAT6 is highly expressed in the in prostate cancer cell lines and it is the singularly most important factor, which regulates the genetic transcriptional program for the progression of prostate cancer<sup>194</sup>. STAT6 has been related to the immune diseases such as asthma. Asthma is associated with increase production of interleukins (IL)-4 and (IL)-13 whose signaling events are mediated by STAT6 proteins<sup>73,195,196</sup>. Highly activated STAT6 has been found in cancerous cells and chronic diseases like asthma. Type 2 helper (Th2) cells as well as production of immunoglobulin E (IgE) by B-cells were impaired in STAT6 deficient mice<sup>197</sup>.

However, a better understanding of STAT still remains an attractive goal for anti-cancer and anti-inflammatory drug development. Any mechanism which blocks the activation of STAT can be a prime goal for drug targeting. Recently 4-benzylamino-2-[(4-morpholin-4-ylphenyl) amino] pyrimidine-5-carboxamide derivatives which could inhibit the activity of STAT6 with an IC<sub>50</sub> of 0.70 nM and also inhibited Th2 differentiation in mouse spleen T cells induced by interleukin (IL)-4 with an IC<sub>50</sub> of 0.28 nM without affecting type 1 helper T (Th1) cell differentiation induced by IL-12 was shown in the paper published by Shinya Nagashima *et. al.*, 2008<sup>198</sup>. Designing a semisynthetic truncated light switchable STAT6 as a system to test for selective dimerization (activation inhibitors), translocation inhibitors was a step forward in understanding its bioactivity *in vivo* and *in vitro*. Hence, to explore the signal transduction pathway of STAT6, several modifications were introduced into STAT6 to test the effects of phosphorylation of the crucial phosphorylation site Tyr<sup>641</sup> by which STAT6 can be investigated in its monomeric and dimeric state *in vivo* and *in vitro*. Significant research has been carried out on STAT6 by expressing STAT6 in mammalian cells. In order to construct, the largest semisynthetic truncated isoform of STAT6 (aa 668) the N-terminal portion of STAT6 (aa 1 - 634) with an intein fusion protein *MxeGyrA*, His<sub>7</sub>-tag and a chitin binding domain (STAT6*MxeCBD*) at the C-terminus was expressed in *E.coli* cells which upon transthoesterification reaction in presence of MesNa generated STAT6 MesNa α-COSR (aa 1 - 634). The C-terminal fragment of the wild type STAT6 was chemically synthesized which facilitated

## Discussion

---

the demonstration of various modifications at Tyr<sup>641</sup> and coupling with a small fluorophore such as Cy5. Chemical Synthesis of the full length STAT6 protein was impossible as the large size of STAT6 led to difficulties in obtaining significant quantities of correctly folded protein. The EPL technique subverted the problem of synthesizing full length STAT6 (95 kDa), while still allowing the flexibility of chemical synthesis at the C-terminus, to explore its functionality. The main aim was to carry out the post translational modifications (PTMs) at the C-terminus transactivation domain (TAD) of STAT6, which was 200 aa long, requires two to three NCL to generate the entire TAD peptide. As such, restoring the essential Tyr<sup>641</sup> for which C-TAD peptide (aa 635 - 660) was synthesized allowing to carry out various PTMs such as addition of un-natural amino acids such as caged phosphorylated tyrosine, phosphorylated tyrosine, non-phosphorylated tyrosine, peptides with and without Cy5 as fluorophore and His<sub>6</sub>-tag for purification. Such semisynthetic truncated STAT6 (aa 1 - 668) will never carry out gene transcription due to its TAD which is essential for the gene transcription. In this investigation, a light switchable semisynthetic truncated STAT6 along with their variants was prepared and characterized for the first time using expressed protein ligation (EPL) to investigate their interaction with GAS-DNA the dimerization of the chimeric protein *in vivo* and *in vitro*.

In order to construct semisynthetic truncated STAT6 (section 4.1 and 4.2), chemical and biochemical methods were applied. Six semisynthetic truncated STAT6 **-(1-6)** were obtained which were site specifically modified at Tyr<sup>641</sup> by ligating chemo selectively STAT6 MesNa  $\alpha$ -COSR (aa 1 - 634) with six variants of C-terminal peptides **1-6** (aa 635 - 668). SPPS generated Peptides **1**, **3** and **6** with Cy5 labeled and peptides **2**, **4** and **5** with non-labeled analogues of **1**, **3** and **6** respectively (chapter 4, section 4.1 and figure 4.3). Peptides **1** and **2** had caged phosphorylated Tyr at position 641 related to the native STAT6 sequence. Peptides **3** and **4** had phosphorylated Tyr at position 641. Peptides **5** and **6** had no phosphorylation on Tyr at position 641. The peptides **1-6** had minor differences in the size between 4.7 kDa to 3.7 kDa due to the presence of modifications on them. In all chimeric proteins, Glycine 635 was mutated to Cysteine to facilitate EPL (as explained in the section 4.1.1- 4.1.6). To conjugate fluorophore Cy5

## Discussion

---

lysine at position 661 and a spacer as Glycine at position 662 was incorporated into the peptide chain.

EPL generated light switchable STAT6-1 with caged phosphorylated Tyr<sup>641</sup> along with Cy5 label at Lys<sup>661</sup>. STAT6-2 was prepared with caged phosphorylated Tyr<sup>641</sup>, which enabled STAT6 to maintain in its monomeric native form. STAT6-3 was prepared with non-caged phosphorylated Tyr<sup>641</sup> along with a Cy5 label at Lys<sup>661</sup>. STAT6-4 was prepared with non-caged phosphorylated Tyr<sup>641</sup>. Non-caged phosphorylated STAT6-3 and -4 were synthesized to investigate dimeric variants of these proteins. STAT6-5 was prepared with non phosphorylated Tyr<sup>641</sup> and STAT6-6 was similar to STAT6-5 but with the presence of Cy5 as fluorophore at Lys<sup>661</sup>. The biological activity of semisynthetic truncated STAT6 isoform (1-6) was assessed by several methods such as western blotting, electrophoretic mobility shift assays (EMSA) and microinjection.

### 5.2 Caged phosphorylated tyrosine building block

Chemical synthesis was considered to obtain caged compounds since it allows rapid synthesis with high yields as compared other modes for generating proteins<sup>199,200</sup>. Proteins and peptides have been caged with commercially available reagents that covalently modify specific amino acid residues<sup>147,201</sup>. In recent times many groups have shown these reagents can be used for spatio-temporal control of biological activities for studies in *in vivo* or *in vitro*<sup>200,201</sup>. Caged compounds are widely used with cysteine, arginine, lysine, glutamic acid, serine, threonine and tyrosine residues. Cell penetrating caged peptides and caged proteins were recently studied to understand many protein-protein interactions, enzymatic processes, among other biologically relevant phenomena<sup>202</sup>. Phosphorylation is an important post translational modification on proteins, and in the case of STAT6, caging the phosphate has a dramatic effect on protein behavior. Earlier work reported by David Humphrey *et. al.*<sup>203</sup> showed that phosphorylation of Tyr<sup>397</sup> is responsible for the downstream signaling events cascaded by the focal adhesion kinase (FAK). FAK-mediated signaling plays a critical role in cell adhesion. Decaging of Tyr<sup>397</sup> FAK peptide in the migrating cells led to temporary arrest

## Discussion

---

of migration, similar to observations with non caged active variant of FAK showing that decaged FAK behaves like the native protein.

1-(2-nitrophenyl) ethyl (NPE) is one of the widely used caging compounds (section 1.2.3) and thus was chosen to cage STAT6 due to its rapid decaging capacity on illumination by UV. The NPE moiety was synthesized using phosphoramidite chemistry which is one of the widely used methods to phosphorylate a residue on a peptide or protein by using Fmoc based SPPS and can be incorporated at any position of the peptide chain. NPE-IP<sub>3</sub> has been successfully applied to study the signaling in Ca<sup>2+</sup> voltage gated channels present in neurons. Pyridine nucleotides NAD and NADP<sup>204</sup> most abundantly found in the eukaryotic cells have been caged and characterized for use in enzymology, cell biology, metabolism and have been studied<sup>205</sup>. NPE was also used to caged fluorophore such as NPE- coumarins<sup>206</sup> which are non-fluorescent when key functional groups of fluorophore are masked by caging groups. Photoactivation with ultraviolet (UV) light removes the protecting group and switches on the fluorescence of parent dyes.

The photo byproducts from NPE are water soluble at physiological conditions causing no harm to the cells and did not cause the protein or peptide to aggregate nor modify the activity of the protein during the photolysis experiment. The NPE group was selected because it releases a ketone rather than an aldehyde as a photo-byproduct, which is highly reactive in the cellular environment. The NPE group has a maximum absorption at 259 nm, with an extinction coefficient ( $\epsilon_{\max} = 5,700 \text{ M}^{-1}\text{cm}^{-1}$ ). The absorption spectrum is broad, and thus the aromatic group still absorbs significantly at high-end UV (365 nm). Deprotecting NPE group by UV light is rapid depending on the light source. The majority of decaging experiments use flash lamps (for example, pulsed xenon or mercury arc lamps focused with a parabolic mirror) or lasers as the light source. The intensity of the light source plays essential role in determining the rate of decaging. The large number of photons from the laser of the confocal microscope could enable uncaging during the *in vivo* experiments much more quickly than the photons generated from the UV lamp which was used during the *in vitro* decaging of the peptide. Analysis of the decaging of

## Discussion

---

NPE group from peptide can be carried out over RP-HPLC or directly by ESI-MS which is an advantage since the analysis can be performed in a short time with more accuracy.

Caging STAT6 was performed by synthesizing the caged phosphorylated tyrosine building block (Tyr<sup>641</sup>) which was carried out efficiently over five steps in solution phase as described by Rothman D.M, *et al.*, 2003<sup>176</sup>. First NPE group was synthesized with the help of phosphoramidite chemistry to generate trivalent phosphate product (section 3.2.2) which was later incorporated with the Fmoc protected Tyrosine to yield the final product, caged phosphorylated Fmoc protected Tyrosine (section 3.2.3 - 3.26). Inert atmosphere was maintained for the required synthesis steps. Yields of the products in each step were in good agreement with the original paper from Rothman D.M, *et al.*, 2003<sup>176</sup>. Yield for product (**7**) (section 3.3.4) was found to be higher by 18% than reported in the original paper. Product (**6**) was synthesized by 1-H tetrazole in acetonitrile instead of pure 1-H tetrazole because of the non availability of the latter. The overall yield of the synthesis was ~50 % which was 10 % higher than reported in the original paper. Fmoc protected caged phosphorylated Tyrosine had  $\beta$ - cyanoethyl group which was removed during base treatment rendering non chirality to the amino acid. All the products were characterized using NMR, ESI-MS and MALDI.

Further, product (**8**) was incorporated at position 641 of the growing peptide chain of **1** and **2** which generated the caged phosphorylated Tyr<sup>641</sup> variants. The un-natural Tyr<sup>641</sup> which was modified to have the caged (NPE) phosphate as the bulkier group in its side chain required 2 h of coupling time, compared to 20 min usually needed for the coupling of Fmoc protected amino acid with smaller side chains and protecting groups. Peptide **1** was further labeled with Cy5 which eased the detection during HPLC purification, NCL and *in vivo* experiments. Peptide **2** was similar to peptide **1** in sequence except it had no Cy5. The yield of peptide **1** was lower than peptide **2** in spite of the similarities in the purification conditions it was assumed than the former peptide which only differentiated from the latter by possessing one Cy5 and an  $M_{(obs)}$ : 3831 Da was an artifact generated from HPLC column as the artifact was not observed during the purification of peptide **2**.

## Discussion

---

Peptide **3** having non-caged phosphorylated tyrosine and Cy5 labeled variant when compared with its counterpart peptide **4** had no fluorophore showed similar pattern of low yield after the purification from HPLC. The improvement in the yield for purification of Cy5 labeled peptide was observed when compared between peptide **4** over **1** even though there was no difference in the strategy of purification. Peptide **5** and **6** which are the variants for wild type STAT6 sequence also showed similar trend in the yield when compared with peptide **1** and the detection of peptide **6** in ESI-MS showed high signal to noise ratio. It was concluded that Cy5 containing peptides always gave low yield than its counterpart peptides.

### 5.3 Generation of semisynthetic STAT6 variants

Many papers have reported the use of expressed protein ligation to engineer the proteins. However, there was no report on the semisynthesis of STAT proteins before the start of this work. EPL was used to generate light switchable STAT6 by caging the phosphorylation site on Tyr<sup>641</sup> and investigating its behavior as monomer and upon decaging its dimeric behavior which will help to investigate STAT6 at molecular level. Hahn *et al*, 2007<sup>146</sup> prepared a caged Smad-2 using semisynthesis and expressed protein ligation (EPL) strategy. Smad-2 which is a key element of the intracellular response to cytokines of the transforming growth factor  $\beta$  (TGF $\beta$ ) super family, which are involved in myriad of normal and disease processes. The caged form only entered the nucleus as hetero-trimer after photoactivation.

Based on the general guidelines of EPL explained in section 1.3, recombinant Human STAT6MxeCBD plasmid was generated and the protein was expressed in *E.coli* cells. STAT6 MesNa  $\alpha$ -COSR was obtained after STAT6MxeCBD was mainly found in the inclusion bodies with a lesser amount found in the cytosol. STAT6 was purified from the cytosolic fraction of *E.coli* in order to generate folded native protein; hence induction with IPTG was carried out at a low temperature from 14 - 18°C to obtain soluble protein with higher yield.



## Discussion

---

Purification of expressed STAT6MxeCBD (95 kDa) from crude lysate was carried out by double affinity tag containing His<sub>7</sub>-tag at the C-terminus, after the intein, and the chitin binding domain (CBD) attached to the C-terminal part of the intein was found to be very useful enabling STAT6 to purify twice. It was observed that STAT6MxeCBD was eluted from the Ni-NTA resin at a very low imidazole concentration (30 mM) since binding between the Ni<sup>2+</sup> and His<sub>7</sub> tag was not very strong hence more washing with the STAT6 buffer favored a high level of purification. STAT6 MesNa α-COSR at the C-terminus was prepared by splicing the MxeGyrA by addition of thiols such as MesNa after loading STAT6MxeCBD on the chitin beads via chitin binding domain. Intein splicing was carried out very efficiently over 12 h. However, an excess of MesNa resulted in precipitation of the protein hence it was observed that 250 mM concentration of MesNa was ideal for splicing the intein to form STAT6 MesNa α-COSR without any precipitation.

Aggregation was the main problem during preparation of STAT6MxeCBD. Precipitation of protein was observed during the thawing of frozen sample, removal of imidazole from the protein solution by dialysis or ultra filtration, in the presence of excess MesNa and during storage. Stabilization of proteins using detergent micelles has been successful in several cases. To prevent STAT6 from aggregation, a non-ionic detergent n-dodecyl-β-D-maltopyranoside (DDM) in varying concentration (0.1% to 0.05%) was added as a stabilizer. DDM (0.1% to 0.05%) proved to give protein without any precipitation. Later removing protein from detergent was the most problematic part of the purification. DDM has a very low critical micelle concentration (CMC) value (~0.2 mM) hence breaking detergent micelle containing protein and peptide was very difficult. This was in agreement with the report from Pavel *et. al.* 2005.<sup>207</sup> who showed in their work that the micelle size of DDM was 70 kDa which is comparable to 62 kDa for STAT6 MesNA α-COSR. Thus, DDM with STAT6 MesNa α-COSR cannot be removed by a 100 kDa cutoff dialysis tube or membranes found in centrifuges. Purifying STAT6MxeCBD with glycerol (25% - 50%) was found to be an ideal solution. Using glycerol showed no of precipitation in any stage of purification. STAT6 MesNa α-COSR in glycerol (25% - 50%) solution could also be stored at 4°C for months without any precipitation. Frozen STAT6

## Discussion

---

MesNa  $\alpha$ -COSR also was thawed without any observation of precipitation. Disadvantage of glycerol is due to its high viscosity of the STAT6 buffer.

After successful preparation of recombinant STAT6  $\alpha$ -COSR, ligation with six different peptides (**1-6**) generated six different ligation products of STAT6 (**1-6**). Ligations were carried out at physiological pH (pH 7.0) without observing any precipitation of the protein. The shielding effect caused by the detergent hindering the ligation between STAT6 MesNa  $\alpha$ -COSR and its peptides (**1-6**) was improved by using glycerol (25%-50%) in the STAT6 buffer. The complete formation of the ligation was 72 h and RT was found to be ideal for the ligation reaction.

Each peptide carried a His<sub>6</sub>-tag at its C-terminus, which was useful to separate ligation product from the STAT6  $\alpha$ -COSR, but excess peptide could not be separated due to the presence of the His<sub>6</sub>-tag on the sample peptide. Gel filtration, which is commonly used to separate compounds with very different molecular weight as proteins and peptides, was found to be unsuccessful due to the micelle formation of DDM. Due to this peptide and the ligation product was eluted at the same time. As it is reported by Pavel *et. al.* that size of DDM micelle is 70 kDa which is equal to the size of ligation product of STAT6 (75 kDa), detergent micelle was very difficult to remove by gel filtration. Due to the minor amounts obtained after several steps of synthesis to generate the ligation product, loss in yield was a greater concern and non achievable separation of peptide from ligation products gel filtration method was discontinued. Ultra filtration of the ligation product by using protein concentrators was able to remove large concentrations of the peptide though traces remained. Final yield of the ligations were from 33% to 20%, which is very good after several steps of synthesis. The yields were measured by Bradford test or by observing the difference between the ligation product band and the protein marker on SDS-PAGE.

### 5.4 Choice of Fluorophore

Fluorescent markers like Cy5 and Tamra were used to study semisynthetic truncated STAT6. Cy5 was selected as a fluorophore due to its small size compared to large fluorescent proteins, such as GFP<sup>208</sup> or YFP. Using semisynthetic truncated STAT6 (75 kDa), it was possible to couple Cy5 directly to the peptides synthesized by SPPS. The distance of Cy5 from Tyr<sup>641</sup> on STAT6 peptides was 20 aa which was reasonable since no loss of activity of STAT6 was observed during any bioactivity experiments.

Cy5 fluorophore emits in the far-red range which did not interfere with the aromatic amino acids present in the proteins and hence was easily detected by confocal microscopy, RP-HPLC and Fluoromax 3 machines. There was no auto fluorescence in the far red range in the cells during the *in vivo* experiments. Cy5 excitation (649 nm) and emission (670 nm) was well separated from the wavelengths required for decaging of the caged group, which needed UV light at 365 nm. During the *in vivo* experiments, no bleaching of Cy5 was observed. The extinction coefficient of Cy5 ( $250,000 \text{ M}^{-1} \text{ cm}^{-1}$ ) gave an advantage to study the protein at low concentration. Cy5 was easily detected by flashing He laser and the decaging experiments were carried out with ease by using UV laser which did not show any change in the Cy5 fluorescence. During ligation of the recombinant STAT6 with the Cy5 labeled peptides, the ligated protein did not denature. Due to high solubility of Cy5 in organic solvents, and its blue color, a Kaiser's test could not be performed, during the procedure of coupling the Cy5 to Lys661. Hence each test cleavage was carried out after the coupling of Cy5 to the peptide and its absorption at 595 nm light in RP-HPLC and corresponding ESI-MS of the peptide, before and after purification of the peptides showed the complete coupling of Cy5. This only delayed working time and loss of important peptide because of cleavage.

Tamra was used for the EMSA experiments to study the DNA binding of STAT6. Its ex 510 nm and em 575 nm was easily detected in fluorescence scanner. Tamra and Cy5 gave reasonably good signals during FRET experiments, which enabled the measurement of the dynamics of DNA binding to STAT6.

### 5.5 Bioactivity of STAT6 proteins

Phosphorylation is essential for signaling by STAT<sup>209</sup>. It is known that STAT is also phosphorylated not only on the Tyr<sup>641</sup> but also on the Ser<sup>232</sup> and Ser<sup>250</sup> present at the C-termini. Phosphorylation of serine is essential for transcriptional activity of STAT1, STAT2, STAT3 and STAT4 but not for STAT5A or STAT5B and STAT6. Maiti. N.R, *et. al.*, 2005<sup>210</sup> showed that serine phosphorylation occurs when PP2A is inhibited which reduces the DNA binding capacity of STAT6. Phosphorylation of serine residues does not affect the phosphorylation of Tyr<sup>641</sup> and dimer formation but phosphorylation of multiple serine residues changes the STAT6 dimers, causing the loss of DNA binding ability of the protein. Hence the single serine phosphorylation works independently of tyrosine phosphorylation.

More in depth knowledge about the importance of tyrosine phosphorylation along with its GAS-DNA binding mechanism for native STAT6 has to be investigated. Phosphorylation of semisynthetic variants of STAT6 was thereby, analyzed by various experiments first by monitoring the removal of NPE group from peptides and proteins. Actual functionality of semisynthetic STAT6 was proved by DNA binding experiments (with the approach of EMSA and FRET) and confocal nuclear localization studies.

The NPE group was successfully removed from peptide-7 upon irradiation with UV light from a Xenon lamp. ESI-MS data indicated that in 20 min the caged group was completely removed. This provided preliminary evidence that decaging works on a 34 aa long STAT6 peptide. The same technique was applied to the semisynthetic truncated STAT6-2 protein. An antibody-based method was found to be the ideal solution to detect the decaged STAT6-2 with high specificity as explained in section 4.3.1.

Dot blot experiments with phosphorylated peptide **3** and phosphorylated protein (STAT6-3) as positive control, non phosphorylated Tyr containing peptide **5** and caged phosphorylated containing peptide **2** as negative control showed the specificity of the antibody against the phosphorylated tyrosine. Decaging experiments over the protein on

## Discussion

---

SDS-PAGE showed a very specific signal for caged and decaged samples. These experiments revealed that the antibody did not bind to caged phosphorylated Tyr<sup>641</sup> (eg STAT6-2) but the decaged STAT6-2 was bound by the antibody, resulting in an intense signal showing the presence of free phosphate group on Tyr<sup>641</sup>. A minor amount of dimer of STAT6-2 was also observed when it was compared with the dimer of phosphorylated tyrosine STAT6-3.

Further the method did not require the purification of the ligation product because the decaging of the NPE group from protein was monitored via SDS-PAGE which facilitated the separation of peptide (~ 4 kDa) from semisynthetic truncated STAT6 variants (~75 kDa) as peptide migrates faster than the protein thereby loss of the ligation product during Ni-NTA purification or ultra filtration was completely avoided and many experiments could be performed. Native gel analysis of decaged STAT6-2 showed very high intense band which only proves that UV light did not denature STAT6-2 during removal of caged group as it was able to migrate through the gel in nearly one hour which was always required for binding experiments with STAT6-4.

Western blotting allowed detection of the removal of NPE group with highest specificity at low concentration of sample which was difficult with RP-HPLC and ESI-MS. However, the long experimental time required to perform western blots and the resulting semi-quantitative data were a disadvantage. The evidence gathered from dot blot for the peptides and western blots for STAT6-2 and -4 protein variants can be compared with the work published by Banala *et. al.*, 2008<sup>211</sup> who prepared caged substrates of O<sup>6</sup>-benzylguanine (BG) which were used by them for labeling protein such as O<sup>6</sup>-alkylguanine-DNA alkyl transferase (AGT or SNAP-tag). They successfully showed the removal of caged group NPE by using dot blot experiments along with other methods, the dimerization of SNAP-tag fusion protein by using caged derivatives of BG such as 1-(2-nitrophenyl)-ethyl-O<sup>6</sup>-benzylguanine.

Proof of functionality of semisynthetic truncated STAT6 variants was demonstrated by dimerization of STAT6-4 and its specific binding to its recognized GAS-DNA sequence

## Discussion

---

and the lack of binding by the monomeric STAT6-1 and -2 with its GAS-DNA shown by EMSA (section 4.3.2) indicating the strong dependency on tyrosine phosphorylation to form a dimer by STAT6 and its DNA binding ability while simultaneously proving that semisynthetic truncated STAT6-1, -2 and -4 are functional proteins. When compared with the EMSA data obtained from semisynthetic truncated STAT6 and the investigation reported by Chen W.G, *et. al.*, 2004<sup>212</sup> who explored methylation on STAT6, it is very evident that semisynthetic truncated STAT6 dimerizes and bind to its GAS-DNA independent of its methylation on arginine and phosphorylation on serine residues at its N-and C-termini respectively.

The challenging part was to detect the presence of detergent in the STAT6 buffer which prevented binding to the GAS-DNA sequence. It was observed during the EMSA experiments that presence of DDM in the STAT6 buffer caused the presence of an unidentified fluorescent band near the region of the STAT6 dimer which interfered with the interpretation of the binding of STAT6 with the Tamra ds GAS-DNA. This result was in agreement with the Pavel, *et. al.*, who investigated that DDM's micelle can only pass through 100 kDa cutoff but 100 kDa cutoff membranes cannot be used for semisynthetic STAT6 (75 kDa). The presence of glycerol in STAT6MxeCBD not only prevented the precipitation of STAT6 but also prevented the appearance of the unidentified fluorescence band that was seen in the presence of DDM during EMSA experiments. Therefore, glycerol did not interfere with the DNA binding activity of the protein.

Demonstrating FRET provided more evidence towards the proof of functionality for semisynthetic STAT6 variants by showing the binding with GAS-DNA. STAT6-3 which was phosphorylated variant labeled with Cy5 was used as an acceptor and Tamra ds GAS-DNA and Tamra ds random DNA was used as donor. Successful generation of FRET produced during the binding reaction between STAT6-3 and Tamra ds GAS-DNA against the background emission signal from non-binding reaction with Tamra ds random DNA indicates very fast dimerization of semisynthetic STAT6 which binds specifically to their recognized GAS-DNA in a functionally active form. FRET was an advantage to postulate the fast binding of the dimerized STAT6-3 with its specific DNA

## Discussion

---

as it is concentration independent. It also proved that presence of fluorophore did not interfere with the binding reactions. This is advantageous to future exploration of binding kinetics. The disadvantage of using spectrophotometer Fluoromax-3 was the generation of overheating of the instrument after few hours of experiments, it was difficult to reproduce the same data in similar conditions.

DNA binding activity of semisynthetic STAT6 is in good agreement with published work by Thomas Mitika *et. al.*<sup>213</sup> who had shown that even after deletion of TAD domain from STAT6 it binds to their GAS-DNA in spite of its inability to activate IL-4 responsive reporter construct.

The study of the functional genomics involves constructing the protein of interest in the form of DNA cloning and expressing them in bacterial cells, mammalian cells or yeast. Along with the *in vitro* data, *in vivo* experiments are proved by transferring the protein or peptide of interest into the live cells. Many methods are used for protein delivery such as electroporation, viral protein fusion, cationic lipids, projet-protein transfection reagent and microinjection. To investigate *in vitro* bioactivity of caged STAT6 variants, electroporation was not considered since short electrical pulse used for inserting the protein often damages many cells giving low efficiency. Viral protein fusion was not carried out since STAT6 was already 95 kDa long protein further modifying to insert the small protein transducing domain would have created difficulties in purification. It is also known for PTDs is that after insertion in the cells the protein of interest has to refold since PTDs are denatured during the insertion process. Microinjection is considered the most suitable method over transfection since data can be interpreted in a very short time which also overcomes the barrier of plasma membrane permeability. The only disadvantage is that only few cells can be studied at a time and the method is a very laborious.

Therefore, microinjection was used to demonstrate the *in vivo* activity of light switchable semisynthetic truncated STAT6-1 in physiological conditions. STAT6-1 in its caged form is assumed to behave as a monomer in the cytoplasm upon microinjection and after

## Discussion

---

photolysis with UV laser should transform into a dimer which should migrate to the nucleus. Microinjection was performed with various mammalian cell-lines such as A431, COS-7 and MDCK. A431 cell lines were used because of its larger cell size compared with COS-7 cell lines which showed STAT6-1 only in the cytoplasm proving the presence of monomeric native state. During several attempts of microinjection it was observed that STAT6-1 was seen both in the nucleus and cytoplasm without exposure to UV. This was impossible since STAT6 (75 kDa) cannot migrate to nucleus before becoming functionally active by forming a dimer. The observation can be explained by the results obtained during the difficulty of removing Peptide 1 (4.7 kDa) from STAT6 buffer due to the presence of DDM which can lead to the rapid migration to nucleus because of its small size resulting in the appearance of Cy5 fluorescence in the nucleus. Some minor amount of precipitation was observed during the microinjection of STAT6-1 which occurred for the reason that STAT6 is instable at low salt concentration of injection buffer (PBS buffer), and it is stable at high salt concentration (1 M NaCl).

The unavailability of the UV laser had halted the experiment for further trials until Leica SP5 with 405 diode laser was available. The difficulty during microinjection occurred due to the low concentrations of STAT6-1 available to be used for the experiments which made it difficult to analyze the data. Concentrating STAT6 was not reasonable since it had a tendency to precipitate hence always the diluted protein solutions were used. It was also observed that cells started to disintegrate when microcapillary tube loaded with STAT6-1 was brought close to the cell surface for injection. It was assumed that presence of detergent in STAT6-1 might cause the disintegration of the cells, hence as a control STAT6 buffer + DDM (0.1%) was injected but it did not show any disintegration of the cells. Cell lines were changed from A431 to COS-7 which did not make any difference in the observation.

Finally MDCK cell lines which are known to be more robust for microinjection were used. The change in the cell lines produced dramatic change in the results. In chapter 4, section 4.3.3 and figure 4.36, A shows the caged STAT6-1 in the cytoplasm, on exposure to UV light caged group was removed and STAT6-1 migrated rapidly from



## Discussion

---

cytosol to nucleus with an increase in Cy5 fluorescence showing the successful formation of the dimer. The migration of STAT6-1 from the cytoplasm to the nucleus was further evaluated by plotting a graph of Cy5 intensities in the cytoplasm and the nucleus against time which showed an exponential increase of Cy5 due to the formation of dimeric STAT6 upon removal of caged group by UV light and exponential decrease of the same in cytoplasm because of the migration of the functionally active dimer to the nucleus.

The result successfully proved that semisynthetic truncated STAT6-1 in physiological conditions switched from monomeric state to dimeric state showing the presence of bioactive STAT6 by mimicking native STAT6 behavior. Nuclear protein transporters such as importins were not added externally neither any scavenger to trap the photo by product was used. As described in many reports on microinjection that decaging with UV laser occurs in few micro seconds which had good agreement with the observed results of light switchable STAT6-1. Laser 405 diode could very well remove the caged group. It was also observed that on exposing UV light for 20 min dimer of STAT6-1 did not localize to the cytoplasm since STAT has an ability to relocate in the cytosol after the completion of transcription of gene by undergoing dephosphorylation to convert into its inactive monomeric state. No natural phosphatases which are always found in cells could dephosphorylate dimeric STAT6 into monomeric form followed by their migration from nucleus to cytosol was observed in 20 min which proves that C-TAD was essential for relocation from nucleus to cytosol. The lifetime of STAT in nucleus was reported from 15 min to few hours. Hoechst 33445 was excited at 405 nm, and the increased intensity in the Hoechst channel compared to Cy5 channel was due to higher intensity of UV 405 for decaging the caged group from STAT6-1.

The result obtained from microinjection experiment can be compared with the published work carried out by Thomas Meyer *et. al.*, 2004<sup>214</sup> where recombinant STAT1-GFP tagged protein was microinjected in HeLa cells which did not relocalize to the cytoplasm after stimulation with IFN $\gamma$ . They concluded that the presence of GFP-tag and nuclear barrier was responsible for inhibition for translocation activity of the protein from nucleus

## Discussion

---

to cytoplasm. However C-TAD was carrier independent in translocating protein into the nucleus. Thus, variants of semisynthetic truncated STAT6 proteins which miss the transactivation domain (TAD) showed its DNA binding activity successfully via *in vitro* experiments (EMSA and FRET) and their physiological behavior of dimerization in native environment through *in vivo* experiments (microinjection in MDCK cells). Semisynthetic truncated STAT6 thereby cannot induce transcription produced by IL-4 respective signals. Thus, by using EPL technique, systems biology of light switchable STAT6 which successfully mimicked their native form of dimerization has opened new areas in understanding their behavior at molecular level.

# Chapter 6

---

Summary and Outlook

### 6.1. Summary

Signal transducer and activators of transcription (STAT) proteins comprise a family of transcription factors that usually reside in the cytoplasm in a monomeric state. They are essential constituents of the JAK-STAT pathway. In this pathway a ligand binds to its respective receptor thereby activating JAKs, which upon activation phosphorylate the receptor. The phosphorylated tail becomes a docking site for monomeric STAT proteins from the cytoplasm. Upon binding to the receptor tail STAT proteins become themselves phosphorylated by JAKs and are released from the receptor tail. Such a phosphorylation event is followed by formation of homo- and heterodimers that translocalize to the nucleus. At this stage STAT proteins bind to specific DNA promoter regions that induce expression of cytokine responsive genes. This signal transduction pathway plays a key role in case of cell proliferation (cancer), controlled cell death, during viral infections as well as in inflammatory processes. Here the semisynthesis of a light-switchable variant of STAT6 is described that provides temporal control over STAT6 activation together with *in vitro* and *in vivo* visualization.

To achieve this aim, a semisynthetic approach termed expressed protein ligation (EPL), which combines chemical and biochemical methods was used. A C-terminally truncated STAT6-intein fusion protein was expressed in *E.coli*. The intein fusion comprised the *Mxe* GyrA intein for generating STAT6-  $\alpha$ -COSR consisting of amino acids 1 - 634 and a chitin-binding domain as a purification tag. Following expression it was essential to stabilize STAT6 during purification and generation of the thioester moiety ( $\alpha$ -COSR) with stabilizers such as detergent or glycerol to prevent aggregation and increase protein yields.

Six semisynthetic truncated STAT6 variants (numbered **1-6**) were obtained with site specific modifications at Tyr<sup>641</sup>. This was achieved by native chemical ligation of recombinantly generated STAT6-  $\alpha$ -COSR with six different variants of a chemically synthesized peptide comprising amino acids 635 - 668 of STAT6. The site specific modifications of Tyr<sup>641</sup> were introduced by incorporating specifically modified tyrosine building blocks during SPPS and this process led to caged phosphorylated Tyr, phosphorylated Tyr and non phosphorylated Tyr in position 641 of STAT6. No

## Summary and Outlook

---

enzyme-based phosphorylation strategy was used. Thus, seven different peptides **1-7** were generated by using SPPS and peptides **1-6** were incorporated in STAT6 thereby giving access to the following variants: STAT6-1 carrying a caged phosphorylated Tyr<sup>641</sup> and a Cy5 fluorophore for visualization, STAT6-2 with caged phosphorylated Tyr<sup>641</sup> without Cy5, STAT6-3 with phosphorylated Tyr<sup>641</sup> with Cy5, STAT6-4 with phosphorylated Tyr<sup>641</sup> without Cy5, STAT6-5 with non-phosphorylated Tyr<sup>641</sup> without Cy5 and STAT6-6 with non-phosphorylated Tyr<sup>641</sup> with Cy5. Peptide 7 was not used in ligation reactions but for studying the photo-release of the caged group.

To investigate the bioactivity of semisynthetic STAT6 proteins **1-6** *in vitro* DNA binding assay based on electrophoretic mobility shift assays (EMSA) and fluorescence resonance energy transfer (FRET) were performed with different caged and non-caged phosphorylated STAT6 variants such as STAT6-2 and STAT6-4, respectively. STAT6-4 successfully recognized its specific DNA binding motif (GAS) and did not recognize a random DNA sequence of the same length. This indicated that semisynthetic, C-terminally truncated STAT6 can form bioactive dimers and that the absence of the C-TAD domain does not affect DNA binding. STAT6-2 did not recognize GAS-DNA demonstrating that the caged group effectively prevents dimerization via an SH2-mediated interaction. The presence of detergent such as DDM, required to stabilize STAT6 during semisynthesis and *in vitro* assays, inhibited the interpretation of EMSA data and hence it should be avoided in future EMSA experiments. However, glycerol did not inhibit the interpretation of data from EMSA experiments. Mixing of activated, semisynthetic STAT6 carrying Cy5 as an acceptor fluorophore with commercially available DNA equipped with a TAMRA label showed successful binding of STAT6-3 with GAS-DNA by energy transfer only for non-caged phosphorylated STAT variants. To study the removal of the caged group, western blot experiments and ESI-MS analysis were performed with STAT6-2 and peptide 7. Western blot experiments using a pTyr-specific antibody showed intense signals for decaged STAT6-2, STAT6-4 and peptide 3 and no signal for caged phosphorylated STAT6-2 and peptide 5. ESI-MS showed 100% removal of caged group from Tyr of peptide 7 after illumination with 365 nm light for 20 min.

## Summary and Outlook

---

*In vivo* visualization of STAT6 was very challenging due to the size of the semisynthetic product and its tendency to aggregate. Transfer of STAT6 variants into cells was achieved by microinjection into different eukaryotic cell lines such as A431, COS7 and MDCK cells. Finally microinjection of MDCK cells with STAT6-1 showed that this caged variant remains in the cytoplasm but after illuminating the cells with UV light (and release of the caged group) the protein became activated and translocated to the nucleus. This result provides proof that semisynthetic STAT6 variant behave similar to their native counterparts under physiological conditions and that they can become valuable tools for studying the JAK-STAT pathway *in vitro* and *in vivo*.

### 6.2. Outlook

Thus the successful semisynthesis and application of STAT6-variants requires the synthesis of a crucial amino acid building block (caged phosphorylated tyrosine) starting from the round bottom flask to procedures such as microinjection of living cells. The data produced here gives evidence not only about the importance of controlling phosphorylation as a major posttranslational modification of STAT6 but also that very large semisynthetic protein can be generated successfully.

The experiments described here, which combine chemical and biological techniques established a new platform on which STAT6 can be investigated in the future. Demonstrating FRET *in vivo* could provide a better understanding of the kinetics of dimerization and the effect of DNA binding on STAT6. Thus systems biology approaches can be used to investigate STAT6 and connected proteins in more detail. Microinjection with Cy5 labeled variants such as STAT6-3 and STAT6-6 can increase our knowledge about localization of these variants. Labeling caged phosphorylated variants of STAT6 with two different fluorophores followed by microinjecting and observation via two different channels can also provide more knowledge about the dimerization pattern of STAT6 thus, protein-protein interactions could be evaluated more efficiently *in vivo*. Inhibitors of STAT6, which were recently published, can be studied with these semisynthetic variants *in vitro* and *in vivo*. Even new screening systems could be set up using these molecules. Cytokine signaling and JAK proteins can be further investigated.

### 6.1. Zusammenfassung und Ausblick

Die Signaltransducer und Aktivatoren der Transkription (STAT) bilden eine Familie von Transkriptionsfaktoren, die im Cytoplasma in monomerer Form vorliegen. Sie können durch extrazelluläre Signale, wie Cytokinen, aktiviert und daraufhin in den Zellkern transportiert werden. Dort wird dann die Transkription spezifischer Gene initiiert. Dieser Mechanismus verläuft über den so genannten JAK-STAT Signalweg, wobei, zunächst ein Ligand an den zugehörigen Rezeptor bindet und damit dessen Phosphorylierung durch Janus-Kinase (JAKs) aktiviert. So entsteht eine Bindestelle für monomere STAT-Proteine, die im Rezeptor-gebundenen Zustand wiederum durch JAKs phosphoryliert werden und sich dann vom Rezeptorende lösen. Die phosphorylierten STATs bilden Homo- und Heterodimere, die in den Zellkern wandern. In dieser Phase binden die STAT-Proteine an spezifische DNA-Sequenzen und induzieren die Expression. Dieser Signalübertragungsweg ist bedeutend für die Kontrolle der Zellproliferation sowie bei Entzündungsprozessen und bei der Entstehung von Krebs. Das Ziel dieser Arbeit war es licht-aktivierbares humanes STAT6 herzustellen, das eine gezielte Aktivierung der Dimerisierung und damit der DNA-Bindung des STAT6 *in vitro* und *in vivo* erlaubt.

Um dieses Ziel zu erreichen wurde ein Verfahren gewählt, das chemische und biochemische Methoden kombiniert und als Expressed Protein Ligation (EPL) bezeichnet wird.. Ein C-terminales Segment des STAT6 Proteins, das den für die Dimerisierung entscheidende Tyrosinrest 641 enthält konnte erfolgreich chemisch synthetisiert und ortsspezifisch modifiziert werden. Es war jedoch erforderlich die C-terminale Transaktivierungsdomäne (TAD) des STAT6-Protein zu entfernen, um die modifizierten Tyrosinreste und den Fluoreszenzfarbstoffe in das STAT6 mittels einer EPL Reaktion einzuführen. In *E. coli* wurde das multidomänen Protein STAT6 in Fusion mit dem GyrA-Intein aus *Mycobacterium Xenopi* und einer Chitin-bindenden Domäne als Aufreinigungstag exprimiert Nach Spaltung des Fusionskonstruktes in Anwesenheit von MesNa konnte STAT MesNa  $\alpha$ -COSR (AS 1-634) dargestellt werden. Die Stabilisierung des Fusionskonstruktes war essentiell für der Generierung von STAT6 MesNa  $\alpha$ -COSR, da häufig Aggregation beobachtet wurden, und die Zugabe von Stabilisatoren, wie Detergenz oder Glycerin nötig war.

## Zusammenfassung und Ausblick

---

Es wurden sechs semisynthetische STAT6 Varianten (**1-6**) mit ortsspezifischen Modifikationen im C-terminalen Bereich des Proteins (Tyr<sup>641</sup>, Fluoreszenzmarkierung, Hexahistidin-Tag) nach chemoselektiver Ligation mit sechs unterschiedlichen C-terminalen Peptiden (Peptide **1-6**, AS 635-668) generiert. Als ortsspezifische Modifikation wurde bei der chemischen Synthese der C-terminalen Peptide geschütztes, phosphoryliertes Tyrosin und phosphoryliertes Tyrosin eingeführt sowie der Fluoreszenzmarker Cy5. Auf diese Weise wurden sieben unterschiedliche Peptide durch SPPS generiert. Durch EPL wurde Tyr<sup>641</sup> in STAT6 mit geschütztem, phosphoryliertem Tyrosin und Cy5 (STAT6-1) dargestellt. STAT6-2 wurde mit geschütztem, phosphoryliertem Tyr<sup>641</sup> ohne Cy5 generiert, STAT6-3 mit phosphoryliertem Tyr<sup>641</sup> mit Cy5 und STAT6-4 mit phosphoryliertem Tyr<sup>641</sup> ohne Cy5. STAT6-5 wurde ohne Phosphorylierung am Tyr<sup>641</sup> und ohne Cy5 und STAT6-6 mit nicht-phosphoryliertem Tyr<sup>641</sup> mit Cy5 dargestellt. Peptid **7** weist ein geschütztes phosphoryliertes Tyr<sup>641</sup> auf und wurde in den Ligationsversuchen nicht verwendet, jedoch wurde es zur Untersuchungen zum Entschützen der photolabilen Gruppen genutzt.

Um die Bioaktivität der sechs semisynthetischen STAT6 Varianten zu testen wurden *in vitro* Methoden, wie DNA Bindungstests mit Hilfe elektrophoretischer Methoden (EMSA) und Fluoreszenzresonanz-Energietransfer (FRET) genutzt. Dabei wurde mit den phosphorylierten Varianten STAT6-4 und STAT6-3 gearbeitet. STAT6-4 erkannte die zugehörige GAS-DNA, wohingegen keine zufälligen DNA-Sequenzen erkannt wurden. So konnte gezeigt werden, dass semisynthetisches, verkürztes STAT6 richtig gefaltet und biologisch aktiv in dimerer, nativer Form vorliegt und die Abwesenheit der C-terminalen TAD Domäne die DNA Erkennung und Bindung nicht verhindert. STAT6-2 (mit geschütztem phosphorylierten Tyr<sup>641</sup>) konnte die zugehörige GAS-DNA nicht erkennen, was auf das Vorliegen von monomerem STAT6 zurückzuführen ist. Die Anwesenheit von Detergenz erschwerte die Interpretation der EMSA Daten und es wurde durch Glycerin ersetzt, das keinen solchen Effekt zeigte. FRET Experimente mit Cy5-markiertem STAT6 Protein und Tamra-gelabelter DNA zeigen eine Bindung von STAT6-3 an die GAS-DNA.

Die Abspaltung der Phosphat-Schutzgruppe in Peptiden und den semisynthetischen STAT6 Proteinen wurde durch Western-Blot Experimente mit einem Phospho-



## Zusammenfassung und Ausblick

---

Tyrosin spezifischen Antikörper nachgewiesen, sowie durch ESI-MS Messungen mit Peptid **7**. Die Western-Blot Experimente zeigten starke Signale für STAT6-**2**, STAT6-**4** und Peptid **3**, die jeweils Phospho-Tyrosin enthalten, jedoch kein Signal für geschütztes, phosphoryliertes STAT6-**2** und Peptid **5**. ESI-MS Daten zeigten, dass die Schutzgruppe am Tyrosinrest des Peptids **7** quantitativ entfernt werden (Bestrahlung mit UV-Licht bei 365 nm für 20 min).

Zur *in vivo* Visualisierung von STAT6 wurde geschütztes, phosphoryliertes und Cy5 gelabeltes STAT6-**1** durch Mikroinjektion in unterschiedliche Zelllinien wie A431, COS7 and MDCK eingebracht. In MDCK Zellen verblieb diese STAT6 Variante vor Bestrahlung mit UV-Licht im Cytoplasma, wie es für die monomere Form erwartet wird. Nach Bestrahlen mit UV-Licht und entschützen des phosphorylierten Tyrosin wurde das Protein im Zellkern gefunden. Dies zeigt, dass spezifisch modifiziertes semisynthetisches STAT6 (wie z.B. STAT6-**1**) die Möglichkeit bietet die aktivierte phosphorylierte Variante des STAT6 gezielt freizusetzen und intrazellulär zu beobachten.

Die durchgeführten Experimente, die chemische und biologische Techniken verreinen, konnten einen neuen Zugang zu ortsspezifisch modifizierten STAT6-Varianten aufzeigen, die in der Zukunft neue Einblicke in die STAT6 vermittelte Signalweiterleitung erlauben. Das erfolgreiche Einbringen in Zellen erlaubt die Anwendung systembiologischer Ansätze, z.B. auch unter Verwendung unterschiedlich markierter STAT-Proteine. Die kontrollierte Freisetzung der phosphorylierten STAT6 Varianten ermöglicht auf die gezielte Untersuchung des Einflusses von STAT-Inhibitoren auf die Dimersierungsgleichgewichte in Zellen und die Translokation.

## Acknowledgment

---

I would take this opportunity to thank many people.

Prof. Dr. Christian Becker my direct supervisor for his extreme patience, endless support over these years and giving me lots of freedom to carry out STAT project successfully.

Prof. Dr. Martin Engelhard for being my referee and for his advices on my project.

Prof. Dr. Peter Eilbracht for reading my thesis and being my referee.

Prof. Dr. Roger. S. Goody for accepting me in his department, and for his support.

Dr. Ralf Seidel and Anke Raulen for providing me not only with the plasmid for STAT6 but also for his advices on STAT project.

Sascha Gentz and Martina Wischnewski for providing me with peptides and helping me with HPLC techniques.

Dr. Anne Adida who first introduced me to tissue culture. Nachiket Varket for helping me with microinjection experiments, discussions and correcting my manuscript together with Tulika Dhar and Dr. Christine Delon till the n<sup>th</sup> moment. Thanks to Ines Heinrich for converting my abstract in German language.

Thanks to my friends and colleagues without their support and friendship the path to reach the goal would have been a very difficult journey.

I thank the MPI for providing a fascinating scientific atmosphere which kept me motivated all the time during these periods. I would honestly say that I completely enjoyed my time in MPI. I thank IMPRS for providing me funding and their past and present coordinators for easing my work during bureaucratic hassels.

Finally there is no word called "thanks" for mom, dad and sister this will definitely insult them because without their extreme courage to send me abroad, without their support and motivation from far away, I would not have reached at this stage of my life.

## Reference list

---

1. Sprang, S. R.; Fernando Bazan, J. Cytokine structural taxonomy and mechanisms of receptor engagement : Current opinion in structural biology 1993, 3:815-827. *Current Opinion in Structural Biology* **1993**, 3 (6), 815-827.
2. Levy, J. P.; Gomard, E.; Wybier-Franqui, J. [Primary generation in vitro of T killer lymphocytes specific against viral tumors, in the presence of interleukine 2]. *C. R. Seances Acad. Sci. III* **1981**, 292 (12), 759-761.
3. Claudinon, J.; Monier, M. N.; Lamaze, C. Interfering with interferon receptor sorting and trafficking: Impact on signaling. *Biochimie* **2007**, 89 (6-7), 735-743.
4. Arai, K.; Lee, F.; Miyajima, A.; Miyatake, S.; Arai, N.; Yokota, T. Cytokines - Coordinators of Immune and Inflammatory Responses. *Annual Review of Biochemistry* **1990**, 59, 783-836.
5. Darnell, J. E. STATs and gene regulation. *Science* **1997**, 277 (5332), 1630-1635.
6. Haque, S. J.; Sharma, P. Interleukins and STAT signaling 313. *Interleukins* **2006**, 74, 165-206.
7. James N Ihle . The STAT family in cytokine signaling. *Current Opinion in Cell Biology*13[2],211-217.2001.
8. Patel, B. K.; Keck, C. L.; O'Leary, R. S.; Popescu, N. C.; LaRochelle, W. J. Localization of the human STAT6 gene to chromosome 12q13.3-q14.1, a region implicated in multiple solid tumors. *Genomics* **1998**, 52 (2), 192-200.
9. Jacqueline Bromberg STAT proteins and oncogenesis. *Journal of Clinical Investigation* **2002**, 109 (9), 1139-1142.
10. Calo, V.; Migliavacca, M.; Bazan, V.; Macaluso, M.; Buscemi, M.; Gebbia, N.; Russo, A. STAT proteins: From normal control of cellular events to tumorigenesis. *Journal of Cellular Physiology* **2003**, 197 (2), 157-168.
11. Bromberg, J.; Darnell, J. E. The role of STATs in transcriptional control and their impact on cellular function. *Oncogene* **2000**, 19 (21), 2468-2473.
12. Coffey, P. J.; Koenderman, L.; de Groot, R. P. The role of STATs in myeloid differentiation and leukemia. *Oncogene* **2000**, 19 (21), 2511-2522.
13. Darnell, J. E. Transcription factors as targets for cancer therapy. *Nat Rev Cancer* **2002**, 2 (10), 740-749.
14. Ortmann A .R, Cheng.T. Visconti. R, Frucht. M. D, O'Shea. J,O.J Janus kinases and signal transducers and activators of transcription: their roles in cytokine signaling, development and immunoregulation. *Arthritis Research and therapy* **1999**, 2, 16-32.
15. Park, C.; Lecomte, M. J.; Schindler, C. Murine STAT2 is uncharacteristically divergent. *Nucleic Acids Res.* **1999**, 27 (21), 4191-4199.

## Reference list

---

16. Park, C.; Li, S.; Cha, E.; Schindler, C. Immune response in STAT2 knockout mice. *Immunity* **2000**, *13* (6), 795-804.
17. Zhong, Z.; Wen, Z.; Darnell, J. E., Jr. STAT3 and STAT4: members of the family of signal transducers and activators of transcription. *Proc. Natl. Acad. Sci U S A* **1994**, *91* (11), 4806-4810.
18. Park, S. J.; Nakagawa, T.; Kitamura, H.; Atsumi, T.; Kamon, H.; Sawa, S.; Kamimura, D.; Ueda, N.; Iwakura, Y.; Ishihara, K.; Murakami, M.; Hirano, T. IL-6 regulates in vivo dendritic cell differentiation through STAT3 activation. *J. Immunol* **2004**, *173* (6), 3844-3854.
19. Germain, D.; Frank, D. A. Targeting the cytoplasmic and nuclear functions of signal transducers and activators of transcription 3 for cancer therapy. *Clin. Cancer Res.* **2007**, *13* (19), 5665-5669.
20. Watford, W. T.; Hissong, B. D.; Bream, J. H.; Kanno, Y.; Muul, L.; O'Shea, J. J. Signaling by IL-12 and IL-23 and the immunoregulatory roles of STAT4. *Immunol Rev* **2004**, *202*, 139-156.
21. Remmers, E. F.; Plenge, R. M.; Lee, A. T.; Graham, R. R.; Hom, G.; Behrens, T. W.; de Bakker, P. I.; Le, J. M.; Lee, H. S.; Batliwalla, F.; Li, W.; Masters, S. L.; Booty, M. G.; Carulli, J. P.; Padyukov, L.; Alfredsson, L.; Klareskog, L.; Chen, W. V.; Amos, C. I.; Criswell, L. A.; Seldin, M. F.; Kastner, D. L.; Gregersen, P. K. STAT4 and the risk of rheumatoid arthritis and systemic lupus erythematosus. *N. Engl. J Med* **2007**, *357* (10), 977-986.
22. Yu, H.; Jove, R. The STATs of cancer--new molecular targets come of age. *Nat Rev Cancer* **2004**, *4* (2), 97-105.
23. Garcia, R.; Yu, C. L.; Hudnall, A.; Catlett, R.; Nelson, K. L.; Smithgall, T.; Fujita, D. J.; Ethier, S. P.; Jove, R. Constitutive activation of STAT3 in fibroblasts transformed by diverse oncoproteins and in breast carcinoma cells. *Cell Growth & Differentiation* **1997**, *8* (12), 1267-1276.
24. Hou, J.; Schindler, U.; Henzel, W. J.; Ho, T. C.; Brasseur, M.; McKnight, S. L. An interleukin-4-induced transcription factor: IL-4 STAT. *Science* **1994**, *265* (5179), 1701-1706.
25. Kaplan, M. H.; Schindler, U.; Smiley, S. T.; Grusby, M. J. STAT6 is required for mediating responses to IL-4 and for development of Th2 cells. *Immunity* **1996**, *4* (3), 313-319.
26. Szabo, S. J.; Glimcher, L. H.; Ho, I. C. Genes that regulate interleukin-4 expression in T cells. *Curr. Opin. Immunol* **1997**, *9* (6), 776-781.
27. Takeda, K.; Kishimoto, T.; Akira, S. STAT6: its role in interleukin 4-mediated biological functions. *J Mol Med* **1997**, *75* (5), 317-326.
28. Guiter, C.; Dusanter-Fourt, I.; Copie-Bergman, C.; Boulland, M. L.; Le Gouvello, S.; Gaulard, P.; Leroy, K.; Castellano, F. Constitutive STAT6

## Reference list

---

- activation in primary mediastinal large B-cell lymphoma. *Blood* **2004**, *104* (2), 543-549.
29. Ritz, O.; Guiter, C.; Dorsch, K.; Dusanter-Fourt, I.; Wegener, S.; Jouault, H.; Gaulard, P.; Castellano, F.; Moller, P.; Leroy, K. STAT6 activity is regulated by SOCS-1 and modulates BCL-XL expression in primary mediastinal B-Cell lymphoma. *Leukemia* **2008**.
  30. Barth, T. F.; LeithSuser, F.; Joos, S.; Bentz, M.; M÷ller, P. Mediastinal (thymic) large B-cell lymphoma: where do we stand? *The Lancet Oncology* **2002**, *3* (4), 229-234.
  31. Zhang, W. J.; Li, B. H.; Yang, X. Z.; Li, P. D.; Yuan, Q.; Liu, X. H.; Xu, S. B.; Zhang, Y.; Yuan, J.; Gerhard, G. S.; Masker, K. K.; Dong, C.; Koltun, W. A.; Chorney, M. J. IL-4-induced STAT6 activities affect apoptosis and gene expression in breast cancer cells. *Cytokine* **2008**, *42* (1), 39-47.
  32. Gooch, J. L.; Christy, B.; Yee, D. STAT6 mediates interleukin-4 growth inhibition in human breast cancer cells. *Neoplasia* **2002**, *4* (4), 324-331.
  33. Roth, M.; Black, J. L. Transcription factors in asthma: are transcription factors a new target for asthma therapy? *Curr. Drug Targets* **2006**, *7* (5), 589-595.
  34. Chen, X.; Vinkemeier, U.; Zhao, Y.; Jeruzalmi, D.; Darnell, J. E., Jr.; Kuriyan, J. Crystal structure of a tyrosine phosphorylated STAT-1 dimer bound to DNA. *Cell* **1998**, *93* (5), 827-839.
  35. Becker, S.; Groner, B.; Muller, C. W. Three-dimensional structure of the STAT3 beta homodimer bound to DNA. *Nature* **1998**, *394* (6689), 145-151.
  36. Hoey, T.; Schindler, U. STAT structure and function in signaling. *Current Opinion in Genetics & Development* **1998**, *8* (5), 582-587.
  37. Horvath, C. M. STAT proteins and transcriptional responses to extracellular signals. *Trends in Biochemical Sciences* **2000**, *25* (10), 496-502.
  38. Levy, D. E.; Darnell, J. E. STATs: transcriptional control and biological impact. *Nat Rev Mol Cell Biol* **2002**, *3* (9), 651-662.
  39. K Shuai . Modulation of STAT signaling by STAT-interacting proteins. 19[21], 2638-2644.20-5-2000.
  40. Akira, S. Roles of STAT3 defined by tissue-specific gene targeting. *Oncogene* **2000**, *19* (21), 2607-2611.
  41. Takeda, K.; Akira, S. STAT family of transcription factors in cytokine-mediated biological responses. *Cytokine & Growth Factor Reviews* **2000**, *11* (3), 199-207.
  42. Lucet, I. S.; Fantino, E.; Styles, M.; Bamert, R.; Patel, O.; Broughton, S. E.; Walter, M.; Burns, C. J.; Treutlein, H.; Wilks, A. F.; Rossjohn, J. The structural

## Reference list

---

- basis of Janus kinase 2 inhibition by a potent and specific pan-Janus kinase inhibitor. *Blood* **2006**, *107* (1), 176-183.
43. Kisseleva, T.; Bhattacharya, S.; Braunstein, J.; Schindler, C. W. Signaling through the JAK/STAT pathway, recent advances and future challenges. *Gene* **2002**, *285* (1-2), 1-24.
  44. Ihle, J. N. The Janus protein tyrosine kinase family and its role in cytokine signaling. *Adv. Immunol* **1995**, *60*, 1-35.
  45. Shuai, K.; Liu, B. Regulation of JAK-STAT signalling in the immune system. *Nature Reviews Immunology* **2003**, *3* (11), 900-911.
  46. Heinrich, P. C.; Behrmann, I.; Muller-Newen, G.; Schaper, F.; Graeve, L. Interleukin-6-type cytokine signalling through the gp130/Jak/STAT pathway. *Biochemical Journal* **1998**, *334*, 297-314.
  47. Heinrich, P. C.; Behrmann, I.; Graeve, L.; Grotzinger, J.; Haan, S.; Horn, F.; Horsten, U.; Kerr, I.; May, P.; Muller-Newen, G.; Terstegen, L.; Thiel, S. Molecular mechanisms of inflammation: interleukin-6-type cytokine signaling through the Jak/STAT pathway. *Nieren-und Hochdruckkrankheiten* **1998**, *27* (3), 123-131.
  48. Briscoe, J.; Guschin, D.; Rogers, N. C.; Watling, D.; Muller, M.; Horn, F.; Heinrich, P.; Stark, G. R.; Kerr, I. M. JAKs, STATs and signal transduction in response to the interferons and other cytokines. *Philosophical Transactions of the Royal Society of London Series B-Biological Sciences* **1996**, *351* (1336), 167-171.
  49. Zhong, M.; Henriksen, M. A.; Takeuchi, K.; Schaefer, O.; Liu, B.; Hoeve, J. t.; Ren, Z.; Mao, X.; Chen, X.; Shuai, K.; Darnell, J. E. Implications of an antiparallel dimeric structure of nonphosphorylated STAT1 for the activation/inactivation cycle. *Proceedings of the National Academy of Sciences of the United States of America* **2005**, *102* (11), 3966-3971.
  50. Aaronson, D. S.; Horvath, C. M. A road map for those who don't know JAK-STAT. *Science* **2002**, *296* (5573), 1653-1655.
  51. Reichel, M.; Nelson, B. H.; Greenberg, P. D.; Rothman, P. B. The IL-4 receptor alpha-chain cytoplasmic domain is sufficient for activation of JAK-1 and STAT6 and the induction of IL-4-specific gene expression. *J Immunol* **1997**, *158* (12), 5860-5867.
  52. McBride, K. M.; Reich, N. C. The Ins and Outs of STAT1 Nuclear Transport. *Sci. STKE* **2003**, *2003* (195), re13.
  53. Starr, R.; Hilton, D. J. Negative regulation of the JAK/STAT pathway. *Bioessays* **1999**, *21* (1), 47-52.
  54. Hebenstreit, D.; Wirnsberger, G.; Horejs-Hoeck, J.; Duschl, A. Signaling mechanisms, interaction partners, and target genes of STAT6. *Cytokine & Growth Factor Reviews* **2006**, *17* (3), 173-188.

## Reference list

---

55. Lee, D. U.; Rao, A. Molecular analysis of a locus control region in the T helper 2 cytokine gene cluster: A target for STAT6 but not GATA3. *Proceedings of the National Academy of Sciences of the United States of America* **2004**, *101* (45), 16010-16015.
56. Ehret, G. B.; Reichenbach, P.; Schindler, U.; Horvath, C. M.; Fritz, S.; Nabholz, M.; Bucher, P. DNA Binding Specificity of Different STAT Proteins. Comparison of in vitro specificity with natural target sites. *J. Biol. Chem.* **2001**, *276* (9), 6675-6688.
57. Kraus, J.; Borner, C.; Holtt, V. Distinct palindromic extensions of the 5' -TTC...GAA-3' motif allow STAT6 binding in vivo. *Faseb Journal* **2002**, *16* (14), 304-+.
58. Kraus, J.; Borner, C.; Holtt, V. High and low affinity binding sites for STAT6 with implications for opioid receptor gene regulation. *Naunyn-Schmiedeberg's Archives of Pharmacology* **2004**, 369, R74.
59. Hebenstreit, D.; Luft, P.; Schmiechlechner, A.; Duschl, A.; Horejs-Hoeck, J. SOCS-1 and SOCS-3 inhibit IL-4 and IL-13 induced activation of Eotaxin-3/CCL26 gene expression in HEK293 cells. *Mol Immunol* **2005**, *42* (3), 295-303.
60. Yoshimura, A.; Naka, T.; Kubo, M. SOCS proteins, cytokine signalling and immune regulation. *Nat Rev Immunol* **2007**, *7* (6), 454-465.
61. Campbell, I. L. Cytokine-mediated inflammation, tumorigenesis, and disease-associated JAK/STAT/SOCS signaling circuits in the CNS. *Brain Res. Brain Res. Rev* **2005**, *48* (2), 166-177.
62. Palvimo, J. J. PIAS proteins as regulators of small ubiquitin-related modifier (SUMO) modifications and transcription. *Biochemical Society Transactions* **2007**, *035* (6), 1405-1408.
63. Schust, J.; Berg, T. A high-throughput fluorescence polarization assay for signal transducer and activator of transcription 3. *Anal. Biochem.* **2004**, *330* (1), 114-118.
64. Siddiquee, K.; Zhang, S.; Guida, W. C.; Blaskovich, M. A.; Greedy, B.; Lawrence, H. R.; Yip, M. L.; Jove, R.; McLaughlin, M. M.; Lawrence, N. J.; Sebt, S. M.; Turkson, J. Selective chemical probe inhibitor of STAT3, identified through structure-based virtual screening, induces antitumor activity. *Proc. Natl. Acad. Sci. U. S A* **2007**, *104* (18), 7391-7396.
65. Thieu, V. T.; Nguyen, E. T.; McCarthy, B. P.; Bruns, H. A.; Kapur, R.; Chang, C. H.; Kaplan, M. H. IL-4-stimulated NF-kappaB activity is required for STAT6 DNA binding. *J Leukoc. Biol* **2007**, *82* (2), 370-379.
66. Razeto, A.; Ramakrishnan, V.; Litterst, C. M.; Giller, K.; Griesinger, C.; Carlomagno, T.; Lakomek, N.; Heimburg, T.; Lodrini, M.; Pfitzner, E.; Becker, S. Structure of the NCoA-1/SRC-1 PAS-B domain bound to the LXXLL motif of

## Reference list

---

- the STAT6 transactivation domain. *Journal of Molecular Biology* **2004**, 336 (2), 319-329.
67. Razeto, A.; Pfitzner, E.; Becker, S. Crystallization and preliminary crystallographic studies of the NCoA-1/SRC-1 PAS-B domain bound to the LXXLL motif of the STAT6 transactivation domain. *Acta Crystallogr. D Biol Crystallogr.* **2004**, 60 (Pt 3), 550-552.
68. Kotanides, H.; Reich, N. C. Interleukin-4-induced STAT6 recognizes and activates a target site in the promoter of the interleukin-4 receptor gene. *J Biol Chem.* **1996**, 271 (41), 25555-25561.
69. Takeda, K.; Tanaka, T.; Shi, W.; Matsumoto, M.; Minami, M.; Kashiwamura, S.; Nakanishi, K.; Yoshida, N.; Kishimoto, T.; Akira, S. Essential role of STAT6 in IL-4 signalling. *Nature* **1996**, 380 (6575), 627-630.
70. Curiel, R. E.; Lahesmaa, R.; Subleski, J.; Cippitelli, M.; Kirken, R. A.; Young, H. A.; Ghosh, P. Identification of a STAT-6-responsive element in the promoter of the human interleukin-4 gene. *Eur. J Immunol* **1997**, 27 (8), 1982-1987.
71. Rothenberg, M. E.; Hogan, S. P. The Eosinophil. *Annual Review of Immunology* **2006**, 24 (1), 147-174.
72. Voehringer, D.; Van Rooijen, N.; Locksley, R. M. Eosinophils develop in distinct stages and are recruited to peripheral sites by alternatively activated macrophages. *J Leukoc. Biol* **2007**, 81 (6), 1434-1444.
73. Kuperman, D.; Schofield, B.; Wills-Karp, M.; Grusby, M. J. Signal transducer and activator of transcription factor 6 (STAT6)-deficient mice are protected from antigen-induced airway hyperresponsiveness and mucus production. *J Exp. Med* **1998**, 187 (6), 939-948.
74. Andrews, R. P.; Ericksen, M. B.; Cunningham, C. M.; Daines, M. O.; Hershey, G. K. Analysis of the life cycle of STAT6. Continuous cycling of STAT6 is required for IL-4 signaling. *J Biol Chem.* **2002**, 277 (39), 36563-36569.
75. Blease, K.; Schuh, J. M.; Jakubzick, C.; Lukacs, N. W.; Kunkel, S. L.; Joshi, B. H.; Puri, R. K.; Kaplan, M. H.; Hogaboam, C. M. STAT6-deficient mice develop airway hyperresponsiveness and peribronchial fibrosis during chronic fungal asthma. *Am. J Pathol.* **2002**, 160 (2), 481-490.
76. Kuperman, D. A.; Schleimer, R. P. Interleukin-4, Interleukin-13, Signal Transducer and Activator of Transcription Factor 6, and Allergic Asthma. *Current Molecular Medicine* **2008**, 8 (5), 384-392.
77. Bruns, H. A.; Kaplan, M. H. The role of constitutively active STAT6 in leukemia and lymphoma. *Crit Rev Oncol. Hematol.* **2006**, 57 (3), 245-253.
78. Watson, C. J. STAT transcription factors in mammary gland development and tumorigenesis. *J Mammary Gland Biol Neoplasia* **2001**, 6 (1), 115-127.



## Reference list

---

79. Benekli, M.; Baer, M. R.; Baumann, H.; Wetzler, M. Signal transducer and activator of transcription proteins in leukemias. *Blood* **2003**, *101* (8), 2940-2954.
80. Skinnider, B. F.; Elia, A. J.; Gascoyne, R. D.; Patterson, B.; Trumper, L.; Kapp, U.; Mak, T. W. Signal transducer and activator of transcription 6 is frequently activated in Hodgkin and Reed-Sternberg cells of Hodgkin lymphoma. *Blood* **2002**, *99* (2), 618-626.
81. Buglio, D.; Georgiakis, G. V.; Hanabuchi, S.; Arima, K.; Khaskhely, N. M.; Liu, Y. J.; Younes, A. Vorinostat inhibits STAT6-mediated TH2 cytokine and TARC production and induces cell death in Hodgkin lymphoma cell lines. *Blood* **2008**.
82. Cui, X.; Zhang, L.; Luo, J.; Rajasekaran, A.; Hazra, S.; Cacalano, N.; Dubinett, S. M. Unphosphorylated STAT6 contributes to constitutive cyclooxygenase-2 expression in human non-small cell lung cancer. *Oncogene* **2007**, *26* (29), 4253-4260.
83. Hanson, E. M.; Dickensheets, H.; Qu, C. K.; Donnelly, R. P.; Keegan, A. D. Regulation of the dephosphorylation of STAT6. Participation of Tyr-713 in the interleukin-4 receptor alpha, the tyrosine phosphatase SHP-1, and the proteasome. *J Biol Chem*. **2003**, *278* (6), 3903-3911.
84. Wold, F. In vivo chemical modification of proteins (post-translational modification). *Annu. Rev Biochem*. **1981**, *50*, 783-814.
85. Merrifield, R. B. Solid-phase peptide synthesis. 3. AN IMPROVED SYNTHESIS OF BRADYKININ. *Biochemistry* **1964**, *3*, 1385-1390.
86. Kimmerlin, T.; Seebach, D. '100 years of peptide synthesis': ligation methods for peptide and protein synthesis with applications to peptide assemblies\*. *Journal of Peptide Research* **2005**, *65* (2), 229-260.
87. Dawson, P. E.; Kent, S. B. H. Synthesis of native proteins by chemical ligation 1. *Annual Review of Biochemistry* **2000**, *69* (1), 923-960.
88. Kochendoerfer, G. G.; Kent, S. B. Chemical protein synthesis. *Curr. Opin. Chem. Biol* **1999**, *3* (6), 665-671.
89. Merrifield, R. B.; Merrifield, E. L.; Juvvadi, P.; Andreu, D.; Boman, H. G. Design and synthesis of antimicrobial peptides. *Ciba Found. Symp.* **1994**, *186*, 5-20.
90. Coin, I.; Beyermann, M.; Bienert, M. Solid-phase peptide synthesis: from standard procedures to the synthesis of difficult sequences. *Nat. Protoc.* **2007**, *2* (12), 3247-3256.
91. Dawson, P. E.; Muir, T. W.; Clark-Lewis, I.; Kent, S. B. Synthesis of proteins by native chemical ligation. *Science* **1994**, *266* (5186), 776-779.

## Reference list

---

92. Muir, T. W.; Dawson, P. E.; Fitzgerald, M. C.; Kent, S. B. Protein signature analysis: a practical new approach for studying structure-activity relationships in peptides and proteins. *Methods Enzymol.* **1997**, *289*, 545-564.
93. Amblard, M.; Fehrentz, J. A.; Martinez, J.; Subra, G. Methods and protocols of modern solid phase Peptide synthesis. *Mol Biotechnol.* **2006**, *33* (3), 239-254.
94. Hackeng, T. M.; Griffin, J. H.; Dawson, P. E. Protein synthesis by native chemical ligation: expanded scope by using straightforward methodology. *Proc. Natl. Acad. Sci U S A* **1999**, *96* (18), 10068-10073.
95. Becker, C. F.; Hunter, C. L.; Seidel, R. P.; Kent, S. B.; Goody, R. S.; Engelhard, M. A sensitive fluorescence monitor for the detection of activated Ras: total chemical synthesis of site-specifically labeled Ras binding domain of c-Raf1 immobilized on a surface. *Chem. Biol* **2001**, *8* (3), 243-252.
96. Ball, H. L.; King, D. S.; Cohen, F. E.; Prusiner, S. B.; Baldwin, M. A. Engineering the prion protein using chemical synthesis. *J. Pept. Res.* **2001**, *58* (5), 357-374.
97. Dawson, P. E. Synthesis of chemokines by native chemical ligation. *Methods Enzymol.* **1997**, *287*, 34-45.
98. Camarero, J. A.; Muir, T. W. Native chemical ligation of polypeptides. *Curr. Protoc. Protein Sci.* **2001**, *Chapter 18*, Unit18.
99. Baca, M.; Alewood, P. F.; Kent, S. B. Structural engineering of the HIV-1 protease molecule with a beta-turn mimic of fixed geometry. *Protein Sci.* **1993**, *2* (7), 1085-1091.
100. Becker, C. F.; Hunter, C. L.; Seidel, R.; Kent, S. B.; Goody, R. S.; Engelhard, M. Total chemical synthesis of a functional interacting protein pair: the protooncogene H-Ras and the Ras-binding domain of its effector c-Raf1. *Proc. Natl. Acad. Sci U. S A* **2003**, *100* (9), 5075-5080.
101. Becker, C. F.; Hunter, C. L.; Seidel, R. P.; Kent, S. B.; Goody, R. S.; Engelhard, M. A sensitive fluorescence monitor for the detection of activated Ras: total chemical synthesis of site-specifically labeled Ras binding domain of c-Raf1 immobilized on a surface. *Chem. Biol.* **2001**, *8* (3), 243-252.
102. Kochendoerfer, G. G.; Chen, S. Y.; Mao, F.; Cressman, S.; Traviglia, S.; Shao, H.; Hunter, C. L.; Low, D. W.; Cagle, E. N.; Carnevali, M.; Gueriguian, V.; Keogh, P. J.; Porter, H.; Stratton, S. M.; Wiedeke, M. C.; Wilken, J.; Tang, J.; Levy, J. J.; Miranda, L. P.; Crnogorac, M. M.; Kalbag, S.; Botti, P.; Schindler-Horvat, J.; Savatski, L.; Adamson, J. W.; Kung, A.; Kent, S. B. H.; Bradburne, J. A. Design and Chemical Synthesis of a Homogeneous Polymer-Modified Erythropoiesis Protein. *Science* **2003**, *299* (5608), 884-887.
103. Kochendoerfer, G. G.; Tack, J. M.; Cressman, S. Total Chemical Synthesis of a 27 kDa TASP Protein Derived from the MscL Ion Channel of *M. tuberculosis* by Ketoxime-Forming Ligation. *Bioconjugate Chem.* **2002**, *13* (3), 474-480.

## Reference list

---

104. Chen, J.; Wan, Q.; Yuan, Y.; Zhu, J.; Danishefsky, S. J. Native Chemical Ligation at Valine: A Contribution to Peptide and Glycopeptide Synthesis. *Angew. Chem. Int. Ed Engl.* **2008**, *47* (44), 8521-8524.
105. Bang, D.; Chopra, N.; Kent, S. B. Total chemical synthesis of crambin. *J Am. Chem Soc.* **2004**, *126* (5), 1377-1383.
106. Camarero, J. A.; Fushman, D.; Cowburn, D.; Muir, T. W. Peptide chemical ligation inside living cells: in vivo generation of a circular protein domain. *Bioorg. Med. Chem* **2001**, *9* (9), 2479-2484.
107. Alsina, J.; Yokum, T. S.; Albericio, F.; Barany, G. Backbone Amide Linker (BAL) Strategy for N- $\alpha$ -9-Fluorenylmethoxycarbonyl (Fmoc) Solid-Phase Synthesis of Unprotected Peptide p-Nitroanilides and Thioesters. *J. Org. Chem.* **1999**, *64* (24), 8761-8769.
108. Hofmann, R. M.; Muir, T. W. Recent advances in the application of expressed protein ligation to protein engineering. *Curr. Opin. Biotechnol.* **2002**, *13* (4), 297-303.
109. Alsina, J.; Jensen, K. J.; Albericio, F.; Barany, G. Solid-phase synthesis with tris(alkoxy)benzyl backbone amide linkage (BAL). *Chemistry-A European Journal* **1999**, *5* (10), 2787-2795.
110. Quaderer, R.; Hilvert, D. Improved Synthesis of C-Terminal Peptide Thioesters on "Safety-Catch" Resins Using LiBr/THF. *Org. Lett.* **2001**, *3* (20), 3181-3184.
111. Axel Sewing, D. H. P. Fmoc-Compatible Solid-Phase Peptide Synthesis of Long C-Terminal Peptide Thioesters. 40[18], 3395-3396. 6-4-2001. Ref Type: Generic
112. Swinnen, D.; Hilvert, D. Facile, Fmoc-Compatible Solid-Phase Synthesis of Peptide C-Terminal Thioesters. *Org. Lett.* **2000**, *2* (16), 2439-2442.
113. Low, D. W.; Hill, M. G.; Carrasco, M. R.; Kent, S. B.; Botti, P. Total synthesis of cytochrome b562 by native chemical ligation using a removable auxiliary. *Proc. Natl. Acad. Sci U. S A* **2001**, *98* (12), 6554-6559.
114. Hunter, C. L.; Kochendoerfer, G. G. Native chemical ligation of hydrophobic [corrected] peptides in lipid bilayer systems. *Bioconjug. Chem* **2004**, *15* (3), 437-440.
115. Clayton, D.; Shapovalov, G.; Maurer, J. A.; Dougherty, D. A.; Lester, H. A.; Kochendoerfer, G. G. Total chemical synthesis and electrophysiological characterization of mechanosensitive channels from Escherichia coli and Mycobacterium tuberculosis. *Proceedings of the National Academy of Sciences of the United States of America* **2004**, *101* (14), 4764-4769.
116. Schnolzer, M.; Kent, S. B. Constructing proteins by dovetailing unprotected synthetic peptides: backbone-engineered HIV protease. *Science* **1992**, *256* (5054), 221-225.

## Reference list

---

117. Muir, T. W.; Williams, M. J.; Ginsberg, M. H.; Kent, S. B. H. Design and Chemical Synthesis of a Neoprotein Structural Model for the Cytoplasmic Domain of a Multisubunit Cell-Surface Receptor: Integrin  $\alpha$ .IIb.beta.3 (Platelet GPIIb-IIIa). *Biochemistry* **1994**, 33 (24), 7701-7708.
118. Fisch, I.; Kunzi, G.; Rose, K.; Offord, R. E. Site-specific modification of a fragment of a chimeric monoclonal antibody using reverse proteolysis. *Bioconjugate Chem.* **1992**, 3 (2), 147-153.
119. Rose, K. Facile synthesis of homogeneous artificial proteins. *J. Am. Chem. Soc.* **1994**, 116 (1), 30-33.
120. Zhang, L.; Torgerson, T. R.; Liu, X. Y.; Timmons, S.; Colosia, A. D.; Hawiger, J.; Tam, J. P. Preparation of functionally active cell-permeable peptides by single-step ligation of two peptide modules. *Proceedings of the National Academy of Sciences of the United States of America* **1998**, 95 (16), 9184-9189.
121. Tornøe, C. W.; Christensen, C.; Meldal, M. Peptidotriazoles on Solid Phase: [1,2,3]-Triazoles by Regiospecific Copper(I)-Catalyzed 1,3-Dipolar Cycloadditions of Terminal Alkynes to Azides. *J. Org. Chem.* **2002**, 67 (9), 3057-3064.
122. Durek, T.; Becker, C. F. W. Protein semi-synthesis: New proteins for functional and structural studies. *Biomolecular Engineering* **2005**, 22 (5-6), 153-172.
123. Muir, T. W.; Kent, S. B. The chemical synthesis of proteins. *Curr. Opin. Biotechnol.* **1993**, 4 (4), 420-427.
124. Muir, T. W.; Sondhi, D.; Cole, P. A. Expressed protein ligation: a general method for protein engineering. *Proc. Natl. Acad. Sci. U. S A* **1998**, 95 (12), 6705-6710.
125. Severinov, K.; Muir, T. W. Expressed protein ligation, a novel method for studying protein-protein interactions in transcription. *J. Biol Chem.* **1998**, 273 (26), 16205-16209.
126. Blaschke, U. K.; Silberstein, J.; Muir, T. W. Protein engineering by expressed protein ligation. *Methods Enzymol.* **2000**, 328, 478-496.
127. Muir, T. W. Semisynthesis of proteins by expressed protein ligation. *Annu. Rev Biochem.* **2003**, 72, 249-289.
128. David, R.; Richter, M. P.; Beck-Sickinger, A. G. Expressed protein ligation. Method and applications. *Eur. J. Biochem.* **2004**, 271 (4), 663-677.
129. Machova, Z.; Beck-Sickinger, A. G. Expressed Protein Ligation for Protein Semisynthesis and Engineering. In *Peptide Synthesis and Applications*, 298 ed.; 2005; pp 105-130.
130. Muralidharan, V.; Muir, T. W. Protein ligation: an enabling technology for the biophysical analysis of proteins. *Nat Methods* **2006**, 3 (6), 429-438.

## Reference list

---

131. Telenti, A.; Southworth, M.; Alcaide, F.; Daugelat, S.; Jacobs, W. R.; Perler, F. B. The Mycobacterium xenopi GyrA protein splicing element: Characterization of a minimal. *Journal of Bacteriology* **1997**, *179* (20), 6378-6382.
132. Southworth, M. W.; Amaya, K.; Evans, T. C.; Xu, M. Q.; Perler, F. B. Purification of proteins fused to either the amino or carboxy terminus of the Mycobacterium xenopi gyrase A intein. *Biotechniques* **1999**, *27* (1), 110-+.
133. Shi, Y.; Massagué, J. Mechanisms of TGF- $\beta$  Signaling from Cell Membrane to the Nucleus. *Cell* **2003**, *113* (6), 685-700.
134. Ottesen, J. J.; Huse, M.; Sekedat, M. D.; Muir, T. W. Semisynthesis of phosphovariants of Smad2 reveals a substrate preference of the activated T beta RI kinase. *Biochemistry* **2004**, *43* (19), 5698-5706.
135. Durek, T.; Alexandrov, K.; Goody, R. S.; Hildebrand, A.; Heinemann, I.; Waldmann, H. Synthesis of fluorescently labeled mono- and diprenylated Rab7 GTPase. *J. Am. Chem. Soc.* **2004**, *126* (50), 16368-16378.
136. Durek, T.; Goody, R. S.; Alexandrov, K. In vitro semisynthesis and applications of C-terminally modified rab proteins. *Methods Mol Biol* **2004**, *283*, 233-244.
137. Shen, K. Analyzing protein tyrosine phosphatases by phosphotyrosine analog integration. *Methods* **2007**, *42* (3), 234-242.
138. Goto, N. K.; Kay, L. E. New developments in isotope labeling strategies for protein solution NMR spectroscopy. *Current Opinion in Structural Biology* **2000**, *10* (5), 585-592.
139. Kimura, R.; Camarero, J. A. Expressed protein ligation: a new tool for the biosynthesis of cyclic polypeptides. *Protein Pept. Lett.* **2005**, *12* (8), 789-794.
140. Trabi, M.; Craik, D. J. Circular proteins -- no end in sight. *Trends in Biochemical Sciences* **2002**, *27* (3), 132-138.
141. Evans, J. R.; Benner, J.; XU, M. Q. Semisynthesis of cytotoxic proteins using a modified protein splicing element. *Protein Sci* **1998**, *7* (11), 2256-2264.
142. Schwarzer, D.; Zhang, Z.; Zheng, W.; Cole, P. A. Negative regulation of a protein tyrosine phosphatase by tyrosine phosphorylation. *J. Am. Chem. Soc.* **2006**, *128* (13), 4192-4193.
143. Beene, D. L.; Brandt, G. S.; Zhong, W.; Zacharias, N. M.; Lester, H. A.; Dougherty, D. A. Cation03C0; Interactions in Ligand Recognition by Serotonergic (5-HT<sub>3A</sub>) and Nicotinic Acetylcholine Receptors: The Anomalous Binding Properties of Nicotine. *Biochemistry* **2002**, *41* (32), 10262-10269.
144. Beene, D. L.; Dougherty, D. A.; Lester, H. A. Unnatural amino acid mutagenesis in mapping ion channel function. *Current Opinion in Neurobiology* **2003**, *13* (3), 264-270.

## Reference list

---

145. Ottesen, J. J.; Bar-Dagan, M.; Giovani, B.; Muir, T. W. An amalgamation of solid phase peptide synthesis and ribosomal peptide synthesis. *Biopolymers* **2008**, *90* (3), 406-414.
146. Hahn, M. E.; Pellois, J. P.; Vila-Perello, M.; Muir, T. W. Tunable photoactivation of a post-translationally modified signaling protein and its unmodified counterpart in live cells. *ChemBiochem* **2007**, *8* (17), 2100-2105.
147. Ellis-Davies, G. C. Caged compounds: photorelease technology for control of cellular chemistry and physiology. *Nat Methods* **2007**, *4* (8), 619-628.
148. Mayer, G.; Heckel, A. Biologically active molecules with a "light switch". *Angew. Chem. Int. Ed Engl.* **2006**, *45* (30), 4900-4921.
149. Douglas D.Young and Alexander Deiters\* Photochemical control of biological processes. *Org. Biomol. Chem* **2006**, *2007* (5), 999-1005.
150. Kaplan, J. H.; Somlyo, A. P. Flash photolysis of caged compounds: new tools for cellular physiology. *Trends Neurosci.* **1989**, *12* (2), 54-59.
151. Kaplan, J. H.; Forbush, B.; Hoffman, J. F. Rapid photolytic release of adenosine 5'-triphosphate from a protected analog: utilization by the sodium:potassium pump of human red blood cell ghosts. *Biochemistry* **1978**, *17* (10), 1929-1935.
152. Humphries, J. D.; Byron, A.; Humphries, M. J. Integrin ligands at a glance. *J Cell Sci* **2006**, *119* (19), 3901-3903.
153. Petersen, S.; Alonso, J. M.; Specht, A.; Duodu, P.; Goeldner, M.; del Campo, A. Phototriggering of cell adhesion by caged cyclic RGD peptides PETERSEN2008. *Angewandte Chemie-International Edition* **2008**, *47* (17), 3192-3195.
154. Aemissegger, A.; Carrigan, C. N.; Imperiali, B. Caged O-phosphorothioyl amino acids as building blocks for Fmoc-based solid phase peptide synthesis. *Tetrahedron* **2007**, *63* (27), 6185-6190.
155. Humphrey, D. H.; Rajfur, Z.; Vazquez, F.; Imperiali, B.; Jacobson, K. Photoactivation of caged FAK phosphotyrosine 397 peptides transiently halts lamellar extension of migrating cells Humphrey2004. *Molecular Biology of the Cell* **2004**, *15*, 401A.
156. Xie, Z.; Sanada, K.; Samuels, B. A.; Shih, H.; Tsai, L. H. Serine 732 Phosphorylation of FAK by Cdk5 Is Important for Microtubule Organization, Nuclear Movement, and Neuronal Migration. *Cell* **2003**, *114* (4), 469-482.
157. Rothman, D.; Imperiali, B. Caged phosphoserine peptides. *Abstracts of Papers of the American Chemical Society* **2002**, *224*, U118.
158. Tatsu, Y.; Shigeri, Y.; Sogabe, S.; Yumoto, N.; Yoshikawa, S. Solid-Phase Synthesis of Caged Peptides Using Tyrosine Modified with a Photocleavable Protecting Group: Application to the Synthesis of Caged Neuropeptide Y.

## Reference list

---

- Biochemical and Biophysical Research Communications* **1996**, 227 (3), 688-693.
159. Ni, J. H.; Auston, D. A.; Freilich, D. A.; Muralidharan, S.; Sobie, E. A.; Kao, J. P. Y. Photochemical gating of intracellular Ca<sup>2+</sup> release channels NI2007. *Journal of the American Chemical Society* **2007**, 129 (17), 5316-+.
160. Samways, D. S. K.; Li, W. H.; Conway, S. J.; Holmes, A. B.; Bootman, M. D.; Henderson, G. Co-incident signalling between mu-opioid and M-3 muscarinic receptors at the level of Ca<sup>2+</sup> release from intracellular stores: lack of evidence for Ins(1,4,5)P-3 receptor sensitization. *Biochemical Journal* **2003**, 375, 713-720.
161. Bayley, H.; Chang, C. Y.; Pan, P. Caged peptides and proteins. *Biophysical Journal* **1997**, 72 (2), WPME7.
162. Kinyanjui, M. W.; Fixman, E. D. Cell-penetrating peptides and proteins: new inhibitors of allergic airways disease. *Can. J Physiol Pharmacol.* **2008**, 86 (1-2), 1-7.
163. Zhang, Y.; Yu, L. C. Single-cell microinjection technology in cell biology. *Bioessays* **2008**, 30 (6), 606-610.
164. Storrie, B. Microinjection as a tool to explore small GTPase function. *Methods Enzymol.* **2005**, 404, 26-42.
165. Shigeri, Y.; Tatsu, Y.; Yumoto, N. Synthesis and application of caged peptides and proteins. *Pharmacology & Therapeutics* **2001**, 91 (2), 85-92.
166. Marriott, G. Caged Protein Conjugates and Light-Directed Generation of Protein Activity: Preparation, Photoactivation, and Spectroscopic Characterization of Caged G-Actin Conjugates. *Biochemistry* **1994**, 33 (31), 9092-9097.
167. Rothman, D. M.; Vazquez, E. M.; Vogel, E. M.; Imperiali, B. General method for the synthesis of caged phosphopeptides: Tools for the exploration of signal transduction pathways. *Organic Letters* **2002**, 4 (17), 2865-2868.
168. Mendel, D.; Ellman, J. A.; Schultz, P. G. Construction of a light-activated protein by unnatural amino acid mutagenesis. *J. Am. Chem. Soc.* **1991**, 113 (7), 2758-2760.
169. Miller, J. C.; Silverman, S. K.; England, P. M.; Dougherty, D. A.; Lester, H. A. Flash Decaging of Tyrosine Sidechains in an Ion Channel. *Neuron* **1998**, 20 (4), 619-624.
170. Pan, P.; Bayley, H. Caged cysteine and thiophosphoryl peptides. *Febs Letters* **1997**, 405 (1), 81-85.
171. Rothman, D. M.; Imperiali, B. Caged phosphoserine peptides and proteins. *Biopolymers* **2005**, 80 (4), 484.

## Reference list

---

172. Pellois, J. P.; Muir, T. W. Semisynthetic proteins in mechanistic studies: using chemistry to go where nature can't. *Current Opinion in Chemical Biology* **2006**, *10* (5), 487-491.
173. Shi, Y.; Massagué, J. Mechanisms of TGF- $\beta$  Signaling from Cell Membrane to the Nucleus. *Cell* **2003**, *113* (6), 685-700.
174. Mendel, D.; Ellman, J. A.; Schultz, P. G. Construction of a light-activated protein by unnatural amino acid mutagenesis. *J. Am. Chem. Soc.* **1991**, *113* (7), 2758-2760.
175. Noren, C. J.; Anthony-Cahill, S. J.; Griffith, M. C.; Schultz, P. G. A general method for site-specific incorporation of unnatural amino acids into proteins. *Science* **1989**, *244* (4901), 182-188.
176. Rothman, D. M.; Vazquez, M. E.; Vogel, E. M.; Imperiali, B. Caged phospho-amino acid building blocks for solid-phase peptide synthesis. *Journal of Organic Chemistry* **2003**, *68* (17), 6795-6798.
177. Terpetschnig, E.; Szmecinski, H.; Ozinskas, A.; Lakowicz, J. R. Synthesis of Squaraine-N-Hydroxysuccinimide Esters and Their Biological Application as Long-Wavelength Fluorescent Labels. *Analytical Biochemistry* **1994**, *217* (2), 197-204.
178. Gruber, H. J.; Kada, G.; Pragl, B.; Riener, C.; Hahn, C. D.; Harms, G. S.; Ahner, W.; Dax, T. G.; Hohenthanner, K.; Knaus, H. G. Preparation of Thiol-Reactive Cy5 Derivatives from Commercial Cy5 Succinimidyl Ester. *Bioconjugate Chem.* **2000**, *11* (2), 161-166.
179. Merrifield, R. B. Solid Phase Peptide Synthesis .1. Synthesis of A Tetrapeptide. *Journal of the American Chemical Society* **1963**, *85* (14), 2149
180. Carpino, L. A.; Han, G. Y. 9-Fluorenylmethoxycarbonyl Amino-Protecting Group. *Journal of Organic Chemistry* **1972**, *37* (22), 3404.
181. Bang, D.; Kent, S. B. His6 tag-assisted chemical protein synthesis. *Proc. Natl. Acad. Sci. U. S A* **2005**, *102* (14), 5014-5019.
182. Schnolzer, M.; Alewood, P.; Jones, A.; Alewood, D.; Kent, S. B. In situ neutralization in Boc-chemistry solid phase peptide synthesis. Rapid, high yield assembly of difficult sequences. *Int. J. Pept. Protein Res.* **1992**, *40* (3-4), 180-193.
183. Kaiser, E.; COLESCOT.RL; BOSSINGE.CD; Cook, P. I. Color Test for Detection of Free Terminal Amino Groups in Solid-Phase Synthesis of Peptides. *Analytical Biochemistry* **1970**, *34* (2), 595.
184. Sarin, V. K.; Kent, S. B.; Tam, J. P.; Merrifield, R. B. Quantitative monitoring of solid-phase peptide synthesis by the ninhydrin reaction. *Anal. Biochem.* **1981**, *117* (1), 147-157.



## Reference list

---

185. Schaeffer, H.; von Jagow, G. Tricine-sodium dodecyl sulfate-polyacrylamide gel electrophoresis for the separation of proteins in the range from 1 to 100 kDa. *Analytical Biochemistry* **1987**, *166* (2), 368-379.
186. Andrea L Wurster<sup>1</sup>, T. T. a. M. J. G. The biology of STAT4 and STAT6. *Oncogene* **2007**.
187. Stein, N. C.; Kreutzmann, C.; Zimmermann, S. P.; Niebergall, U.; Hellmeyer, L.; Goettsch, C.; Schoppet, M.; Hofbauer, L. C. Interleukin-4 and interleukin-13 stimulate the osteoclast inhibitor osteoprotegerin by human endothelial cells through the STAT6 pathway. *Journal of Bone and Mineral Research* **2008**, *23* (5), 750-758.
188. Quelle, F. W.; Shimoda, K.; Thierfelder, W.; Fischer, C.; Kim, A.; Ruben, S. M.; Cleveland, J. L.; Pierce, J. H.; Keegan, A. D.; Nelms, K.; . Cloning of murine STAT6 and human STAT6, STAT proteins that are tyrosine phosphorylated in responses to IL-4 and IL-3 but are not required for mitogenesis. *Mol Cell Biol* **1995**, *15* (6), 3336-3343.
189. Atherton, E.; Sheppard, R. C. "Solid Phase Peptide Synthesis: A Practical Approach"; IRL Press at Oxford University Press Oxford, England 1989
190. Ehret, G. B.; Reichenbach, P.; Schindler, U.; Horvath, C. M.; Fritz, S.; Nabholz, M.; Bucher, P. DNA binding specificity of different STAT proteins. Comparison of in vitro specificity with natural target sites. *J Biol Chem.* **2001**, *276* (9), 6675-6688.
191. Schindler, C.; Darnell, J. E., Jr. Transcriptional responses to polypeptide ligands: the JAK-STAT pathway. *Annu. Rev Biochem.* **1995**, *64*, 621-651.
192. Parisien, J. P.; Lau, J. F.; Horvath, C. M. STAT2 acts as a host range determinant for species-specific paramyxovirus interferon antagonism and simian virus 5 replication. *Journal of Virology* **2002**, *76* (13), 6435-6441.
193. Khwaja, A. The role of Janus kinases in haemopoiesis and haematological malignancy. *British Journal of Haematology* **2006**, *134* (4), 366-384.
194. Das, S.; Roth, C. P.; Wasson, L. M.; Vishwanatha, J. K. Signal transducer and activator of transcription-6 (STAT6) is a constitutively expressed survival factor in human prostate cancer. *Prostate* **2007**, *67* (14), 1550-1564.
195. Mullings, R. E.; Wilson, S. J.; Puddicombe, S. M.; Lordan, J. L.; Bucchieri, F.; Djukanovic, R.; Howarth, P. H.; Harper, S.; Holgate, S. T.; Davies, D. E. Signal transducer and activator of transcription 6 (STAT-6) expression and function in asthmatic bronchial epithelium. *Journal of Allergy and Clinical Immunology* **2001**, *108* (5), 832-838.
196. Gernez, Y.; Tirouvanziam, R.; Nguyen, K. D.; Herzenberg, L. A.; Krensky, A. M.; Nadeau, K. C. Altered phosphorylated signal transducer and activator of transcription profile of CD4+CD161+ T cells in asthma: modulation by allergic status and oral corticosteroids. *J Allergy Clin Immunol* **2007**, *120* (6), 1441-1448.

## Reference list

---

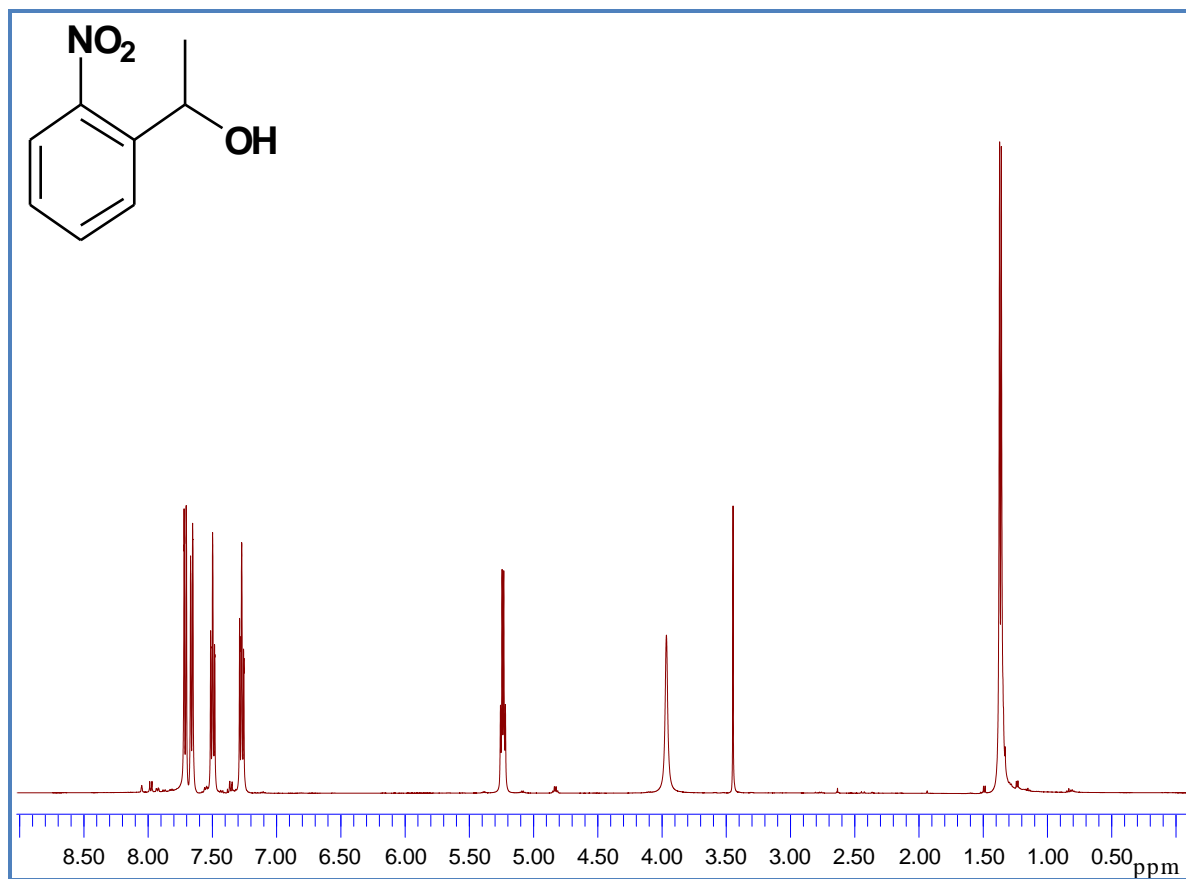
197. Shimoda, K.; van Deursen, J.; Sangster, M. Y.; Sarawar, S. R.; Carson, R. T.; Tripp, R. A.; Chu, C.; Quelle, F. W.; Nosaka, T.; Vignali, D. A.; Doherty, P. C.; Grosveld, G.; Paul, W. E.; Ihle, J. N. Lack of IL-4-induced Th2 response and IgE class switching in mice with disrupted STAT6 gene. *Nature* **1996**, *380* (6575), 630-633.
198. Nagashima, S.; Nagata, H.; Iwata, M.; Yokota, M.; Moritomo, H.; Orita, M.; Kuromitsu, S.; Koakutsu, A.; Ohga, K.; Takeuchi, M.; Ohta, M.; Tsukamoto, S. Identification of 4-benzylamino-2-[(4-morpholin-4-ylphenyl)amino]pyrimidine-5-carboxamide derivatives as potent and orally bioavailable STAT6 inhibitors. *Bioorg. Med Chem.* **2008**, *16* (13), 6509-6521.
199. Marriott, G.; Roy, P.; Jacobson, K. [11] Preparation and light-directed activation of caged proteins. In *Methods in Enzymology Biophotonics, Part A*, Volume 360 ed.; Gerard Marriott and Ian Parker, Ed.; Academic Press: 2003; pp 274-288.
200. Gorostiza, P.; Isacoff, E. Optical switches and triggers for the manipulation of ion channels and pores. *Molecular Biosystems* **2007**, *3* (10), 686-704.
201. Grell, E.; Geoffroy, A.; Stolz, M.; Lewitzki, E.; von Raumer, M. Membrane proteins in thin films. *Journal of Thermal Analysis and Calorimetry* **2007**, *89* (3), 723-727.
202. Kinyanjui, M. W.; Fixman, E. D. Cell-penetrating peptides and proteins: new inhibitors of allergic airways disease. *Canadian Journal of Physiology and Pharmacology* **2008**, *86* (1-2), 1-7.
203. Humphrey, D.; Rajfur, Z.; Vazquez, M. E.; Scheswohl, D.; Schaller, M. D.; Jacobson, K.; Imperiali, B. In Situ photoactivation of a caged phosphotyrosine peptide derived from focal adhesion kinase temporarily halts lamellar extension of single migrating tumor cells. *Journal of Biological Chemistry* **2005**, *280* (23), 22091-22101.
204. Cohen, B. E.; Stoddard, B. L.; Koshland, D. E., Jr. Caged NADP and NAD. Synthesis and characterization of functionally distinct caged compounds. *Biochemistry* **1997**, *36* (29), 9035-9044.
205. Momotake, A. Current topics of caged compounds for biological application. *Seikagaku* **2007**, *79* (12), 1153-1158.
206. Zhao, Y. R.; Zheng, Q.; Dakin, K.; Xu, K.; Martinez, M. L.; Li, W. H. New caged coumarin fluorophores with extraordinary uncaging cross sections suitable for biological imaging applications. *Journal of the American Chemical Society* **2004**, *126* (14), 4653-4663.
207. Strop, P.; Brunger, A. T. Refractive index-based determination of detergent concentration and its application to the study of membrane proteins. *Protein Sci* **2005**, *14* (8), 2207-2211.

## Reference list

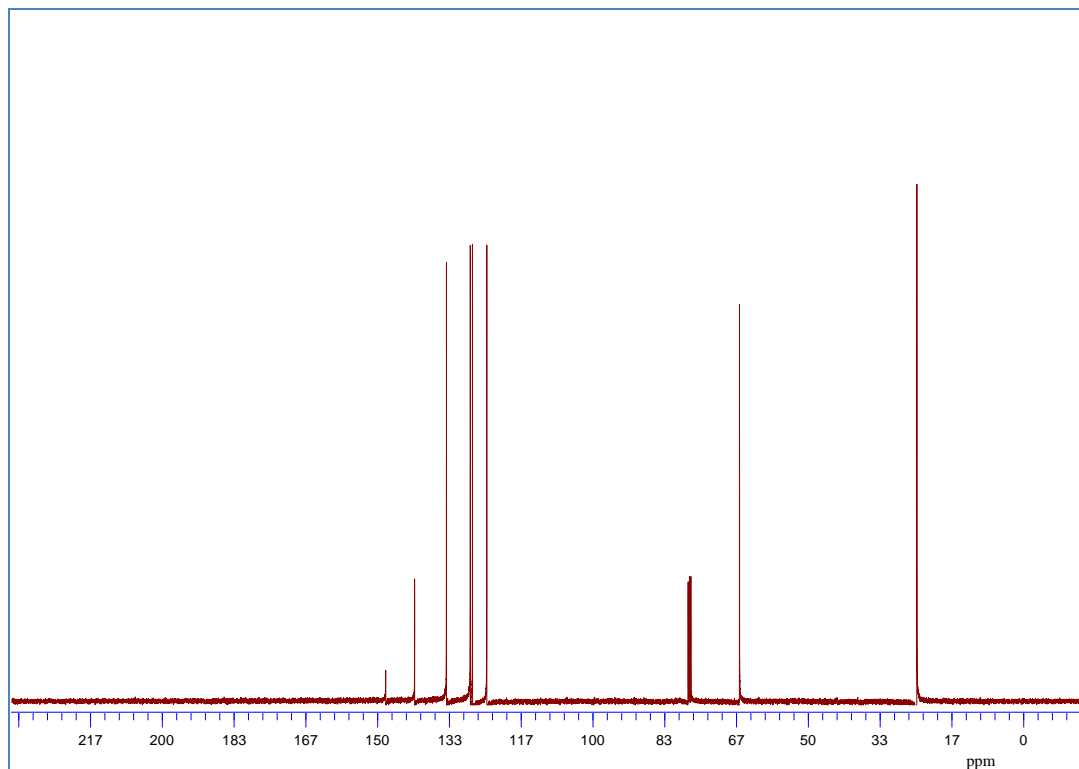
---

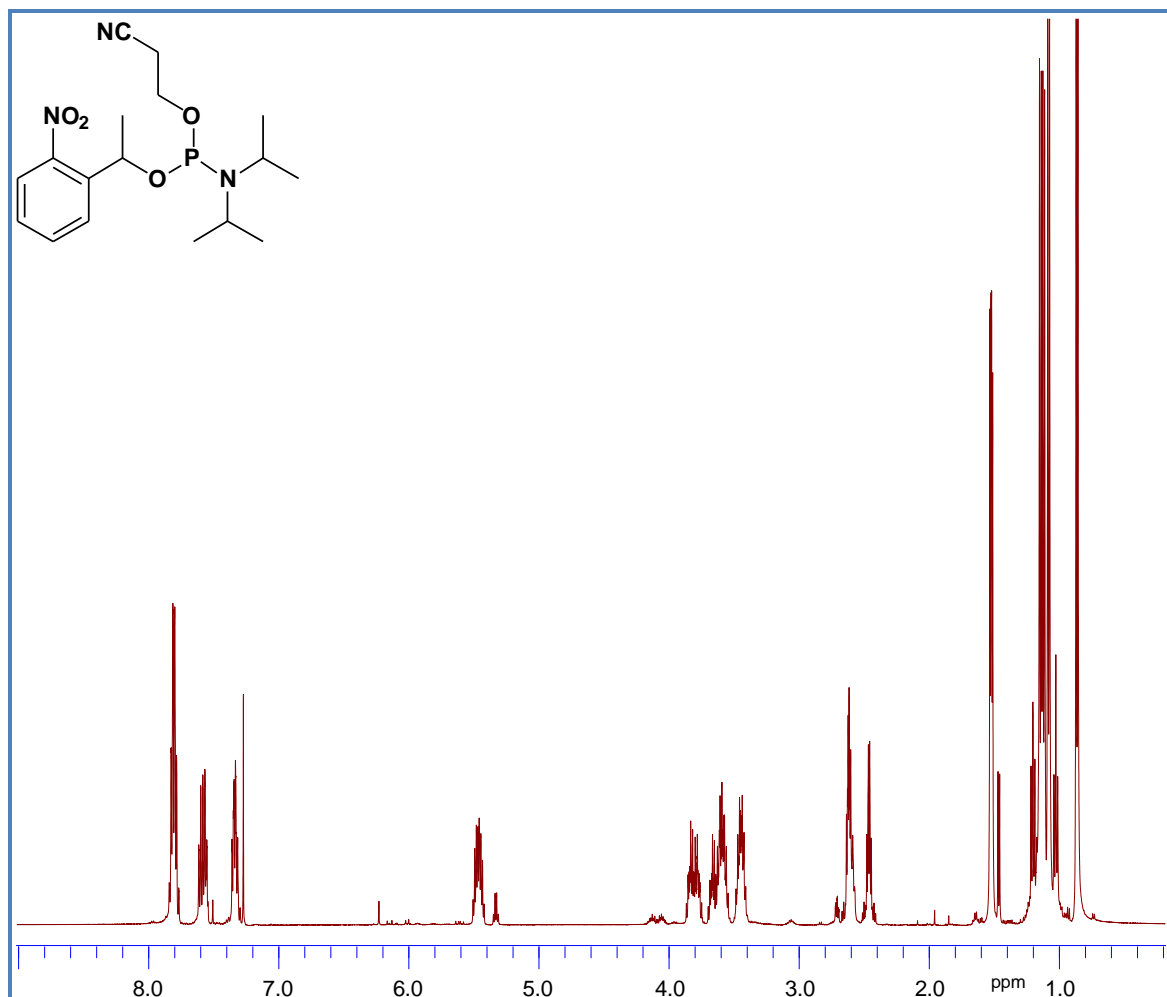
208. Begitt, A.; Meyer, T.; van Rossum, M.; Vinkemeier, U. Nucleocytoplasmic translocation of STAT1 is regulated by a leucine-rich export signal in the coiled-coil domain. *Proc. Natl. Acad. Sci U S A* **2000**, *97* (19), 10418-10423.
209. Decker, T.; Kovarik, P. Serine phosphorylation of STATs. *Oncogene* **2000**, *19* (21), 2628-2637.
210. Maiti, N. R.; Sharma, P.; Harbor, P. C.; Haque, S. J. Serine phosphorylation of STAT6 negatively controls its DNA-binding function. *Journal of Interferon and Cytokine Research* **2005**, *25* (9), 553-563.
211. Banala, S.; Arnold, A.; Johnsson, K. Caged substrates for protein labeling and immobilization. *Chembiochem* **2008**, *9* (1), 38-41.
212. Chen, W. G.; Daines, M. O.; Hershey, G. K. K. Methylation of STAT6 modulates STAT6 phosphorylation, nuclear translocation, and DNA-binding activity. *Journal of Immunology* **2004**, *172* (11), 6744-6750.
213. Mikita, T.; Campbell, D.; Wu, P.; Williamson, K.; Schindler, U. Requirements for interleukin-4-induced gene expression and functional characterization of STAT6. *Mol Cell Biol* **1996**, *16* (10), 5811-5820.
214. Meyer, T.; Begitt, A.; Vinkemeier, U. Green fluorescent protein-tagging reduces the nucleocytoplasmic shuttling specifically of unphosphorylated STAT1. *FEBS J* **2007**, *274* (3), 815-826.

**1-(2-nitrophenyl) ethanol (*NPE-OH*) (2),  $^1\text{H}$  NMR**

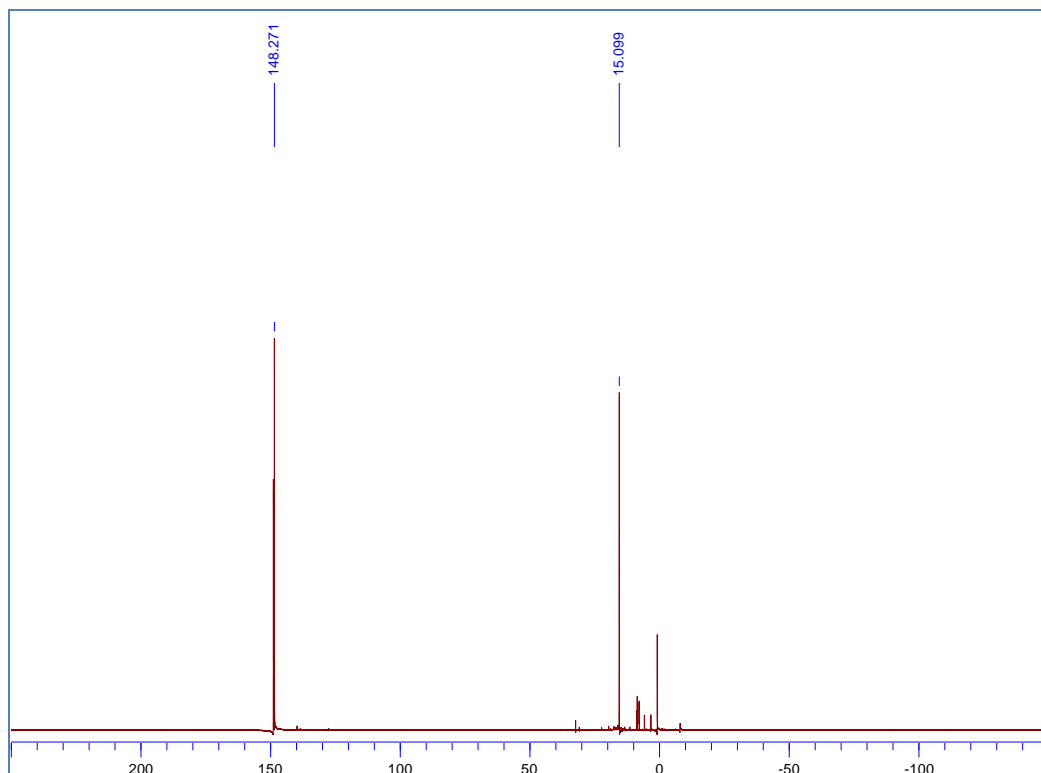


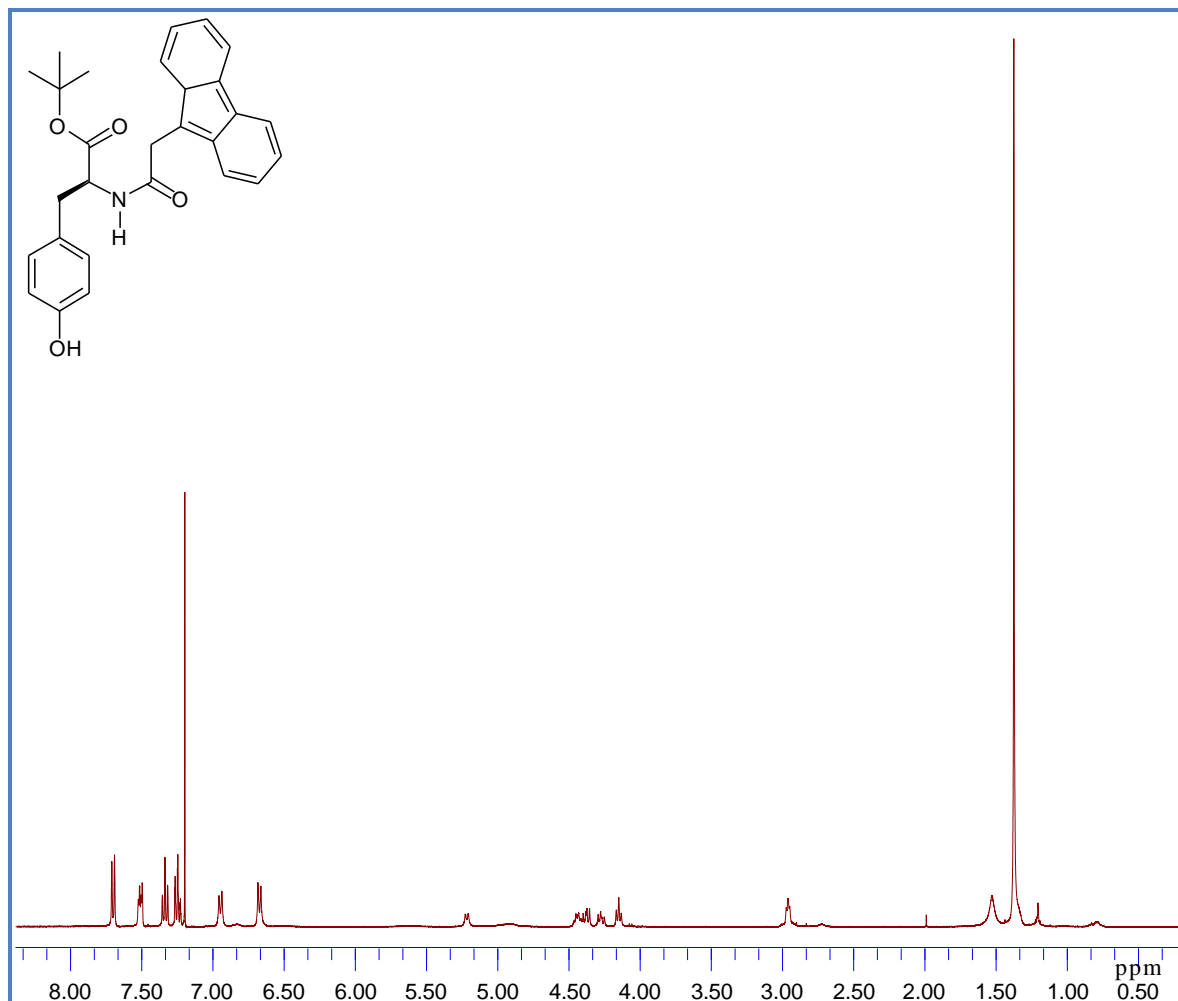
**1-(2-nitrophenyl)-ethanol (*NPE-OH*) (2),  $^{13}\text{C}$  NMR**



**O-1-(2-nitrophenyl)ethyl-O'-β-cyanoethyl-N,N-diisopropyl phosphoramidite (3), <sup>1</sup>H NMR**

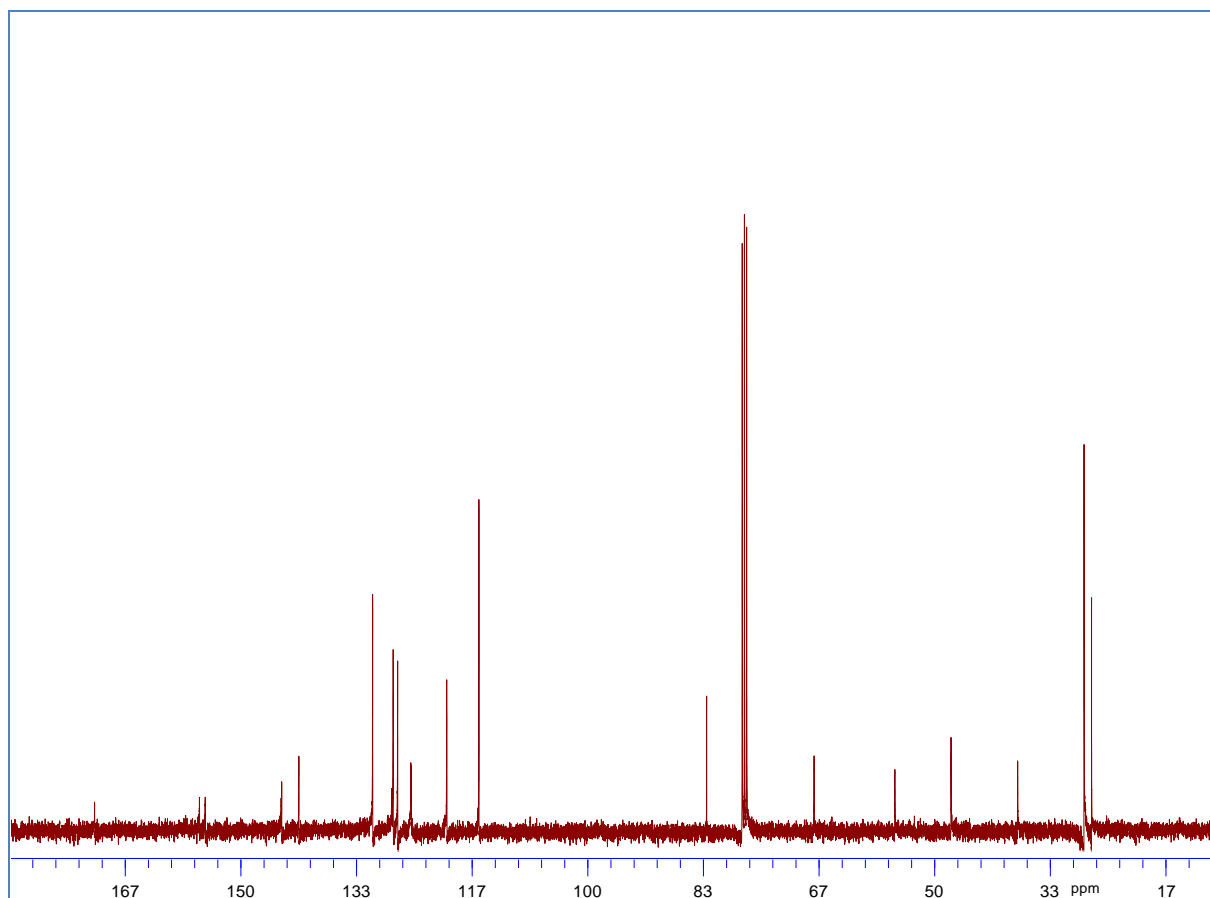
**O-1-(2-nitrophenyl)ethyl-O'- $\beta$ -cyanoethyl-N,N-diisopropyl phosphoramidite (3),  $^{31}\text{P}$  NMR**

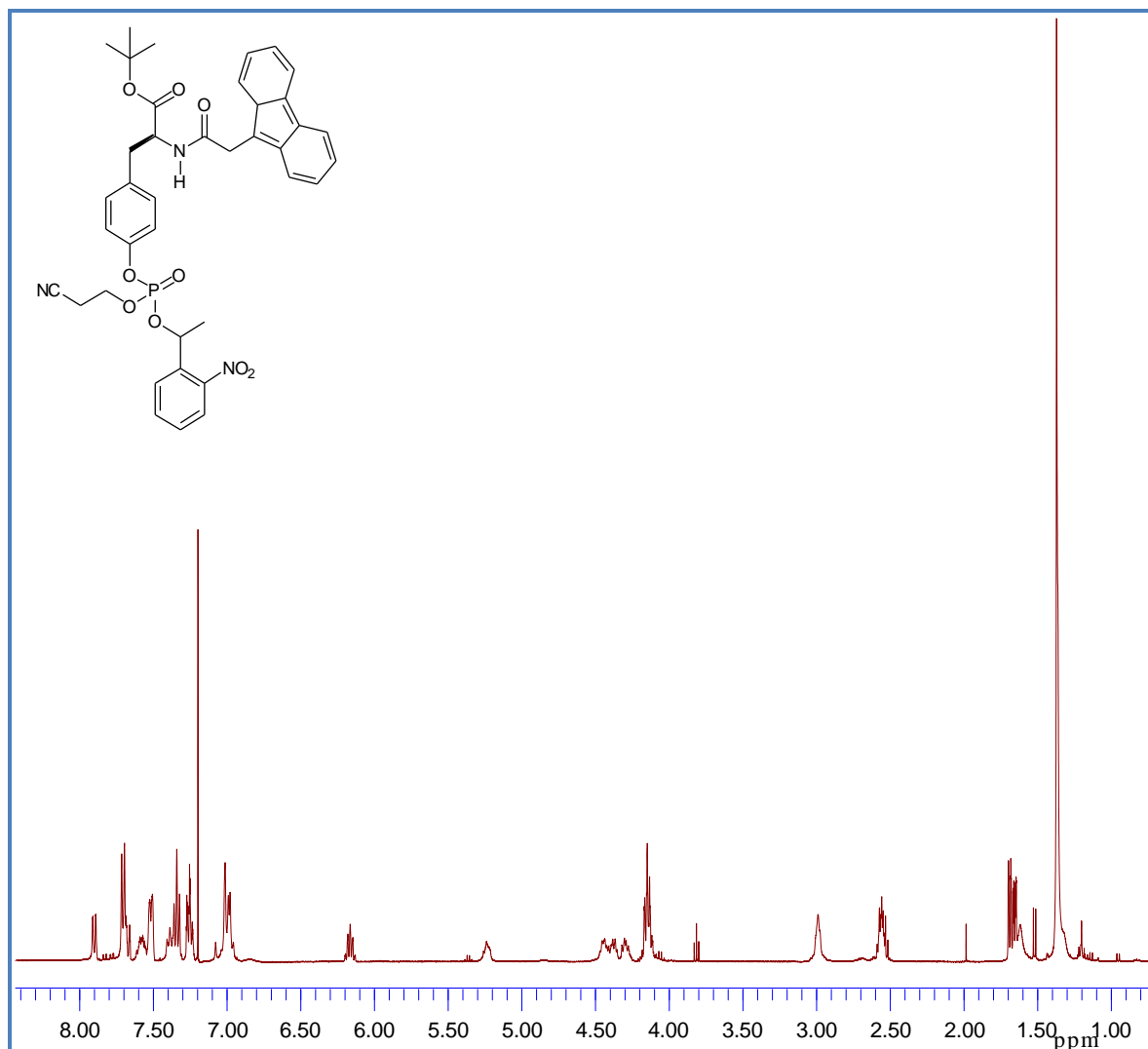


**N- $\alpha$ -Fmoc-L-tyrosine tert-butyl Ester (5),  $^1\text{H}$  NMR**

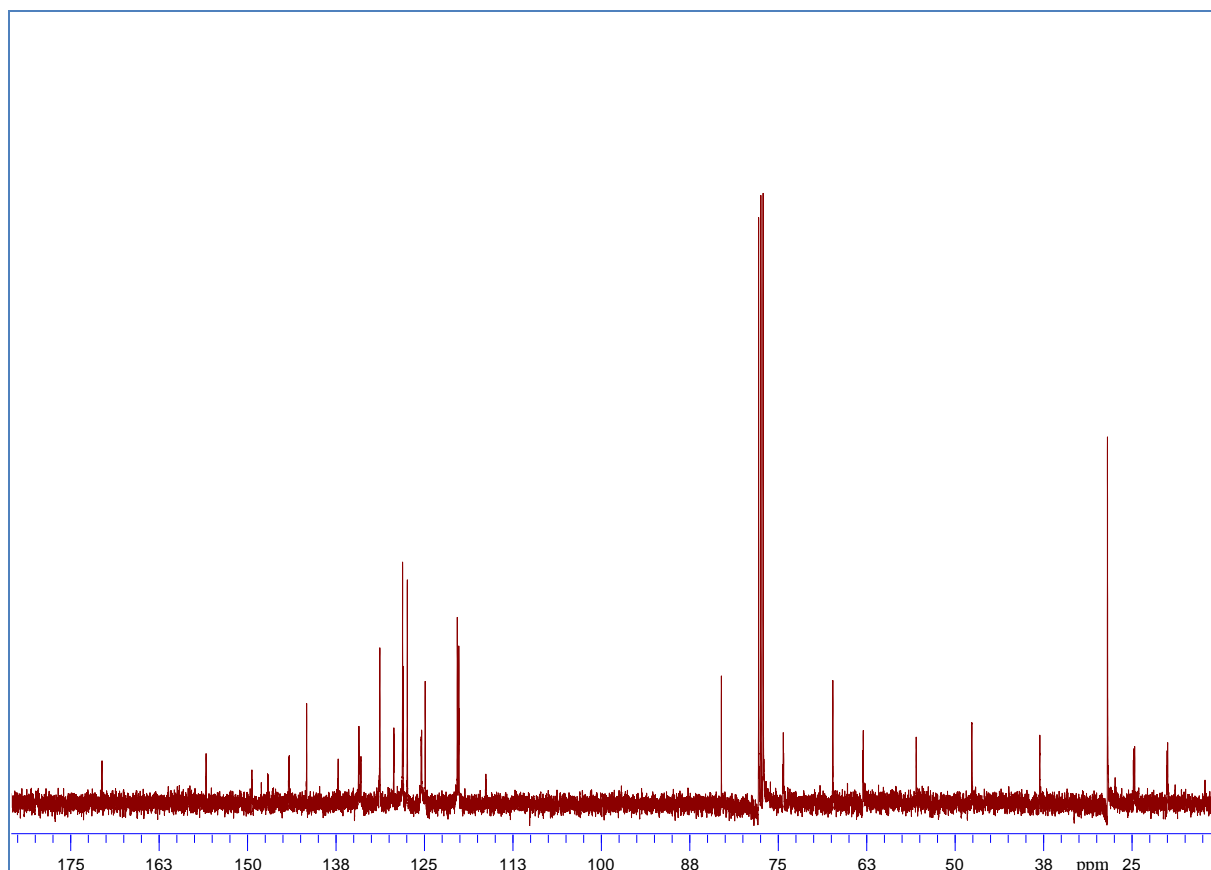


**N- $\alpha$ -Fmoc-L-tyrosine tert-butyl Ester (5),  $^{13}\text{C}$  NMR**

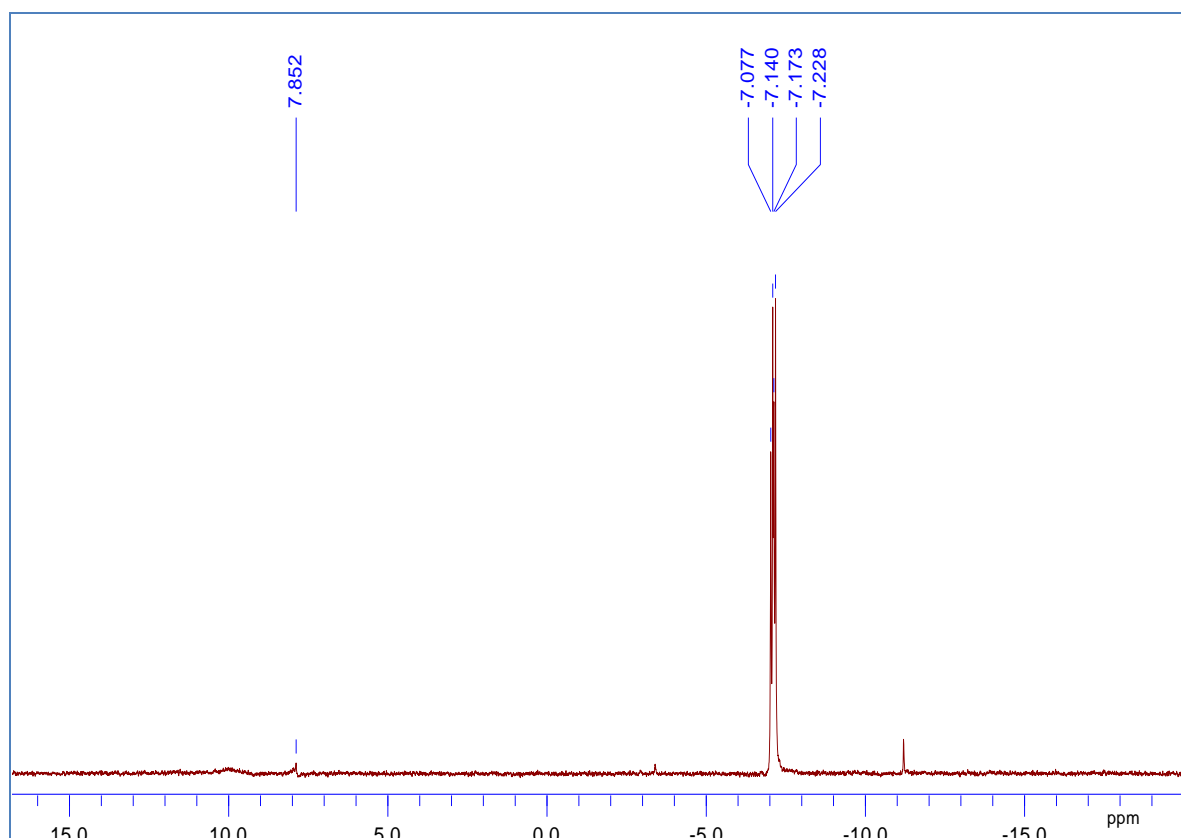


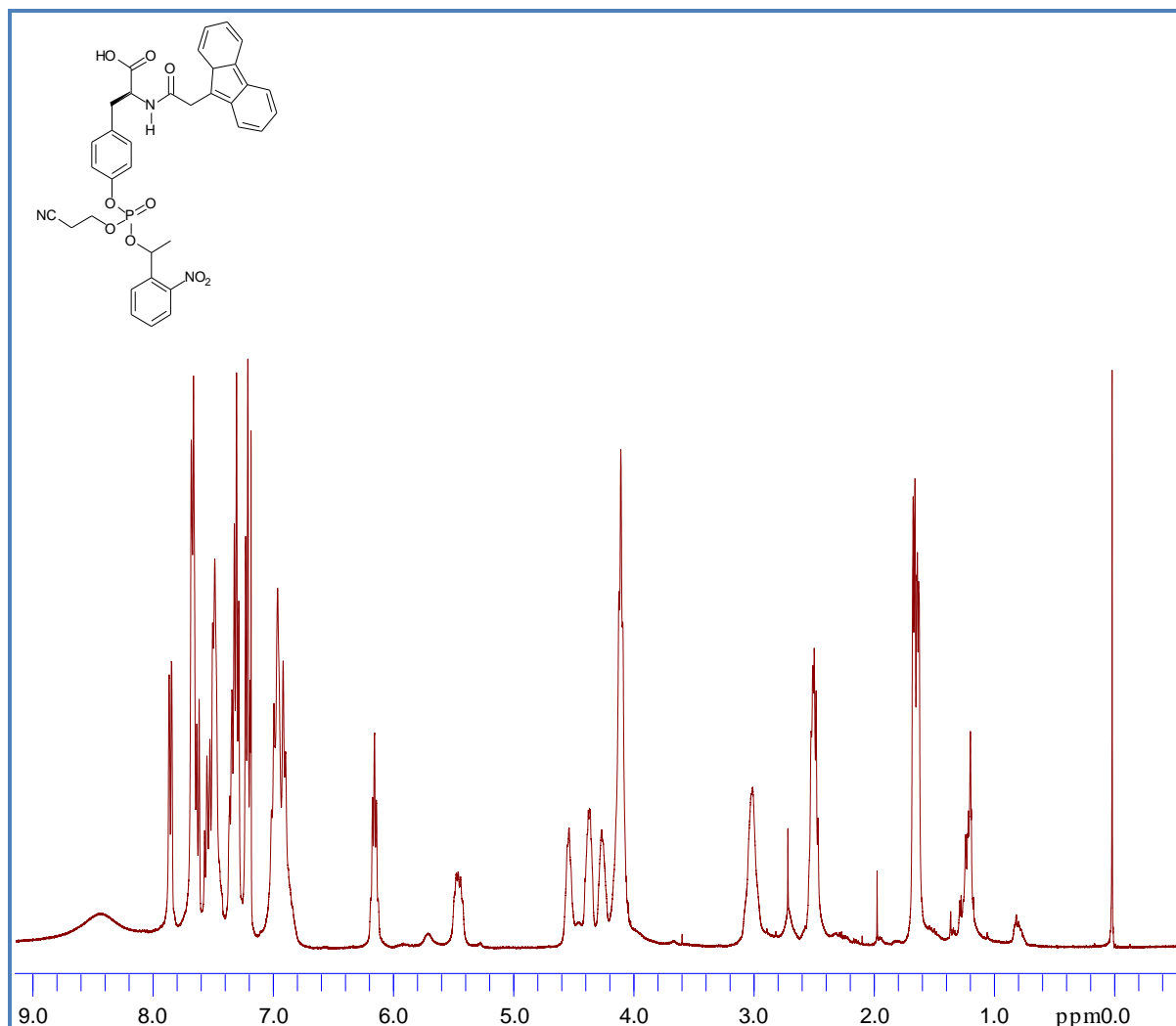
**N- $\alpha$ -Fmoc-phospho-(1-nitrophenyl ethyl-2-cyanoethyl)- L-tyrosine tert-butyl ester. (7),  $^1\text{H}$  NMR**

**N- $\alpha$ -Fmoc-phospho-(1-nitrophenylethyl-2-cyanoethyl)- L-tyrosine tert-butyl ester. (7),  $^{13}\text{C}$  NMR**

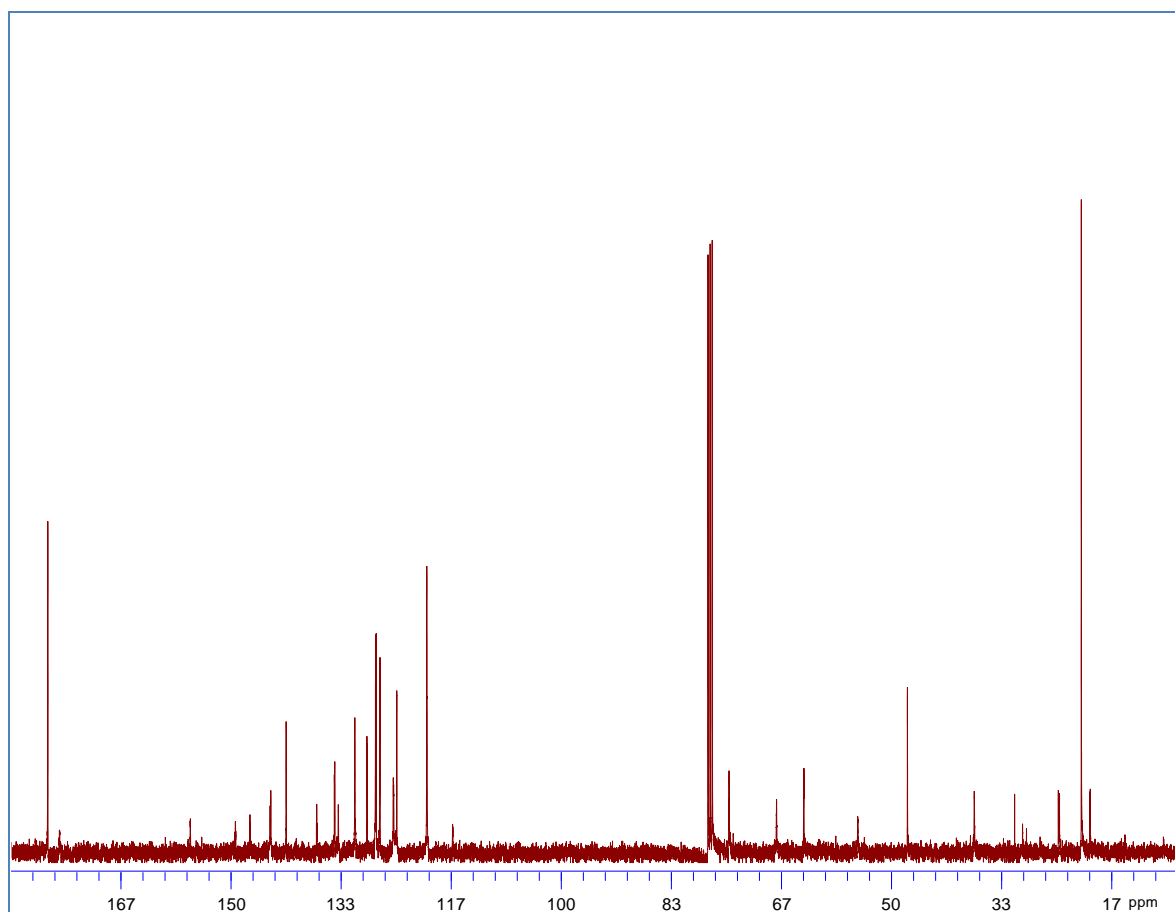


**N- $\alpha$ -Fmoc-phospho (1-nitrophenylethyl-2-cyanoethyl)-L-tyrosine tert-butyl ester. (7),  $^{31}\text{P}$  NMR**

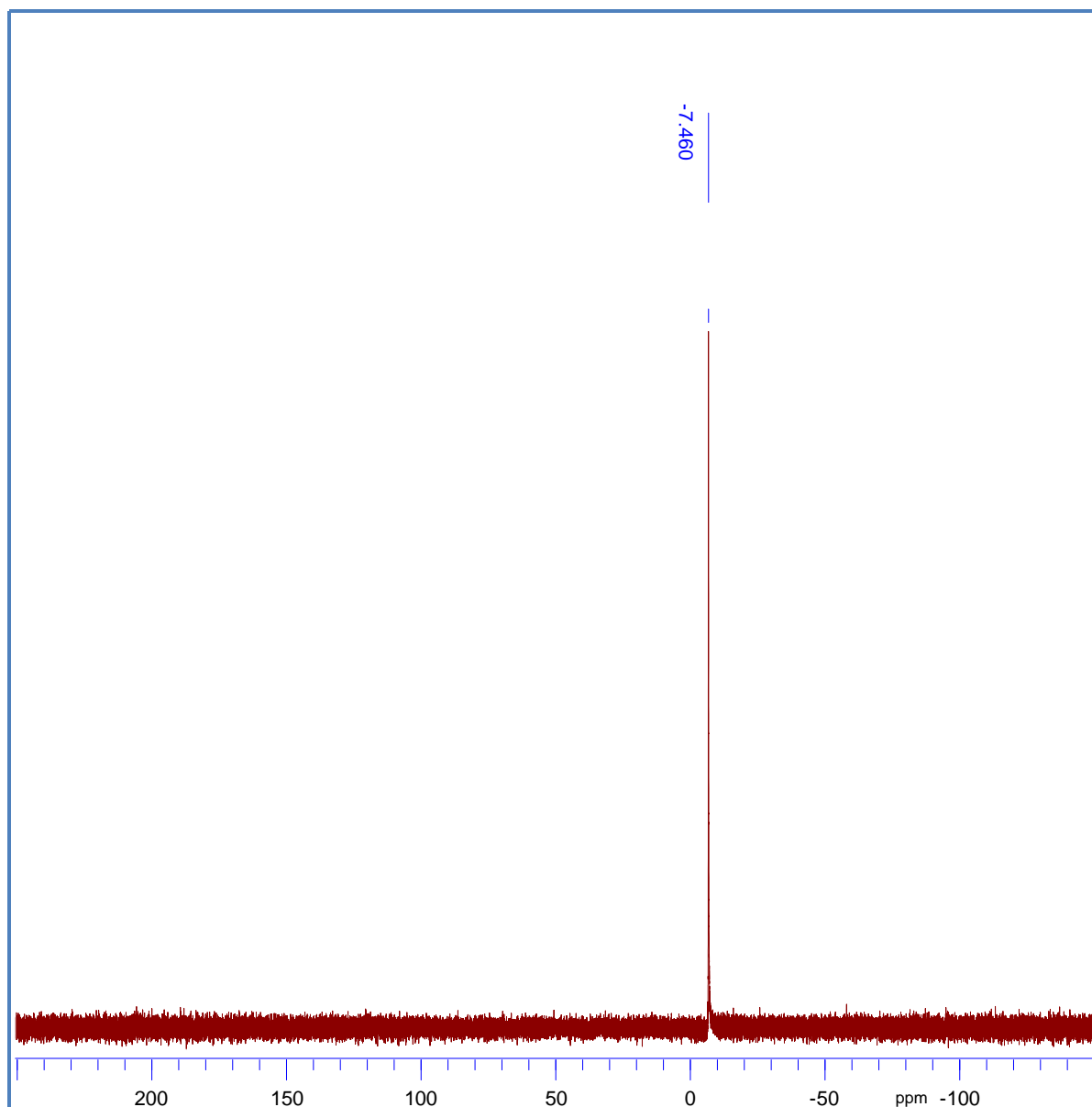


**N- $\alpha$ -Fmoc-phospho (1-nitrophenylethyl-2-cyanoethyl)-L-tyrosine (8),  $^1\text{H}$  NMR**

**N- $\alpha$ -Fmoc-phospho (1-nitrophenyl ethyl-2-cyanoethyl)-L-tyrosine (8),  $^{13}\text{C}$  NMR**



**N- $\alpha$ -Fmoc-phospho-(1-nitrophenyl ethyl-2-cyanoethyl)-L-tyrosine (8),  $^{31}\text{P}$  NMR**



## ***Personal Data***

Name	Sunanda Lahiri
Birth place	Mumbai, India
Date of birth	5-12-1979
Nationality	Indian

## ***University Education***

September 2004:	PhD, Supervisor Dr. Christian Becker, Prof Dr. Roger .S. Goody Max Planck Institute of Molecular Physiology, Dortmund, Germany.
2003-2004:	Internship with Prof Dr. Peter Langer working on the synthesis based on 1,3 –Bis silyl enol ethers Chemistries, University of Greifswald (EMAU), Germany.
2002-2003:	Project Student with Dr. M. Ravikanth “The Synthesis of Dendrimeric Porphyrin”, Indian Institute of Technology, Mumbai, India.
2002-2000:	Master of Science ( <i>MSc</i> ) in Organic Chemistry, Kelkar V. G College, Mulund, University of Mumbai, India.
1997-2000:	Bachelor of Science ( <i>BSc</i> ) in Chemistry, Kelkar V.G. College, Mulund, University of Mumbai, India.
1995-1997:	Higher Secondary Certificate ( <i>HSc</i> ), Mumbai, India.
1984-1995:	Secondary School Certificate ( <i>SSc</i> ), Mumbai, India.

## ***Conference and Publications***

- Presented poster in Gordon Research Conference, Bioorgani Chemistry, New Hampshire, USA
- Semisynthesis of caged phosphorylated and fluorescently labeled STAT6 proteins" by Sunanda Lahiri, Ralf Seidel, Martin Engelhard and Christian F. W. Becker Paper in the Proceedings of the 29th European Peptide Symposium, Gdansk, Poland, 2006
- Domino "[3+3]-Cyclization-Homo-Michael" Reactions of 1,3-Bissilyl Enol Ethers with 1,1-Diacylcyclopropanes Bose, G.; Hong Nguyen, V. T.; Ullah, E.; Lahiri, S.; Gorls, H.; Langer, P.; *J. Org. Chem.*; (Article); 2004; 69(26); 9128-9134. DOI:10.1021/jo0485278